2010

The role of bone marrow in SIV pathogenesis using the Rhesus macaque model

Amy F. Gill
Louisiana State University and Agricultural and Mechanical College

THE ROLE OF BONE MARROW IN SIV PATHOGENESIS USING THE RHESUS MACAQUE MODEL

A Dissertation

Submitted to the Graduate Faculty of the
Louisiana State University and
Agricultural and Mechanical College
in partial fulfillment of the
requirements for the degree of
Doctor of Philosophy

in
The Interdepartmental Program in
Veterinary Medical Sciences
Through the Department of Pathobiological Sciences

by
Amy F. Gill
D.V.M., Louisiana State University, 1994
August 2010

DEDICATION

To Elizabeth and Don Michael Jr.,
My dear children who always have and always will love me in spite of myself
as much as
I always have and always will love them in spite of themselves,

And

To my parents, Dale and Sally Fleniken,
My dear parents who have supported me 200% in all my endeavors and
Taught me how to love myself and others in spite of ourselves,

And

To God
Who is the teacher for loving us in spite of ourselves.

ACKNOWLEDGEMENTS

Books are doors to worlds of pleasure.
Books are keys to wisdom's treasure.
Books are stairs that upward lead.
Books are friends. Come let us read.
Author Unknown

Overwhelming thanks are due to many family members and friends that have supported me during my second professional student era or is that now just professional student. I hope ya'll enjoy reading this book and take special note of the buckets of tears, liters of sweat, gallons of diet Coke, countless sleepless nights, unending carpool hours, passing 2nd grade two more times, numerous Sonic trips (best Reese's blasts are on Wardline Road in Hammond considering East Baton Rouge Parish, Livingston Parish, Tangipahoa Parish and St. Tammany Parish), ever growing loads of laundry, gained and lost weight, new hairstyles (but no gray hairs!), passing the "40" mark, surviving as the Girl Scout cookie Mom, attending Cub Scout campouts (2 Polar Bear awards), and several other rites of passage entwined between the lines of this auspicious undertaking. See kids, you are never too old to go to school or to succeed in anything you dream to undertake!

Thanks to Drs. Andrew Lackner, director for the Tulane National Primate Research Center (TNPRC), and Thomas Klei, dean of academic research for the LSU School of Veterinary Medicine (LSU-SVM). Both of these esteemed researchers accepted me into the NIH T32 Training Grant for my PhD research. I am grateful for the career opportunity and academic guidance they offered me and hope to show them many exciting works in my future.

Thanks to my research mentor, Dr. Ron Veazey at the Tulane National Primate Research Center. He offered space in his busy laboratory for me to learn invaluable basic science research including collaborative research. I am grateful to his guidance and the ability for me to learn by

trial and error. For after being forged in fire we are rid of our impurities and shine with brilliance we didn't know existed but others knew was hidden within. I hope I did not cause your eye sight to worsen too much with all the trees I have passed over your desk as flow cytometry gates… I know I am seeing dots all the time.

Thanks to Dr. Xiaolei Wang for sharing an office with me for over 3 years. We shared work, lots of flow analyses, motherhood and life. I loved having someone in the room to share ideas and happy times. I appreciate her careful and detailed explaining my complicated 10 color flow analysis and helping me find cross reactive antibodies. She showed by example how great life can be if we are open to all possibilities and of course that good things do happen to good people. I will miss you Xiaolei and Eddie!

Thanks to Dr. Peter Didier who had the misfortune of having his office next door to mine for over three years. His misfortune was that his door was always open as his intellect to offer an innovative research approach, to offer a second opinion on pathology issues, or to offer supportive advice to a struggling graduate student. His numerous years with experience of primate pathology and basic sciences research were invaluable to the naïve scientist within me. Pete also showed by example how to balance family and hobbies with work for a well-rounded, happy life. I am very appreciative for his willingness to invest his time for my career.

Thanks to the Molecular Core Laboratory at the Tulane National Primate Research Center. Ms. Terri Rasmussen was a great mentor in molecular pathology and raising kids. She always had a smile on her face and NEVER ran when she saw me coming toward her with a worried look on my face. She devoted endless hours of discussion and work to my immunohistochemistry without ever complaining compared to my endless babbling.

Thanks to the TNPRC Necropsy service for their allowing me to participate in necropsies, working with me to finalize protocols, collecting my endless samples and answering all my questions. Necropsy prosectors that worked diligently to collect whole blood and bone marrow were Mr. Maurice Duplantis, Ms. Cristina Polizzi, and Ms. Melinda Martin. Keep up the good work!

Thanks to Dr. Veazey's research laboratory personnel and post-doctorate students for their assistance and friendship: Ms. MaryJane Dodd (research assistant), Ms. Kelsi Rasmussen (research assistant) , Mrs. Janell Leblanc (research assistant), Mrs. Charlene Bartholomae (administrative assistant), and Dr. Linda Green (research faculty coordinator), Dr. Xiaolei Wang (research faculty) and Dr. Huanbin Xu (senior post-doctorate associate). Also in the Department of Comparative Pathology were Additionally were Dr. Bernice Kaack whom showed to always have wonder about what you will learn in a new day and Mrs. Nancy Parr whom kept us all on track being the department secretary and lent me a hot meal and spare bedroom for late nights. All were welcoming to me and offered invaluable technical assistance and life assistance while listening to me often talk to myself and occasionally complain. I am grateful for their patience and support.

Thanks to Dr. David Liu for offering advice when I knocked at his door. He urged me to stay the course for my PhD and finish so that I could study for veterinary pathology boards and be able "to count all my money" some day. He has been a great sounding board for life after a PhD and to be optimistic about new challenges.

Thanks to my "clin path moms" for no matter where I was physically located, I had lots of "moms" watching over me for the past nearly seven years. For the first three years, I had the pleasure of Mrs. Essie Mack, Mrs. Catherine Christensen, Mrs. Natalie Simpson, Ms. Suzanne

Mouch, and Mrs. Cindy Berry all excellent medical technologists at the LSU-SVM Clinical Pathology Laboratory. The last four years I had the pleasure of Mrs. Nancy Hartzog, Mrs. Gail Plauche and Mrs. Robin Sherar also premier medical technologists located at the Tulane National Primate Research Center Clinical Pathology Laboratory. All of these ladies welcomed me into the laboratory and into their lives as both mentors and friends. Not only did these ladies answer endless questions from me about clinical pathology equipment, protocols, and procedures but they kept me aware of the weather, current events, GREAT places to eat, how to be a mom to my kids, and that family and friends are to be savored daily. Most importantly though they were acutely aware of my mental and physical health as only a mom can provide and made sure I ate my veggies and got good rest! I consider myself lucky to have had so many "moms" in such a short time.

Thanks to behind the scenes employees of the TNPRC. In the IT department Ms. Jean Geddis for helping me data mine the TNPRC records, Mrs. Karla Stelly for handling my computer requests, Mr. Steve Coy and Mr. Neil Guillot for fixing my computer problems, and Mrs. Robin Rodriguez for graphic design help at the 12th hour on numerous occasions.

Thanks to my pathology resident mates even though they entered the "darker" side of pathology at the LSU School of Veterinary Medicine. Dr. Andrew David and Dr. Michael Walden were study and office mates through years of rigorous pathology classes and resident training. Dr. Wes Baumgartner joined us later. I got a *real* graduate education with our many discussions about everything under the sun. We kept each other in line when necessary to study and laughing when stressed. I am proud to call ya'll my friends and colleagues. Good luck guys!

Thanks to the Flow Cytometry Core Laboratory at the Tulane National Primate Research Center: Dr. Bapi Pahar, Mrs. Julie Bruhn, Mr.Calvin Lanclos, and Mrs. Desiree Waguespack. I am appreciative of their longsuffering with me during my numerous long flow runs. Even though they always cringed when they saw my name on the run list they were patient and supportive of my work. They never let me down no matter what samples I surprised them with for analysis!

Thanks to the histology department at the LSU School of Veterinary Medicine, Ms. Cheryl Crowder, Mr. Hal Holloway, and Mrs. Kendra Shultz. Thanks to the histology department at the Tulane National Primate Research Center, Mrs. Carol Coyne, Mrs. Junli Huang, and Mrs. Monica Mayer for sectioning and staining tissues . All of these histology technicians were always welcoming of my presence even though I was training as a clinical and not anatomic pathologist. They offered their services and time to me without hesitation or expectation. I appreciate their guidance and support. They always greeted me with a kind word and smile!

Thanks to my LSU School of Veterinary Medicine clinical pathology resident mentors, Dr. Stephen Gaunt and Dr. Jeffrey Sirninger. They were willing to take a chance on a mature (older anyway) with children graduate student eager to learn. These two men trained endlessly with me and showed me how unique we all are yet that we can all work together. I admire their patience and dedication to my growth in clinical pathology. Without their continuous support and guidance I would not be able to write this today!

I would like to acknowledge Dr. Michael Kearney at the LSU-SVM for his contribution to my PhD by SAS analysis. I also acknowledge Dr. Lisa Morici at Tulane University for her contribution to my PhD by performing the cytokine data acquisition and support for preparation,

analysis, and interpretation. I would like to acknowledge Mr. Peter Mottram at the LSU-SVM for his apoptosis IHC staining protocol. I would like to acknowledge Ms. Cecily Conerly and Dr. Xavier Alvarez at the TNPRC for their contribution to tissue staining and confocal microscopy (TNPRC base grant RR00164). I wish to acknowledge Ms. Dot Kuebler for her contribution by performing *in situ* hybridization and frozen sectioning of tissues. I wish to acknowledge Dr. Bapi Pahar and Ms. Terri Rasmussen for providing DNA sense and anti-sense for *in situ* hybridization. I wish to acknowledge Ms. Linda Rogers for performing DNA polymerase chain reaction and her technical support. I wish to acknowledge Dr. Binhua Ling for providing DNA primers for polymerase chain reaction. I wish to acknowledge Dr. Mahesh Mohan for performing quantitative real time polymerase chain reaction and providing RNA primers and his technical support. I wish to acknowledge Dr. Mahesh Mohan for performing quantitative real time polymerase chain reaction and providing RNA primers and his technical support.

Almost last but by no way least, thanks to my wonderfully supportive parents. They have been there for me in my many adventures in school and life without hesitation or questioning. Their love is boundless. I can never repay them for everything they have given me and unselfishly continue to give to me and my family.

Finally, overwhelming thanks to my two children. They have kept me grounded, real, and practical through this journey. They have studied with me in books, articles, and online. They have spent many hours at the LSU School of Veterinary Medicine including the library. They have reminded me to play just as hard as I was studying and teaching. I hope I have showed them how to balance life and go for your dreams. Good luck guys with your graduate studies!

TABLE OF CONTENTS

LIST OF TABLES

LIST OF FIGURES

LIST OF ABBREVIATIONS

AC	activated caspase
AC3	activated caspase 3
AC8	activated caspase 8
ACD	Anemia of chronic inflammatory disease
AIDS	acquired immune deficiency syndrome
AIRD	Anemia of iron deficiency
AmCyan	*Anemonia mohjona* Cyanine
ANOVA	one way analysis of variance
Apaf-1	apoptotic protease-activating factor -1
APC	Allophycocyanin
APCs	antigen presenting cells
APC-Cy7	Allophycocyanin Cyanine 7
ARC	AIDS related complex
ART	anti-retroviral therapy
ASD	advanced SIV disease
ASY	asymptomatic SIV disease
AZT	azidothymidine
β7	βeta7
BFU-E	burst forming unit-erythroid
BFU-Meg	burst forming unit-megakaryocyte
BFU-Meg/E	burst forming unit-megakaryocyte/erythroid
BM	Bone marrow
BMLA	bone marrow lymphoid aggregates
BMMC	bone marrow mononuclear cells
BrdU	bromodeoxyuridine
CBC	complete blood count
CDC	Centers for Disease Control
CFU-B	colony forming unit-B lymphocyte
CFU-Baso	colony forming unit-basophil
CFU-E	colony forming unit-erythroid
CFU-Eo	colony forming unit-eosinophil
CFU-G	colony forming unit-granulocyte
CFU-GEMM	colony forming unit-granulocyte, erythroid, megakaryocyte, monocyte
CFU-GM	colony forming unit-granulocyte, macrophage
CFU-L	colony forming unit-lymphoid
CFU-M	colony forming unit-macrophage
CFU-Mast	colony forming unit-mast cell
CFU-Meg	colony forming unit-megakaryocyte
CFU-MK	colony forming unit-megakaryocyte
CFU-T	colony forming unit-T lymphocyte
CLP	common lymphoid progenitor
CMP	common myeloid progenitor
CM	central memory

CSF-G	Granulocyte Colony Stimulating Factor
CSF-GM	Granulocyte-Macrophage Colony Stimulating Factor
DC	dendritic cells
DCLD	Dendritic Cell-Lymphoid Derived
DCMD	Dendritic Cell-Myeloid Derived
DEPC	diethylpyrocarbonate
DNAse	deoxyribonuclease
DPI	days post-inoculation
dUTP	deoxyuridine-triphosphatase
ED	experimental database(s)
EDTA	ethylenediaminetetraacetic acid
EM	effector memory
ER	endoplasmic reticulum
F	female
FADD	Fas-associated death domains
FGF	Basic Fibroblast Growth Factor
FIHC	Fluorescent immunohistochemistry
FISH	Fluorescent *in situ* hybridization
FITC	fluorescein isothiocyanate
FSC	forward scatter
FSG	fish skin gelatin
GALT	gut associated lymphoid tissue
GM	sum of the marrow granulocyte and monocyte populations or myeloid lineage
GM:MLN	phenotypic lineage ratio
H&E	hematoxylin and eosin
HCT	hematocrit
HIV	human immunodeficiency virus
HSC	hematopoietic stem cells
hpf	high power field
ID	identification
IFN-γ	Interferon gamma
IHC	immunohistochemistry
IL	Interleukin
ILC	immunophenotype lymphocyte count
IMM	inner mitochondrial membrane
IND	indeterminate
INVG	intra-vaginal
IP-10	Interferon Inducible Protein 10
IR	intra-rectal
ISH	*in situ* hybridization
IV	intravenous
K_2EDTA	dipotassium ethylenediaminetetraacetic acid
lpf	low power field
LH	Lymphoid hyperplasia
LNIHC	lineage negative immature hematopoietic cells

LT-HSC	long-term culture hematopoietic stem cells
LTBMC	long term bone marrow culture cells
M	male
M. avium	*Mycobacterium avium*
M:E	myeloid (granulocytic/monocytic lineage) to erythroid lineage
MANOVA	repeated measures of analysis of variance
MCH	mean cell hemoglobin
MCHC	mean cell hemoglobin concentration
MCV	mean cell volume
MCP-1 (MCAF)	Monocyte Chemotactic Protein 1 or CCL2 or Monocyte Chemotactic and Activating Factor
mDC	Myeloid dendritic cells
MIP-1α	Macrophage Inflammatory Protein 1 alpha or CCL3
MIP-1β	Macrophage Inflammatory Protein 1 beta or CCL4
MLN gate	marrow multilineage gate
Mod	moderate
NA	not analyzed
Neg	negative
NK	natural killer
NBT-BCIP	nitro blue tetrazolium chloride/5-Bromo-4-chloro-3-indolyl phosphate
NGS	normal goat serum
NP	not performed
NS	not significant
NSF	no significant lesions found
OI	opportunistic infections
OMM	outer mitochondrial membrane
p	p value
PacBlue (PacBl) (PB)	Pacific Blue
PAS	Periodic Acid Schiff
PBMC	peripheral blood mononuclear cells
PBS	phosphate buffered saline
PCR	polymerase chain reaction
pDC	plasmacytoid dendritic cells
PDGF	Platelet Derived Growth Factor dimer BB
PerCP	Peridinin Chlorophyll Protein
PerCP-Cy5.5	Peridinin Chlorophyll Protein Cyanine 5.5
PE	Phycoerythrin
PE-Cy5	Phycoerythrin Cyanine 5
PE-Cy7	Phycoerythrin Cyanine 7
PE-Tx RED or PE-TxR	Phycoerythrin Texas Red
PHA	phytohemagluttinin
PeLT	peripheral lymphoid tissue
PMA	phorbol 12-myristate 13-acetate
Q	quadrant(s)
QDOT655	Quantum dots 655

qRT-PCR	quantitative real time polymerase chain reaction
RANTES	Regulated upon Activation, normal T cell Expressed and Secreted or CCL5
RIP	receptor interactive protein
RM	Rhesus macaques
SD	standard deviation
SEM	standard error of the mean
SIV	simian immunodeficiency virus
SSC	side scatter
1X SSC	sodium citrate
ST-HSC	short-term culture hematopoietic stem cells
TBS	tris buffered saline
TCP	thrombocytopenia
TDEM	terminally differentiated effector memory
Tdt	terminal deoxynucleotidyl transferase
TNF-α	Tumor Necrosis Factor alpha
TNFR	TNF-α may bind TNF receptors
TNPRC	Tulane National Primate Research Center
TRADD	TNFR-associated death domains
TUNEL	terminal deoxynucleotidyl transferase deoxyuridine-triphosphatase nick end labeling
VEGF	Vascular Endothelial Growth Factor
vs.	versus
WB	whole blood
WBC	white blood cell

ABSTRACT

CD4+ memory T cells are depleted in mucosal tissues post human immunodeficiency virus (HIV) and simian immunodeficiency virus (SIV) infection without restoration to pre-infection levels during progressive course of disease. Bone marrow (BM) as a hematopoietic organ has been investigated for hematologic and morphologic changes during HIV infection. However, BM as a primary lymphoid tissue during HIV infection has been poorly characterized. We proposed BM was also a site of CD4+ T cell depletion driven by increased apoptosis during progressive HIV disease. We chose to investigate bone marrow changes using the premier non-human primate Rhesus macaque SIV model for the study HIV infection.

We observed hematologic abnormalities of anemia, thrombocytopenia, neutropenia and eosinophilia during SIV infection mimicked HIV infection as did morphologic increased BM cellularity, loss of iron marrow storage, and increased marrow fibrosis as infection advanced to AIDS. The increased BM cellularity was characterized by increased erythroid, myeloid including dendritic cells, and lymphoid lineages in the later stages of infection. In fact, numbers of BM CD3+ T lymphocytes increased in absolute numbers and proliferation percentage during progressive SIV infection mainly composed of CD8+ T cells and fewer CD4+ T cells. Naïve and memory CD8+ T cells and CD4+ T cells were maintained in BM during SIV infection. Low numbers of SIV infected BM cells were observed including CD3+ T cells, macrophages, and other hematopoietic cells with detection of both viral RNA and DNA by polymerase chain reaction. However, less than 0.2% of CD3+ BM T cells were apoptotic determined by activated caspase 3 though overall BM cells tended to have increased rates of apoptosis in later stages of SIV. Our data revealed BM T cells were not depleted but maintained to increased during SIV disease without an increase in apoptosis. Future studies into mechanisms of bone marrow

lymphocyte maintenance may reveal homeostatic mechanisms potentially disrupted in mucosal tissues during HIV and SIV infection.

CHAPTER 1: INTRODUCTION AND SIGNIFICANCE

RATIONALE AND SIGNIFICANCE

HIV is a worldwide epidemic in the 21st century. The HIV epidemic has been characterized as the 'worst' epidemic in the history of humankind (Volberding 2003). Numerous global resources have been extended into education, treatment, and prevention of HIV disease and acquired immune deficiency syndrome (AIDS), yet new infections continue in adult and pediatric populations. The complex mechanisms of chronic immune stimulation accompanied by immune dysregulation during progressive HIV infection and ongoing replication still elude the scientific community after many years of stellar research. How the bone marrow is woven into the intricate and detailed pathogenesis of HIV remains unexplored in HIV infection. This body of research was to investigate the bone marrow as a lymphoid organ during progressive SIV infection for a model of changes in bone marrow of HIV infected patients. It is unclear how HIV disease works in this body compartment.

The bone marrow (BM) or marrow is a primary lymphoid organ and lymphocyte compartment or tissue of the body (Jain 1986; Paraskevas 2004; Tizard 2004). Primary lymphoid organs develop early in the fetus, produce immature lymphocytes, and allow maturation of lymphocytes independent of antigen stimulation (Jain 1986; Paraskevas 2004; Tizard 2004). Early T cell lymphoid progenitors leave the bone marrow and migrate to the thymus for differentiation into CD4+ and CD8+ lymphocytes whereas early B cell lymphoid progenitors remain in the bone marrow to differentiate into immature naïve B lymphocytes (Jain 1986; Paraskevas 2004; Tizard 2004).

It is estimated that billions of lymphocytes migrate through the bone marrow daily even though it is only fed by the blood vascular circulation and not the lymphoid circulation(Wei

2006). Homeostatic mechanisms exist within the bone marrow to protect levels of CD4 and CD8 resident lymphocytes. Basal homeostatic proliferation (BHP) is an inherent function of T memory cells to self-renew under non-antigenic conditions (Nugeyre 2003). Homeostatic bone marrow regulation is mostly controlled by the colony stimulating factors (Doweiko 1993).

PURPOSE OF THE STUDY

The objective of this research was to investigate the role of the bone marrow as a primary and extra-thymic lymphoid tissue in the replenishment of CD4+ lymphocytes during HIV infection. CD4+ lymphocyte depletion in HIV occurs predominantly in mucosal lymphoid tissues during HIV and SIV infection but particularly in early and late stages, corresponding with high viremia (Veazey 2000b). During infection, mucosal and peripheral depletion of activated memory CD4+ lymphocytes is ongoing without return to pre-infection levels (Veazey 2000). The bone marrow may contribute to the repression of CD4+ lymphocytes during HIV infection; however, the CD4+ lymphocyte pool in the bone marrow lymphoid compartment has been poorly characterized.

Examination and comparison of the bone marrow as a lymphoid compartment could determine the extent of CD4+ lymphocyte depletion that is attributed to lack of production, turnover, and lymphocyte homing, as compared to rates of destruction in secondary lymphoid tissues such as lymph nodes, gut, and blood during progressive infection. Additionally, examining bone marrow during progressive disease could determine and define possible disruptions of bone marrow homeostasis in relation to CD4+ lymphocyte depletion in this compartment.

SPECIFIC AIMS

Hypothesis

The hypothesis is ongoing apoptosis of CD4+ lymphocytes within the BM lymphocyte compartment during progressive SIV, despite low numbers of SIV infected cells in the bone marrow, contributes to BM exhaustion of CD4+ lymphocytes due to loss of BM homeostasis. The following represents a logical analytical approach for addressing our hypothesis and for describing the changes that occur in this compartment throughout SIV infection.

Research Model

All research was conducted at the Tulane National Primate Research Center (TNPRC) using Rhesus macaques (RM) for the animal model of HIV disease. All animals were housed and treated according to the Animal Welfare Act and Guide for the Care and Use of Laboratory Animals, Institute of Laboratory Resources National Research Council. All protocols and research procedures were approved by the Tulane Institutional Animal Care and Use Committee. TNPRC is accredited by the Association for Assessment and Accreditation of Laboratory Animal Care. Four experimental database(s) (ED) of research subjects were utilized as defined in Appendix II as ED I-EDIV.

Specific Aim 1 (Chapter 3)

The objective was to validate the SIV model for study of bone marrow changes during HIV infection. Marrow derived hematopoietic cells circulate in blood. Hematologic values are interpreted by reported laboratory parameters from the complete blood count (CBC) as below or above the reference interval or reference range values for evidence of hematologic abnormalities. First, the occurrence of hematologic abnormalities during progressive, non-treated SIV infection in the Rhesus macaque was determined and compared to reported hematologic abnormalities

during HIV infection for confirmation of similarities. Second, the impact of SIV disease on circulating cells was established to confirm the effect of SIV on bone marrow derived hematopoietic cells without confounding effects of intervention by therapeutic drugs or vaccinations, inadequate diet, or co-infections.

Specific Aim 2 (Chapter 4)

The objective was to validate the SIV model for occurrences of BM disruption or loss of homeostasis in HIV infection. The occurrence of morphologic and histologic changes during progressive, non-treated SIV infection in the Rhesus macaque was determined and compared to reported abnormalities during HIV infection for confirmation of similarities. Marrow cellularity, marrow iron storage, and marrow fibrosis were evaluated for alteration during periods of SIV infection.

Specific Aim 3 (Chapter 5 and Chapter 6)

The objective was to determine the shifts of hematopoietic lineage populations, lymphocyte populations, and dendritic cell populations in BM during progressive, non-treated SIV infection in the Rhesus macaque. Flow cytometry analysis of bone marrow was performed to identify percentage shifts of hematopoietic cells during periods of SIV infection.

Specific Aim 4 (Chapter 7)

The objective was to determine the number and phenotype of SIV infected cells in the BM during progressive, non-treated SIV infection in the Rhesus macaque for comparison with changes in tissue lymphocyte populations and plasma viral loads. *In situ* hybridization and polymerase chain reaction were performed to reveal SIV infected cells in marrow.

Specific Aim 5 (Chapter 8)

The objective was to determine changes in naïve, memory, and activated $CD4^+$ lymphocyte numbers in the BM lymphocyte compartment during progressive, non-treated SIV infection in the Rhesus macaque to identify the degree of $CD4^+$ lymphocyte bone marrow exhaustion. Flow cytometry and morphometric analyses were performed on marrow tissue and blood to calculate absolute numbers of lymphocytes during various periods of SIV infection.

Specific Aim 6 (Chapter 9)

The objective was to determine percentages of apoptotic and proliferating $CD4^+$ BM lymphocytes during progressive, non-treated SIV infection in the Rhesus macaque. Apoptosis was defined by flow cytometry and immunohistochemistry and correlated with the changes in the CD3+ lymphocyte bone marrow compartment and levels of pro-apoptotic cytokines, as a mechanism for CD4+ bone marrow lymphocyte loss.

REFERENCES

Doweiko, J.P. (1993). Hematologic aspects of HIV infection. AIDS (London, England) *7*, 753-757.

Jain, N.C. (1986). The Lymphocytes and Plasma Cells. In Schalm's Veterinary Hematology (Philadelphia, PA, Lea and Febiger), pp. 790-820.

Nugeyre, M.T., Monceaux, V., Beq, S., Cumont, M.C., Ho Tsong Fang, R., Chene, L., Morre, M., Barre-Sinoussi, F., Hurtrel, B., and Israel, N. (2003). IL-7 stimulates T cell renewal without increasing viral replication in simian immunodeficiency virus-infected macaques. J Immunol *171*, 4447-4453.

Paraskevas, F. (2004). Lymphocytes and Lymphatic Organs. In Wintrobe's Clinical Hematology, J. Greer, J. Foerster, J.N. Lukens, G.M. Rodgers, F. Paraskevas, and B. Glader, eds. (Philadelphia, Lippincott Williams & Wilkins), pp. 410-438.

Tizard, I.R., and Schubot, R.M. (2004). Organs of the Immune System. In Veterinary Immunology: An Introduction, T. Merchant, ed. (Philadelphia, PA, Saunders), pp. 78-91.

Veazey, R.S., Tham, I.C., Mansfield, K.G., DeMaria, M., Forand, A.E., Shvetz, D.E., Chalifoux, L.V., Sehgal, P.K., and Lackner, A.A. (2000). Identifying the target cell in primary simian immunodeficiency virus (SIV) infection: highly activated memory CD4(+) T cells are rapidly eliminated in early SIV infection in vivo. Journal of virology *74*, 57-64.

Volberding, P.A., Baker, K.R., and Levine, A.M. (2003). Human immunodeficiency virus hematology. Hematology Am Soc Hematol Educ Program, 294-313.

Wei, S., Kryczek, I., and Zou, W. (2006). Regulatory T cell compartmentalization and trafficking. Blood.

CHAPTER 2: BACKGROUND AND LITERATURE REVIEW

RETROVIRUSES

Equine infectious anemia, feline immunodeficiency virus, SIV, and HIV are lentiviruses in the *Retroviridae* family of retroviruses (Goff 2001). Lentiviruses have a bar or cone shaped nuclear core which is distinct among the retroviruses (Apetrei 2004). The HIV virus and life cycle are detailed in Figure 2.1 (National Institute of Allergy and Infectious Disease).

A. **B.**

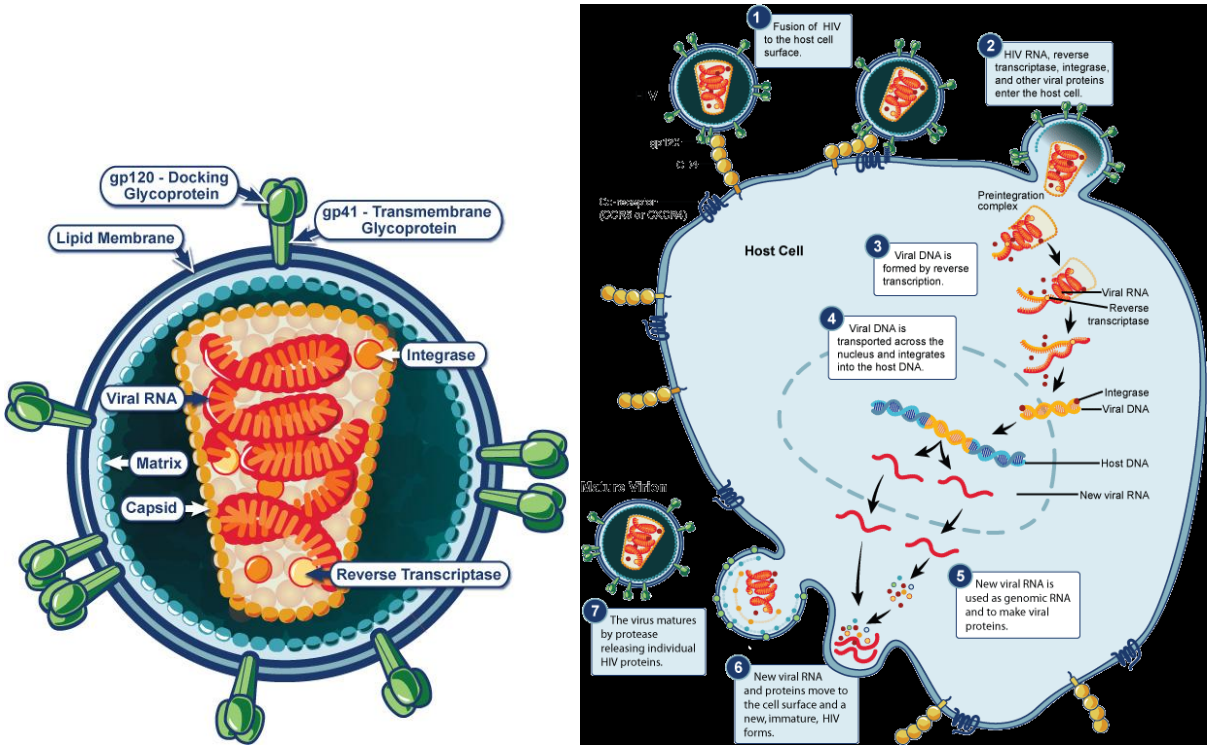

Figure 2.1. HIV virus
Schematic representation of the HIV and SIV virus particle (**A.**) (HIV virus from National Institute of Allergy and Infectious Disease http://www.niaid.nih.gov/topics/HIVAIDS/Understanding/Biology/Pages/structure.aspx.). Schematic representation of the HIV and SIV retrovirus life cycle (**B.**) (HIV life cycle from National Institute of Allergy and Infectious Disease http://www.niaid.nih.gov/topics/HIVAIDS/Understanding/Biology/Pages/hivReplicationCycle.aspx.).

SIV AND HIV INFECTION AND DISEASE

A concise review of the discovery of HIV and SIV has been previously reported (Gardner 1993; Lifson 1988). Three viral inoculations were used in our study of SIV and are their origin are briefly detailed here.

SIVmac251 is a wildtype strain of SIV that originated from the RM with the same name at the New England Regional Primate Research Center. Mm78-72 had retorbital lymphoma and tissue from this monkey was inoculated into macaque Mm 251-79 (Gardner 1996; Letvin 1985). Mm251-79 developed AIDS and the simian T-lymphotrophic virus type III (later reclassified as SIV) was isolated from this RM (Letvin 1985). STLV III isolated from Mm 251-79 was grown in cultures of human T cells (Daniel 1985; Letvin 1985). RM inoculated with STLV III virus isolated from Mm251-179 progressed to AIDS (Letvin 1985).

SIVB670 is a wildtype strain of SIV that originated from the RM with the same name at the Delta Regional Primate Research Center (now call the TNPRC). Lymph node tissue taken at necropsy from Macaque B670 was the source of SIV/DeltaB670 or SIVB670 (Baskin 1986; Gardner 1996; Murphey-Corb 1986). Macaque B670 was inoculated with lymphoma cells isolated from macaque 8664 (Baskin 1986; Murphey-Corb 1986). Macaque 8664 had been inoculated with *Mycobacterium leprae* isolated from Sooty mangabey A022 (Baskin 1986; Murphey-Corb 1986). Macaques inoculated with SIVB670 progressed to AIDS (Murphey-Corb 1986)

SIVmac239 is a molecular clone that originated from the RM with the same name at the New England Regional Primate Research Center Mm239-82 was inoculated with cell-free plasma from Mm61-82 and died 85 days post-inoculation (Daniel 1985). STLV III was recovered from the blood of Mm239-82 (Daniel 1985). Mm61-82 was inoculate with pooled

blood samples from 3 of 7 macaques that had been inoculated with lymphoma tissue from Mm251-79 (Daniel 1985). All inoculated animals had signs of immunodeficiency at necropsy (Daniel 1985).

SIV is a premier model for the study of HIV (Gardner 1993). Mucosal memory CD4+ T cell depletion is the hallmark of acute SIV infection in RM (Lay 2009; Veazey 2000; Walker 2004). Although an increase in proliferating CD4+CCR5+ cells may be observed in progressive SIV disease in blood, mucosal CD4+CD195+ cells are never replenished in patients that progress to disease, likely because they are unable to compete with continued loss of this cell population (Walker 2004). With continual depletion of CD4+ memory cells in the absence of proliferation, the body is unprotected against opportunistic invaders (Walker 2004). Modeling of acute SIV infection in RM and sooty mangabeys revealed lymphoid compartments with highest numbers of the cell populations susceptible to infection along with the highest viral production rate of each infected cell will drive peak viral load (Lay 2009).

T LYMPHOCYTES IN LYMPHOID ORGANS

The primary lymphoid tissues are bone marrow and thymus (Feuerer 2003; Pabst 2007), since a functioning bone marrow and thymus are needed for T cell lymphopoiesis. Bone marrow serves as a secondary lymphoid tissue in addition to its role as primary lymphoid tissue. Naïve T cells transferred into host mice were found one day after transfer in bone marrow, spleen, and lymph nodes but not thymus (Feuerer 2003). Bone marrow DC were observed to act as antigen presenting cells to naïve BM CD4+ and CD8+ T lymphocytes and induce T cell proliferation and differentiation in mice (Feuerer 2003). Other secondary lymphoid tissues are lymph nodes, spleen, tonsils, and intestinal Peyer's patches (Pabst 2007).

Mouse studies indicate that uncommitted lymphocyte/myeloid precursors leave the bone marrow and enter the thymus for T cell/NK cell development (Spits 2002). The daily output by the thymus of T cells in the RM is estimated to be 2-3X10^8 cells which is higher than compared in the humans estimated to be 10^8 cells (Borghans 2005). With age, thymic involution occurs where thymic tissue is replaced with fat, and decreases in function, but thymopoiesis still occurs (Spits 2002). Volume and size of the thymus compared to body weight is relatively stable with age (Pabst 2007). Thymic output appears to be related to the bone marrow pool of thymic precursors and functional thymic parenchyma (Nikolich-Zugich 2007).

The T cell pool is fairly consistent in 'normal' individuals under the control of homeostatic regulation considering age as a factor (Surh 2005). Single positive T cells are released from the thymus as 'naïve' or non-antigen stimulated (Lackner 2007; Tizard 2004). Naïve T cells circulate in the blood and to secondary lymphoid sites (Obhrai 2006; Tizard 2004). Once naive T cells are activated, differentiation into effector T cells occurs with the ability to enter non-lymphoid tissues (Obhrai 2006; Tizard 2004). Many effector T cells undergo apoptosis but remaining long-lived central memory cells can be found within lymphoid and non-lymphoid tissues (Obhrai 2006).

Naïve T cells that encounter antigen become short-lived effector memory T cells and long-lived central memory T cells (Paraskevas 2004; Lackner 2007). Naïve T cells home to lymphocyte compartments or lymphoid tissues (Paraskevas 2004). Memory proliferation in response to antigen allows daughter cells to expand and differentiate into "secondary" effector cell populations (Paraskevas 2004; Kaech 2002). Activated T cells undergo programmed cell death after immune stimulation. During the contraction stage or death stage, large numbers (>90%) of effector T cells made after contact with antigen are eliminated (Douek 2003; Kaech

2002). The effector T cells that survive the death stage move into the long-lived memory T cell stage (Douek 2003; Kaech 2002). Effector memory cells lose lymph node homing capabilities but are able to produce greater levels cytokines for Th responses (Lanzavecchia 2002). In contrast, central memory cells retain lymph node homing capabilities but produce perforin and lesser levels of restricted cytokines for immune response (Lanzavecchia 2002). CD4+ T cells can follow a linear progression from naïve cell to effector memory to central memory cells, but central memory cells may also be generated from earlier activated T cells (Obhrai 2006; Sallusto 2004). Homeostasis of memory cells occurs by slow division of long-lived memory cells for maintenance of the clonal cell line (Lanzavecchia 2002; Sallusto 2004). Memory homeostatic or "self-renewal" proliferation occurs but is mechanistically different from antigenic "pluripotent" memory proliferation (Kaech 2002).

T CELLS AND BONE MARROW

Athymic and nude mice are T cell deficient with normocellular BM, an arrest of granulocytic immature myeloid cells, lymphopenia, low numbers of marrow erythroblasts, and normal concentrations of blood monocytes and platelets (Monteiro 2005). In studies of T cell deficient mice by Montiero et al., reconstitution of these mice with fetal thymic grafts or CD4+ T cells allowed maturation of the granulocytic cells and restoration of circulating and bone marrow lymphocytes, though erythroid precursors were not affected, which was attributed to the presence of activated CD4+ BM cells (Monteiro 2005). However, Montiero et al. did not find CD8+ T cells to restore granulocytes and lymphocytes to T cell deficient mice (Monteiro 2005). Montiero et al. suggested CD4+ T cell depletion during HIV may lead to neutropenia and disruption of hematopoiesis in bone marrow (Monteiro 2005). Di Rosa et al. proposed BM has a role in maintenance of naïve and memory T cells and that BM may have a role in restoring BM

function in periods of loss of BM steady state (Di Rosa 2009). Development of hematopoietic cells is under the influence of a complex microenvironment involving interactions of multitudes of growth factors, cytokines, chemokines, stromal cells and non-stromal cells, and stromal support.

HEMATOPOIESIS

Hematopoiesis is the development of cells found in blood and tissue from a pluripotent hematopoietic stem cell within the bone marrow (BM) environment (Bondurant 2004; Gasper 2000; Huang 2007; Scott 2008a; Travlos 2006). The bone marrow environment is identified within the medullary cavity of long bones and axial bones (Travlos 2006). Hematopoiesis is maintained in flat bones as mammals age (Gasper 2000). The medullary cavity consists of blood vessels, stromal tissue, and multiple lineages of cells (Scott 2008b). BM mesenchymal stem cells are approximately 0.01-0.0001% of total BM nucleated cells (Dazzi 2006). Adipose tissue is part of the normal stroma or supportive BM tissue (Scott 2008b). Large amounts of adipose tissue in BM imparts a 'yellow' color and is referred to 'yellow marrow' in contrast to 'red marrow' where BM is composed of mostly hematopoietic tissue (Scott 2008b; Stasney 1936). As hematopoiesis increases density of cells, adipose tissue decreases by resorption to allow the space occupying mass of cells (Gurkan 2008). Hematopoiesis occurs within defined areas of the medullary cavity described as niches. The niche comprises supportive cells and signals to support HSC populations and provide necessary signals for differentiation and maturation (Wagers 2005).

One niche of bone marrow is the osteoblastic, bony, or endosteal niche of bone marrow (Calvi 2003; Huang 2007; Jung 2005; Sacchetti 2007; Wagers 2005). Osteoblasts are found within and upon bone endosteum or lining of bony surfaces (Travlos 2006). Osteoblasts are

mesenchymal bone marrow cells that regulate bone production. Another important osteoblast function is to provide support for hematopoietic stem cells (HSC) by increasing numbers of long term hematopoietic stem cells (LT-HSC) as proven in transgenic mice (Calvi 2003; Huang 2007; Zhang 2003). Increased numbers of LT-HSCs in mice were observed at 76% within the marrow cavity and 24% at the bone surface with the majority in the cancellous or trabecular bone surface including the epiphysis and metaphysis, and the remaining dispersed at the endosteal surface of the diaphysis or long bone (Travlos 2006; Zhang 2003).

Another niche of bone marrow is the vascular niche of sinusoidal endothelium (Huang 2007; Kiel 2005). Components of the vascular niche including endothelial and other associated mesenchymal cells support HSC differentiation (Huang 2007; Kiel 2005; Wagers 2005). In long bone, a specific vascular system is present (Dazzi 2006; Gurkan 2008; Travlos 2006; Zhang 2003). A nutrient artery enters the long bone feeding the central artery. The central artery branches into radial arteries toward the inner lining of the bone (endosteum) where it forms sinuses and sinusoids. The sinuses and sinusoids are drained into the central vein or central sinus which is located in the center of the bone. The central vein exits bone by the nutrient vein. Blood flow is from the center nutrient artery toward the peripheral bone into sinuses then back into the central vein again. The majority of blood vessels are distributed closer to the endosteal bone. Hematopoiesis occurs mostly in the vascular rich regions of bone marrow. Even though bone marrow has an intricate network of vessels, this organ is not drained by lymphatic vessels despite BM being a primary lymphoid organ (Di Rosa 2005; Travlos 2006).

Long term culture hematopoietic stem cells (HSC) can self renew and gives rise to short term culture hematopoietic stem cells (ST-HSC) that cannot further self renew or differentiate into stem cells (Huang 2007; Wagers 2005). The ST-HSC are pluripotent stem cells that under

direct intracellular and extracellular signals differentiate into a common myeloid progenitor (CMP) or common lymphoid progenitor (CLP) (Figure 2.2). The CMP is influenced by the cytokine colony forming unit-granulocyte, erythroid, megakaryocyte, monocyte (CFU-GEMM) while the CLP is directed by the cytokine colony forming unit-lymphoid (CFU-L). Precursor cells include the following groups: mitotically active dividing cells, immature and mature post-mitotic cells, and storage pools of cells (Gasper 2000).

The CLP cells further differentiates into B lymphocyte, T lymphocyte, natural killer (NK) cell, and dendritic cell progenitors. B lymphocyte progenitors remain in the bone marrow and become immature B cells, then migrate to other lymphoid organs of spleen or lymph node to develop into active or memory B cells including plasma cells. T lymphocyte progenitors leave the bone marrow to enter the thymus as early thymic progenitors for differentiation into CD4+ T cells, CD8+ T cells, T regulatory CD4+CD25+ T cells, and γδ T cells.

The CMP further differentiates into myeloid cells including erythrocytes, megakaryocytes, monocytes, neutrophil, eosinophils, and basophils in bone marrow. Monocytes differentiate into macrophages within tissue. Mast cell precursors leave the bone marrow and differentiate into mature mast cells in tissue. DC, from myeloid progenitors, differentiate in the tissue. Erythroid lineage is referred to with the prefix '*rubri*' in veterinary medicine instead of 'erythro' or 'normo' in humans (Scott 2008b). Erthropoiesis occurs in erythroblastic islands while megakaryocytopoiesis occurs near endothelium, and granulocytopoiesis occurs in less defined areas (Travlos 2006). Evaluation of bone marrow can be performed by multiple methods and has been reviewed (Bolliger 2004; Cotelingam 2003; Grindem 2002; Huser 1970; Travlos 2006). Bone marrow aspiration or cytology, bone marrow biopsy or histopathology, and flow cytometry may be utilized to obtain information about the status of hematopoiesis. In

Figure 2.2. Bone marrow hematopoiesis

Schematic representation of bone marrow hematopoiesis as defined in the text. (Bondurant 2004; Gasper 2000; Scott 2008a; Travlos 2006).

BFU-E	burst forming unit-erythroid
BFU-Meg	burst forming unit-megakaryocyte
BFU-Meg/E	burst forming unit-megakaryocyte/erythroid
CFU-B	colony forming unit-B lymphocyte
CFU-Baso	colony forming unit-basophil
CFU-E	colony forming unit-erythroid
CFU-Eo	colony forming unit-eosinophil
CFU-G	colony forming unit-granulocyte
CFU-GEMM	colony forming unit-granulocyte, erythroid, megakaryocyte, monocyte
CFU-GM	colony forming unit-granulocyte, macrophage
CFU-L	colony forming unit-lymphoid
CFU-M	colony forming unit-macrophage
CFU-Mast	colony forming unit-mast cell
CFU-Meg	colony forming unit-megakaryocyte
CFU-MK	colony forming unit-megakaryocyte
CFU-T	colony forming unit-T lymphocyte
DCLD	Dendritic Cell-Lymphoid Derived
DCMD	Dendritic Cell-Myeloid Derived
HSC	hematopoietic stem cells
NK	natural killer cell

Figure on next page.

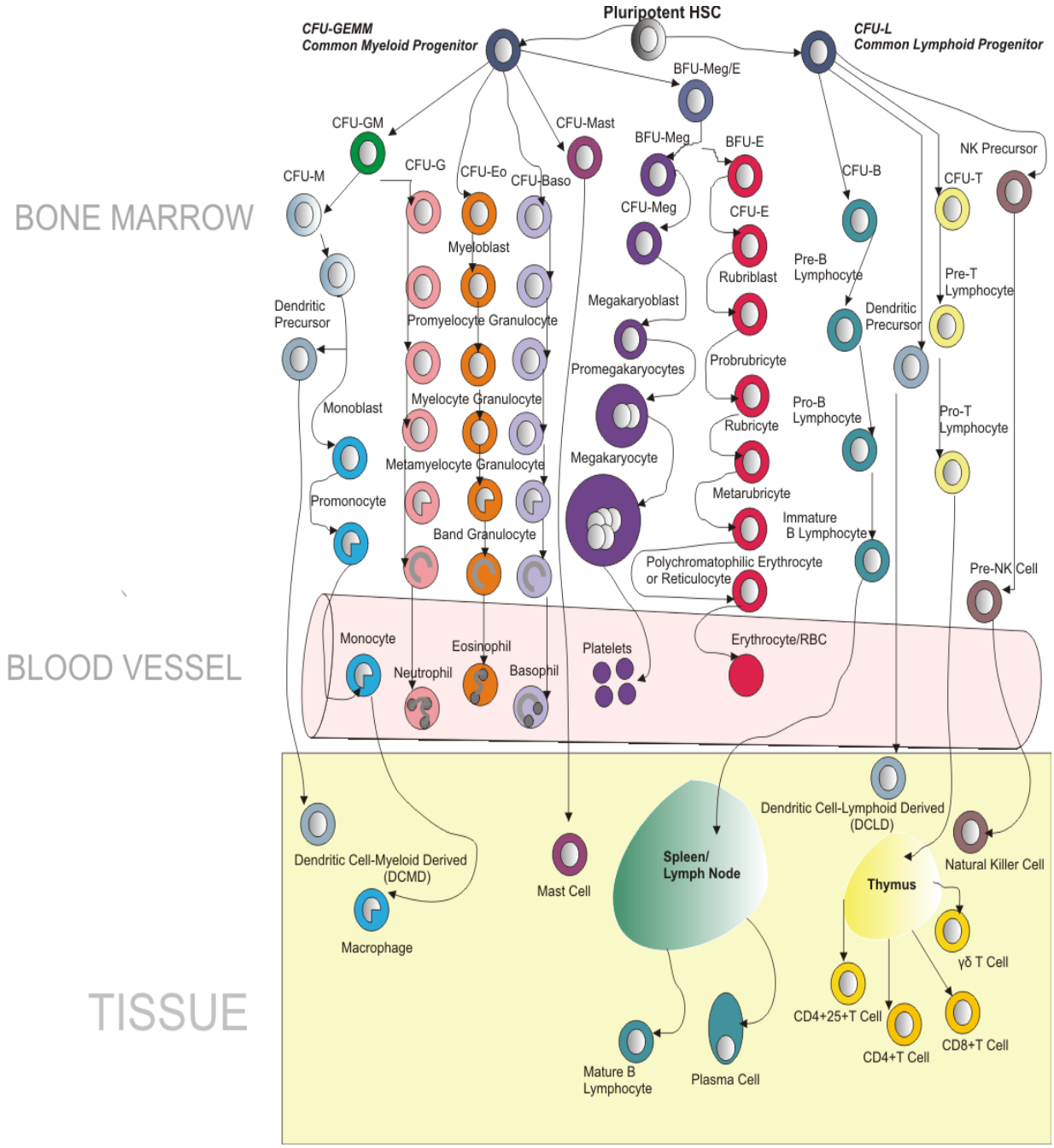
BONE MARROW
BLOOD VESSEL
TISSUE
Pluripotent HSC
CFU-GEMM
Common Myeloid Progenitor
CFU-L
Common Lymphoid Progenitor
BFU-Meg/E
CFU-GM
CFU-Mast
BFU-Meg
BFU-E
NK Precursor
CFU-M
CFU-G
CFU-Eo
CFU-Baso
CFU-Meg
CFU-E
CFU-B
CFU-T
Myeloblast
Rubriblast
Pre-B Lymphocyte
Pre-T Lymphocyte
Dendritic Precursor
Promyelocyte Granulocyte
Megakaryoblast
Dendritic Precursor
Promegakaryocytes
Probrubricyte
Myelocyte Granulocyte
Monoblast
Rubricyte
Pro-B Lymphocyte
Pro-T Lymphocyte
Megakaryocyte
Metamyelocyte Granulocyte
Promonocyte
Metarubricyte
Immature B Lymphocyte
Band Granulocyte
Polychromatophilic Erythrocyte or Reticulocyte
Pre-NK Cell
Monocyte
Eosinophil
Platelets
Erythrocyte/RBC
Neutrophil
Basophil
Dendritic Cell-Lymphoid Derived (DCLD)
Dendritic Cell-Myeloid Derived (DCMD)
Natural Killer Cell
Mast Cell
Spleen/ Lymph Node
Thymus
Macrophage
γδ T Cell
CD4+25+T Cell
CD4+T Cell
CD8+T Cell
Mature B Lymphocyte
Plasma Cell

conjunction with direct evaluation of bone marrow, the peripheral blood should also be examined to define changes noted in BM hematopoiesis.

Bone marrow histopathology can define the architecture of tissue and megakaryocyte numbers but cell identification is more difficult (Scott 2008b). The myeloid (granulocytic/monocytic lineage) to erythroid lineage (M:E) ratio is a quantitative, calculated, yet only semi-quantitative or subjective assessment of the granulocytic/monocytic myeloid lineage to erythroid lineage. The M of the M:E ratio refers to non-erythroid myeloid cells including granulocytic and monocytic lineages and occasionally megakaryocytic lineages (Scott 2008b). Therefore, the M:E is a misnomer since the erythroid lineage is also of myeloid descent and is not included in the 'M' aspect (Scott 2008b). The M:E ratio may or may not encompass numbers of megakaryocytes, also myeloid cells, present of which the megakaryocytes can be easily identified by their characteristic large size and multi-lobed nuclei (Travlos 2006). Neither does the M:E ratio account for mast cells and macrophages, of myeloid lineage, nor lymphoid cells as expected by the name myeloid (Scott 2008b). Thus much more careful and less subjective assessments of cells and phenotype is necessary to assess the impact of an infection or other condition in bone marrow.

APOPTOSIS PATHWAY

Mechanisms of failure of bone marrow to support orderly and effective hematopoiesis in HIV infection are not know, but could be from either direct viral destruction, bystander apoptosis, pronounced bystander apoptosis from T lymphocytes/monocytes/macrophages/megakaryocytes, a suppressive cytokine milieu, and/or loss of stromal cell structure (Isgro 2005). Our hypothesis is immature BM CD4+ T lymphocytes are lost through apoptosis during progressive SIV disease.

Caspases are involved in apoptosis by an endoplasmic reticulum (ER) disruption pathway, ligand-mediated or death domain pathway, and a mitochondrial pathway (Elmore 2007; Gupta 2007). Activated caspase 3 is a late pathway effector or 'executioner' caspase involved in all three pathways (Figure 2.3) (Elmore 2007; Gupta 2007). Activation of caspase 3 leads to degradation of DNA and cytoskeletal proteins leading to formation of apoptotic bodies (Elmore 2007).

Endoplasmic reticulum mediated apoptosis is induced by alterations to protein processing or the ER calcium pool (Gupta 2007). Protein processing in the ER includes post-translational changes, folding, and sorting, and a disruption of normal processing may induce apoptosis (Gupta 2007). Calcium dysregulation within the ER can lead to and induce apoptosis (Gupta 2007). The highest amount of intracellular calcium is within the ER where concentrations are 10,000 fold-lower than cytosolic ER concentrations (Gupta 2007). Also, disturbances leading to shift of the ER calcium pool (higher or lower) may induce apoptosis (Gupta 2007). ER disruption can directly activate the caspase system involved in apoptosis (Dong 2006). Though controversial, in humans, caspase 12 appears to be the first activated caspase (Dong 2006). The Bcl2 family appears to be involved in ER disruption induced apoptosis (Szegezdi 2006). Additionally, stress imposed upon the ER can sends signals to the mitochondria and may trigger mitochondrial apoptosis (Szegezdi 2006). Caspases involved in ER disruption induced apoptosis include 3,4,6,7,8,9, and 12 (Szegezdi 2006). Gupta and Gollapudi observed in thapsigargi-induced apoptosis that activation of the ER disruption pathway through increased calcium, CD8+ T cells were induced into apoptosis. Naïve CD8+ T cells and CD8+ central memory T cells were more sensitive to apoptosis than CD8+ effector memory T cells by ER stress activation (Gupta 2007).

TNF-α ligand binding and CD95 ligand binding both may induce ligand-mediated or death receptor pathways (Gupta 2007). TNF-α may bind TNF receptors (TNFR) which activate the adapter protein TNFR-associated death domains (TRADD) which in turn activate Fas-associated death domains (FADD) which in turn activates caspase 8 (Gupta 2007; Hurtrel 2005). TRADD may activate other adapter proteins, TNFR-associated factor 2 and receptor interactive protein (RIP) that lead to stimulation of MAP kinase (apoptosis inducer or inhibitor) and NF-κB (apoptosis inhibitor) that in turn upregulate transcription factors to inhibit or stimulate apoptosis (Gupta 2007). Gupta and Gollapudi observed in TNF-α induced apoptosis with activation of the death domain pathway, T cells responded differently. Naïve CD8+ T cells and CD8+ central memory T cells were observed to undergo apoptosis while CD8+ effector memory T cells were observed to be resistant to apoptosis by death domain activation (Gupta 2007).

Mitochondrial mediated apoptosis is induced by changes to either the outer mitochondrial membrane (OMM) or inner mitochondrial membrane (IMM) (Gupta 2007). Stress to the cell leading to breach of the OMM allows leakage of cytochrome *c*, apoptosis-inducing factor, some pro-caspases, and other molecules from the intermembrane space (Gupta 2007). The OMM contains anion channels that are voltage dependent along with Bcl-2 found on the IMM which are involved in maintenance of the mitochondrial membrane potential(Gupta 2007). Cytochrome *c* when free in the cytoplasm can bind an adapter protein apoptotic protease-activating factor -1 (Apaf-1) (Gupta 2007). Pro-caspase 9 is activated without cleavage in the presence of ATP/dATP (Gupta 2007). Gupta and Gollapudi observed in H_2O_2 induced apoptosis with activation of the mitochondrial pathway, T cells responded differently. Naïve CD4+ and CD8+ T cells and CD4+ and CD8+ central memory T cells were observed to undergo apoptosis while

CD4+ and CD8+ effector memory T cells were observed to be resistant to apoptosis by H_2O_2 stress (Gupta 2007).

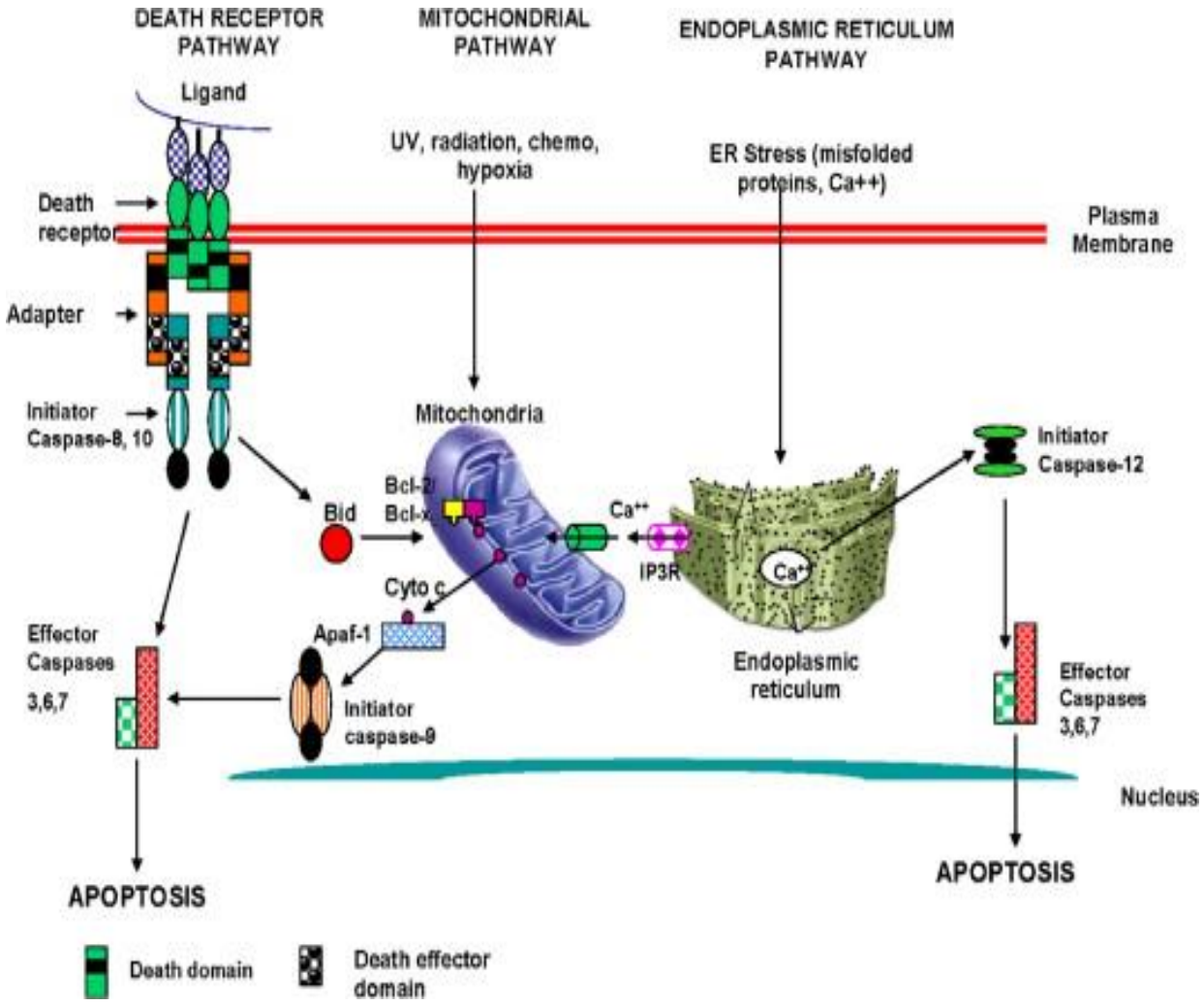

Figure 2.3. Apoptosis pathway
Schematic representation of apoptosis pathways as described in text. All pathways have a common sequence of initiation of effector caspases (Gupta 2007). (With permission see Appendix V).[1]

[1] Gupta S and Gollapudi S (2007). "Susceptibility of naive and subsets of memory T cells to apoptosis via multiple signaling pathways." Autoimmun Rev 6(7): 476-481.

REFERENCES

Apetrei, C., Robertson, D.L., and Marx, P.A. (2004). The history of SIVS and AIDS: epidemiology, phylogeny and biology of isolates from naturally SIV infected non-human primates (NHP) in Africa. Front Biosci *9*, 225-254.

Baskin, G.B., Martin, L.N., Rangan, S.R., Gormus, B.J., Murphey-Corb, M., Wolf, R.H., and Soike, K.F. (1986). Transmissible lymphoma and simian acquired immunodeficiency syndrome in rhesus monkeys. J Natl Cancer Inst *77*, 127-139.

Bolliger, A.P. (2004). Cytologic evaluation of bone marrow in rats: indications, methods, and normal morphology. Vet Clin Pathol *33*, 58-67.

Bondurant, M.C., and Koury, M.J. (2004). Origin and Development of Blood Cells. In Wintrobe's Clinical Hematology, J. Greer, J. Foerster, J.N. Lukens, G.M. Rodgers, F. Paraskevas, and B. Glader, eds. (Philadelphia, Lippincott Williams & Wilkins), pp. 169-194.

Borghans, J.A., Hazenberg, M.D., and Miedema, F. (2005). Limited role for the thymus in SIV pathogenesis. Eur J Immunol *35*, 42-45.

Calvi, L.M., Adams, G.B., Weibrecht, K.W., Weber, J.M., Olson, D.P., Knight, M.C., Martin, R.P., Schipani, E., Divieti, P., Bringhurst, F.R., *et al.* (2003). Osteoblastic cells regulate the haematopoietic stem cell niche. Nature *425*, 841-846.

Cotelingam, J.D. (2003). Bone marrow biopsy: interpretive guidelines for the surgical pathologist. Advances in anatomic pathology *10*, 8-26.

Daniel, M.D., Letvin, N.L., King, N.W., Kannagi, M., Sehgal, P.K., Hunt, R.D., Kanki, P.J., Essex, M., and Desrosiers, R.C. (1985). Isolation of T-cell tropic HTLV-III-like retrovirus from macaques. Science *228*, 1201-1204.

Dazzi, F., Ramasamy, R., Glennie, S., Jones, S.P., and Roberts, I. (2006). The role of mesenchymal stem cells in haemopoiesis. Blood Rev *20*, 161-171.

Di Rosa, F. (2009). T-lymphocyte interaction with stromal, bone and hematopoietic cells in the bone marrow. Immunol Cell Biol *87*, 20-29.

Di Rosa, F., and Pabst, R. (2005). The bone marrow: a nest for migratory memory T cells. Trends in immunology *26*, 360-366.

Dong, Z., Saikumar, P., Weinberg, J.M., and Venkatachalam, M.A. (2006). Calcium in cell injury and death. Annual review of pathology *1*, 405-434.

Douek, D.C., Picker, L.J., and Koup, R.A. (2003). T cell dynamics in HIV-1 infection. Annu Rev Immunol *21*, 265-304.

Elmore, S. (2007). Apoptosis: a review of programmed cell death. Toxicol Pathol *35*, 495-516.

Feuerer, M., Beckhove, P., Garbi, N., Mahnke, Y., Limmer, A., Hommel, M., Hammerling, G.J., Kyewski, B., Hamann, A., Umansky, V., *et al.* (2003). Bone marrow as a priming site for T-cell responses to blood-borne antigen. Nat Med *9*, 1151-1157.

Gardner, M.B. (1993). The importance of nonhuman primate research in the battle against AIDS: a historical perspective. Journal of medical primatology *22*, 86-91.

Gardner, M.B. (1996). The history of simian AIDS. Journal of medical primatology *25*, 148-157.

Gasper, P.W. (2000). The Hematopoietic System. In Schalm's Veterinary Hematology, B.V. Feldman, J.G. Zinkl, and N.C. Jain, eds. (Baltimore, Maryland, LIppincott Williams & Wilkins), pp. 63-68.

Goff, S., Cohen, O.J., and Fauci, A.S. (2001). Fields Virology, Vol 2, 4 edn (Philadelphia, PA, Lippincott Williams & Wilkins).

Grindem, C.B., Neel, J.A., and Juopperi, T.A. (2002). Cytology of bone marrow. The Veterinary clinics of North America *32*, 1313-1374, vi.

Gupta, S., and Gollapudi, S. (2007). Susceptibility of naive and subsets of memory T cells to apoptosis via multiple signaling pathways. Autoimmun Rev *6*, 476-481.

Gurkan, U.A., and Akkus, O. (2008). The mechanical environment of bone marrow: a review. Annals of biomedical engineering *36*, 1978-1991.

Huang, X., Cho, S., and Spangrude, G.J. (2007). Hematopoietic stem cells: generation and self-renewal. Cell death and differentiation *14*, 1851-1859.

Hurtrel, B., Petit, F., Arnoult, D., Muller-Trutwin, M., Silvestri, G., and Estaquier, J. (2005). Apoptosis in SIV infection. Cell death and differentiation *12 Suppl 1*, 979-990.

Huser, H.-J. (1970). Atlas of comparative primate hematology, First edn (New York, Academic Press, Inc.).

Isgro, A., Aiuti, A., Leti, W., Gramiccioni, C., Esposito, A., Mezzaroma, I., and Aiuti, F. (2005). Immunodysregulation of HIV disease at bone marrow level. Autoimmun Rev *4*, 486-490.

Jung, Y., Wang, J., Havens, A., Sun, Y., Jin, T., and Taichman, R.S. (2005). Cell-to-cell contact is critical for the survival of hematopoietic progenitor cells on osteoblasts. Cytokine *32*, 155-162.

Kaech, S.M., Wherry, E.J., and Ahmed, R. (2002). Effector and memory T-cell differentiation: implications for vaccine development. Nat Rev Immunol *2*, 251-262.

Kiel, M.J., Yilmaz, O.H., Iwashita, T., Terhorst, C., and Morrison, S.J. (2005). SLAM family receptors distinguish hematopoietic stem and progenitor cells and reveal endothelial niches for stem cells. Cell *121*, 1109-1121.

Lackner, A.A., and Veazey, R.S. (2007). Current concepts in AIDS pathogenesis: insights from the SIV/macaque model. Annu Rev Med *58*, 461-476.

Lanzavecchia, A., and Sallusto, F. (2002). Progressive differentiation and selection of the fittest in the immune response. Nature reviews *2*, 982-987.

Lay, M.D., Petravic, J., Gordon, S.N., Engram, J., Silvestri, G., and Davenport, M.P. (2009). Is the gut the major source of virus in early simian immunodeficiency virus infection? Journal of virology *83*, 7517-7523.

Letvin, N.L., Daniel, M.D., Sehgal, P.K., Desrosiers, R.C., Hunt, R.D., Waldron, L.M., MacKey, J.J., Schmidt, D.K., Chalifoux, L.V., and King, N.W. (1985). Induction of AIDS-like disease in macaque monkeys with T-cell tropic retrovirus STLV-III. Science *230*, 71-73.

Lifson, A.R., Rutherford, G.W., and Jaffe, H.W. (1988). The natural history of human immunodeficiency virus infection. J Infect Dis *158*, 1360-1367.

Monteiro, J.P., Benjamin, A., Costa, E.S., Barcinski, M.A., and Bonomo, A. (2005). Normal hematopoiesis is maintained by activated bone marrow CD4+ T cells. Blood *105*, 1484-1491.

Murphey-Corb, M., Martin, L.N., Rangan, S.R., Baskin, G.B., Gormus, B.J., Wolf, R.H., Andes, W.A., West, M., and Montelaro, R.C. (1986). Isolation of an HTLV-III-related retrovirus from macaques with simian AIDS and its possible origin in asymptomatic mangabeys. Nature *321*, 435-437.

Nikolich-Zugich, J. (2007). Non-human primate models of T-cell reconstitution. Semin Immunol *19*, 310-317.

Obhrai, J.S., Oberbarnscheidt, M.H., Hand, T.W., Diggs, L., Chalasani, G., and Lakkis, F.G. (2006). Effector T cell differentiation and memory T cell maintenance outside secondary lymphoid organs. J Immunol *176*, 4051-4058.

Pabst, R. (2007). Plasticity and heterogeneity of lymphoid organs. What are the criteria to call a lymphoid organ primary, secondary or tertiary? Immunology letters *112*, 1-8.

Paraskevas, F. (2004). Lymphocytes and Lymphatic Organs. In Wintrobe's Clinical Hematology, J. Greer, J. Foerster, J.N. Lukens, G.M. Rodgers, F. Paraskevas, and B. Glader, eds. (Philadelphia, Lippincott Williams & Wilkins), pp. 409-438.

Sacchetti, B., Funari, A., Michienzi, S., Di Cesare, S., Piersanti, S., Saggio, I., Tagliafico, E., Ferrari, S., Robey, P.G., Riminucci, M., *et al.* (2007). Self-renewing osteoprogenitors in bone marrow sinusoids can organize a hematopoietic microenvironment. Cell *131*, 324-336.

Sallusto, F., Geginat, J., and Lanzavecchia, A. (2004). Central memory and effector memory T cell subsets: function, generation, and maintenance. Annu Rev Immunol *22*, 745-763.

Scott, M.A., and Stockham, S.L. (2008a). Leukocytes. In Fundamentals of Veterinary Clinical Pathology (Ames, Iowa, Blackwell Publishing Professional), pp. 53-106.

Scott, M.A., and Stockham, S.L. (2008b). Bone Marrow and Lymph Nodes. In Fundamentals of Veterinary Clinical Pathology (Ames, Iowa, Blackwell Publishing Professional), pp. 323-368.

Spits, H. (2002). Development of alphabeta T cells in the human thymus. Nature reviews *2*, 760-772.

Stasney, J., and Higgines, G.M. (1936). The Bone Marrow in the Monkey (Macacus Rhesus). The Anatomical Record *67*, 219-231.

Surh, C.D., and Sprent, J. (2005). Regulation of mature T cell homeostasis. Semin Immunol *17*, 183-191.

Szegezdi, E., Logue, S.E., Gorman, A.M., and Samali, A. (2006). Mediators of endoplasmic reticulum stress-induced apoptosis. EMBO reports *7*, 880-885.

Tizard, I.R., and Schubot, R.M. (2004). Lymphocytes. In Veterinary Immunology: An Introduction, T. Merchant, ed. (Philadelphia, PA, Saunders), pp. 92-104.

Travlos, G.S. (2006). Normal structure, function, and histology of the bone marrow. Toxicol Pathol *34*, 548-565.

Veazey, R.S., Tham, I.C., Mansfield, K.G., DeMaria, M., Forand, A.E., Shvetz, D.E., Chalifoux, L.V., Sehgal, P.K., and Lackner, A.A. (2000). Identifying the target cell in primary simian immunodeficiency virus (SIV) infection: highly activated memory CD4(+) T cells are rapidly eliminated in early SIV infection in vivo. Journal of virology *74*, 57-64.

Wagers, A.J. (2005). Stem cell grand SLAM. Cell *121*, 967-970.

Walker, J.M., Maecker, H.T., Maino, V.C., and Picker, L.J. (2004). Multicolor flow cytometric analysis in SIV-infected rhesus macaque. Methods in cell biology *75*, 535-557.

Zhang, J., Niu, C., Ye, L., Huang, H., He, X., Tong, W.G., Ross, J., Haug, J., Johnson, T., Feng, J.Q., *et al.* (2003). Identification of the haematopoietic stem cell niche and control of the niche size. Nature *425*, 836-841.

CHAPTER 3: HEMATOLOGIC ABNORMALITIES DURING PROGRESSIVE SIV INFECTION MIRROR HIV DISEASE

INTRODUCTION

Hematologic abnormalities including anemia, lymphopenia, thrombocytopenia, neutropenia, and leukopenia have been reported in HIV infection and AIDS (Castella 1985; Morris 1982; Moyle 2002; Spivak 1984). However, there is considerable debate whether these abnormalities are caused by HIV infection alone, concurrent opportunistic infections, anti-retroviral therapy (ART), intravenous (IV) drug usage, or other lifestyle factors.

Early studies usually involved patients with advanced HIV disease, often using opportunistic infections as diagnostic criteria, so the hematologic changes were often attributed to the opportunistic infection such as Pneumocystis pneumonia. Furthermore, early studies were often confounded by the use of anti-microbials and later studies by ART. For example azidothymidine (AZT) trials started in 1986 in the USA, and this and other drugs were eventually shown to have significant side effects including anemia and other hematologic abnormalities (Fischl 1987). An increased risk of anemia in HIV patients naïve for antiviral therapy was observed in African Americans (Sullivan 1998). Also, older patients, African Americans, and males are more likely to become thrombocytopenic during HIV disease (Sloand 1992). HIV patients infected by heterosexual relations were reported to be at higher risk to develop thrombocytopenia compared to homosexuals, bisexual, IV drug users, transfusion recipients, or hemophiliacs (Sloand 1992). Neutropenia is observed often in HIV patients on drug therapy or in late stages of AIDS (Street 1996; Coyle 1997). Thus, studies of hematologic abnormalities in HIV infected patients are difficult to interpret and it is not known whether pathogenesis involves direct viral destruction of hematopoietic cells and/or precursors or secondary effects from

immune dysfunction (i.e. autoimmune hemolytic anemia) caused by the virus, drugs, or concurrent infections (Coyle 1997; Curkendall 2007; Olayemi 2008; Treacy 1987; Zon 1987).

The objective of the study was to determine the frequency of hematologic abnormalities in SIV infected macaques during various periods of infection under well-controlled conditions for comparison with HIV infected patients. We hypothesized hematologic changes during progressive non-interventional SIV infection of RM in well-controlled studies would be similar to those of untreated HIV infected patients and represent changes due to SIV infection alone without impact of confounding factors. Close approximations in prevalence of hematologic abnormalities between SIV and HIV would validate the SIV model for bone marrow studies in HIV infection and AIDS. Currently, SIV infected RM are the premier animal model for studying HIV infection in humans, as SIV-induced disease recapitulates essentially all features of HIV infection and AIDS in the macaque model.

MATERIAL AND METHODS

Database Selection

A retrospective longitudinal evaluation of SIV pathogenesis complete blood count (CBC) data collected from Indian RM inoculated with SIV viral strains between January 1986 and December 2006 was conducted at TNPRC. Criteria for inclusion included the following: >1.75 years old at time of inoculation; a single inoculation with SIVB670, SIVmac239, or SIVmac251; slow progression to AIDS (≥260 days post-inoculation or DPI); and serial CBC data collected from 0 DPI until humane sacrifice. Further, all animals were devoid of SIV-related experimental therapy or vaccination throughout the study. AIDS criteria were defined based on the 1993 Centers for Disease Control (CDC) guidelines and limited to opportunistic infections (OI), encephalitis, and/or multi-organ lymphoma confirmed by histopathologic examination at

necropsy. Data collected from age-matched Indian RM served as the controls. Controls included RM beginning research protocols for the first time and macaques were naïve to experimental inoculation or therapy. RM inclusive in the study were referred to as experimental database (ED) I and further defined in this chapter and Appendix II.

Hematologic Data and Definitions

Hematologic data and definitions are described in Appendix I.

Statistical Analysis

Hematologic data from pre-inoculation to humane sacrifice for SIV inoculated RM was organized for evaluation and statistical analyses according to viral inoculation or period of infection. Viral inoculation group(s) was identified by individual inoculum with one of three wildtype strains: SIVB670, SIVmac239, or SIVmac251. Period of infection was assigned by DPI due to inconsistent sampling among SIV infected RM as uninfected or pre-inoculation (0 DPI or Period 1), early (1-42 DPI or Period 2), chronic (43-120 DPI or Period 3), and slowly progressive to AIDS (AIDS or >120 DPI until sacrifice or Period 4). Control hematologic data analysis consisted of a one-time CBC sample.

Differences of hematologic values between the control macaques and infected RM were statistically compared using the Mann Whitney non-parametric unpaired t test in GraphPad Prism 5 (GraphPad Software; San Diego, CA). Correlation of CBC data was compared using non-parametric Spearman correlation coefficients in GraphPad Prism 5 (GraphPad Software).

Prevalence rate was defined as the percentage of total macaques with a hematologic abnormality. Incidence rate was defined as the percentage of total macaques observed with the first event of a hematologic abnormality within a defined period. Statistical differences in prevalence between the control and infected subjects arranged by inoculum groups or periods

were compared using the Tukey Kramer one way analysis of variance (ANOVA) test in GraphInstat 3 (GraphPad Software). Statistical differences in prevalence and incidence between infected subjects arranged by inoculum groups or periods were compared using the Tukey ANOVA test in GraphInStat 3 (GraphPad Software). Graphs represent the mean of the data evaluated.

The SAS® (Version 9.1.3) statistical package was used to analyze the CBC data values of SIV inoculated subjects by repeated measures analysis of variance (MANOVA) in a split-plot arrange of treatments. Effects on the main plot included sex, group*sex, and animal within group*sex. Subplot factors included period and the interactions of period, group and sex. Since any factor which included sex was non-significant in the initial analysis, sex was absorbed as an effect and the models were rerun. Where overall significance was found, post hoc pairwise comparisons of means were conducted with Tukey's HSD test for main effects and t tests of least-squares means for interaction effects.

Graphs represent the means and error bars represent the standard error of the mean (SEM). Statistical analyses were considered significant at p value (p) ≤ 0.05.

RESULTS

Experimental Database I

Retrospective analysis of the TNPRC animal database revealed 61 Indian RM inoculated with a single dose of SIVmac239, 129 Indian RM inoculated with a single dose of SIVmac251, and 427 Indian RM inoculated with a single dose of SIVB670 during the twenty year time period. However, only a subset of animals met the stringent inclusion criteria that excluded animals younger than 1.75 years at inoculation, those vaccinated/immunized/ and/or challenged with other viruses, treated for SIV or other diseases, treated with ART or other anti-microbials,

or rapid progressors. Finally, only macaques that had serial CBC data collected at all defined periods of infection were included. Thus only data from five SIVmac239 infected, six SIVmac251 infected, and ten SIVB670 infected RM were included in this study as the infected cohort (Appendix II). Thirty-one control macaques comprised the uninfected cohort (Appendix II).

Hematologic Differences Between Control and SIV Infected Rhesus macaques

CBC data and prevalence rates were compared between control and SIV infected macaques to detect hematologic changes present during untreated progressive SIV infection (Figure 3.1 and Table 3.1 respectively). Change in prevalence for hematologic abnormalities between SIV infected and control RM was similar to differences observed by evaluation of CBC data. Hemoglobin and hematocrit (HCT) values were significantly decreased in SIV infected RM paralleled by significant increase in anemia prevalence compared to control macaques. SIV macaques had a significantly lower mean cell hemoglobin concentration (MCHC) however hypochromia prevalence was not significant compared to non-infected macaques. Platelet counts were depressed in SIV macaques with increased significance for thrombocytopenia (TCP) prevalence compared to controls. Significant increases in prevalence for neutropenia and neutrophilia was detected in SIV macaques with overall significantly lower neutrophil counts compared to controls. SIV macaques were observed with significantly low lymphocyte counts and increased prevalence of lymphopenia compared to non-infected subjects. Increased prevalence for monocytosis ($p \leq 0.001$) and monocytopenia was present in SIV subjects though a difference in monocyte count was not present compared to controls. Eosinophilia prevalence was significantly increased with a trend for increased eosinophil count compared to control

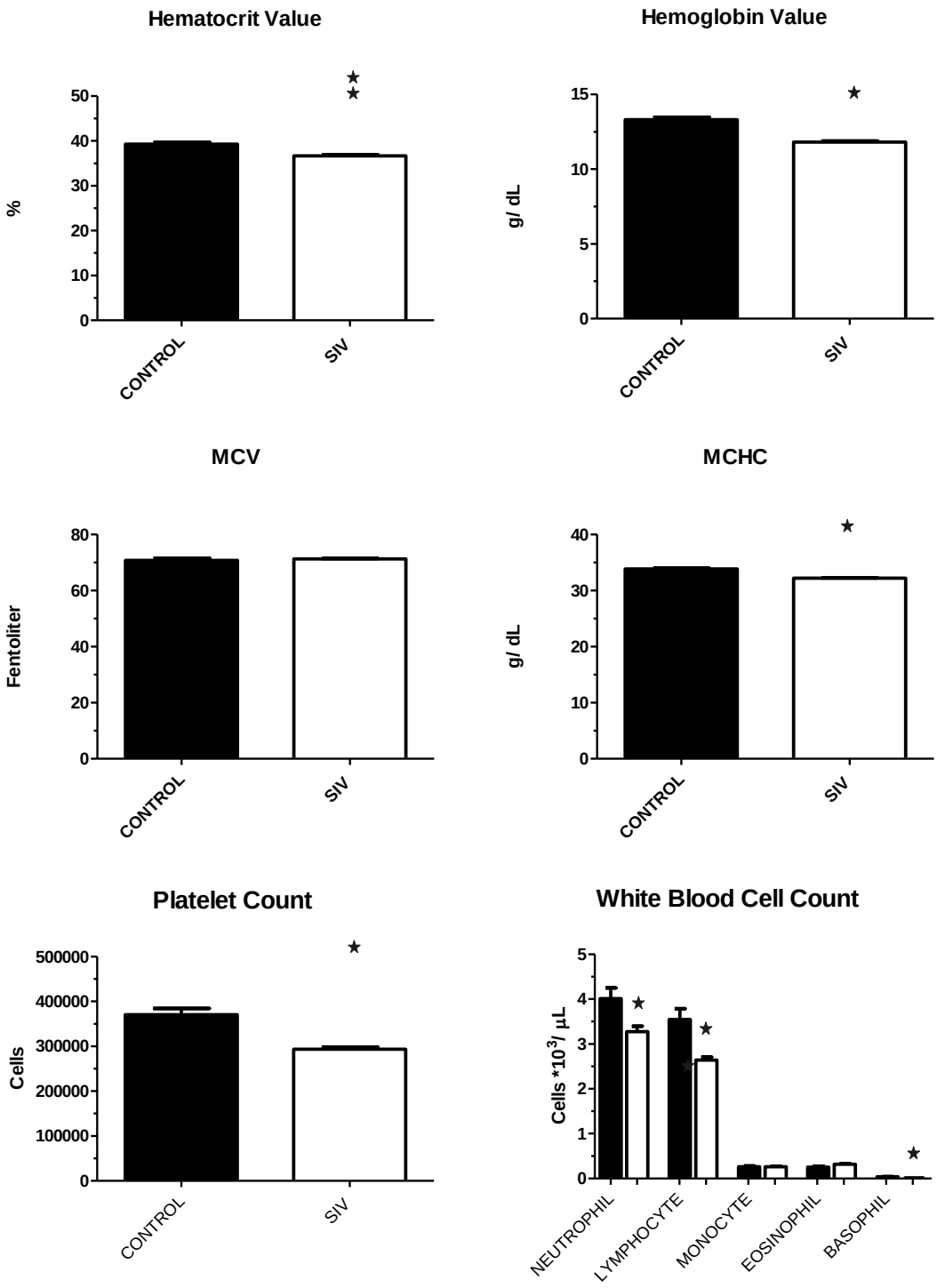

Figure 3.1. Hematologic values of control and SIV infected macaques
Comparison of CBC values between data from control macaques and data from SIV infected macaques. MCV is mean cell volume. MCHC is mean cell hemoglobin concentration. Significant differences by Mann Whitney t tests (*$p \leq 0.0001$ and **$p \leq 0.001$) are shown. Values indicate mean $\pm$ SEM.

Table 3.1. Prevalence Rate of Hematologic Abnormalities in Control and SIV Infected Rhesus macaques

Hematologic Abnormality	Control Subjects (%)	SIV Infected Subjects (%)
Lymphopenia	23	100**
Anemia	3	90**
Eosinophilia	13	90**
Neutropenia	0	90**
Neutrophilia	10	76**
Thrombocytopenia	3	67**
Monocytopenia	3	62
Monocytosis	3	48**
Basophilia	0	24****
Microcytosis	6	5
Lymphocytosis	0	5
Hypochromia	0	6
Macrocytosis	0	0

**Significance $p \leq 0.001$ when compared to control cohort by ANOVA analysis
****Significance $p \leq 0.05$ when compared to control cohort by ANOVA analysis

subjects. Basophilia was noted with significantly increased prevalence in SIV subjects and significantly higher absolute numbers in controls when comparisons were applied.

Classification of SIV infected subjects by strain of inoculum revealed differences when compared to controls for prevalence of hematologic abnormalities (Table 3.2). All hematologic changes were present in SIVB670 macaques. A significant difference was observed between the control group and each SIV inoculum group for prevalence of anemia, neutropenia, lymphopenia, eosinophilia, and basophilia. SIVB670 and SIVmac251 macaques displayed significance for TCP and neutrophilia compared to controls. Monocytopenia was significant for SIVmac239 and SIVB670 compared to control macaques. Both SIVmac groups were significant for monocytosis compared to non-infected macaques. Basophilia was only statistically different for SIVB670 macaques.

Classification of SIV infected subjects by time period revealed differences when compared to the controls for prevalence of hematologic abnormalities (Table 3.3). All time periods showed significant differences compared to controls for prevalence of neutropenia. Post-inoculation periods significantly differed compared to control macaques for both lymphopenia

and eosinophilia prevalence. Early and AIDS periods showed significant prevalence differences compared to non-infected controls for anemia. Interestingly, only the AIDS period showed a significantly increased prevalence of thrombocytopenia, neutrophilia, and monocytosis when compared to control macaques. Lymphocytosis and monocytopenia prevalence rates were too low to be statistically analyzed.

Table 3.2. Significance by p Value Comparing Prevalence Rates of Hematologic Abnormalities for Control and SIV Infected Rhesus macaques by Inoculum

Hematologic Abnormality	SIVmac239	SIVmac251	SIVB670
Anemia	<0.001	<0.001	<0.001
Thrombocytopenia	NS	<0.001	<0.001
Neutropenia	<0.001	<0.001	<0.001
Neutrophilia	NS	<0.01	<0.001
Lymphopenia	<0.001	<0.001	<0.001
Lymphocytosis	NS	NS	NS
Monocytopenia	<0.001	NS	<0.001
Monocytosis	<0.01	<0.001	NS
Eosinophilia	<0.01	<0.001	<0.001
Basophilia	NS	NS	<0.01

NS = not significant

Table 3.3. Significance by p Value Comparing Prevalence Rates of Hematologic Abnormalities for Control and SIV Infected Rhesus macaques by Period

Hematologic Abnormality	Period 1	Period 2	Period 3	Period 4
Anemia	NS[a]	<0.001	NS	<0.001
Thrombocytopenia	NS	NS	NS	<0.001
Neutropenia	<0.001	<0.001	<0.001	<0.001
Neutrophilia	NS	NS	NS	<0.001
Lymphopenia	NS	<0.001	<0.01	<0.001
Lymphocytosis	NA[b]	NA	NA	NA
Monocytopenia	NA	NA	NA	NA
Monocytosis	NS	NS	NS	<0.001
Eosinophilia	NS	<0.001	<0.001	<0.001
Basophilia	NS	NS	NS	NS

a) NS = not significant; b) NA = not analyzed

Prevalence and Incidence of Hematologic Values in SIV Infected Rhesus macaques

CBC data of SIV infected RM were evaluated for differences by group and period (Table 3.4). Significance in group effect, period effect, and group by period effect was noted for

hematocrit, platelet count, neutrophil count, and lymphocyte count. The monocyte count was significant for a group effect and period effect. Only significance for a group effect was detected for eosinophil and basophil count.

Table 3.4. Significance by p Value Comparing CBC Data of SIV Infected Rhesus macaque by Group and Period

CBC Value	Group Effect	Period Effect	Group*Period Effect
Hematocrit	<0.0001	<0.0001	<0.0001
Platelet Count	<0.0001	<0.0001	0.0311
Neutrophil count	<0.0001	<0.0001	0.0066
Lymphocyte count	<0.0001	0.0053	0.0382
Monocyte count	<0.0001	0.0004	NS
Eosinophil count	0.0233	NS	NS
Basophil count	0.0435	NS	NS

NS = not significant

Incidence rates for hematology changes in SIV infected macaques were calculated to detect the first time a specific hematologic abnormality occurred within a time period by viral inoculum (Table 3.5). Evaluation of incidence rates aided in the determination of recurrence of a hematologic event. Several changes in circulating cells were noted during SIV, although incidence rates were detected most commonly for anemia, TCP, neutropenia, neutrophilia, lymphopenia, and eosinophilia.

Prevalence rates for hematologic abnormalities during SIV infection were determined by period for each viral strain (Table 3.6). Prevalence rates for neutropenia and lymphopenia were noted during all periods for all viral strains. Anemia and eosinophilia prevalence rates were the next most common followed by prevalence rates for TCP and neutrophilia.

Hematologic Abnormalities During Progressive SIV Infection

Anemia

Anemia was frequently observed in early and AIDS periods of SIV infected RM for all inoculums (Figure 3.2). Overall, the anemia was mild, normocytic and normochromic, yet

Table 3.5. Incidence Rate of Hematologic Abnormalities for SIV infected RM

	SIVmac239 (%)					SIVmac251 (%)					SIVB670 (%)				
Hematologic Abnormality	***Total***	***0 DPI[a]***	***1-42 DPI***	***43-120 DPI***	***>120 DPI***	***Total***	***0 DPI***	***1-42 DPI***	***43-120 DPI***	***>120 DPI***	***Total***	***0 DPI***	***1-42 DPI***	***43-120 DPI***	***>120 DPI***
Anemia	100	20	60	0	20	83	0	50	0	33	90	14	52	5	19
TCP[b]	40	0	0	0	40	84	0	17	0	67	67	0	10	14	43
Neutropenia	100	40	40	20	0	84	17	50	17	0	90	38	38	14	0
Neutrophilia	60	0	0	20	40	83	33	0	0	50	77	10	5	5	57
Lymphopenia	100	60	40	0	0	100	33	50	0	17	100	28	43	10	19
Lymphocytosis	0	0	0	0	0	0	0	0	0	0	5	0	0	0	5
Monocytopenia	80	20	0	0	60	0	0	0	0	0	62	38	5	0	19
Monocytosis	60	0	0	20	40	66	0	0	33	33	47	0	0	14	33
Eosinophilia	80	0	40	20	20	100	0	100	0	0	91	10	57	10	14
Basophilia	0	0	0	0	0	17	0	0	0	17	40	0	10	5	10

a) DPI = days post-inoculation; b) TCP = thrombocytopenia

Table 3.6. Prevalence Rate of Hematologic Abnormalities for SIV infected RM

	SIVmac239 (%)					SIVmac251 (%)					SIVB670 (%)				
Hematologic Abnormality	***Total***	***0 DPI[a]***	***1-42 DPI***	***43-120 DPI***	***>120 DPI***	***Total***	***0 DPI***	***1-42 DPI***	***43-120 DPI***	***>120 DPI***	***Total***	***0 DPI***	***1-42 DPI***	***43-120 DPI***	***>120 DPI***
Anemia	100	20	60	0	80	83	0	50	0	83	90	20	70	60	90
TCP[b]	40	0	0	0	40	83	0	17	0	67	70	0	10	40	60
Neutropenia	100	40	80	80	80	83	17	67	83	67	90	50	80	80	70
Neutrophilia	60	0	0	20	40	83	33	0	0	83	80	0	10	10	80
Lymphopenia	100	60	100	60	100	100	33	83	67	100	100	10	40	70	100
Lymphocytosis	0	0	0	0	0	0	0	0	0	0	10	0	0	0	10
Monocytopenia	80	20	0	0	60	0	0	0	0	0	90	70	80	80	90
Monocytosis	60	0	0	20	60	67	0	0	33	50	30	0	0	0	30
Eosinophilia	80	0	40	60	80	100	0	100	67	83	90	20	40	60	90
Basophilia	0	0	0	0	0	17	0	0	0	17	40	0	20	10	20

a) DPI = days post-inoculation; b) TCP = thrombocytopenia

highly prevalent in infected animals. Reticulocyte counts were not available to ascertain regenerative capacity of the anemia, but several causes for anemia were ruled out including hemolysis, renal disease, endocrine disease, bone marrow infiltrative disease, and myelodysplasia. The occurrence of a mild normocytic and normochromic anemia was suggestive of a non-regenerative process such as anemia of chronic inflammatory disease or early iron-deficiency anemia (Glader 2004; Means 2004).

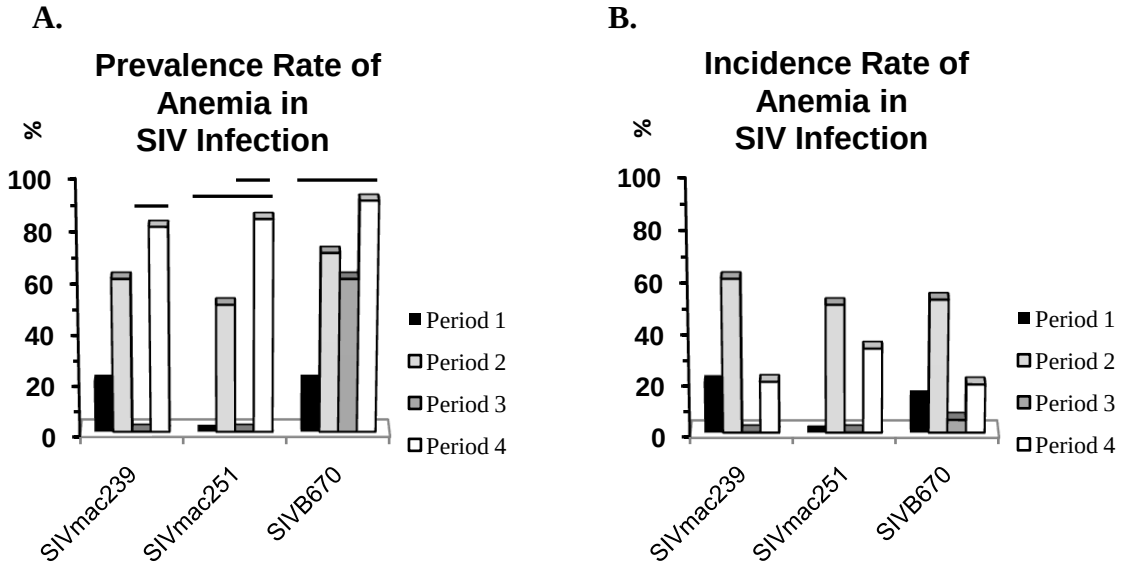

Figure 3.2. Prevalence and incidence of anemia during SIV infection
Prevalence rates (**A.**) and incidence rates (**B.**) for anemia by period for each viral inoculum. Significance between periods within groups represented by horizontal lines by ANOVA ($p \leq 0.05$).

Anemia was often recurrent but was rarely persistent in SIV infected RM. The early period had the highest rate of incidence for anemia (at least 50%) compared to later time periods. Only one subject inoculated with B670 was persistently anemic after inoculation. A mild anemia was detected in animals chronically infected with SIVmac251 and SIVmac239 but varied from mild to severe in SIVB670 subjects as infection progressed. Severe yet transient and recurrent anemia was detected in two subjects chronically infected with SIVB670.

Anemia was not apparent in all periods of infection, but when observed was mostly in the AIDS, with lower prevalence in the early period and much less in the chronic period. All except one subject in each inoculation group displayed anemia in the AIDS stage. Interestingly, subjects inoculated with SIVmac239 and SIVmac251 did not manifest anemia in the chronic phase, while a 60% prevalence of anemia was present in the chronic period of SIVB670 inoculated RM.

Thrombocytopenia

Incidence of thrombocytopenia increased toward progression to AIDS but the degree of thrombocytopenia did not parallel this finding (Figure 3.3). Thrombocytopenia in SIV infected RM was moderately prevalent, while rarely recurrent as it was observed in only three SIVB670 inoculated subjects, including one subject displaying persistent and variably mild to severe thrombocytopenia in chronic and AIDS periods. In the early period of infection, one subject in the SIVmac251 and one subject in the SIVB670 group were observed with mild thrombocytopenia. Subjects infected with SIVB670 were more likely to demonstrate thrombocytopenia as SIV infection progressed compared to macaques with SIVmac239 and SIVmac251.

Thrombocytopenia during the chronic period was only detected in group SIVB670 at 40% prevalence while absent in the SIVmac239 and SIVmac251 groups, similar to prevalence for anemia. During the AIDS stage, all three inoculum groups had thrombocytopenic subjects with prevalence of 40% of SIVmac239 inoculated subjects, 67% of SIVmac251 inoculated subjects, and 60% of SIVB670 inoculated subjects.

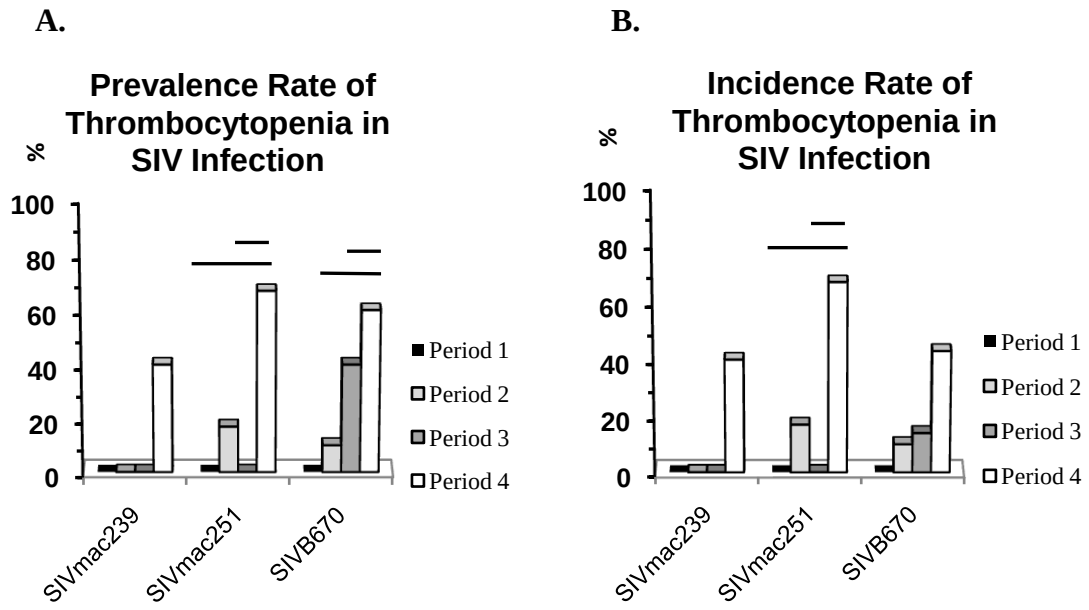

Figure 3.3. Prevalence and incidence of thrombocytopenia during SIV
Prevalence rates (**A.**) and incidence rates (**B.**) for thrombocytopenia by period for each viral inoculum. Significance between periods within groups represented by horizontal lines by ANOVA ($p \leq 0.05$).

Neutropenia

Neutropenia was another frequent finding in SIV-infected macaques, as 90% of infected subjects were found to have neutropenia at some period of infection (Figure 3.4). Incidence of neutropenia was greater than 50% for all time periods and fairly consistent between time periods and inoculum groups but tended to decline with progression of disease. Again, however, although highly prevalent, neutropenia was usually transient, yet often recurrent, although mostly mild to occasionally moderate. All subjects in the SIVmac239 group displayed neutropenia at some stage of infection, and all but one each in both SIVmac251 and SIVB670 groups displayed neutropenia. Neutropenia was always mild in SIVmac251-infected subjects, but often moderate in SIVmac239 and SIVB670 infected subjects.

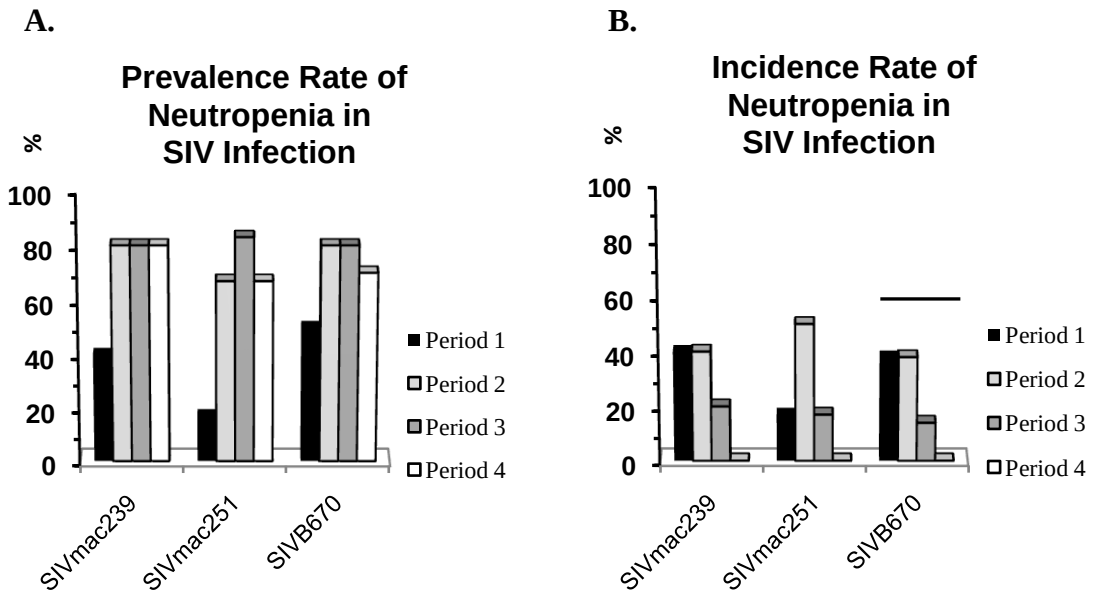

Figure 3.4. Prevalence and incidence of neutropenia during SIV infection
Prevalence rates (**A.**) and incidence rates (**B.**) for neutropenia by period for each viral inoculum. Significance between periods within groups represented by horizontal lines by ANOVA ($p \leq 0.05$).

Lymphopenia

Total prevalence of lymphopenia was highest of all hematologic variances over time by inoculum but incidence varied (Figure 3.5). Essentially every animal experienced lymphopenia at least during some stage of SIV infection. Lymphopenia was present in all inoculum groups at all time periods with at least 40% prevalence ending with 100% prevalence in the progressive phase. Inoculated RM had lymphopenia that was often mild, occasionally moderate, rarely severe, and also rarely persistent in only two subjects infected with SIVmac239 during progressive infection.

Eosinophilia

Prevalence of eosinophilia was high in SIV infected macaques (Figure 3.6). Nevertheless, eosinophilia was mild and often recurrent in SIV infected RM but never persistent.

At least two subjects from all infected time periods for all inoculums groups displayed eosinophilia.

DISCUSSION

Although several hematologic anomalies were occasionally observed in individual control animals, virtually all SIV-infected animals displayed anemia, thrombocytopenia, neutropenia, neutrophilia, lymphopenia, or eosinophilia at some stage of SIV infection. CBC data, prevalence rates, and incidence rates were evaluated between SIV infected and uninfected macaques to identify differences and ascertain relevance of hematologic abnormalities during non-treated SIV infection. Hematologic abnormalities were compared by period and viral group during SIV by prevalence and incidence to identify trends.

Comparison of HCT, hemoglobin, MCV, and MCHC as hematologic parameters for classification of anemia were significantly lower in SIV infected macaques than controls with the exception of MCV. HCT and hemoglobin values and prevalence for anemia were significantly different during SIV compared to controls interpreted as an important hematologic abnormality during SIV infection. Anemia prevalence was highest in AIDS but incidence was highest in period 2 for all viral strains. Of note, anemia was not present in SIVmac infected RM during period 3. The SIV RM model simplifies the ability to rule out many causes for anemia such as drug, diet, and acute or chronic blood loss. Reticulocyte count was not available to ascertain regeneration during anemic episodes but MCHC and MCV were evaluated to classify anemias.

Initially, MCHC was significantly decreased in SIV infected macaques compared to controls but prevalence for hypochromia was low compared to controls and this finding was regarded as unimportant during SIV infection. The lack of significant difference in MCV between RM infected and uninfected with SIV indicated this value was not important during SIV

. **A**. **B.**

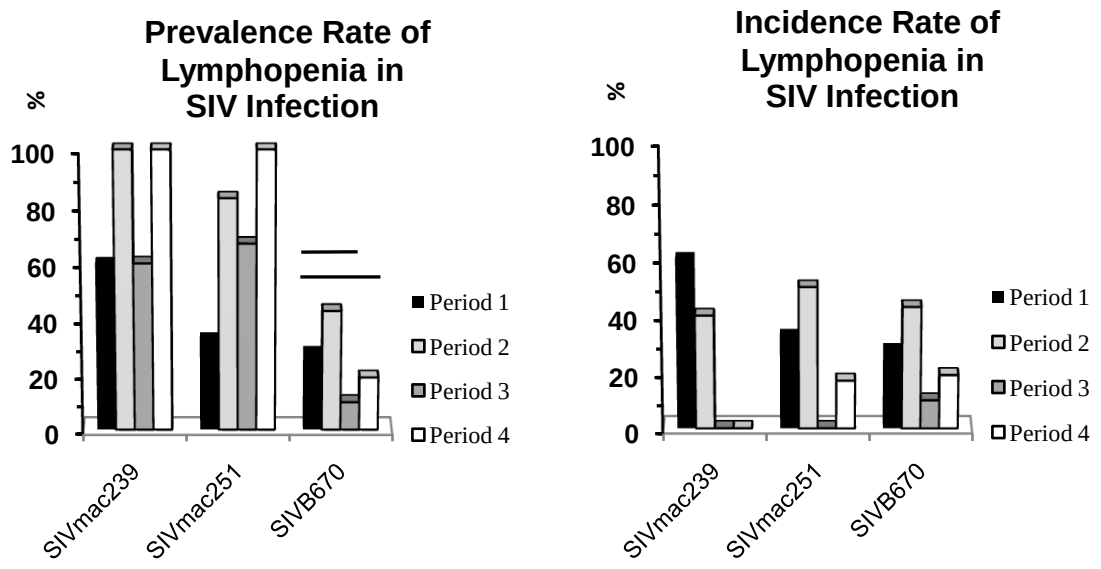

Figure 3.5. Prevalence and incidence of lymphopenia during SIV infection
Prevalence rates (**A.**) and incidence rates (**B.**) for lymphopenia by period for each viral inoculum. Significance between periods within groups represented by horizontal lines by ANOVA ($p \leq 0.05$).

A. **B.**

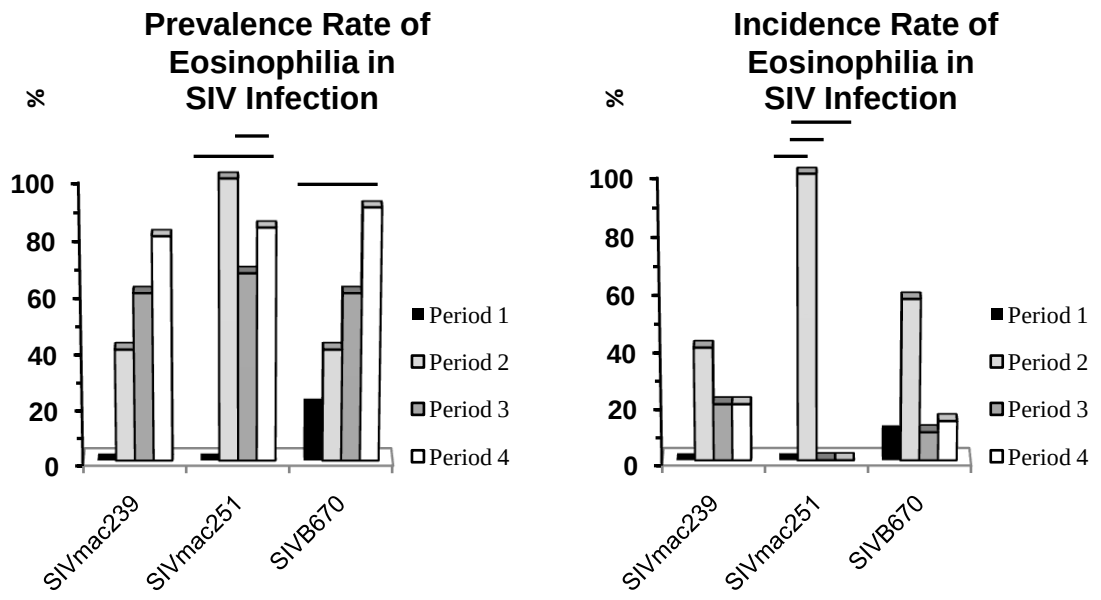

Figure 3.6. Prevalence and incidence of eosinophilia during SIV infection
Prevalence rates (**A.**) and incidence rates (**B.**) for eosinophilia by period for each viral inoculum. Significance between periods within groups represented by horizontal lines by ANOVA ($p \leq 0.05$).

infection. In fact, prevalence for macrocytosis was absent in both control and SIV infected macaques with low prevalence rate comparisons for microcytosis, thus MCV changes were considered inconsequent to SIV infection.

Platelet count and TCP were significantly different between controls and SIV infected macaques indicating thrombocytopenia was a relevant hematologic abnormality during SIV infection. TCP prevalence was low compared to other hematologic abnormalities and early time periods were less likely to manifest this anomaly with highest incidence and prevalence in AIDS for all three inoculums. Similar to anemia, TCP was not observed in SIVmac infected RM during period 3.

A significantly low neutrophil count in SIV infected macaques compared to controls was observed even though both neutropenia and neutrophilia prevalences were significantly higher in

SIV infected macaques compared to controls. Multiple causes could not be discounted for neutrophilia such as epinephrine-mediated physiologic neutrophilia, corticosteroid-induce stress neutrophilia, and inflammation (Smith Graham S. 2000). Therefore neutrophilia was regarded as equivocal in this study for SIV disease. Neutropenia, however, may be observed during periods of increased tissue demand/ destruction or due to reduced bone marrow production or acute inflammation. Absence of neutropenia in controls and occurrence post- SIV infection in all viral groups supported neutropenia to be a common hematologic event during SIV. Most infected RM had detectable neutropenia prior to AIDS.

Lymphocyte count during SIV was significantly lower compared to controls observed as the highest prevalence for a hematologic abnormality during SIV infection. Lymphopenia was a hallmark hematologic abnormality in all SIV periods for all viral inoculums whereas only one RM in AIDS inoculated with SIVB670 was detected with lymphocytosis (1 event from 557 CBCs) indicating this event to be rare.

The likelihood of circulating monocytes to be elevated or decreased during SIV infection was similar by prevalence rates (near 50%) resulting in minimal absolute count differences from controls. We interpreted monocyte count shifts to be non-conclusive during SIV infection even though significant prevalence differences were noted for prevalence by group and period.

Even though only an increased trend for eosinophilia in SIV infected macaques compared to controls was noted, the high prevalence of eosinophilia in SIV infected macaques compared to controls indicated a relevant change during progressive SIV infection. Parasite data was evaluated to determine if parasitism alone could account for the eosinophilia. Rare parasite fecal direct smear and flotation results were available during progressive SIV infection, that included all AIDS diagnoses, with at least one RM evaluated per period. Only two controls had fecal

evaluation on the day of CBC collection. Intestinal parasites (roundworms and protozoa) were detected on all fecal analyses for two SIVmac239 infected RM, two SIVmac251 infected RM, and seven SIVB670 infected RM plus the two controls. However, one SIVmac239 infected RM had only 3 of 4 fecal results positive for parasites and 1 fecal examination negative at 362 DPI. Parasitism could not account for the eosinophilia alone so this hematologic abnormality was considered pertinent to SIV.

Basophil granulocytes represented <1% of total circulating cells indicating shifts would minimally impact total WBC and may be difficult to discern as a specific change in SIV disease. Basophil count and basophilia prevalence in SIV infected macaques was significantly lower than in controls. Consequently, basophilia was considered an unremarkable event during SIV infection.

Overall, prevalences in SIV infected RM from our study mirrored prevalences in HIV patients exclusive of AIDS related therapies. Fairly consistent characterization of hematologic abnormalities were found in HIV cohorts with the note that anemia was determined by hemoglobin concentration that varied by sex and global location. HIV patients naïve to ART, chemotherapy, radiation therapy, or anti-microbials by self-declaration and/or preceding enrollment in clinical trials were found with the following frequencies of hematologic abnormalities: anemia 10-95%; TCP 10-83%; lymphopenia 64%; neutropenia 17-40%; and eosinophilia 3% (Adediran 2006; Alaei 2002; Babadoko 2008; Erhabor 2005; Malyangu 2000; Marroni 1995; Moore 1998; Mugisha 2008; Peltier 1991; Sa 2007; Sloand 1992; Walsh 1985). AIDS patients naïve to antiretroviral therapy displayed frequencies of 30-88% anemia, TCP 16-66%, lymphopenia 31-83%, neutropenia 8-29%, eosinophilia 23% (Adewuyi 1999; Murphy 1987; Spivak 1984; Zon 1987) which was similarly represented in our prevalence of SIV

infected RM with AIDS. Lower values were noted for earlier stages of HIV disease as 6-40% anemia, TCP 0-20%, lymphopenia 15-30%, neutropenia 0-30%, eosinophilia 16-18% (Adewuyi 1999; Murphy 1987; Zon 1987). Comparative non-AIDS stages in the RM of this study revealed anemia, TCP, lymphopenia, neutropenia, and eosinophilia were all lower than in macaques in AIDS with the exception of neutropenia which revealed minimal differences.

We observed significant differences between macaques infected with different strains of virus. The RM SIV model using three different strains allowed hematologic abnormalities in the AIDS population to be evaluated according to progression of infection. SIVmac239 infected RM had the highest incidence and prevalence for lymphopenia and neutropenia. SIVB670 inoculated RM had the highest incidence and prevalence for anemia and TCP. SIVmac251 diseased RM had the highest incidence and prevalence for eosinophilia. The choice to compare three SIV inoculum groups in this retrospective study was to mimic biological variability of HIV strains in the human population. HIV-1 group M and SIVsm lineages share molecular methods of diversification (Apetrei 2005; Apetrei 2004). Natural infections of Sooty mangabey monkeys with SIVsm housed at primate centers in the United States were the origin for SIVmac and SIVB670 viruses (Apetrei 2005). However, SIVB670 and SIVmac251 represent distinct lineages (Apetrei 2005). Therefore, SIVmac239, SIVmac251 and SIVB670 inoculated RM may reflect demographics of HIV infection in viral diversification, and thus affect hematologic abnormalities. In our study of SIV infected RM, slow progressors devoid of therapeutic intervention defined explicitly the incidence and prevalence and observance of hematologic parameters during untreated HIV disease.

The retrospective database investigation of natural SIV disease progression in Rhesus macaques revealed prevalence of hematologic abnormalities during progressive SIV infection in

Macaca mulatta that mirrored progressive HIV infection in *Homo sapiens*. These results suggest that, like in HIV infection, lymphopenia, anemia, thrombocytopenia, and neutropenia are major complications of progressive SIV infection. Advantages of the Rhesus macaque model for studies of HIV pathogenesis allow the researcher to control for variables including antiretroviral drug therapy, sexual preference/lifestyle, socio-economic strata, and recreational drug use, hemophilia, and blood transfusion, duration of infection, diet, and race. However, in our study, SIV inoculum and stage of infection were significant determinants of several hematologic abnormalities suggesting the strain of virus and chronicity of disease may be important in the development of certain hematologic disorders in HIV infection.

SUMMARY

Studies of hematologic abnormalities in HIV infected patients are confounded by a multitude of factors such as unknown duration or strain of viral infection, sexual activity, drug usage, race, geography (i.e. endemic disease, availability of healthcare), chronic conditions/diseases including multiple infections, and diet (i.e. iron availability). A retrospective data analysis of SIV infected Rhesus macaques of Indian origin was performed at the Tulane National Primate Research Center to determine the prevalence of hematologic abnormalities without the effect of anti-retroviral therapy, lifestyle, diet, or race. Hematologic data from RM inoculated with SIV and without antiviral therapy or vaccination from 1987-2006 was collected pre-inoculation and during development of AIDS were studied. Anemia, thrombocytopenia, lymphopenia, eosinophilia, and neutropenia increased in prevalence with progression of SIV disease, but some variances were noted with different SIV strains and during different periods of progressive SIV infection. Concordance of hematologic abnormalities during progressive SIV infection to similar changes in HIV disease suggest that, like in HIV infection of humans,

hematologic abnormalities are major complications of SIV infection and that such hematologic abnormalities are often attributed to SIV infection alone rather than intervening therapeutic regimens. Additionally, this study confirms the SIV Rhesus macaque model to study hematologic and bone marrow changes during HIV disease.

REFERENCES

Adediran, I.A., and Durosinmi, M.A. (2006). Peripheral blood and bone marrow changes in patients with acquired immunodeficiency syndrome. Afr J Med Med Sci *35 Suppl*, 85-91.

Adewuyi, J.O., Coutts, A.M., Latif, A.S., Smith, H., Abayomi, A.E., and Moyo, A.A. (1999). Haematologic features of the human immunodeficiency virus (HIV) infection in adult Zimbabweans. Cent Afr J Med *45*, 26-30.

Alaei, K., Alaei, A., and Mansoori, D. (2002). Thrombocytopenia in HIV-infected patients, Islamic Republic of Iran. East Mediterr Health J *8*, 758-764.

Apetrei, C., Kaur, A., Lerche, N.W., Metzger, M., Pandrea, I., Hardcastle, J., Falkenstein, S., Bohm, R., Koehler, J., Traina-Dorge, V., *et al.* (2005). Molecular epidemiology of simian immunodeficiency virus SIVsm in U.S. primate centers unravels the origin of SIVmac and SIVstm. Journal of virology *79*, 8991-9005.

Apetrei, C., Robertson, D.L., and Marx, P.A. (2004). The history of SIVS and AIDS: epidemiology, phylogeny and biology of isolates from naturally SIV infected non-human primates (NHP) in Africa. Front Biosci *9*, 225-254.

Babadoko, A.A., Aminu, S.M., and Suleiman, A.N. (2008). Neutropenia and human immunodeficiency virus-1 infection: analysis of 43 cases. Niger J Med *17*, 57-60.

Castella, A., Croxson, T.S., Mildvan, D., Witt, D.H., and Zalusky, R. (1985). The bone marrow in AIDS. A histologic, hematologic, and microbiologic study. Am J Clin Pathol *84*, 425-432.

Coyle, T.E. (1997a). Hematologic complications of human immunodeficiency virus infection and the acquired immunodeficiency syndrome. Med Clin North Am *81*, 449-470.

Coyle, T.E. (1997b). Hematologic complications of human immunodeficiency virus infection and the acquired immunodeficiency syndrome. Med Clin North Am *81*, 449-470.

Curkendall, S.M., Richardson, J.T., Emons, M.F., Fisher, A.E., and Everhard, F. (2007). Incidence of anaemia among HIV-infected patients treated with highly active antiretroviral therapy. HIV Med *8*, 483-490.

Erhabor, O., Ejele, O.A., Nwauche, C.A., and Buseri, F.I. (2005). Some haematological parameters in human immunodeficiency virus (HIV) infected Africans: the Nigerian perspective. Niger J Med *14*, 33-38.

Fischl, M.A., Richman, D.D., Grieco, M.H., Gottlieb, M.S., Volberding, P.A., Laskin, O.L., Leedom, J.M., Groopman, J.E., Mildvan, D., Schooley, R.T., *et al.* (1987). The efficacy of azidothymidine (AZT) in the treatment of patients with AIDS and AIDS-related complex. A double-blind, placebo-controlled trial. N Engl J Med *317*, 185-191.

Glader, B. (2004). Anemia: General Considerations. In Wintrobe's Clinical Hematology, J. Greer, J. Foerster, J.N. Lukens, G.M. Rodgers, F. Paraskevas, and B. Glader, eds. (Philadelphia, Lippincott Williams & Wilkins), pp. 947-978.

Malyangu, E., Abayomi, E.A., Adewuyi, J., and Coutts, A.M. (2000). Aids is now the commonest clinical condition associated with multilineage blood cytopenia in a central referral hospital in Zimbabwe. Cent Afr J Med *46*, 59-61.

Marroni, M., Gresele, P., Vezza, R., Papili, R., Francisci, D., De Socio, G., Di Candilo, F., Baldelli, F., Fiorio, M., Longo, F., *et al.* (1995). Thrombocytopenia in HIV infected patients. Prevalence and clinical spectrum. Recenti Prog Med *86*, 103-106.

Means, R.T., Jr. (2004). Anemias Secondary to Chronic Disease and Systemic Disorders. In Wintrobe's Clinical Hematology, J. Greer, J. Foerster, J.N. Lukens, G.M. Rodgers, F. Paraskevas, and B. Glader, eds. (Philadelphia, Lippincott Williams & Wilkins), pp. 1445-1465.

Moore, R.D., Keruly, J.C., and Chaisson, R.E. (1998). Anemia and survival in HIV infection. J Acquir Immune Defic Syndr Hum Retrovirol *19*, 29-33.

Morris, L., Distenfeld, A., Amorosi, E., and Karpatkin, S. (1982). Autoimmune thrombocytopenic purpura in homosexual men. Ann Intern Med *96*, 714-717.

Moyle, G. (2002). Anaemia in persons with HIV infection: prognostic marker and contributor to morbidity. AIDS reviews *4*, 13-20.

Mugisha, J.O., Shafer, L.A., Van der Paal, L., Mayanja, B.N., Eotu, H., Hughes, P., Whitworth, J.A., and Grosskurth, H. (2008). Anaemia in a rural Ugandan HIV cohort: prevalence at enrolment, incidence, diagnosis and associated factors. Trop Med Int Health *13*, 788-794.

Murphy, M.F., Metcalfe, P., Waters, A.H., Carne, C.A., Weller, I.V., Linch, D.C., and Smith, A. (1987). Incidence and mechanism of neutropenia and thrombocytopenia in patients with human immunodeficiency virus infection. British journal of haematology *66*, 337-340.

Olayemi, E., Awodu, O.A., and Bazuaye, G.N. (2008). Autoimmune hemolytic anemia in HIV-infected patients: a hospital based study. Ann Afr Med *7*, 72-76.

Peltier, J.Y., Lambin, P., Doinel, C., Courouce, A.M., Rouger, P., and Lefrere, J.J. (1991). Frequency and prognostic importance of thrombocytopenia in symptom-free HIV-infected individuals: a 5-year prospective study. AIDS (London, England) *5*, 381-384.

Sa, M.S., Sampaio, J., Haguihara, T., Ventin, F.O., and Brites, C. (2007). Clinical and laboratory profile of HIV-positive patients at the moment of diagnosis in Bahia, Brazil. Braz J Infect Dis *11*, 395-398.

Sloand, E.M., Klein, H.G., Banks, S.M., Vareldzis, B., Merritt, S., and Pierce, P. (1992). Epidemiology of thrombocytopenia in HIV infection. European journal of haematology *48*, 168-172.

Smith, G.S. (2000). Neutrophils. In Schalm's Veterinary Hematology, B.V. Feldman, J.G. Zinkl, and N.C. Jain, eds. (Baltimore, Maryland, Ippincott Williams & Wilkins), pp. 281-307.

Spivak, J.L., Bender, B.S., and Quinn, T.C. (1984). Hematologic abnormalities in the acquired immune deficiency syndrome. Am J Med *77*, 224-228.

Street, A.M., and Gibson, J. (1996). Managing HIV. Part 5: Treating secondary outcomes. 5.12 HIV and haematological disease. Med J Aust *164*, 487-488.

Sullivan, P.S., Hanson, D.L., Chu, S.Y., Jones, J.L., and Ward, J.W. (1998). Epidemiology of anemia in human immunodeficiency virus (HIV)-infected persons: results from the multistate adult and adolescent spectrum of HIV disease surveillance project. Blood *91*, 301-308.

Treacy, M., Lai, L., Costello, C., and Clark, A. (1987). Peripheral blood and bone marrow abnormalities in patients with HIV related disease. British journal of haematology *65*, 289-294.

Walsh, C., Krigel, R., Lennette, E., and Karpatkin, S. (1985). Thrombocytopenia in homosexual patients. Prognosis, response to therapy, and prevalence of antibody to the retrovirus associated with the acquired immunodeficiency syndrome. Ann Intern Med *103*, 542-545.

Zon, L.I., Arkin, C., and Groopman, J.E. (1987). Haematologic manifestations of the human immune deficiency virus (HIV). British journal of haematology *66*, 251-256.

CHAPTER 4: BONE MARROW CHANGES EARLY AND LATE DURING SIV INFECTION

INTRODUCTION

Detection of changes in erythrocytes, platelets, and leukocytes as anemia, thrombocytopenia, and neutropenia respectively during SIV and HIV infection reflect, likely, alterations in bone marrow hematopoiesis (Chapter 3). Geller et al. in 1985 initially defined a BM pattern pathognomonic for AIDS, prior to identification of HIV as causative agent (Geller 1985). This pattern was defined as granulocytic left shift and hyperplasia, including eosinophils, and erythroid hypoplasia with an increased M:E ratio. In addition, the hypercellular marrow included megakaryocytic hyperplasia, lymphocytic infiltration, and evidence of fibrosis. Studies over time have determined the marrow to be more variable than Geller first observed and without a pathognomonic pattern. However, BM studies of HIV infected patients are complicated by inconsistent defined stages of disease (e.g. AIDS related complex or ARC, symptomatic, "pre-AIDS"), classifications of AIDS (e.g. total CD4+ count, opportunistic infection, neoplasia), erratic report for anti-microbial or ART, variable methods of BM collection (e.g. aspirate, biopsy, ante-mortem, post-mortem), and divergent morphologic characterization of BM which makes patterns of disease and comparisons difficult to interpret (Thiele 1992).

The objective of this study was to examine bone marrow changes during progressive SIV infection in subjects devoid of ART or any pharmacoligic intervention, including vaccination, for comparison with HIV patients. Our earlier study of SIV infection revealed hematologic abnormalities were present in primary pathogenesis studies uncomplicated by drug therapy, diet, lifestyle, and economic factors present in populations of HIV patients (Chapter 3). We hypothesized bone marrow disruption from a steady state environment would be present during progressive stages of SIV disease identified by time post-infection and detection of clinical

disease, but variable for hematopoietic cell lineages, consistent with the observed hematologic abnormalities. We also hypothesized bone marrow morphologic assessment during SIV would mirror HIV as did hematologic abnormalities. Morphologic assessment of bone marrow tissue for changes in nucleated cells, iron storage, and fibrosis along with phenotype of hematopoietic stem cells was performed to elucidate evidence of bone marrow dysregulation as foretold by the common occurrence of hematologic abnormalities.

MATERIAL AND METHODS

Experimental Database II

Experimental database and definitions are described in Appendix II.

Hematologic Data and Definitions

Hematologic data and definitions are described in Appendix I.

Plasma Viral Load

Plasma viral loads and definitions are described in Appendix IV.

Flow Cytometry Analysis

Whole blood and BM tissue collection, flow cytometry analysis, and definitions are described in Appendix III.

Flow cytometry was performed to identify CD34+ HSC in WB and BM. CD34-PE (Clone 563) monoclonal antibody for surface staining from BD Biosciences (San Jose, CA) was utilized to detect HSC. HSC were identified by CD34 versus (vs.) side scatter (SSC) plot gating in a parent gate (Figure 4.1).

Bone Marrow Morphologic Assessment

Five µm sections of paraffin-embedded formalin fixed bone marrow tissue were processed and special stains applied for examination of each tissue. A blinded evaluation by one microscopist of random, non-touching fields using a Zeiss Axiostar Plus microscope (Zeiss;

Thornwood, NY) was performed. Representative photographs of inspected fields at the 20X objective from Leica DMLb microscope (Leica; Bannockburn, IL) using Spot Insight color camera and Spot Imaging Software (Diagnostic Instruments; Sterling Heights, MI) were collected and scored.

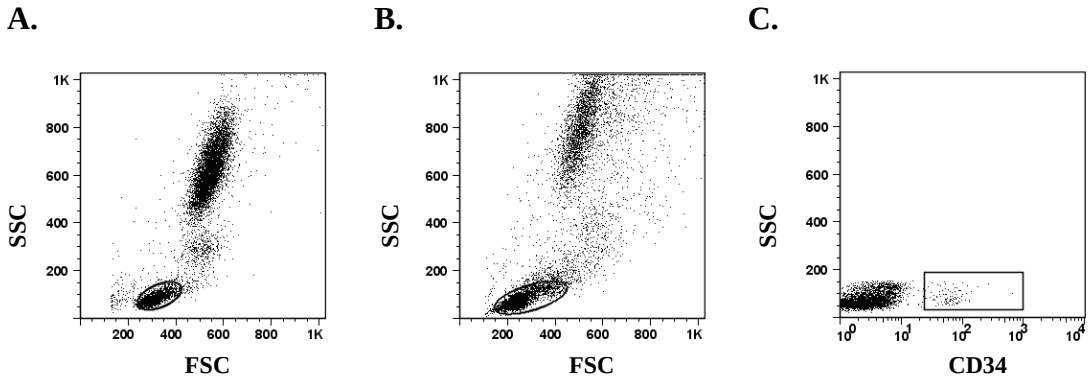

Figure 4.1. Identification of hematopoietic stem cells by flow cytometry gating
Determination of CD34+ hematopoietic stem cells (HSC). **A.** Lymphocyte gate of whole blood by FSC versus SSC plot. **B.** Multilineage gate of bone marrow including lymphocytes by FSC versus SSC plot. **C.** Gate of interest by CD34 versus SSC plot within the parent gate identified CD34+ HSC.

Bone Marrow Cellularity and Bone Marrow Megakaryocyte Numbers

Routine hematoxylin and eosin (H&E) stain was applied to marrow tissue. Each field was subjectively graded using the 10X objective or microscopic low power field (lpf) for mean percentage of bone marrow cellularity in relation to adipose tissue over 20 fields (Table 4.1 and Figure 4.2). Conjointly, megakaryocytes were counted in the same fields to obtain the mean megakaryocyte number per lpf.

Bone Marrow Nucleated Lineage Cell Ratio

Periodic Acid Schiff (PAS) stain was applied to BM tissue. A 300 nucleated cell differential count was performed to count populations of cells based on morphologic appearance and PAS staining. Cells were counted as PAS positive myeloid lineage cells (granulocytic and monocytic lineage excluding lymphocytes and macrophages) or PAS negative erythroid lineage

Table 4.1. Grade of Bone Marrow Cellularity

Grade	% Cellularity of Field
0	0
1	1-5
2	6-24
3	25
4	26-49
5	50
6	51-74
7	75
8	76-89
9	90-99
10	100

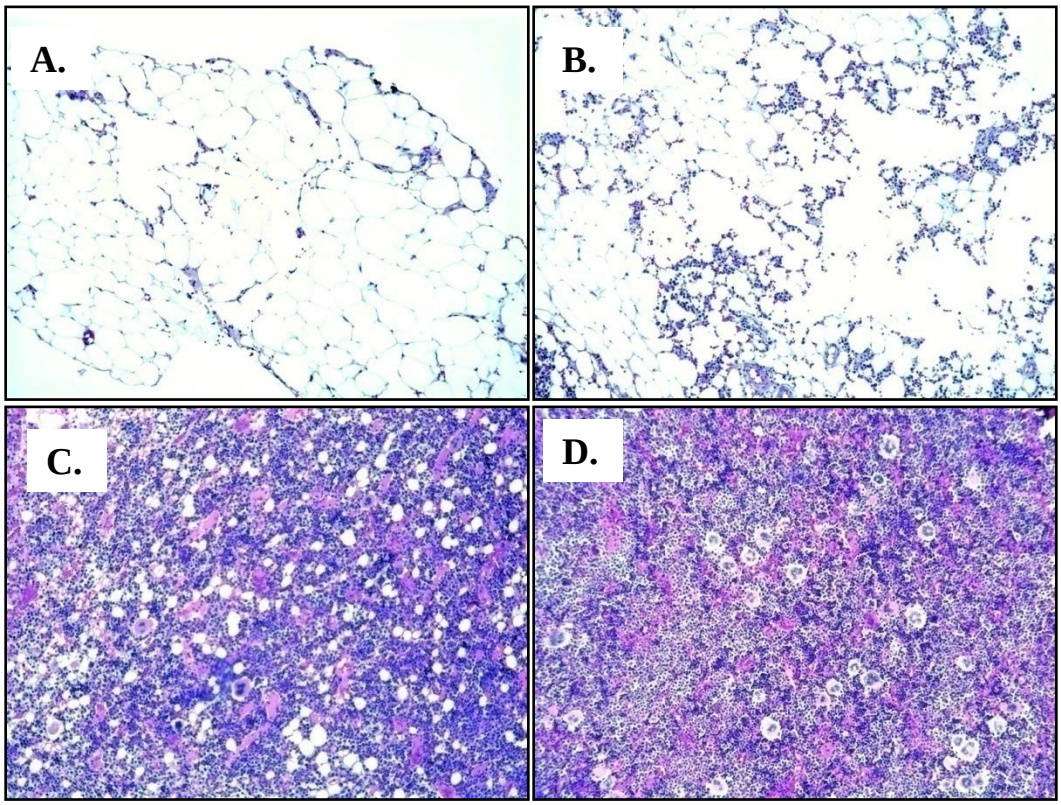

Figure 4.2. Images of bone marrow tissue cellularity by grade
Photomicrographs of hematoxylin and eosin stained bone marrow tissue representing cellularity by grade or percentage of nucleated cells (Table 4.1). **A**. Grade 1 or 1-5% cellularity (macaque R908). **B**. Grade 2 or 6-25% cellularity (macaque L880). **C**. Grade 8 or 76-89% cellularity (macaque AP53). **D**. Grade 9 or 90-99% cellularity (macaque R544). Field represents a 10X objective image (100X) on a Leica DMLb microscope (Leica; Bannockburn, IL) using Spot Insight color camera and Spot Imaging Software (Diagnostic Instruments; Sterling Heights, MI).

cells. Plasma cells and cells of the megakaryocytic lineage were also excluded. Sections were evaluated using the Olympus BX41 microscope (Olympus; Center Valley, PA) at 100X oil immersion objective with a minimum of 3 fields observed. The M:E ratio was calculated.

Bone Marrow Iron Store

Gomori's iron stain was applied to marrow tissue sections. Marrow sections were subjectively graded for stainable iron in marrow particles at the 20X objective for the degree of iron staining over 7 fields as mean marrow iron stores per field (Table 4.2 and Figure 4.3) (Gale 1963; Stuart-Smith 2005).

Table 4.2. Grade of Bone Marrow Iron Storage

Grade	Description
0	Absent or not visible
1	Small particles visible, normal minimal
2	Large particles visible, normal adequate
3	Dense clumps visible, moderate to high
4	Large deposits visible, excessive

Bone Marrow Lymphocyte Aggregates

H&E stained marrow sections were graded using the 10X objective to determine the number of bone marrow lymphocyte aggregates (BMLA) in 10 lpfs as a measure of the degree of lymphocytic infiltration (Table 4.3). Morphologic evaluation of the lymphocyte aggregates was performed.

Bone Marrow Fibrosis

Gordon and Sweet's reticulin stain for type III collagen in marrow stroma was applied to marrow tissue sections. Sections were subjectively graded at the 20X magnification for the degree of intercellular reticulin staining over 7 fields as measure of marrow fibrosis per tissue (Table 4.4 and Figure 4.4) (Thiele 2005).

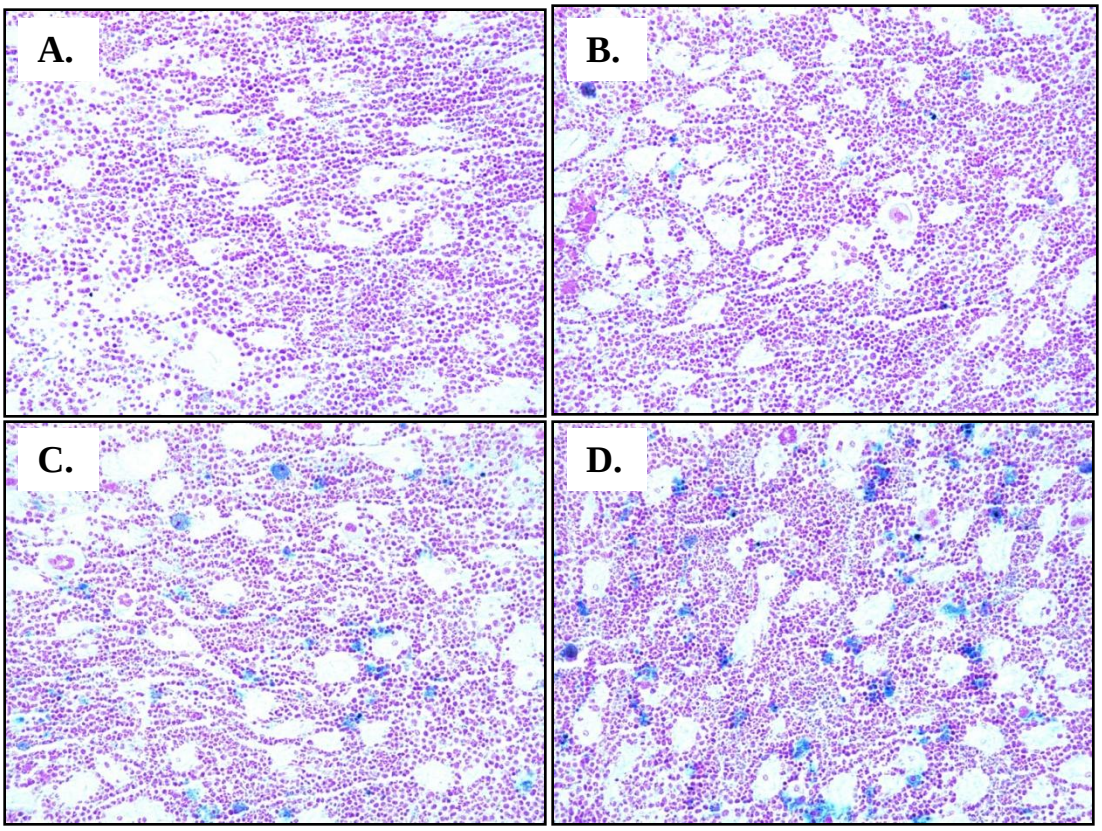

Figure 4.3. Images of bone marrow tissue iron content by grade
Photomicrographs of Gomori's iron stained bone marrow tissue representing iron content (blue staining) by grade (Table 4.2). **A**. Grade 0 or absent iron stores (macaque AV63). **B**. Grade 1 or normal iron storage (macaque AJ79). **C**. Grade 2 or mild iron storage (macaque AP53). **D**. Grade 3 or moderate iron storage (macaque I553). Field represents a 20X objective image (200X) on a Leica DMLb microscope (Leica; Bannockburn, IL) using Spot Insight color camera and Spot Imaging Software (Diagnostic Instruments; Sterling Heights, MI).

Table 4.3. Grade of Bone Marrow Lymphoid Aggregates

Grade	Description
0	Absent
1	Minimal to Mild, 1 follicle in 10 fields
2	Moderate, 2-4 follicles in 10 fields
3	Severe, $\geq$ 5follicles in 10 fields

Table 4.4. Grade of Bone Marrow Fibrosis

Grade	Description
0	Minimal , normal
1	Mild
2	Moderate with minimal bundles
3	Excessive with moderate bundles

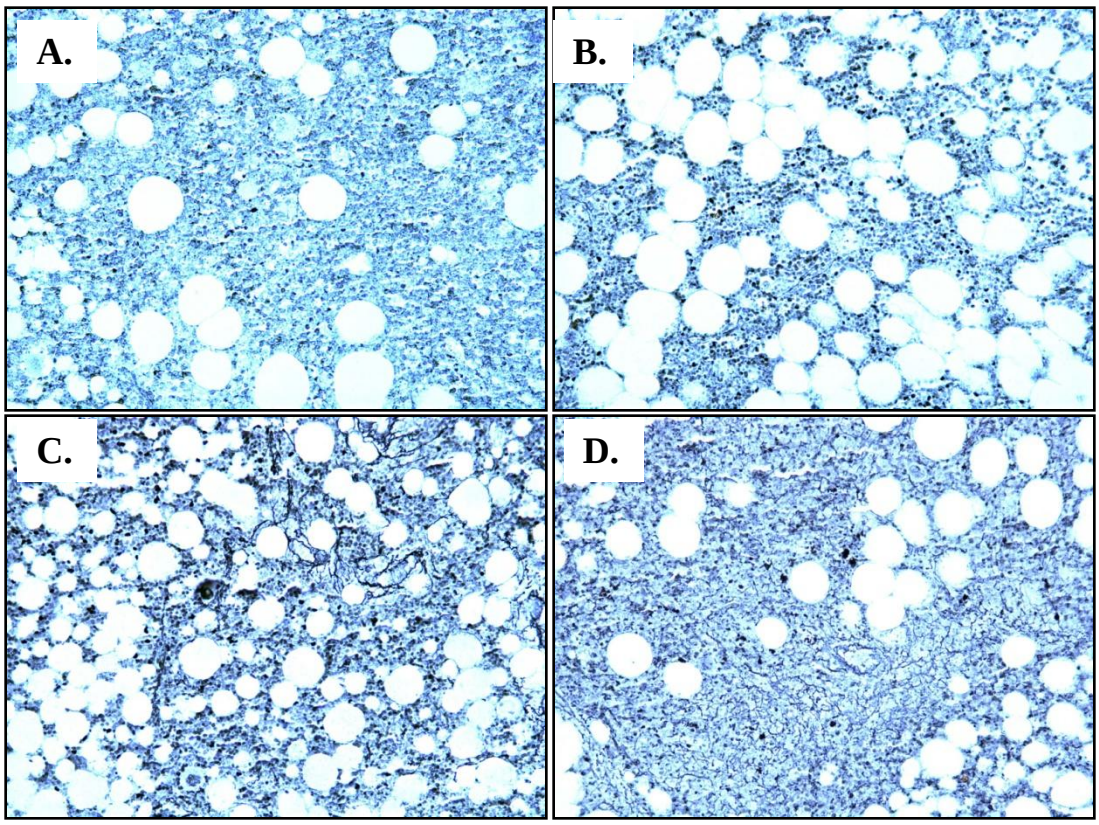

Figure 4.4. Images of bone marrow tissue fibrosis by grade
Photomicrographs of Gordon and Sweet's stained bone marrow tissue representing fibrosis by grade as black staining (Table 4.4). **A**. Grade 0 or minimal fibrosis, normal (macaque L750). **B**. Grade 1 mild fibrosis (macaque BI58). **C**. Grade 2 moderate fibrosis with minimal bundles (macaque L164). **D**. Grade 3 or excessive fibrosis with moderate bundles (macaque CB74). Field represents a 20X objective image (200X) on a Leica DMLb microscope (Leica; Bannockburn, IL) using Spot Insight color camera and Spot Imaging Software (Diagnostic Instruments; Sterling Heights, MI).

Statistical Analysis

For data evaluation, controls were non-SIV infected macaques and SIV infected subjects were grouped into periods defined as early and chronic based on disease progression as chronic asymptomatic SIV disease (ASY), chronic advanced SIV disease (ASD), and AIDS (Appendix II). Macaques developing AIDS were slow progressors at ≥260 DPI.

Statistical analyses were performed using non-parametric tests. Differences between the control group and each infected RM group for mean grade of BM morphologic assessments were

examined statistically using the one-sample t test (GraphPad Software; San Diego, CA) where the mean of the control RM served as the theoretical mean. Mean prevalence CBC data were examined statistically between the control group and each infected RM group using the Kruskal-Wallis one way analysis of variance (ANOVA) analysis (GraphPad Software). Differences between the control group and each infected RM group for hematologic data and phenotypic assessment were examined statistically using the Mann Whitney t test in GraphPad Prism (GraphPad Software). Correlations were compared using Spearman correlation coefficients (GraphPad Software). The mean of the data was represented in graphic illustration by phase of infection with the standard error of the mean (SEM) presented by the error bars. All comparisons were considered significant at $p \leq 0.05$.

RESULTS

Bone Marrow Cellularity During SIV Infection

One RM in the control group was not represented in BM morphologic analyses due to lack of detectable BM tissue in paraffin blocks (H741). One control had a hypocellular marrow and decreased M:E ratio attributed to decreased myeloid cells and increased erythroid cells (R534). A moderate correlation was detected between BM cellularity and BM M:E ratio (Spearman r =0.6032, p=0.0011).

Early in SIV infection, marrow cellularity was minimally changed from the control group, with no significant change to the M:E ratio (Figure 4.5). Macaques within the early period of SIV infection were 3/10 with a hypercellular marrow: 2 RM with unchanged M:E ratio (BI58, CB74) and 1 macaque as a decreased M:E ratio attributed to erythroid hyperplasia in response to anemia and myeloid hypoplasia (BN37). Only 1/10 macaques during the same period had an increased M:E ratio attributed to increased granulocytic cells, normocellular

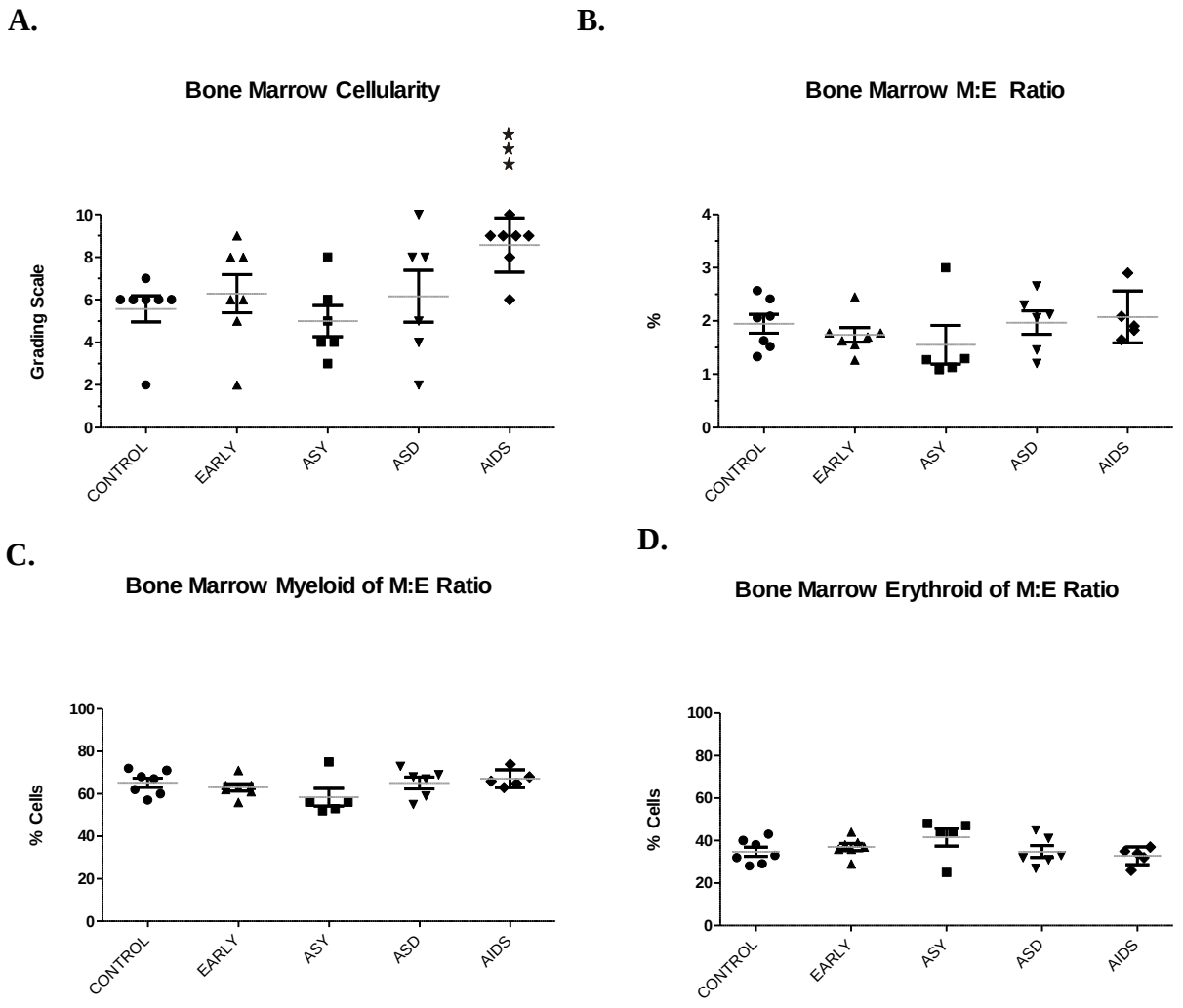

Figure 4.5. Comparison of bone marrow cellularity and M:E ratio during SIV infection Evaluation of control and SIV infected subjects by period of infection for bone marrow cellularity and myeloid to erythroid (M:E) ratio. **A.** Mean bone marrow cellularity by grade. **B.** Mean bone marrow M:E ratio. **C.** Myeloid component of M:E ratio by percentage of cells in bone marrow. **D.** Erythroid component of M:E ratio by percentage of cells in bone marrow. Comparisons between control cohort and each period of infection for cellularity and M:E ratio were determined by one sample t test (***$p \leq 0.01$). Periods of SIV infection were early, chronic asymptomatic SIV disease (ASY), chronic advanced SIV disease (ASD), and AIDS. Grey lines represent means $\pm$ SEM.

marrow, and neutropenia (BA17). One macaque had a hypocellular marrow and unchanged M:E ratio (BV13). A trend for hematologic abnormalities was noted in this phase (Table 4.5). Three macaques in this time period were not evaluated for cellularity or M:E ratio due to poor cellular preservation of marrow tissue sections (C419, L880, and T139).

Table 4.5. Prevalence Rate of Hematologic Abnormalities by Phase of SIV Disease

	Control (%)	Early (%)	Asymptomatic SIV Disease (%)	Advanced SIV Disease (%)	AIDS (%)
Anemia	0	20	14	67****	63
Thrombocytopenia	0	0	14	83****	25
Neutropenia	0	50	71****	33	13
Neutrophilia	0	20	0	33	30
Lymphopenia	50	60	71	67	100
Eosinophilia	25	0	14	0	13

****Significance $p \leq 0.05$ when compared to control cohort by ANOVA analysis

The M:E ratio of BM remained unchanged until decrease during the asymptomatic (ASY) period that paralleled a decrease in marrow cellularity and peak neutropenia ($p \leq 0.05$). Only 1/7 ASY period macaques had a hypercellular marrow with decreased M:E ratio attributed to increased erythroid cells (DE09). One macaque in this period had a hypocellular marrow but the M:E ratio was not evaluated (DB53). In the ASY period, 4/7 had a normocellular marrow. This included 2/4 with low M:E ratio attributed to decreased myeloid cells and increased erythroid cells (BV74) and neutropenia (DI28); 1/4 with anemia, thrombocytopenia, neutropenia and decreased M:E ratio attributed increased erythroid cells (N998); and 1/4 with increased M:E ratio, increased myeloid series, decreased erythroid series, and neutropenia (CF35). Additionally in the ASY phase, neutropenia prevalence peaked and TCP was observed which was also present in later stages of SIV. One macaque was not evaluated for marrow cellularity or M:E ratio due to minimal BM tissue in the formalin block (R908).

In the advanced SIV disease (ASD) period, cellularity of BM started to increase above non-infected levels as 50% macaques had a hypercellular BM: 2/3 with unchanged M:E ratios

and neutrophilia with anemia (AP53) and neutrophilia with TCP (BD78); 1/3 with increased M:E ratio attributed to increased granulocytic cells and decreased erythroid cells with anemia and TCP (BE64). One macaque had an unchanged marrow cellularity with a decreased M:E ratio characterized by decreased granulocytic cells and increased erythroid cells and neutropenia (CD95). One macaque had a hypocellular marrow with an unchanged M:E ratio and neutropenia (V205). Concurrently in ASD, as neutropenia prevalence dropped, neutrophilia and thrombocytopenia ($p \leq 0.05$), and anemia ($p \leq 0.05$) increased to peak prevalence (Table 4.5).

The apex of BM cellularity was in AIDS macaques with ~ 1.5X increase above the cellularity of controls ($p \leq 0.01$). None of the AIDS macaques had decreased marrow cellularity, as was observed in previous periods, though 1 had an unchanged marrow cellularity and anemia (BA25). The M:E ratio of macaques in AIDS was similar to control macaques with only 1 macaque detected with an increased M:E ratio characterized by an increase in granulocytic cells greater than the rise in erythroid cells (P045). One macaque was not evaluated for BM cellularity or M:E ratio due to observation of BM amyloid (I553). Two other macaques were not evaluated for M:E ratio due to poor PAS staining (R544, T798).

Hematopoietic CD34+ Stem Cells in During SIV Infection

CD34+ hematopoietic stem cells were detected in bone marrow and blood (Figure 4.6). Circulating stem cells were increased in the early period ($p \leq 0.001$) (Figure 4.7). In marrow, only the early and asymptomatic periods showed an increased trend of HSCs. The highest marrow percentage of stem cells was noted in the ASY period as total BM cellularity was the most depressed. Significant correlations were not detected between BM CD34 percentages and BM cellularity or BM M:E ratios.

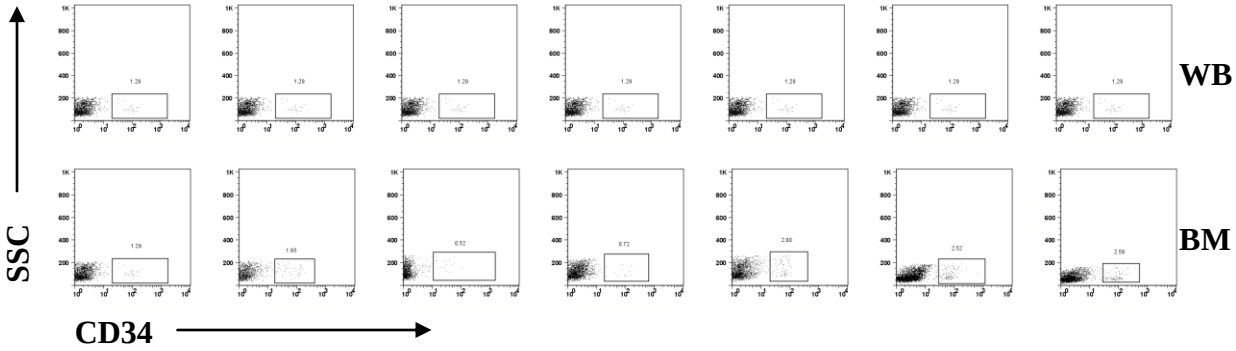

Figure 4.6. Hematopoietic stem cell identification
Phenotypic representation of CD34+ hematopoietic stem cell dot plots for the control cohort defined by flow cytometry gating (Figure 4.4). Upper panel is whole blood (WB). Lower panel is bone marrow (BM).

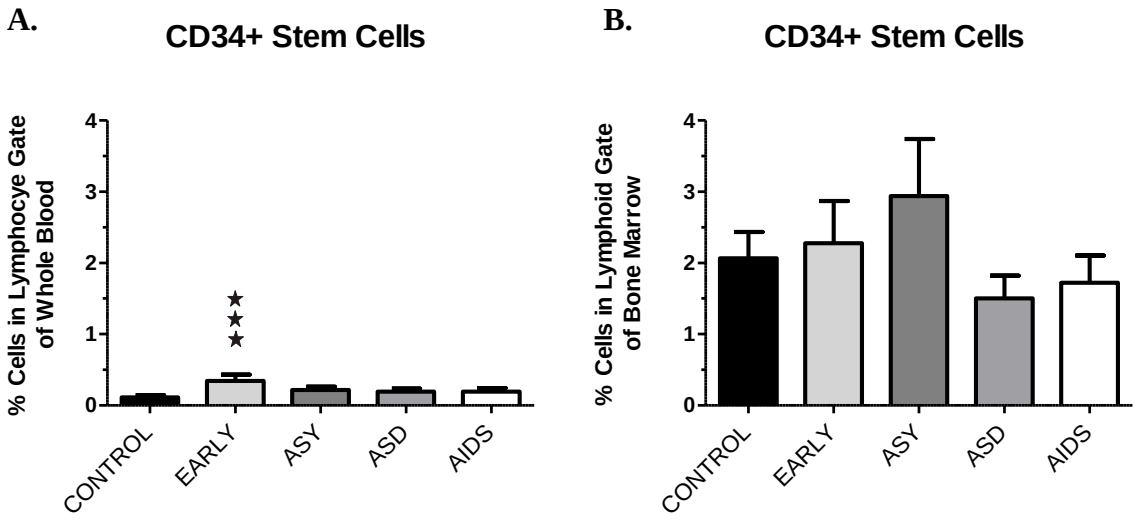

Figure 4.7. Comparison of hematopoietic stem cells during SIV infection
Percentage of CD34+ hematopoietic stem cells within the parent gate as shown in figure 4. 6 for blood (**A**.) or bone marrow (**B**.) in SIV infection. Comparison of control cohort and each period during SIV infection by Mann Whitney t tests (***$p \leq 0.01$). Periods of SIV infection were early, chronic asymptomatic SIV disease (ASY), chronic advanced SIV disease (ASD), and AIDS. Grey lines represent means $\pm$ SEM.

Bone Marrow Megakaryocytes During SIV Infection

The mean of the platelet concentration was lower in the early phase compared to controls without evidence of TCP and megakaryocyte hyperplasia was noted in 2 macaques (BI58, BN37) (Figure 4.8). Megakaryocytes were decreased in the ASY group, from the earlier phase, including 2 megakaryocytic hyperplastic and 1 hypoplastic macaques. TCP was present in the ASY phase in 1 macaque. During the ASD phase megakaryocytes were increased in BM ($p \leq 0.05$), with an almost double compared to the control group. TCP prevalence rates peaked at 83% ($p \leq 0.001$) in the ASD group, observed as 1/5 mildly TCP macaque with megakaryocyte hypoplasia (V205), and 4/5 were severely TCP. The four macaques with TCP included 2/4 with adequate megakaryocytes (BD78, L164), 1/4 with low megakaryocytes (CD95), and 1/4 with increased megakaryocytes (BE64). One macaque in the ASD group had BM megakaryocyte hyperplasia without TCP (AP53). Nearly 3X as many megakaryocytes compared to controls were present in 5/6 AIDS macaques including 1/6 with mild TCP (BE65), 1/6 with moderate TCP (R544), and 3/6 with adequate platelet concentrations (AE55, BI33, PO45, T798). Only 1 AIDS macaque was not observed with megakaryocyte hyperplasia (BA25). BM megakaryocyte positively correlated with BM cellularity (Spearman $r = 0.8239$, $p \leq 0.0001$) but not platelet count. Megakaryocytes were not identified with dysplastic changes and always were intact with multi-lobulated nuclei.

Bone Marrow Iron Content During SIV Infection

Iron content of marrow was adequate in controls without observance of anemia (Figure 4.9). Anemia of macaques post-infection was non-regenerative based on absence of a peripheral reticulocytosis. Depleted iron content in 9/10 macaques ($p \leq 0.0001$) in the early period, when a decreased hematocrit ($p \leq 0.05$) was also noted. During the early period, 2/9 macaques displayed

A. **B.**

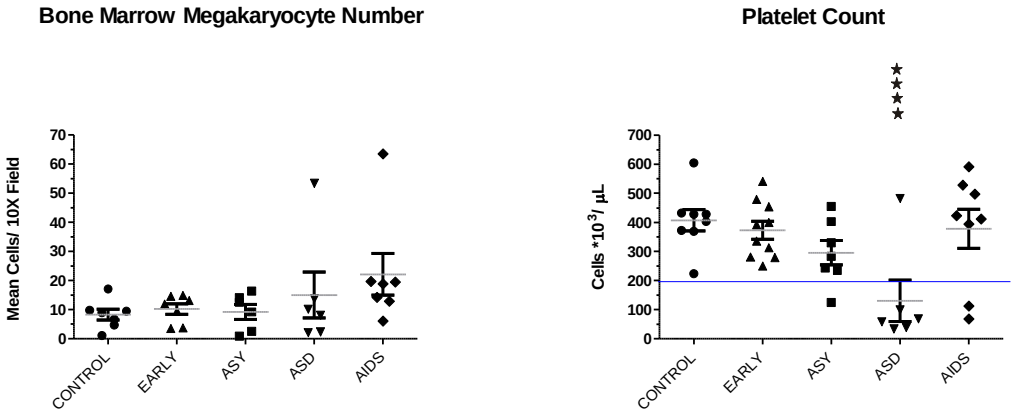

Figure 4.8. Comparison of megakaryocyte number and platelet count during SIV infection Evaluation of control and SIV infected subjects by period of infection for bone marrow megakaryocyte number and CBC platelet count. **A.** Mean megakaryocyte count of bone marrow per low power field. **B.** CBC platelet count with thrombocytopenia represented as values below blue horizontal line. Comparisons between control cohort and each period of infection for megakaryocyte numbers was determined by one sample t test and platelet counts by Mann Whitney t test (****$p \leq 0.05$). Periods of SIV infection were early, chronic asymptomatic SIV disease (ASY), chronic advanced SIV disease (ASD), and AIDS. Grey lines represent means $\pm$ SEM.

A. **B.**

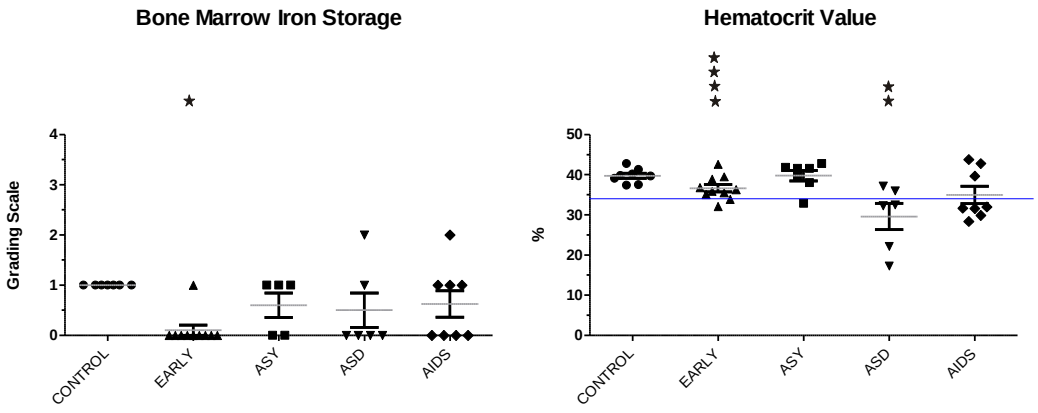

Figure 4.9. Comparison of bone marrow iron content and hematocrit value during SIV infection

Evaluation of control and SIV infected subjects by period of infection for grade of bone marrow iron content and CBC hematocrit value. **A.** Subjective grade of bone marrow iron content. **B.** Hematocrit value with anemia represented as values below blue horizontal line. Comparisons between control cohort and each period of infection for iron content was determined by one sample t test and for hematocrit values by Mann Whitney t test (*$p \leq 0.0001$, **$p \leq 0.001$, and ****$p \leq 0.05$). Periods of SIV infection were early, chronic asymptomatic SIV disease (ASY), chronic advanced SIV disease (ASD), and AIDS. Grey lines represent means $\pm$ SEM.

a normocytic normochromic anemia consistent with AIRD (BI58, BN37). In the ASY period, anemia prevalence decreased from 20% to 14%, as 1/7 macaques showed normocytic normochromic anemia and Grade 1 BM iron content (N998). In the asymptomatic phase, 2/7 macaques lacked anemia but had decreased BM iron stores (BV74, DI28). Anemia prevalence tripled to 67% ($p \leq 0.05$) in the ASD period with minimal changes in BM iron content from the ASY phase. Infected macaques in ASD revealed 4/6 had Grade 0 BM iron content but only 2/4 showed a normocytic normochromic anemia (CD95, L164) and 2/4 were not anemic (BD78, V205). One macaque in this period had increased marrow iron content and microcytic hypochromic anemia (AP53) and one macaque had normal iron content with microcytic

normochromic anemia (BE64). Anemia prevalence (63%) and BM iron storage did not change in AIDS with 3/8 having a normocytic normochromic anemia and decreased iron content (AE55, BE65, R544) and 2/8 macaques with a normocytic normochromic anemia and adequate iron storages suggestive of ACD (BA25, T798). The remaining 3/8 macaques were not anemic, and 1/8 had low BM iron (BI33); 1/8 with adequate BM iron (P045); and 1/8 had increased BM iron (I553). Microscopically, erythroid dysplasia was not observed in the marrow of any macaques. Anemia was not associated with AIDS diagnosis. A low correlation was noted between BM iron storage and BM M:E ratio (Spearman r =0.4663, p=0.0041). A correlation was not present between bone marrow iron stores and BM cellularity, mean cell hemoglobin concentration (MCHC), mean cell volume (MCV), or HCT.

Lymphoid Aggregates in Bone Marrow During SIV Infection

Lymphocyte aggregates were observed in cellular areas of BM, but were not defined follicles with germinal centers, similar to described patterns of poorly defined aggregates in random distribution by Shenoy and Lin, and Delacrétaz et al. (Delacrétaz 1987; Shenoy 1986).

BMLA Grade 1 composed of mature small lymphocytes was considered a normal finding, therefore BMLA Grade 1 composed of variably sized lymphocytes or BMLA Grade 2 and higher were considered abnormal morphologic findings.

BMLA were increased in number during the early period ($p \leq 0.05$) with variable morphologic sizes (Table 4.6). Highest grades of BMLA were observed in AIDS macaques also with different morphologic sizes. Lymphoid neoplasia, plasma cells, and atypical lymphocytes were not observed in BMLA or bone marrow sections examined. BMLA grades were not correlated with the absolute lymphocyte concentration in blood.

Table 4.6. Bone Marrow Lymphoid Aggregates (BMLA) during SIV infection

Subject Identification	Phase of SIV Disease, Histologic Diagnosis	Age years, Necropsy	BMLA Grade	Lymphocyte Population, Size	Histiocyte Population
EH70	Uninfected	3	1	>95% Small	<5%
AV85	Early	8	2	>90% Small	<10%
BA17	Early	8	2	~50% Variable	~50%
BI58	Early	3	2	~50% Variable	~50%
BN37	Early	2	2	>95% Small	<5%
C419	Early	20	1	>90% Small	<10%
BV74	ASY[a]	5	1	>90% Small	<10%
CD95	ASD[b], Right heart failure	8	2	>90% Small	<10%
L164	ASD[c], Colitis	13	1	>90% Small	<10%
BE65	AIDS, *Mycobacterium avium*	6	1	~50% Large	~50%
R544	AIDS, Meningoencephalitis	9	3	>90% Small	<10%
T798	AIDS, *Mycobacterium avium*	9	2	~90% Large	~10%

a) ASY = asymptomatic SIV disease; b) ASY = asymptomatic SIV disease; c) ASD = advanced SIV disease

Bone Marrow Fibrosis During SIV Infection

Marrow fibrosis was not detected in non-infected RM or in the ASY period (Figure 4.10). Marrow fibrosis was noted in almost 50% of RM in other periods of SIV infection with peak in the early phase ($p \leq 0.05$). Reticulin staining of marrow was focally located and linear in appearance yet not associated with lymphoid follicles or blood vessels.

DISCUSSION

Our findings of increased BM cellularity in 26% of non-AIDS macaques, 50% ASD, and 86% of AIDS macaques were higher than reports of 16% hypercellular marrow in HIV infected non-AIDS patients (Tripathi 2005), 31% symptomatic non-AIDS HIV patients (Namiki 1987; Sun 1989), and 18-50% HIV AIDS patients (Namiki 1987; Ricci 1995; Sun 1989; Tripathi 2005). Although conceivable, the SIV model could be an exaggeration of these changes, discrepancies in detection may occur due to lack of standardized categorization of infected subjects, or selection criteria in human studies, as described in the earlier chapter, may also make direct comparisons invalid.

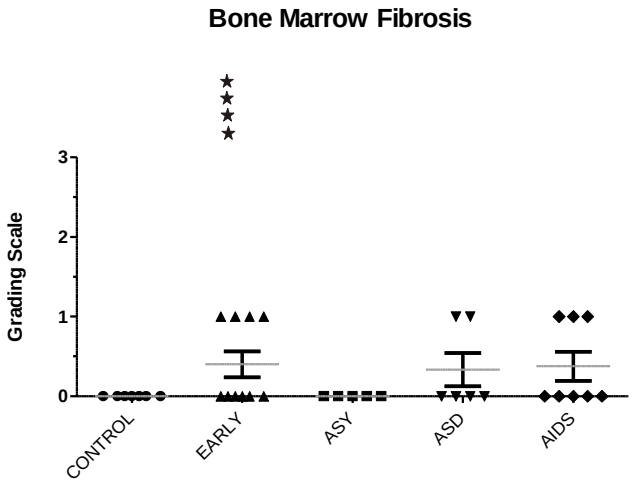

Figure 4.10. Comparison of bone marrow fibrosis during SIV infection
Evaluation of control and SIV infected subjects by period of infection for grade of bone marrow fibrosis. Comparisons between control cohort and each period of infection for fibrosis was determined by one sample t test (****$p \leq 0.05$). Periods of SIV infection were early, chronic asymptomatic SIV disease (ASY), chronic advanced SIV disease (ASD), and AIDS. Grey lines represent means $\pm$ SEM.

Here, we detected 42% of RM in the early phase of SIV infection with hypercellular BM consistent with findings of Mandell et al. of hypercellular bone marrow in 50% of early SIVmac239 infected RM (Mandell 1993). Kitagawa et al. reported 46% of SIV infected RM with BM hypercellularity (Kitagawa 1991). Baskin et al. reported 7/24 RM infected with hypercellular marrow in AIDS (Baskin 1988). A few macaques in each group of our study were noted with a hypocellular BM except in the AIDS phase. Delacrétaz identified megakaryo- and erythrodysplastic BM changes in HIV patients but noted these two conditions are easier to identify on plastic embedded specimens compared to detection of granulodysplastic changes (Delacrétaz 1987). Myelodysplastic changes may be due to indirect or direct HIV infection, anti-microbial or ART drugs, or secondary infections (Ryu 2001). However, evidence of myelodysplasia was not identified in our study.

The BM morphologic M:E mean of the control group of macaques was 1.94±0.46 which was similar to reported reference intervals for RM at 0.86-1.91:1 (Huser 1970; Jain 1986; Stasney 1936; Switzer 1967). In general we observed, a decreased M:E ratio due to BM cellular decline in granulocytic/monocytic lineage and an equal or greater cellular rise in erythroid lineage. We observed an increased M:E ratio was attributed to increased BM granulocytic/monocytic cells and an equal or lesser relative drop in erythroid cells. Post-infection the lowest M:E ratio was 1.88 in the asymptomatic phase and the highest 2.076 in AIDS, all within the control study range means. Nearly twice as many infected macaques (52%) were within the M:E control range than below (22%) or above the range (26%). Similarly, 25% of SIV infected RM were noted with an increased M:E ratio (Kitagawa 1991). Of note, in the ASY phase all macaques were outside the M:E control range with 4/5 below and 1/5 above and all AIDS macaques were within or above the control range M:E ratio. Infected macaque M:E ratios were similar in distribution to M:E ratios of HIV patients with reports of normal 50-72 %, 5-40% elevated, and 10-22% decreased (Castella 1985; Delacrétaz 1987; Ricci 1995).

CD34+ circulating hematopoietic stem cells remained similar between control and SIV infected macaques in our study as supported by findings in HIV patients reported by Costantini et al (Costantini 2009; Marandin 1996). Increases in BM CD34+ cells early in SIV infection were supported by findings in SIV infected RM by Hillyer et al (Hillyer 1993b). Our finding of decreased marrow CD34+ HSC in later stages of SIV was supported by by SIV studies by Hillyer et al. and van Wely et al. but contrary to reports by Marandin et al. (De Luca 1993; Hillyer 1993b; Marandin 1996; van Wely 1993).

Culture studies of BM CD34+ stem cells from HIV infected patients revealed decreased HSC in later stages with most effect noted in AIDS (Marandin 1996). Steinberg et al. found

lower numbers of BM precursor cells when HIV was incubated with pure cultures of CD34+ BM HSC (Steinberg 1991). In vitro growth of hematopoietic progenitor colonies was decreased from the BM mononuclear cells obtained in AIDS and symptomatic HIV patients (De Luca 1993; Leiderman 1987; Stella 1987), SIVmac infected RM (Watanabe 1990), and SHIV inoculated cynomolgus macaques within 21 DPI (Thiebot 2001). Overnight incubation of HIV with human BM cells from non-HIV infected patients and depleted of accessory cells resulted in decreased in vitro growth of myeloid, erythroid, lymphoid, and CD34+ precursor cells (Steinberg 1991). One theory proposed is that HIV progenitor cells may become infected with HIV but hematopoiesis is unlikely to be disturbed unless HIV antibodies suppress myelopoiesis (Donahue 1987; Leiderman 1987; Stella 1987). CD34+ marrow HSC were shown to be infected wihtin HIV patients, *in vivo* (Carter 2010). *In vitro*, CD34+ HSC sorted from bone marrow aspirates were incubated with HIV89.6 and 3 days later, infection of HSC was detected by Gag protein (Carter 2010). However, the lower percentage of HSC in SIV macaques in our study did not affect overall BM cellularity and megakaryocytes in AIDS macaques though prevalence of hematologic abnormalities increased over time. In fact, BM cellularity was lowest in the ASY phase as percentage of HSC was highest.

Mandell et al. reported 2/6 RM infected with SIVmac239, <14 DPI, displayed megakaryocytic hyperplasia (Mandell 1993) similar to our findings of 2/7 RM in the early phase of SIV infection. Both the ASY and ASD phases of SIV infection were noted to have 2 macaques with megakaryocyte hyperplasia and 1 macaque with megakaryocyte hypoplasia compared to the final phase with hyperplasia in 6/7 macaques. Higher numbers of megakaryocytes were noted in BM from HIV infected patients ranging from 33-78% (Castella 1985; Khalil 1996; Ricci 1995; Shenoy 1986; Zucker-Franklin 1989) and 38% from SIV infected

RM (Kitagawa 1991). Megakaryocyte hypoplasia has been reported rarely in HIV patients (Castella 1985) and in 3 infected RM and 1 control RM in our study. Denuded nuclei or hypolobulation and megakaryocytic emperipolesis have been observed in megakaryocytes of HIV patients (Gordon 1994; Karcher 1991; Khandekar 2005; Ricci 1995; Tripathi 2005; Zucker-Franklin 1989) though not detected in our study.

Correlations were not present between BM megakaryocytes, and platelet concentration, or mean platelet volume in our study. Koenig et al. observed 92% of TCP HIV patients had low mean platelet volume and few non-TCP HIV patients had low mean platelet volume and theorized HIV had a direct effect on megakaryocytes to produce small platelets (Koenig 1991). Alternatively, Karcher and Frost identified a correlation between megakaryocyte hypoplasia and thrombocytopenia in HIV patients (Karcher 1991) and Castella et al. noted ~30% of HIV patients had adequate to increased megakaryocytes with concurrent TCP (Castella 1985).

Megakaryocyte numbers were increased over the controls for all post-infection phases while blood platelet concentrations were decreased during the same time periods. With increased BM megakaryocytes, shown here, peripheral platelet counts would be expected. Decreased megakaryocyte precursors have been reported in HIV patients with megakaryocyte hyperplasia indicating possible HIV effect on megakaryocytopoiesis possibly through ineffective production by direct infection or inhibitory cytokines (Cole 1998). Thrombocytopenic HIV patients were observed with splenic sequestration of platelets, increased marrow megakaryocytes, ineffective marrow platelet production, shortened platelet life spans, and antiplatelet antibodies to glycoprotein IIIa (Cole 1998). Autoantibody platelet production, elevated mean platelet volume or production of large platelets, absence of marrow megakaryocyte abnormalities, and appropriate marrow response to low platelet concentrations are hallmarks of immune mediated

TCP (Cole 1998; Harris 1990). TCP may be due to marrow and peripheral mechanisms during HIV infection which could explain TCP and marrow findings of the SIV infected macaques in this study.

A moderate positive correlation was found between BM cellularity and BM megakaryocyte numbers (Spearman correlation $r=0.6439$, $p<0.0001$) with both climaxing during AIDS. A moderate positive correlation was noted between BM megakaryocytes and both BM fibrosis (Spearman correlation $r=0.6439$, $p<0.0001$) and iron storage (Spearman correlation $r=0.6439$, $p<0.0001$). The megakaryocyte count showed a low positive correlation to the M:E ratio (Spearman correlation $r=0.4459$, $p=0.0174$) though peak in AIDS was absent. Finally, megakaryocytes also positively correlated with BM lymphoid follicle hyperplasia though low (Spearman correlation $r=0.3616$, $p=0.0387$) without similarities in patterns.

Anemia in SIV infected macaques was more severe in symptomatic versus asymptomatic macaques over controls in our study. This was previously reported by Hillyer et al. findings of "well" versus "sick" SIV infected macaques (Hillyer 1993a). Infected macaques in our study were not observed with histologic, CBC abnormalities, or erythrocyte morphologic changes supportive of hemolysis or bleeding or regenerative anemias. Infected macaques displayed depleted BM iron stores at 53% and 13% displayed adequate to increased BM iron stores compared to HIV patients at 11-25% and 10-85% respectively (Castella 1985; Harris 1990; Karcher 1991; Khalil 1996; Sun 1989; Zhao 2004).

Anemia of iron deficiency (AIRD) is characterized by absent BM iron stores and early in the condition is a normocytic normochromic anemia that progressively develops into a microcytic hypochromic anemia (Glader 2004). Anemia of chronic inflammatory disease (ACD) is characterized by normal to increased BM iron stores and a normocytic normochromic anemia

(Glader 2004). Anemia was absent in controls in this particular study, but detected in the early period and was consistent with AIRD by normocytic and normochromic profile and low marrow iron content. During the ASY period, AIRD persisted but macaques also had normocytic normochromic anemia and Grade 1 BM iron content supportive of ACD, indicating mixed mechanisms for anemia were present, which may be related to stage of infection. Non-regenerative anemia, AIRD or ACD, was noted in our studies with occasional erythroid marrow hyperplasia and without marrow erythroid dysplasia. Mixed mechanisms for anemia continued to be detected in the ASD and AIDS periods.

Hillyer et al. observed regenerative anemias in infected macaques with diagnoses of autoimmune hemolytic anemias, increased to normal erythropoietin levels, BM erythroid hyperplasia, dyserythropoiesis, and decreased *in vitro* BFU-E colony formation (Hillyer 1993a). ACD is associated in humans with blunted erythropoietin levels (Khandekar 2005) which may not be the cause in SIV as Hillyer et al. found increased erythropoietin in SIV infected RM (Hillyer 1993a). Multifactorial causes for anemia include destruction of erythrocytes, folic acid/B_{12} deficiencies, decreased BM erythroid stem cells, cytokine inhibition, iron deficiency, anti-microbial or ART drugs, or OI (Costantini 2009; de Monye 1999; Hillyer 1993a; Khandekar 2005; Schneider 1985; Steinberg 1991; Thiebot 2001; Zhao 2004). A retrospective study of BM iron content in 348 adult HIV patients revealed markedly increased grades were associated with low hemoglobin values, decreased survival time, BM dysplasia, and pneumocystis or mycobacterial infections (de Monye 1999). Associations were not noted in our study with BM iron storage to CBC values, viral load, fibrosis, or AIDS diagnosis. A study of AIDS patients observed high marrow iron content in HIV patients diagnosed with myocbacterial disease, Pneumocystis pneumonia, or candidiasis (de Monye 1999). A positive correlation was noted

between BM iron storage and M:E ratio and based on our study, hematocrit is not based on BM changes alone. A negative low correlation was present between BM iron content and BMLA (Spearman correlation= -0.3418, p=0.0413).

BMLA were detected during the early period (40%) as viral load crested then again in the final stage of AIDS (38%). Our study results for BMLA were higher than 16% reported in SIV infected RM by Kitagawa et al. (Kitagawa 1991). King et al. observed 3/16 SIV infected macaques in AIDS demonstrated lymphoid aggregates composed of small lymphocytes (King 1983) compared to our 2/8 AIDS macaques Grade 1 or 2 BMLA composed of mostly large-sized lymphocytes, and 1/8 AIDS macaques with Grade 3 BMLA composed of small-sized lymphocytes. In our study, both AIDS RM co-infected *M. avium* displayed BMLA accentuated with variable sized lymphocytes and histiocytes while AIDS RM co-infected with *Pneumocystis spp* did not have BMLA. Personal communication from Dr. Peter Didier, TNPRC Anatomic Pathologist, noted he frequently found BMLA in AIDS RM diagnosed with *M. avium* (Didier 2009).

Our findings of lymphoid aggregates have been suggested by Karcher et al. as non-specific HIV findings in BM caused by inflammation or immune stimulation, not OI or lymphoma (Karcher 1991). BMLA composed of small mature lymphocytes have been reported in healthy younger humans while frequency increases with age (Castella 1985). Geller et al. in 1985 originally described the 'AIDS pattern' of BM including defined clusters of large-sized lymphocytes (Geller 1985). Further, Karcher et al. and others have documented most lymphoid aggregates of HIV patients by morphologic characteristics as poorly defined clusters of mostly small mature lymphocytes with few aggregates containing larger-sized lymphocytes occasionally with histiocytes (Castella 1985; Delacrétaz 1987; Harris 1990; Karcher 1991; Khalil 1996;

Shenoy 1986; Sun 1989; Zhao 2004). Our study of SIV infected RM showed variable morphology with multiple lymphoid aggregates compared to small mature lymphocytes in single lymphoid aggregates per tissue. Additionally, BM plasmacytosis was absent in our study though 13-78% has been reported in HIV patients (Castella 1985; Delacrétaz 1987; Harris 1990; Karcher 1991; Khalil 1996; Shenoy 1986; Zhao 2004). Finally, 0-37% BM lymphoma and 0-15% BM Kaposi's sarcoma has been reported in HIV patients (Castella 1985; Delacrétaz 1987; Harris 1990; Karcher 1991; Khalil 1996; Shenoy 1986; Sun 1989; Zhao 2004) while these findings were not expected in our RM with prior reports of 0% and 0% respectively (Baskin 2001).

Myelofibrosis is increased connective tissue or collagen in bone marrow (Scott 2008). Myelofibrosis and disruption of stromal elements to support bone marrow homeostasis can lead to dysregulation of hematopoiesis (O'Malley 2005). Marrow fibrosis may consist of reticulin fibrosis characterized by reticulin staining or collagen fibrosis characterized by collagen IV staining (Apaja-Sarkkinen 1986). Reticulin staining exposes type III procollagen which is a component of the marrow extracellular matrix and identified by Gomori's reticulin stain (Apaja-Sarkkinen 1986). Fibrosis was present early (40%) and during symptomatic phases of SIV infection, 33% ASD and 37% AIDS, in macaques of this study. Reticulin stain of BM from HIV patients ranged from 0-83% though the type of stain was not defined (Castella 1985; Delacrétaz 1987; Harris 1990; Karcher 1991; Khalil 1996; Tripathi 2005). Less than half of SIV infected macaques of our study displayed BM fibrosis in AIDS while O'Malley at al. described 100% BM fibrosis in HIV AIDS patients by reticulin staining and minimal actin or collagen IV positive staining (O'Malley 2005).

BM fibrosis may be a non-specific HIV finding related more to inflammation or immune stimulation (Karcher 1991; O'Malley 2005), similar to lymphocyte aggregations in marrow of HIV infected patients. However, here we demonstrated a low correlation between the occurrence of BMLA and fibrosis in marrow from SIV infected RM (Spearman correlation r=0.3662, p=0.0281). Gelatinous transformation of marrow, another stromal abnormality of bone marrow, is defined by BM hypoplasia, BM adipose tissue atrophy, and extracellular gelatinous material (Alcian blue stain positive, PAS stain variable) seen in starving or cachectic people has been identified in 9-38% of HIV patients including reports of up to 100% AIDS patients (Delacrétaz 1987; Karcher 1991; Murugan 2007). We observed 1 AIDS macaque with a hypercellular marrow and extracellular material Alcian blue stain positive attributed to amyloid (I553).

Histiocytic infiltration of BM and evidence of phagocytosis have been reported in HIV patients but were not observed as the sole composition of aggregates or in increased numbers in this study (Harris 1990; Karcher 1991; Khalil 1996; Khandekar 2005; Sun 1989). Granulomas were rarely indentified in BM of SIV infected macaques in this study but reported 12-35% in HIV patients often associated with the identification of fungi and acid fast bacteria by special stains (Castella 1985; Harris 1990; Khalil 1996; Shenoy 1986; Sun 1989; Zhao 2004).

A common finding of marrow in HIV patients has been myelodysplasia (Karcher 1991). Myelodysplasia in HIV patients has been attributed to direct effect of marrow by HIV disease and drug therapy (Karcher 1991). Criteria for diagnosis of myelodysplasia may be variable (Karcher 1991), but diagnosis is commonly made by microscopic evaluation of bone marrow aspirates that were not evaluated in this study. Delacretaz et al. first reported myelodysplastic changes evident in de-calcified paraffin embedded formalin fixed bone marrow sections from

HIV infected patients (Delacrétaz 1987). Future studies of bone marrow aspirates in SIV infected macaques may reliably detect myelodysplasia.

Lymphopenia, anemia, thrombocytopenia, neutropenia, and neutrophilia occurred in RM following infection with SIV. However, response of BM to increased or decreased peripheral cell changes could not be fully evaluated because all observations in this study observation were one-time evaluations. CBC abnormalities during progressive SIV infection were consistent and supported the hypothesis that loss of bone marrow homeostasis contributes to the hematologic changes observed during progression to AIDS. Hematologic abnormalities from this study were supported by the preceding serial CBC results of SIV infected RM (Chapter 3).

Observed BM morphologic and phenotypic changes along with hematologic abnormalities during progressive SIV infection were characteristic of HIV disease and reports of HIV myelopathy. Increased BM cellularity, myeloid and erythroid lineage shifts, fibrosis, iron depletion, and BMLA were observed morphologic changes during periods of SIV disease also reported in HIV patients. Additionally, decline of BM HSC percentages in later stages of SIV were detected by phenotypic BM examination, and also consistent with HIV patients. Our study verifies BM changes are evident during SIV infection and representative of progressive HIV disease. Also, our study confirms SIV alone contributes to BM deviations from homeostasis regardless of therapeutic intervention, and that BM changes contribute to occurrence of hematologic abnormalities.

SUMMARY

Rhesus macaques inoculated with SIV without interventional drug or vaccine therapy were evaluated to fully assess changes in bone marrow from early to late stages of disease. Patterns of BM and hematologic changes were noted during progressive phases of SIV infection

defined by clinical signs and days post-inoculation. SIV infected macaques in the early phase of infection with high viremia had BM changes including increased circulating and BM CD34+ hematopoietic stem cells, BM iron depletion, increased BM lymphoid aggregates, and BM fibrosis, though correlations with viral load were not detected. Neutropenia prevalence spiked in the next asymptomatic SIV disease (ASY) period as BM cellularity dropped to lowest levels, characterized by loss of granulocytic/monocytic lineage cells and rise in erythroid lineage cells that lead to a depressed M:E ratio, while BM CD34+ hematopoietic stem cells peaked. However, in advanced SIV disease or AIDS, BM CD34+ cells were depressed and fibrosis was detected in almost 50% of macaques as BM cellularity started to rise and the M:E ratio returned to within control intervals. In the ASD phase, anemia, thrombocytopenia, and neutrophilia prevalence climaxed. Pan hyperplasia of BM with resultant hypercellularity including lymphoid aggregation was present consistently as were most hematologic abnormalities during AIDS. In AIDS, the M:E ratio was characterized by a return of the myeloid series to control intervals and a loss of the erythroid lineage. Observed BM abnormalities in SIV infected macaques were characteristic of reported changes and ranges in HIV patients and implicate SIV infection alone rather than therapeutics for observed bone marrow disturbances. Finally, hematologic changes involved BM and peripheral mechanisms.

Again, natural SIV disease progression in the macaque model emulates bone marrow changes and hematologic abnormalities well documented during HIV disease. Deviation of bone marrow from the steady state was present during early and later stages of SIV disease in macaques. Examination of phenotypic population changes in bone marrow during early and late SIV infection is described in subsequent chapters to confirm and expand these morphologic observations.

REFERENCES

Apaja-Sarkkinen, M., Autio-Harmainen, H., Alavaikko, M., Risteli, J., and Risteli, L. (1986). Immunohistochemical study of basement membrane proteins and type III procollagen in myelofibrosis. British journal of haematology *63*, 571-580.

Baskin, G.B., Cremer, K.J., and Levy, L.S. (2001). Comparative pathobiology of HIV- and SIV-associated lymphoma. AIDS research and human retroviruses *17*, 745-751.

Baskin, G.B., Murphey-Corb, M., Watson, E.A., and Martin, L.N. (1988). Necropsy findings in rhesus monkeys experimentally infected with cultured simian immunodeficiency virus (SIV)/delta. Veterinary pathology *25*, 456-467.

Carter, C.C., Onafuwa-Nuga, A., McNamara, L.A., Riddell, J.t., Bixby, D., Savona, M.R., and Collins, K.L. (2010). HIV-1 infects multipotent progenitor cells causing cell death and establishing latent cellular reservoirs. Nat Med *16*, 446-451.

Castella, A., Croxson, T.S., Mildvan, D., Witt, D.H., and Zalusky, R. (1985). The bone marrow in AIDS. A histologic, hematologic, and microbiologic study. Am J Clin Pathol *84*, 425-432.

Cole, J.L., Marzec, U.M., Gunthel, C.J., Karpatkin, S., Worford, L., Sundell, I.B., Lennox, J.L., Nichol, J.L., and Harker, L.A. (1998). Ineffective platelet production in thrombocytopenic human immunodeficiency virus-infected patients. Blood *91*, 3239-3246.

Costantini, A., Giuliodoro, S., Butini, L., Silvestri, G., Leoni, P., and Montroni, M. (2009). Abnormalities of erythropoiesis during HIV-1 disease: a longitudinal analysis. Journal of acquired immune deficiency syndromes (1999) *52*, 70-74.

De Luca, A., Teofili, L., Antinori, A., Iovino, M.S., Mencarini, P., Visconti, E., Tamburrini, E., Leone, G., and Ortona, L. (1993). Haemopoietic CD34+ progenitor cells are not infected by HIV-1 in vivo but show impaired clonogenesis. British journal of haematology *85*, 20-24.

de Monye, C., Karcher, D.S., Boelaert, J.R., and Gordeuk, V.R. (1999). Bone marrow macrophage iron grade and survival of HIV-seropositive patients. AIDS (London, England) *13*, 375-380.

Delacrétaz, F., Perey, L., Schmidt, P.M., Chave, J.P., and Costa, J. (1987). Histopathology of bone marrow in human immunodeficiency virus infection. Virchows Arch A Pathol Anat Histopathol *411*, 543-551.

Didier, P. (2009). Bone marrow follicular hyperplasia during AIDS in SIV infected RM with Mycobacterium avium, A.F. GIll, ed. (Covington, LA).

Donahue, R.E., Johnson, M.M., Zon, L.I., Clark, S.C., and Groopman, J.E. (1987). Suppression of in vitro haematopoiesis following human immunodeficiency virus infection. Nature *326*, 200-203.

Gale, E., Torrance, J., and Bothwell, T. (1963). The quantitative estimation of total iron stores in human bone marrow. J Clin Invest *42*, 1076-1082.

Geller, S.A., Muller, R., Greenberg, M.L., and Siegal, F.P. (1985). Acquired immunodeficiency syndrome. Distinctive features of bone marrow biopsies. Archives of pathology & laboratory medicine *109*, 138-141.

Glader, B. (2004). Anemia: General Considerations. In Wintrobe's Clinical Hematology, J. Greer, J. Foerster, J.N. Lukens, G.M. Rodgers, F. Paraskevas, and B. Glader, eds. (Philadelphia, Lippincott Williams & Wilkins), pp. 947-978.

Gordon, S., and Lee, S. (1994). Naked megakaryocyte nuclei in bone marrows of patients with acquired immunodeficiency syndrome: a somewhat specific finding. Mod Pathol *7*, 166-168.

Harris, C.E., Biggs, J.C., Concannon, A.J., and Dodds, A.J. (1990). Peripheral blood and bone marrow findings in patients with acquired immune deficiency syndrome. Pathology *22*, 206-211.

Hillyer, C.D., Klumpp, S.A., Hall, J.M., Lackey, D.A., 3rd, Ansari, A.A., and McClure, H.M. (1993a). Multifactorial etiology of anemia in SIV-infected rhesus macaques: decreased BFU-E formation, serologic evidence of autoimmune hemolysis, and an exuberant erythropoietin response. Journal of medical primatology *22*, 253-256.

Hillyer, C.D., Lackey, D.A., 3rd, Villinger, F., Winton, E.F., McClure, H.M., and Ansari, A.A. (1993b). CD34+ and CFU-GM progenitors are significantly decreased in SIVsmm9 infected rhesus macaques with minimal evidence of direct viral infection by polymerase chain reaction. Am J Hematol *43*, 274-278.

Huser, H.-J. (1970). II. Morphology and Meylograms. In Atlas of Comparative Primate Hematology (New York, Academic Press, Inc.), pp. 160-178.

Jain, N.C. (1986). Normal Values in Blood of Laboratory, Fur-Bearing, and Miscellaneous Zoo, Domestic, and Wild Animals. In Schalm's Veterinary Hematology (Philadelphia, PA, Lea & Febiger), pp. 274-349.

Karcher, D.S., and Frost, A.R. (1991). The bone marrow in human immunodeficiency virus (HIV)-related disease. Morphology and clinical correlation. Am J Clin Pathol *95*, 63-71.

Khalil, S.H., Nounou, R.M., Frayha, H., Halim, M.A., Ellis, M., and Black, F.T. (1996). Bone marrow morphologic findings in patients with human immunodeficiency virus (HIV) infection. Ann Saudi Med *16*, 16-19.

Khandekar, M.M., Deshmukh, S.D., Holla, V.V., Rane, S.R., Kakrani, A.L., Sangale, S.A., Habbu, A.A., Pandit, D.P., Bhore, A.V., Sastry, J., *et al.* (2005). Profile of bone marrow examination in HIV/AIDS patients to detect opportunistic infections, especially tuberculosis. Indian journal of pathology & microbiology *48*, 7-12.

King, N.W., Hunt, R.D., and Letvin, N.L. (1983). Histopathologic changes in macaques with an acquired immunodeficiency syndrome (AIDS). The American journal of pathology *113*, 382-388.

Kitagawa, M., Lackner, A.A., Martfeld, D.J., Gardner, M.B., and Dandekar, S. (1991). Simian immunodeficiency virus infection of macaque bone marrow macrophages correlates with disease progression in vivo. The American journal of pathology *138*, 921-930.

Koenig, C., Sidhu, G.S., and Schoentag, R.A. (1991). The platelet volume-number relationship in patients infected with the human immunodeficiency virus. Am J Clin Pathol *96*, 500-503.

Leiderman, I.Z., Greenberg, M.L., Adelsberg, B.R., and Siegal, F.P. (1987). A glycoprotein inhibitor of in vitro granulopoiesis associated with AIDS. Blood *70*, 1267-1272.

Mandell, C.P., Jain, N.C., Miller, C.J., Marthas, M., and Dandekar, S. (1993). Early hematologic changes in rhesus macaques (Macaca mulatta) infected with pathogenic and nonpathogenic isolates of SIVmac. Journal of medical primatology *22*, 177-186.

Marandin, A., Katz, A., Oksenhendler, E., Tulliez, M., Picard, F., Vainchenker, W., and Louache, F. (1996). Loss of primitive hematopoietic progenitors in patients with human immunodeficiency virus infection. Blood *88*, 4568-4578.

Murugan, P., Chandrakumar, S., Basu, D., and Hamide, A. (2007). Gelatinous transformation of bone marrow in acquired immunodeficiency syndrome. Pathology *39*, 287-288.

Namiki, T.S., Boone, D.C., and Meyer, P.R. (1987). A comparison of bone marrow findings in patients with acquired immunodeficiency syndrome (AIDS) and AIDS related conditions. Hematol Oncol *5*, 99-106.

O'Malley, D.P., Sen, J., Juliar, B.E., and Orazi, A. (2005). Evaluation of stroma in human immunodeficiency virus/acquired immunodeficiency syndrome-affected bone marrows and correlation with CD4 counts. Archives of pathology & laboratory medicine *129*, 1137-1140.

Ricci, D., Ponzoni, M., Zoldan, M.C., Germagnoli, L., and Faravarelli, A. (1995). Bone marrow biopsy in 50 AIDS patients: a diagnostic approach. Pathologica *87*, 640-645.

Ryu, T., Ikeda, M., Okazaki, Y., Tokuda, H., Yoshino, N., Honda, M., Kimura, S., and Miura, Y. (2001). Myelodysplasia associated with acquired immunodeficiency syndrome. Intern Med *40*, 795-801.

Schneider, D.R., and Picker, L.J. (1985). Myelodysplasia in the acquired immune deficiency syndrome. Am J Clin Pathol *84*, 144-152.

Scott, M.A., and Stockham, S.L. (2008). Bone Marrow and Lymph Nodes. In Fundamentals of Veterinary Clinical Pathology (Ames, Iowa, Blackwell Publishing Professional), pp. 323-368.

Shenoy, C.M., and Lin, J.H. (1986). Bone marrow findings in acquired immunodeficiency syndrome (AIDS). Am J Med Sci *292*, 372-375.

Stasney, J., and Higgines, G.M. (1936). The Bone Marrow in the Monkey (Macacus Rhesus). The Anatomical Record *67*, 219-231.

Steinberg, H.N., Crumpacker, C.S., and Chatis, P.A. (1991). In vitro suppression of normal human bone marrow progenitor cells by human immunodeficiency virus. Journal of virology *65*, 1765-1769.

Stella, C.C., Ganser, A., and Hoelzer, D. (1987). Defective in vitro growth of the hemopoietic progenitor cells in the acquired immunodeficiency syndrome. J Clin Invest *80*, 286-293.

Stuart-Smith, S.E., Hughes, D.A., and Bain, B.J. (2005). Are routine iron stains on bone marrow trephine biopsy specimens necessary? Journal of clinical pathology *58*, 269-272.

Sun, N.C., Shapshak, P., Lachant, N.A., Hsu, M.Y., Sieger, L., Schmid, P., Beall, G., and Imagawa, D.T. (1989). Bone marrow examination in patients with AIDS and AIDS-related complex (ARC). Morphologic and in situ hybridization studies. Am J Clin Pathol *92*, 589-594.

CHAPTER 5: ERYTHROID, LYMPHOCYTIC, AND MONOCYTIC LINEAGES ARE MAINTAINED IN THE CHRONIC PERIOD OF SIV INFECTION

INTRODUCTION

SIV infection in Rhesus macaques is a well-established research animal model for study of HIV and AIDS. The RM SIV model correlates well to HIV-1 human infection (Lee 2004). The SIV RM model mimics HIV hematologic abnormalities and bone marrow changes during all phases of infection as demonstrated in Chapters 3 and 4.

Bone marrow changes during SIV infection have been primarily characterized by morphologic and microscopic (Chapter 4). Our prior study of marrow morphologic changes during SIV infection revealed pan hyperplasia in the early and later stages of disease characterized by overall BM hypercellularity with a stable myeloid (granulocytic/monocytic) to erythroid ratio despite lineage shifts. Phenotypic analysis of bone marrow is another method of assessment for lineages and M:E ratio as performed by flow cytometry to determine the precise measurements of cell size, complexity, and immunophenotype of cells. Immunophenotypic analysis of marrow may provide additional information about observed changes in hematopoietic lineages during SIV disease.

The objective of this study was to define the immunophenotype of hematopoietic cells in the Rhesus macaque and further analyze the shifts of bone marrow erythroid, granulocytic, lymphoid, and monocytic hematopoietic lineages during progressive SIV infection as previously documented in Chapter 4. We hypothesized phenotypic shifts in bone marrow hematopoietic cells during HIV infection would mirror morphologic hypercellularity for granulocytic, monocytic and erythroid lineages as SIV disease progresses. Additionally, we hypothesized that marrow pan hypercellularity could include lymphoid lineages which would be deteted by

phenotypic analysis. Blood was analyzed to determine if changes in blood paralleled those in marrow. Flow cytometry was utilized to determine phenotype of hematopoietic cells in marrow and blood by based on forward scatter (FSC), side scatter (SSC), CD45, and CD14 staining intensity.

MATERIAL AND METHODS

Experimental Database III

Experimental database and definitions are described in Appendix II.

Hematologic Data and Definitions

Hematologic data and definitions are described in Appendix I.

Flow Cytometry Analysis

Whole blood and BM tissue collection, flow cytometry preparation, flow cytometry acquisition, flow cytometry analysis, and definitions are described in Appendix III.

Flow cytometry was performed using monoclonal antibodies: CD45-FITC (clone MB4-6D6; Miltenyi; Auburn, CA), CD34-PE (clone 563; BD Biosciences; San Jose, CA), and CD14-PE (clone M5E2; BD Biosciences).

Immunophenotype of Bone Marrow and Whole Blood

Hematopoietic cells were defined by phenotypic analyses of populations within the FSC vs. SSC plot, CD45 vs. SSC plot, and CD45 vs. CD14 plot as previously described for humans and/or RM in blood and humans in marrow based on cell size, complexity, and staining (Bjornsson 2008; Lafont 2000; Loken 1990; Reimann 1994; Shah 1988; Stelzer 1993; van Lochem 2004; Walker 2004; Zamir 2005). FSC vs. SSC plot analysis defined four distinct populations for marrow and blood that were further defined by CD45 and CD14 staining. FSC

vs. SSC plot analysis is defined in Figure 5.1 for marrow and Figure 5.2 for blood. CD45 vs. SSC plot analysis is presented and defined in Figure 5.3 for marrow and Figure 5.4 for blood.

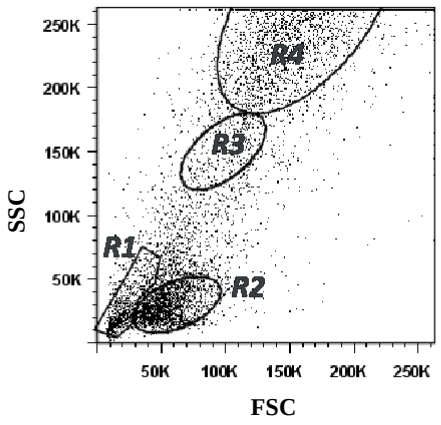

Figure 5.1. Phenotypes of bone marrow populations by forward versus side scatter characteristics

R1 is the marrow debris gate or 'debris gate' composed unlysed erythrocytes, platelets, fragmented cells, debris and rarely intact cells. This gate mainly consists of debris with low FSC and low SSC properties.

R2 is the marrow multilineage gate or 'MLN gate' composed of lineage negative immature hematopoietic stem cells (LNIHC), immature hematopoietic stem cells, erythroid lineage cells, lymphoid lineage (lymphoblasts, T cells, B cells, NK cells) cells, and basophils. This gate contains cells with low FSC and low SSC cells.

R3 is the marrow immature myeloid/monocyte gate or 'monocyte gate' composed of CD34+ hematopoietic stem cells, immature myeloid cells, and monocytes. This gate contains cells with low to moderate FSC and moderate SSC cells.

R4 is the marrow 'granulocyte gate' composed of non-dividing (post-mitotic) granulocytes (predominantly neutrophils and fewer eosinophils without basophils). Cells in this gate have moderate to high FSC, and high SSC, the latter based on their high internal complexity and laser scatter effect, due to their multilobed nuclei.

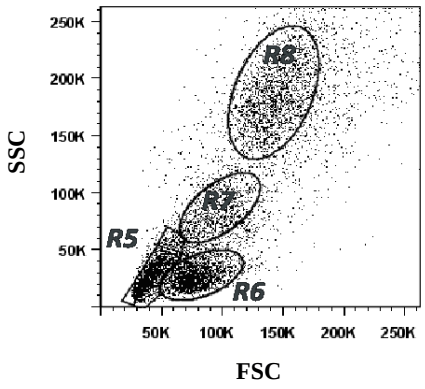

Figure 5.2. Phenotypes of whole blood populations by forward versus side scatter characteristics

R5 is the blood debris gate or 'debris gate' composed of unlysed erythrocytes, platelets, fragmented cells, debris and rarely intact cells.

R6 is the blood lymphocyte gate or 'lymphocyte gate' composed of lymphocytes (predominant population), mature basophils, and if present, metarubricytes (nucleated erythrocytes).

R7 is the blood monocyte gate or 'monocyte gate' composed of monocytes.

R8 is the blood granulocyte gate or 'granulocyte gate' composed of neutrophils (predominant population) and eosinophils.

A. **B.**

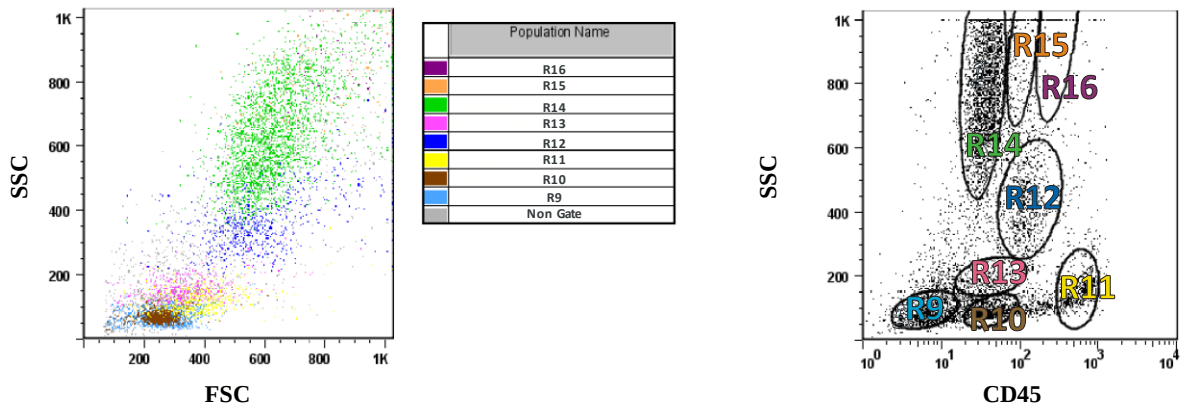

Figure 5.3. Phenotype of bone marrow by CD45 staining

Forward scatter versus side scatter plot of CD45 populations as indicated by color and region (legend in center) (**A.**). Populations of marrow hematopoietic cells by gate as indicated by CD45 versus SSC plot (**B.**).

R9 or 'CD45 marrow erythroid gate' contained cells with low side angle scatter and low forward light scatter staining $CD45^{Neg}$ and smallest and least complex of cells. Debris, erythroid series cells, platelets, and mesenchymal cells are found in this gate.

R10 or 'CD45 marrow blast gate' contained cells with low side angle scatter and low forward light scatter staining $CD45^{Dim\ to\ moderate}$ and less complex mature lymphocytes. Immature B lymphocytes (lymphoblasts), myeloid blasts, CD34+ stem cells, and basophils are found in this gate.

R11 or 'CD45 marrow lymphocyte gate' contained cells with low side angle scatter and low forward light scatter staining $CD45^{Bright}$. B lymphocytes, T lymphocytes, NK cells, and few CD34+ cells are found in this gate.

R12 or 'CD45 marrow monocyte gate' contained cells with moderate side angle scatter and moderate forward angle scatter staining $CD45^{Mod}$ and bigger than mature lymphocytes. The monocytic lineage and CD34+ cells are found in this gate.

R13 or 'CD45 myeloid gate' contained cells with moderate side angle scatter and low forward light scatter staining $CD45^{Dim}$ and similar size to mature monocytes but lower CD45 expression. Immature myeloid cells and CD34+ cells are found in this gate.

R14-R16 or 'CD45 granulocyte gates' contained cells with variable scatter and staining. **R14** gated cells exhibited high side angle scatter and moderate light angle scatter staining $CD45^{Dim}$. **R15** gated cells exhibited high side angle scatter and moderate light angle scatter staining $CD45^{Mod}$. **R16** gated cells exhibited high side angle scatter and high forward light scatter staining $CD45^{Mod}$. Large myeloid cells consisting of immature and mature granulocytic cells are found in these gates.

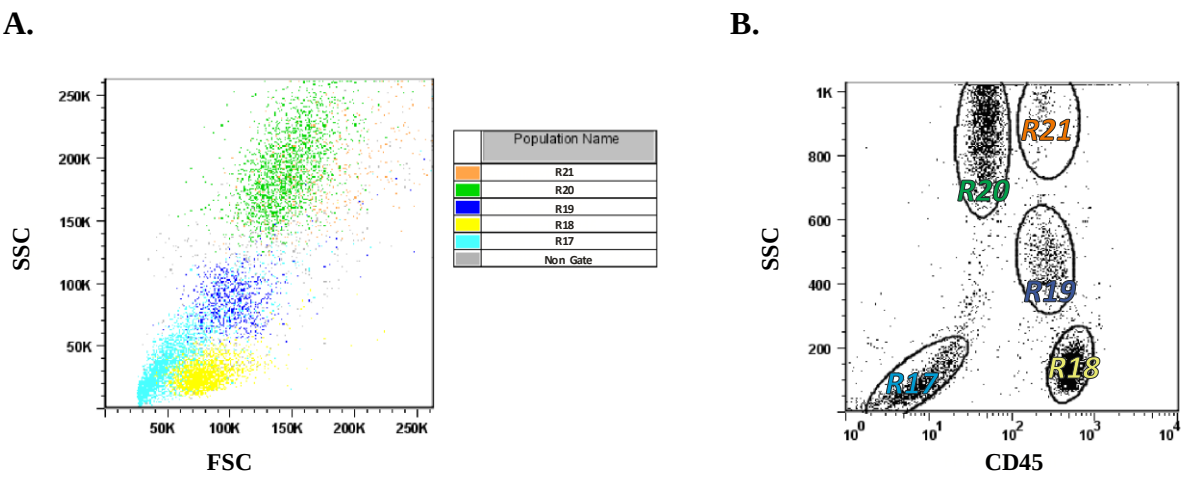

Figure 5.4. Phenotype of whole blood by CD45 staining

Forward scatter versus side scatter plot of CD45 populations (**A.**). Populations of blood cells by gates in the CD45 versus SSC plot (**B.**).

R17 is the 'CD45 debris gate' characterized by $CD45^{Neg}$ staining and low SSC composed of unlysed erythrocytes, platelets, fragmented cells, debris and rare intact cells.

R18 is the 'CD45 lymphocyte gate' characterized by $CD45^{Bright}$ staining and low SSC consisting of lymphocytes (predominant population) and basophils.

R19 is the 'CD45 monocyte gate' characterized by $CD45^{Moderate\ tobright}$ staining and moderate SSC containing monocytes.

R20 and R21 or 'CD45 granulocyte gates' characterized by CD45 variable staining and high SSC. **R20** is characterized by $CD45^{Dim\ to\ moderate}$ staining. **R21** characterized by $CD45^{Mod\ to\ bright}$ staining. Neutrophils (predominantly), eosinophils, and few larger monocytes are found in these gates.

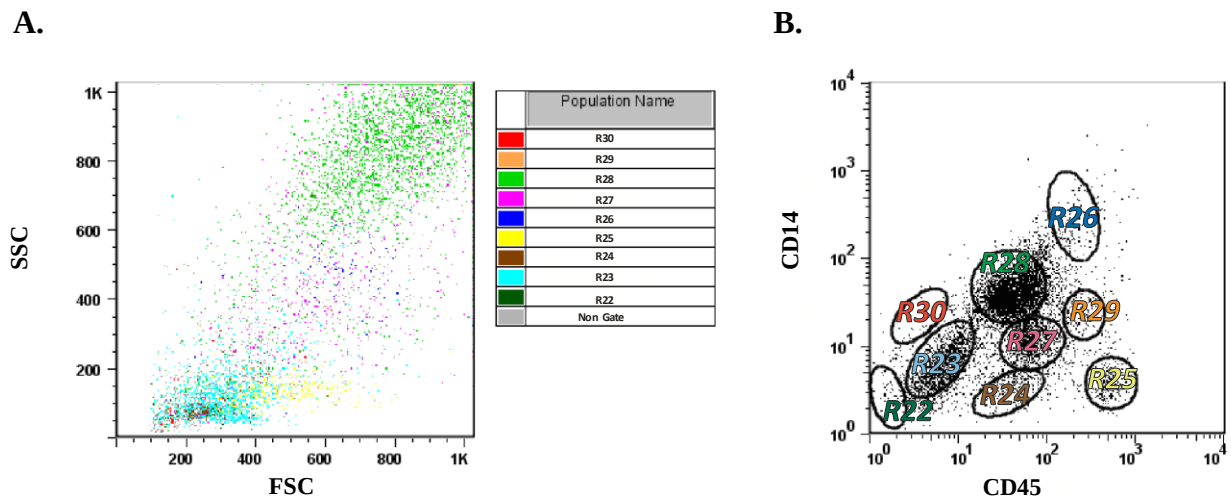

Figure 5.5. Phenotype of bone marrow by CD45 and CD14 staining
Forward scatter versus side scatter plot of CD45 and CD14 populations (**A.**). Populations of blood cells by gates in the CD45 versus CD14 plot (**B.**).

R22 or 'debris gate' contains events with low side angle and low forward light scatter, CD45 and CD14 negative, and moslty platelets, fragmented cells, and debris.

R23 or 'erythroid gate' contains cells with low side angle and low forward light scatter expressing $CD45^{Neg\ to\ dim}$ and $CD14^{Neg}$ mostly erythroid lineage cells and stem cells.

R24 or '$CD14^{Neg}$ blast gate' contains cells with low side angle scatter and low forward light scatter expressing $CD45^{Mod}$ and $CD14^{Neg}$ less complex than mature lymphocytes. Immature B lymphocytes (lymphoblasts), myeloid blasts, CD34+ stem cells, and basophils are found in this gate.

R25 or 'CD45 marrow lymphocyte gate' contained cells with low side angle scatter and low forward light scatter expressing $CD45^{Bright}$ and $CD14^{Neg}$. B lymphocytes, T lymphocytes, NK cells, and few CD34+ cells are found in this gate.

R26 or 'marrow monocyte gate' contained cells with moderate side angle scatter and moderate forward angle scatter expressing $CD45^{Bright}$ $CD14^{Bright}$ and bigger than mature lymphocytes. Monocytic lineage cells and CD34+ cells are found in this gate.

R27 or 'myeloid gate' contained cells with variable side angle scatter and variable forward light scatter expressing $CD45^{Dim}$ and $CD14^{Dim}$. CD34+ stem cells and immature myeloid cells comprised this gate.

R28-30 or 'marrow granulocyte gates' contained cells with variable scatter and staining. **R28** cells exhibited high side angle scatter and high forward light scatter expressing $CD45^{Dim\ to\ mod}$ and $CD14^{Mod}$. **R29** cells exhibited variable side angle scatter and variable forward light scatter expressing $CD45^{Bright}$ and $CD14^{Dim}$. **R30** cells exhibited variable side angle scatter and variable forward light scatter expressing $CD45^{Neg}$ and $CD14^{Neg}$. Immature and mature granulocytes (exclusive of basophils) are found in these gates.

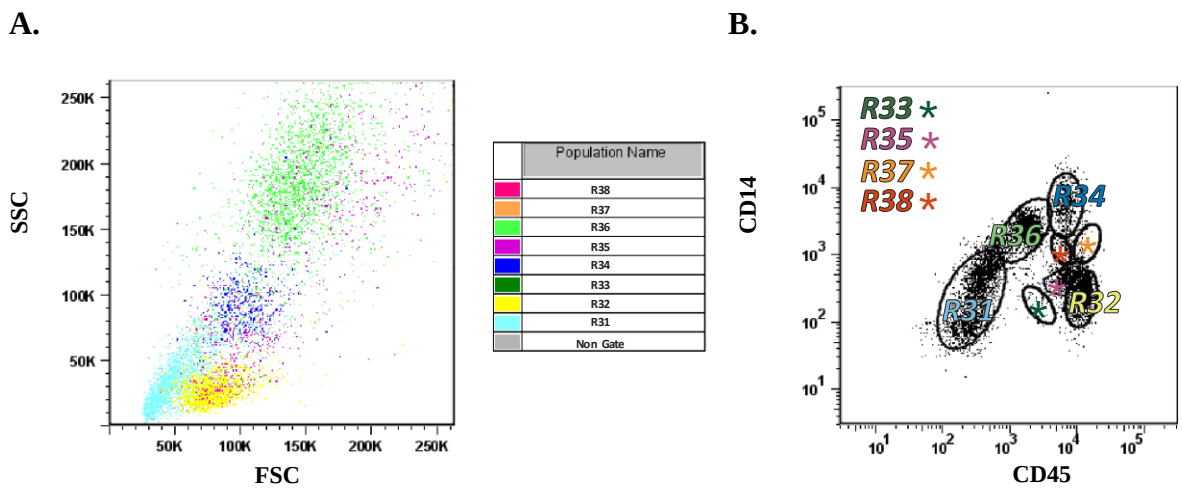

Figure 5.6. Phenotype of whole blood by CD45 and CD14 staining
Forward scatter versus side scatter plot of CD45 and CD14 populations (**A.**). Populations of blood cells by gates in the CD45 versus CD14 plot (**B.**).

R31 or 'debris gate' contained events with low side and forward angle scatter staining $CD45^{Neg}$ and $CD14^{Neg}$ composed of unlysed erythrocytes, platelets, fragmented cells, and debris.

R32 or 'CD45CD14 lymphocyte gate' contained cells with low side angle and low forward light scatter staining $CD45^{Bright}$ and $CD14^{Neg}$. Cells consist of lymphocytes and few CD34+ cells.

R33 and R35-38 or 'CD45CD14 marrow granulocyte gates' contained cells with variable staining and scatter. **R33** contained cells with low side angle and forward light scatter staining $CD45^{Dim}$ and $CD14^{Neg}$. **R35** contained cells with low side angle and forward light scatter staining $CD45^{Mod}$ and $CD14^{Neg}$. **R36** contained cells with high side angle scatter and moderate to high forward light scatter staining $CD45^{Dim\ to\ mod}$ and $CD14^{Mod\ to\ bright}$. **R37** contained cells with variable side angle and forward light scatter staining $CD45^{Bright}$ and $CD14^{Mod}$. **R38** or 'eosinophil gate' contained cells wit side angle and variable to high forward light scatter staining $CD45^{Mod}$ and $CD14^{Mod}$. Cells here consist of immature and mature granulocytes.

R34 or 'CD45CD14 monocyte gate' contained cells with moderate side angle scatter and moderate forward light scatter staining $CD45^{Mod\ to\ bright}$ and $CD14^{Mod\ to\ bright}$. Cells consist of mature monocytes and few CD34+ cells.

CD45 vs. CD14 plot analysis is defined in Figure 5.5 for marrow and Figure 5.6 for blood. CD45 and CD14 staining was defined as negative (Neg), dim, moderate (Mod), or bright based on intensity.

Statistical Analysis

For data evaluation, controls were non-SIV infected macaques and SIV infected subjects were grouped into periods defined as early and chronic (Appendix II). Macaques developing AIDS were fast and slow progressors.

Percentages of immunophenotypic populations for control and SIV infected macaques were compared using the Mann Whitney non-parametric unpaired t test, and correlations were determined using non-parametric Spearman correlation coefficients (GraphPad Software; San Diego, CA).

Graphs represent the means and SEM. Significant differences were defined as $p \leq 0.05$.

RESULTS

Bone Marrow Multilineage Populations and Whole Blood Lymphocyte Populations During SIV infection

The MLN gate represented ~30% nucleated cells in bone marrow of control macaques (Figure 5.7A). The MLN gate consisted of the erthroid (R9 and R23), blast (R10 and R24), and the lymphocyte (R10 and R24) gates. In control macaques, the erythroid gates (Figure 5.7C) represented the highest population (~17%) followed by the lymphocyte (~8%) (Figure 5.7B) and the blast (~6%) gates (Figure 5.7D). Early during SIV infection the MLN gate decreased characterized by a significant drop in all three subsets of the population. During chronic SIV infection, the MLN gate rebounded characterized by a rise in the erythroid and lymphocyte gates but continued significant loss of the blast gates by CD45 staining.

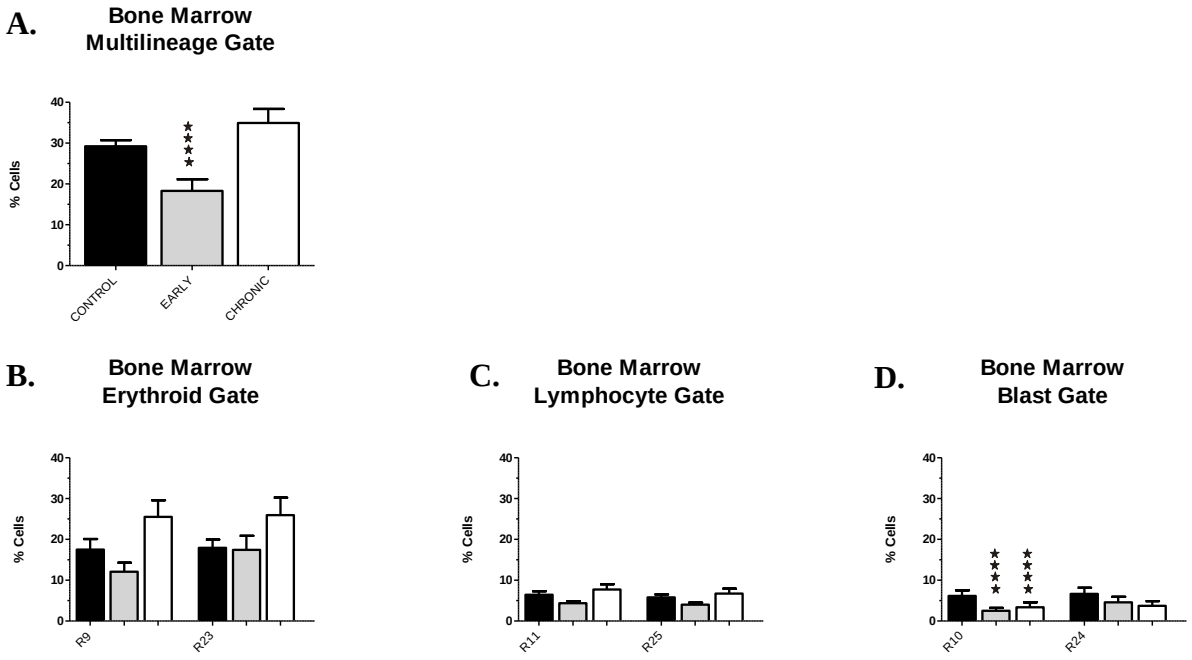

Figure 5.7. Bone marrow multilineage populations
The multilineage gate of bone marrow (R2 gate) consisted of the three subsets: erythroid gate, lymphocyte gate, and blast gate. **A.** The multilineage gate of bone marrow (R2 gate). **B.** The marrow erythroid gates were defined as the R9 gate in CD45 versus SSC plot and the R23 gate in CD45 versus CD14 plot. **C.** The marrow lymphocyte gates were defined as the R11 gate in CD45 versus SSC plot and the R25 gate of CD45 versus CD14 plot. **D.** The marrow blast gates were defined as the R10 gate in CD45 versus SSC plot and the R24 gate of CD45 versus CD14 plot. Comparison of controls to macaques in early and chronic periods of SIV infection by Mann Whitney t tests (****$p \leq 0.05$). Percentages of cells in respective gates are shown as mean $\pm$ SEM.

Lymphocytes in BM (R11 gate) were negatively correlated to viral load (Spearman r = -0.5559, p= 0.0254), however other subsets of the MLN population were not during SIV infection. The BM R9 erythroid gate was positively correlated to the BM R23 gate (Spearman r =0.6826, p=0.0002). The marrow R11 lymphocyte gate was strongly positively correlated to the marrow R25 lymphocyte gate (Spearman r =0.9544, p<0.0001). The R10 marrow blast was positively correlated to the R24 marrow blast gate (Spearman r =0.7938, p<0.0001).

Whole blood lymphocytes were ~15% of circulating cells in control macaques by phenotypic analysis (Figure 5.8). Blood lymphocytes were reported by CBC analysis (Figure 5.8A and 5.8B), the lymphocyte gate in FSC vs. SSC plot (R6) (Figure 5.8C), the lymphocyte gate in CD45 vs. SSC plot (R18) (Figure 5.8D), and the lymphocyte gate in CD45 vs. CD14 plot (R32) (Figure 5.8D). During SIV infection, CBC concentrations of lymphocytes plummeted ($p \leq 0.05$) while phenotypic percentages slightly increased post-infection. Viral load was not correlated to any of the defined blood lymphocyte populations. Strong positive correlations were detected between the defined populations of blood lymphocytes: R6 (FSC vs. SSC plot) compared to R18 (CD45 vs. SSC plot) gated populations (Spearman r =0.9269, p<0.0001); R6 (FSC vs. SSC plot) compared to R32 (CD45 vs. CD14 plot) gated populations (Spearman r =0.8319, p<0.0001); and R18 (CD45 vs. SSC plot) compared to R32 (CD45 vs. CD14 plot) gated populations (Spearman r =0.8628, p<0.0001).

Bone Marrow and Blood Monocyte Populations During SIV Infection

Monocyte populations represented 4-6% of nucleated cells in BM and WB for controls (Figure 5.9 and Figure 5.10). Percentages of marrow monocytes were detected by FSC vs. SSC plot (R3 in Figure 5.9A) and CD45 vs. SSC plot (R12 in Figure 5.9B). Blood monocytes were reported by CBC analysis (Figure 5.10A and 5.10B), the monocyte gate in FSC vs. SSC plot (R7

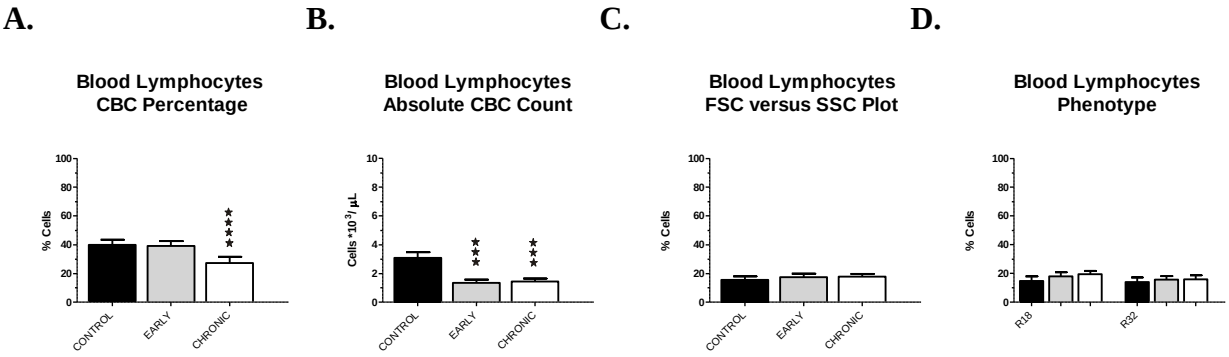

Figure 5.8. Whole blood lymphocyte populations
Whole blood lymphocytes by CBC data and phenotype. **A.** Percent lymphocytes from CBC data. **B.** Absolute lymphocyte count from CBC data. **C.** Lymphocyte gate (R6) in FSC versus SSC plot. **D.** Lymphocyte gate by phenotype: R18 is the lymphocyte gate in CD45 versus SSC plot; R32 is the lymphocyte gate in CD45 versus CD14 plot. Comparison of controls to macaques in early and chronic SIV infection by Mann Whitney t tests (***$p \leq 0.01$ and ****$p \leq 0.05$). Percentages of cells in respective gates are shown as mean $\pm$ SEM.

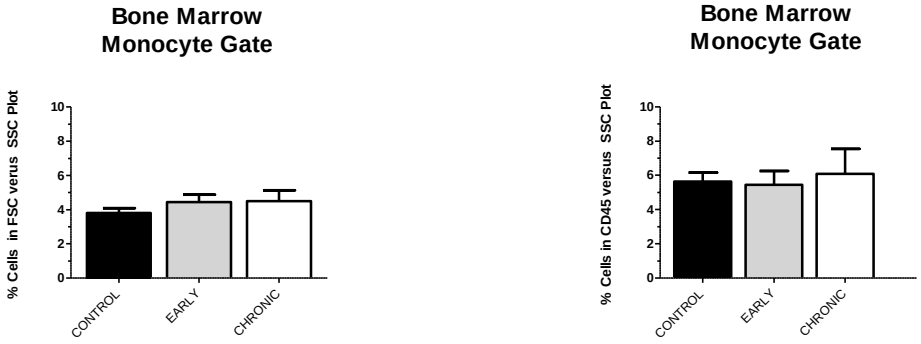

Figure 5.9. Bone marrow monocyte populations
The marrow monocyte populations were defined by two gates: (**A.)** R3 gate in FSC versus SSC plot; and (**B.)** R12 gate in CD45 versus SSC plot. Comparison of controls to macaques in early and chronic SIV infection by Mann Whitney t tests (no significant differences). Percentages of cells in respective gates are shown as mean $\pm$ SEM.

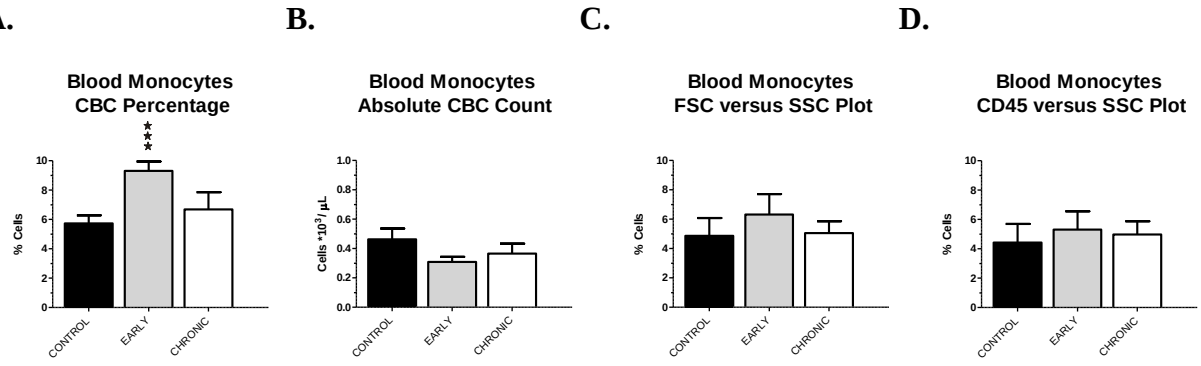

Figure 5.10. Whole blood monocyte populations
Whole blood monocytes by CBC data and phenotype. **A.** Percent monocytes from CBC data. **B.** Absolute monocyte count from CBC data. **C.** Monocyte gate in FSC versus SSC plot (R7). **D.** Monocyte gate by CD45 versus SSC plot (R19). Comparison of controls to macaques in early and chronic SIV infection by Mann Whitney t tests (***$p \leq 0.01$). Percentages of cells in respective gates are shown as mean $\pm$ SEM.

in Figure 5.10C), and the monocyte gate in CD45 vs. SSC plot (R19 in Figure 5.10D). Post-infection, percentages of monocytes were minimally increased from control macaques in BM and WB. Early post-infection, circulating monocytes increased in percentage but decreased in absolute number while marrow cells were unchanged. Later in infection, marrow and blood monocytes maintained percentages, but remained depressed in circulating absolute numbers. Viral load did not correlate with changes in monocytes in WB or BM.

The marrow monocyte gate in the FSC vs. SSC plot (R3) positively correlated with the monocyte gate in the CD45 vs. SSC plot (R12) (Spearman $r = 0.6632$, $p = 0.0004$). The whole blood monocyte gate in the FSC vs. SSC plot (R7 gate) positively correlated with the monocyte gate in the CD45 vs. SSC plot (R19 gate) (Spearman $r = 0.7836$, $p < 0.0001$).

Bone Marrow and Blood Granulocyte Populations During SIV Infection

Granulocyte populations were ~40-50% of BM and WB cells in control macaques (Figure 5.11 and Figure 5.12). Post-infection, percentages of marrow granulocytes decreased significantly in the chronic period ($p \leq 0.05$).

The marrow granulocyte gate (R4) was characterized by subsets of populations (Figure 5.11). Percentages of marrow granulocyte subsets were based on scatter and CD45 intensity as the following (Figure 5.11B) including those with: highest percentage of granulocytes, and moderate sized and $CD45^{Dim}$ (R14 gate); moderate sized and $CD45^{Mod}$ (R15 gate); lowest percentage of granulocytes and largest cells and $CD45^{Mod}$ (R16 gate). The $CD45^{Mod}$ marrow granulocytes increased in the early period of SIV infection as the $CD45^{Dim}$ marrow granulocytes declined. During the chronic period of SIV infection, losses of all subsets of marrow granulocytes was detected. Bone marrow granulocyte populations did not correlated with viral loads.

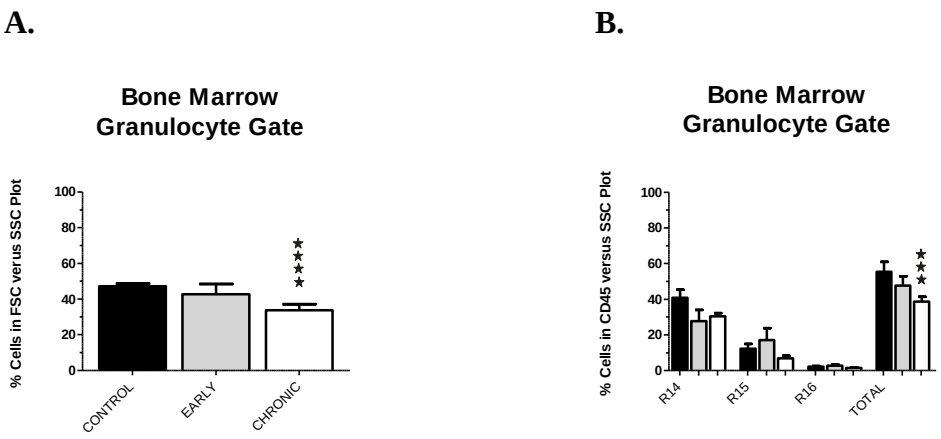

Figure 5.11. Bone marrow granulocyte populations
The marrow monocyte populations were defined by two gates: (**A.**) R4 gate in FSC versus SSC plot; and (**B.**) R14- R16 gates in CD45 versus SSC plot. Comparison of controls to macaques in early and chronic SIV infection by Mann Whitney t tests (no significant differences). Percentages of cells in respective gates are shown as mean $\pm$ SEM.

Percentages of blood granulocytes were detected by CBC analysis (Figure 5.12A and 5.12B), the granulocyte gate in FSC vs. SSC plot (R8 in Figure 5.11C), and the granulocyte gates in CD45 vs. SSC plot (R20 and R21 in Figure 5.11D). The ratio of WB R20 ($CD45^{Mod}$) to R21 ($CD45^{Bright}$) granulocytes was increased in the early phase characterized by parallel losses in both

gates with the loss of R21 in greater proportion. The WB ratio decreased in the chronic phase compared to control macaques defined by a drop in R20 population (granulopenia) and rise in R21 population (granulocytosis). Absolute numbers of total granulocytes, neutrophils and eosinophils, from CBC data declined in the early phase ($p=0.0006$) then rose minimally but were still low in the chronic phase.

The blood granulocyte gate (R8) in FSC vs. SSC plot positively correlated to the sum of the granulocytes gates (R20 and R21) in CD45 vs. SSC plot (Spearman $r=0.9348$, $p<0.0001$). Correlations were not detected between phenotypic gates and CBC data for granulocytes by percentage or absolute numbers. Viral load negatively correlated with CBC absolute concentrations of granulocytes (Spearman $r = -0.6425$, $p=0.0073$) yet positively correlated to CBC percentages of granulocytes (Spearman $r=0.5214$, $p=0.0384$).

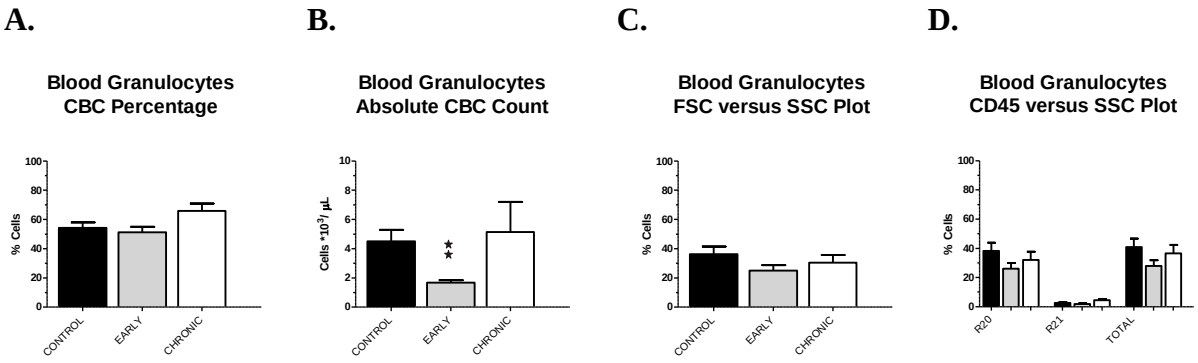

Figure 5.12. Whole blood granulocyte populations
Whole blood granulocytes by CBC data and phenotype. **A.** Sum of neutrophil and eosinophil granulocyte percents from CBC data. **B.** Absolute neutrophil and eosinophil granulocyte counts from CBC data. **C.** Granulocyte gate in FSC versus SSC plot (R8). **D.** Granulocyte gates by CD45 versus SSC plot (R20 and R21). Comparison of controls to macaques in early and chronic SIV infection by Mann Whitney t tests (***$p \leq 0.01$). Percentages of cells in respective gates are shown as mean $\pm$ SEM.

Bone Marrow Phenotypic Lineage Ratio During SIV Infection

A phenotypic lineage ratio (GM:MLN) was determined in bone marrow. The GM:MLN ratio was defined as the sum of the marrow granulocyte and monocyte populations or myeloid

lineage (GM) compared to the MLN population composed of the marrow erythroid and lymphoid lineages and immature stem cells (Figure 5.10). The control macaque GM:MLN ratio was 1.79±0.36 which continually declined post-infection. The drop of the GM:MLN ratio below control values in the early phase was due to a concurrent drop in both granulocyte and MLN populations and minimal change in the monocyte populations. The drop in cells within MLN population (15%) was higher than the drop in the granulocyte population (10%) from the control macaque level. Within the chronic phase, again the monocyte population was minimally changed while the granulocyte population dropped (29%) from the control macaque level and the MNL population rose (20%) to levels near the control macaque level.

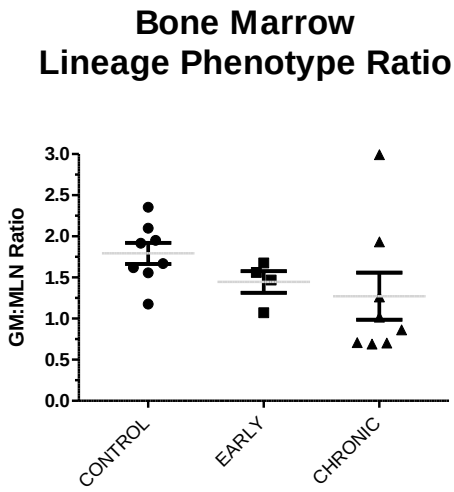

Figure 5.13. Bone marrow lineage phenotype ratio
The GM:MLN ratio defined as the sum of the marrow granulocyte (R4 gate) and monocyte populations (R3 gate) or myeloid lineage (GM) compared to the multilineage MLN gate (R2) population composed of the marrow erythroid and lymphoid lineages and immature stem cells. Comparison of controls to macaques in early and chronic SIV infection by Mann Whitney t tests (no significant differences). Grey lines represent means ± SEM.

DISCUSSION

Phenotypic analysis of BM and WB cells defined populations based on size and complexity by the FSC vs. SSC plot. The main phenotypic populations were defined as the

following: debris, lymphocyte or MLN, monocyte, and granulocyte. Debris usually consists of non-lysed erythrocytes, ghost erythrocytes, particles, cell fragments, and platelets and platelets (Loken 1990). CD45 staining and CD14 staining helped eliminate nonmyeloid cells or debris from marrow populations as the marrow MLN gate occassionally overlapped the debris gate.

Early during SIV infection, percentages of marrow erythroid and lymphocytic lineages, immature hematopoietic cells, and granulocytes were low. Even though total marrow granulocytes were low, the $CD45^{Mod}$ and moderately-sized granulocytes were increased. BM monocytes were unchanged in the early period. In WB, phenotypic percentages and absolute numbers of circulating granulocytes plus absolute numbers of mononuclear cells (lymphocytes and monocytes) were similarly decreased.

The depressed trend in BM continued for percentages of blast cells in the chronic phase but the percentages of erythroid lineage and lymphocytic lineage rebounded in the chronic phase. Percentages of BM granulocytes did not rebound even as the percentage of monocyte cells was unchanged. Circulating lymphocytes remained depressed as did the other mononuclear cells, monocytes. Viral load negatively correlated with lymphocyte populations in BM and the sum of absolute numbers of total granulocytes from CBC data. Viral load positively correlated with percentages of granulocytes from CBC data.

The phenotypic study GM:MLN mean ratio was 1.79 ± 0.03 for control macaques while the morphologic M:E mean ratio was 1.94 for controls in our earlier study (Chapter 4). Phenotypically, the marrow GM:MLN ratio dropped early in infection due to decrease in the majority of hematopoietic cell populations, erythroid and lymphoid lineages plus immature cells and granulocytes yet monocytes were unchanged. Morphologically, the marrow M:E ratio dropped in the early period of infection due to loss of myeloid cells and concurent increase in

erythroid cells. A continued drop in the BM ratio was noted by phenotypic analysis due to increase in percentages of erythroid and lymphoid lineages and monocytes with a sustained loss of granulocytic cells. During chronic SIV infection, the M:E ratio increased to levels noted in non-infected RM characterized by a gradual rise in myeloid cells and loss in erythroid cells.

The GM and M component of the BM ratios were similarly defined in the phenotypic and morphologic studies respectively. Of note, the GM population included macrophages and other mononuclear cells possibly excluded by morphologic appearance. Additionally, the second part of the ratio included lymphocytes, debris, and immature cells for the phenotypic definition but not the morphologic definition. The GM:MLN ratio included a higher percentage of non-myeloid cells thus decreasing the ratio compared to the M:E morphologic ratio. Consistent with marrow ratios was a loss of granulocytic lineage.

Loss of granulocytic cells may be attributed to precursor cells. Reports in HIV and SIV for decreased precursors of the granulocytic series have been documented and may account for changes noted in our study. Committed precursors of the granulocytic lineage occur as colony forming unit-granulocyte, macrophage (CFU-GM). Long term bone marrow cultures from healthy patients infected with HIV showed decreased CFU-GM (Marandin 1995) which was also found in cultures of bone marrow from HIV infected patients (Tomishima 2003). Chronically infected SIVmac251 RM were reported to have persistently low CFU-GM without change to colony forming unit-macrophage (CFU-M) (Thiebot 2005).

One discrepancy from our prior observations was noted in immature hematopoietic cells. In Chapter 4 we defined early increases in percentages of BM CD34+ hematopoietic stem cells then decline as SIV infection progressed. In our current study we observed overall loss in the MLN marrow gate early during infection then rise as the infection progressed characterized by a

rise in the erythroid and lymphocyte gates and loss in the blast gate. The same CD34 manufacturer, clone, and fluorochrome was used in both studies. The CD34+ stem cells may be found in each subset of the MLN marrow gate as lineage negative or lineage differentiated. The percentage of CD34+ cells was <0.5% and poorly reflective of the total MLN population. Further analysis of the stem cells is needed to confirm the trend as LNIHC or lineage differentiated CD34+ cells.

Overall, the phenotypic analysis was comparable to the morphologic analysis in control macaques. The phenotypic trend paralleled the morphologic trend when compared between the early and chronic phases respectively with maintenance of the erythroid and lymphoid lineages, loss of granulocytic lineages, and maintenance of monocytic lineages. Additionally the observed hematologic abnormalities of this study are supported by findings in our prior discoveries described in Chapter 3 and Chapter 4.

SUMMARY

Phenotypic analysis of SIV infected Rhesus macaques defined lineages of hematopoietic cells in bone marrow by CD45 and CD14 staining. The BM erythroid lineage and lineage negative immature hematopoietic cells declined early during infection then increased in later phases. Granulocytes cells and immature hematopoietic cells in BM remained low during progressive infection. During infection, the BM monocytic lineage and immature myeloid cells were minimally increased. BM lymphocytes were low in the early phase then rose to levels observed in control macaques in the chronic phase. Trends observed phenotypically in bone marrow were similar to morphologic trends in bone marrow identified for lineages and the myeloid to erythroid lineage ratio as loss of granulocytes during infection. Viral load was

negatively correlated to the percentage of BM mature lymphocytes. Hematologic abnormalities were consistent with prior findings of lymphopenia, monocytopenia, and neutropenia.

Our study confirms phenotypic analysis of bone marrow recapitulates morphologic observations. Immunophenotype of lymphocytes and dendritic cells, cells essential for antigen presenting function, will be subsequently determined to identify which subsets shifted during SIV infection with respect to BM and WB gated populations.

REFERENCES

Bjornsson, S., Wahlstrom, S., Norstrom, E., Bernevi, I., O'Neill, U., Johansson, E., Runstrom, H., and Simonsson, P. (2008). Total nucleated cell differential for blood and bone marrow using a single tube in a five-color flow cytometer. Cytometry B Clin Cytom 74, 91-103.

Lafont, B.A., Gloeckler, L., D'Hautcourt, J.L., Gut, J.P., and Aubertin, A.M. (2000). One-round determination of seven leukocyte subsets in rhesus macaque blood by flow cytometry. Cytometry 41, 193-202.

Lee, C.I., Cowan, M.J., Kohn, D.B., and Tarantal, A.F. (2004). Simian immunodeficiency virus infection of hematopoietic stem cells and bone marrow stromal cells. J Acquir Immune Defic Syndr 36, 553-561.

Loken, M.R., Brosnan, J.M., Bach, B.A., and Ault, K.A. (1990). Establishing optimal lymphocyte gates for immunophenotyping by flow cytometry. Cytometry 11, 453-459.

Marandin, A., Canque, B., Coulombel, L., Gluckman, J.C., Vainchenker, W., and Louache, F. (1995). In vitro infection of bone marrow-adherent cells by human immunodeficiency virus type 1 (HIV-1) does not alter their ability to support hematopoiesis. Virology 213, 245-248.

Reimann, K.A., Waite, B.C., Lee-Parritz, D.E., Lin, W., Uchanska-Ziegler, B., O'Connell, M.J., and Letvin, N.L. (1994). Use of human leukocyte-specific monoclonal antibodies for clinically immunophenotyping lymphocytes of rhesus monkeys. Cytometry 17, 102-108.

Shah, V.O., Civin, C.I., and Loken, M.R. (1988). Flow cytometric analysis of human bone marrow. IV. Differential quantitative expression of T-200 common leukocyte antigen during normal hemopoiesis. J Immunol 140, 1861-1867.

Stelzer, G.T., Shults, K.E., and Loken, M.R. (1993). CD45 gating for routine flow cytometric analysis of human bone marrow specimens. Ann N Y Acad Sci 677, 265-280.

Thiebot, H., Vaslin, B., Derdouch, S., Bertho, J.M., Mouthon, F., Prost, S., Gras, G., Ducouret, P., Dormont, D., and Le Grand, R. (2005). Impact of bone marrow hematopoiesis failure on T-cell generation during pathogenic simian immunodeficiency virus infection in macaques. Blood 105, 2403-2409.

Tomishima, T., Saitoh, Y., Nishida, T., Morris, S., Maruno, M., and Yoshimine, T. (2003). Lymphangiomatosis of the skull. Case illustration. J Neurosurg 98, 1319.

van Lochem, E.G., van der Velden, V.H., Wind, H.K., te Marvelde, J.G., Westerdaal, N.A., and van Dongen, J.J. (2004). Immunophenotypic differentiation patterns of normal hematopoiesis in human bone marrow: reference patterns for age-related changes and disease-induced shifts. Cytometry B Clin Cytom 60, 1-13.

Walker, J.M., Maecker, H.T., Maino, V.C., and Picker, L.J. (2004). Multicolor flow cytometric analysis in SIV-infected rhesus macaque. In Methods in cell biology, Z. Darzynkiewicz, M. Roederer, and H.J. Tanke, eds. (Elsevier), pp. 535-557.

Zamir, E., Geiger, B., Cohen, N., Kam, Z., and Katz, B.Z. (2005). Resolving and classifying haematopoietic bone-marrow cell populations by multi-dimensional analysis of flow-cytometry data. British journal of haematology 129, 420-431.

CHAPTER 6: T LYMPHOCYTES ARE MAINTAINED IN BONE MARROW AS B LYMPHOCYTES AND NK CELLS DECLINE DURING SIV INFECTION

INTRODUCTION

Phenotying by flow cytometry and morphologic analysis of bone marrow revealed decreases in cells within the MLN gate early in SIV infection with return to control macaque levels in chronic infection while monocytes were minimally impacted and granulocytes declined in our studies (Chapter 4 and Chapter 5). Moreover, phenotypic changes were observed to reflect morphologic changes during progressive SIV disease (Chapter 4 and 5). However, prior phenotypic analysis studies of hematopoietic bone marrow cells during SIV infection have been difficult to interpret based on sample preparation (e.g. density gradient, culture purification, aspirate sample, etc.) and gating protocols (single versus multi-color flow cytometry, sorting, starting populations, etc.).

The objective of this study was to define, establish, and compare BM and WB immunophenotypes of lymphocytes and antigen presenting cells based on lineage gating established in Chapter 5 and to determine shifts in populations during SIV infection. It is estimated that billions of lymphocytes migrate through the bone marrow daily even though it is only fed by the blood vascular circulation and not the lymphoid circulation (Wei 2006). Immature B cells leave BM and mature in peripheral lymphoid tissues (Baumgarth 2004). Long-lived plasma cells and memory CD8 T cells may be found in the bone marrow (Wei 2006). Mouse studies indicate that uncommitted lymphocyte/myeloid precursors leave the bone marrow and enter the thymus for T cell/NK cell development (Spits 2002). Natural killer cells have been reported to develop in the bone marrow of adults and children by Blom et al. (Blom 2006). Myeloid dendritic cells (mDC) and plasmacytoid dendritic cells (pDC) are hematopoietic derived

cells that form direct-cell-to-cell contact with T lymphocytes as antigen presenting cells (APC) (Coates 2003). If environmental conditions are appropriate, pDC can act as APC for naïve T cells but are less efficient than mDC at phagocytosis of antigenic material (McKenna 2005). Both plasmacytoid and myeloid dendritic cells can aid memory T cell activation (McKenna 2005). Human pDC have been shown in vitro to recruit and activate NK cells (McKenna 2005). Disruption of percentages of lymphocytes and dendritic cells in bone marrow during SIV infection would confirm another dysfunction in bone marrow and may help explain the pathogensis of HIV infection.

We hypothesized lymphocyte populations of T cells, plasma cells, B cells, and NK cells would be low during early SIV infection but rise during chronic infection compared to control macaque levels in bone marrow based on data showing maintenance of marrow lymphocytes (Chapter 5). Further, we hypothesized populations of dendritic cells would be maintained during SIV infection in bone marrow due to data showing maintenance of the BM monocytoid gate (Chapter 5). Flow cytometry was utilized to determine immunophenotype of multiple populations in bone marrow and whole blood. We compared gating schemes of FSCvs.SSC and CD45 versus SSC for select populations to determine correlation between different identification schemes of populations based on flow gating observations from Chapter 5.

MATERIAL AND METHODS

Experimental Database III

Experimental database and definitions are described in Appendix II.

Hematologic Data and Definitions

Hematologic data and definitions are described in Appendix I.

Flow Cytometry Analysis

Whole blood and BM tissue collection, flow cytometry preparation, flow cytometry acquisition, flow cytometry analysis, and definitions are described in Appendix III. Immunophenotype of hematopoietic cells was performed for select populations of cells based on specific panels and Boolean gating for flow cytometry analysis (Table 6.1).

Lymphocyte Grandparent Gates for T Lymphocytes, B Lymphocytes, and NK Cells

The bone marrow grandparent gate was defined as the marrow multilineage gate, which includes lymphocytes, in the FSC vs. SSC plot (R2 in Figure 5.1) and the marrow lymphocyte gate in CD45 vs. SSC plot (R11 in Figure 5.3). The whole blood grandparent gate was defined as the lymphocyte gate in the FSC vs. SSC plot (R6 in Figure 5.2) and the lymphocyte gate in the CD45 vs. SSC plot (R18 in Figure 5.4).

Immature Lymphocyte Grandparent Gates for Plasma Cells and Immature B Lymphocytes

The bone marrow grandparent gate was defined as the marrow multilineage gate, which includes lymphocytes, in the FSC vs. SSC plot (R2 in Figure 5.1) and the marrow lymphocyte gate in CD45 vs. SSC plot (R11 in Figure 5.3) and the marrow blast gate in CD45 vs. SSC plot (R10 in Figure 5.3). The whole blood grandparent gate was defined as the lymphocyte gate in the FSC vs. SSC plot (R6 in Figure 5.2) and the lymphocyte gate in the CD45 vs. SSC plot (R18 in Figure 5.4) and the debris gate in the CD45 vs. SSC plot (R17 gate in Figure 5.4).

Monocyte Grandparent Gates for Dendritic Cells

The bone marrow grandparent gate was defined as the marrow monocyte gate in the FSC vs. SSC plot (R3 in Figure 5.1) and the marrow monocyte gate in CD45 vs. SSC plot (R12 in Figure 5.3). The whole blood grandparent gate was defined as the monocyte gate in the FSC vs. SSC plot (R7 in Figure 5.2) and the monocyte gate in the CD45 vs. SSC plot (R19 in Figure 5.4).

Table 6.1. Multi-Color Flow Cytometry Panels by Antibody, Clone, and Manufacturer

Flow Cytometric Phenotype	FITC[a]	PE[b]	PE-Texas Red[c]	PE-Cy5[d]	PerCP-Cy5.5[e]	PE-Cy7[f]	APC[g]	APC-Cy7[h]	Pacific Blue[i]	QDOT655
Hematopoietic Cell Panel	CD45 MB4-6D6 Miltenyi	CD34 563 BD		CD184 12G5 BD		HLA-DR L243 BD	CD90 5E10 BD		CD14 M5E2 BD	
T Lymphocyte Panel	CD7 M-T701 BD	CD34 563 BD	CD8 3B5 Caltag	CD2 RPA-2.10 BD		CD3 SP34-2 BD	CD45 MB4-6D6 Miltenyi	CD20 L27 BD	CD14 M5E2 BD	CD4 T4/19Thy5D7 NIH
B Lymphocyte Panel	IgG G18-145 BD	CD38 OKT10 NIH	CD8 3B5 Caltag	IgM G20-127 BD	CD28 L293 BD	HLA-DR L243 BD	CD45 MB4-6D6 Miltenyi	CD20 L27 BD	CD3 SP34-2 BD	
Plasma Cells and Immature B Lymphocyte Panel	CD138 MI15 BD	CD38 OKT10 NIH	CD8 3B5 Caltag	IgG G18-145 BD	CD28 L293 BD	HLA-DR L243 BD	CD45 MB4-6D6 Miltenyi	CD20 L27 BD	CD3 SP34-2 BD	
Natural Killer Cell Panel	CD3 SP34-2 BD	CD335 or NKp46 BAB281 Beckman	CD8 3B5 Caltag			HLA-DR L243 BD	CD45 MB4-6D6 Miltenyi	CD20 L27 BD		CD4 T4/19Thy5D7 NIH
Dendritic Cell Panel	CD3 SP34-2 BD	CD11c S-HCL-3 BD	CD8 3B5 Caltag	CD123 9F5 BD		HLA-DR L243 BD	CD45 MB4-6D6 Miltenyi	CD20 L27 BD	CD14 M5E2 BD	

Fluorescein isothiocyanate (FITC); b) Phycoerythrin (PE); c) Phycoerythrin Texas Red (PE-Tx RED or PE-TxR); d) Phycoerythrin Cyanine 5 (PE-Cy5); e) Peridinin Chlorophyll Protein Cyanine 5.5 (PerCP-Cy5.5); f) Phycoerythrin Cyanine 7 (PE-Cy7); g) Allophycocyanin (APC); h) Allophycocyanin Cyanine 7 (APC-Cy7); i) Pacific Blue (PacBlue or PacBl), Peridinin Chlorophyll Protein (PerCP); and j) Quantom dots 655 (QDOT 655)

Hematopoietic Cell Panel

The hematopoietic cell panel was a specific panel to identify and classify populations within whole blood and bone marrow. Forward scatter versus side scatter plot analysis (Figure 5.1 and Figure 5.2), CD45 vs. SSC plot analysis (Figure 5.3 and Figure 5.4), and CD45 versus CD14 plot analysis (Figure 5.5 and Figure 5.6) revealed several gates for bone marrow and whole blood respectively as defined in Chapter 5.

T Lymphocyte Panel

T cells are characterized by expression of the T cell receptor CD3 (Shah 1988; Szczepanski 2006). CD3+ T lymphocytes were determined by gates in bone marrow and whole blood (Figure 6.1). Populations of T lymphocytes were examined by expression of early maturation markers (Figure 6.1B).

B Lymphocyte Panel

Mature B lymphocytes have been characterized as CD20+ in bone marrow and whole blood (Baumgarth 2004; Loken 1987; Shah 1988; Szczepanski 2006). CD20+ B lymphocytes were determined by gates in bone marrow and whole blood (Figure 6.2).

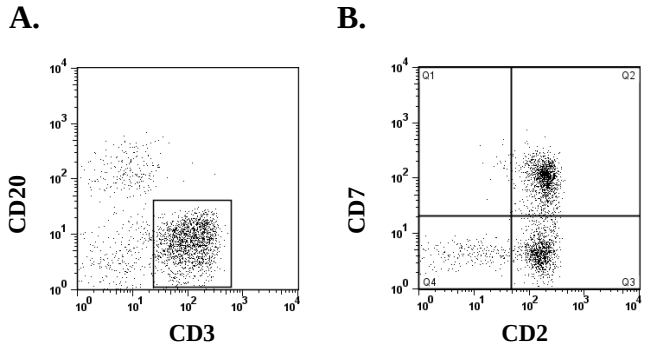

Figure 6.1. Identification of T lymphocytes
Phenotypic determination of T lymphocytes. **A.** The parent gate identified CD3+CD20- T lymphocytes by CD3 versus CD20 plot from the lymphocyte grandparent gates. **B.** Early maturation markers in the CD2 versus CD7 plot of CD3+ T lymphocytes identified four populations of cells as Q1 CD3+CD20- CD2-CD7+ cells, Q2 as CD3+CD20- CD2+CD7+ cells, Q3 as CD3+CD20- CD2+CD7- cells, and Q4 as CD3+CD20- CD2-CD7- cells from the parent gate.

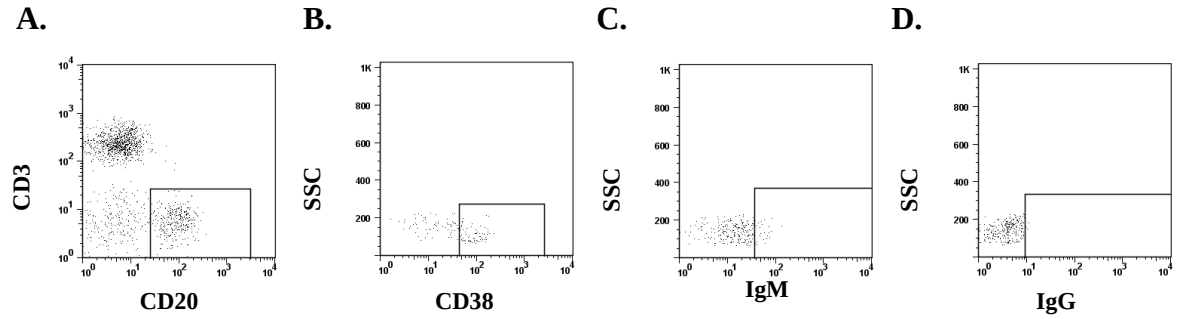

Figure 6.2. Identification of B lymphocytes
Phenotypic determination of B lymphocytes. **A.** The parent gate identified CD20+CD3- B lymphocytes by CD20 versus CD3 plot from the lymphocyte grandparent gates. **B.** CD20+CD3-CD38+ B lymphocytes were identified from the parent gate. **C.-D.** Multiple gating strategies identified CD20+CD3- B lymphocytes by antibody of interest versus SSC plot from the parent gate. **C.** CD20+CD3- IgM+ B lymphocytes. **D.** CD20+CD3- IgG+ B lymphocytes.

Plasma Cells and Immature B Lymphocyte Panel

Plasma cells and immature B cells have been identified based on CD38 and CD138 staining (Medina 2003; Morice 2007; Nowakowski 2005; Rawstron 2002; Sims 2005; Smock 2007). Plasma cells and immature B lymphocytes were determined by gates in bone marrow and whole blood (Figure 6.3).

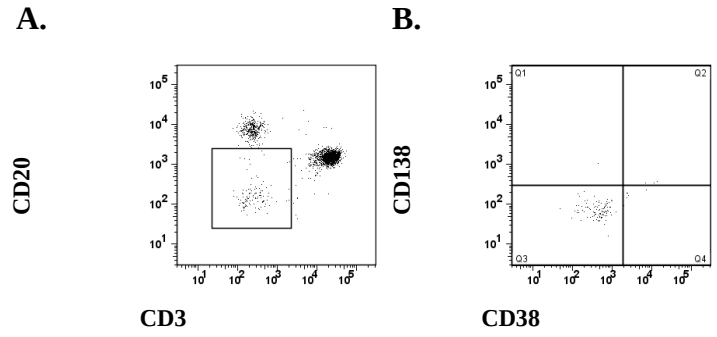

Figure 6.3. Identification of plasma cells and immature B lymphocytes
Phenotypic determination of plasma cells and immature B lymphocytes. **A.** The parent gate identified CD3-CD20- lymphocyte cells by CD3 versus CD20 plot from the immature lymphocyte grandparent gates. **B.** CD38 versus CD138 plot of CD3-CD20- cells identified immature B lymphocytes in Q1 or CD3-CD20-CD38-CD138+ cells and plasma cells in Q2 or CD3-CD20-CD38+CD138+ cells.

Natural Killer Lymphocyte Panel

Natural killer (NK) cells express natural cytotoxicity receptors including NKp46 or CD335 found on human and Rhesus macaque NK cells (Andersen 2004; Szczepanski 2006; Warren 2005). Additionally, NKp46 is expressed on active and resting NK cells (Noessner 2007; Warren 2005). NK cells were determined by gates in bone marrow and whole blood (Figure 6.4).

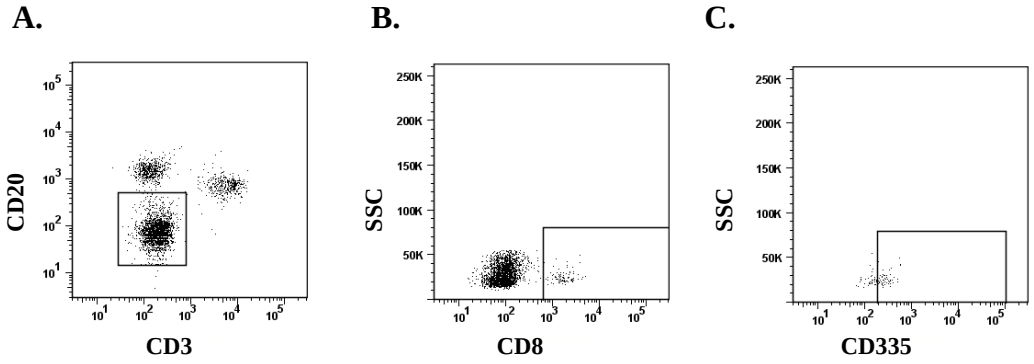

Figure 6.4. Identification of natural killer cells
Phenotypic determination of natural killer (NK) cells. **A.** The parent gate identified CD3-CD20- cells by CD20 versus CD3 plot from the lymphocyte grandparent gates. **B.** CD8+CD3- CD20- cells were identified from the parent gate. **C.** NK cells identified as CD335+CD8+CD3-CD20- from the prior gate.

Dendritic Cell Panel

Dendritic cells display the FSC scatter of monocytes and the SSC scatter of lymphocytes found within a mononuclear gate (Upham 2000). Phenotypic analysis by flow cytometry of dendritic cells identified mononuclear cells absent of mature T cell markers and mature B cell markers, also absent or dim fluorescence for mature granulocytic or monocytic markers (lineage negative) and positive for HLA-DR with either CD11c or CD123 fluorescence (Figure 4.19) (Della Bella 2008; Martin-Martin 2009; Szabolcs 2003; Upham 2000). Dendritic cells are classified as CD11c+CD123- or mDC and pDC or CD11c-CD123+. Dendritic cells were determined by gates from the dendritic cell panel for bone marrow and whole blood (Figure 6.5).

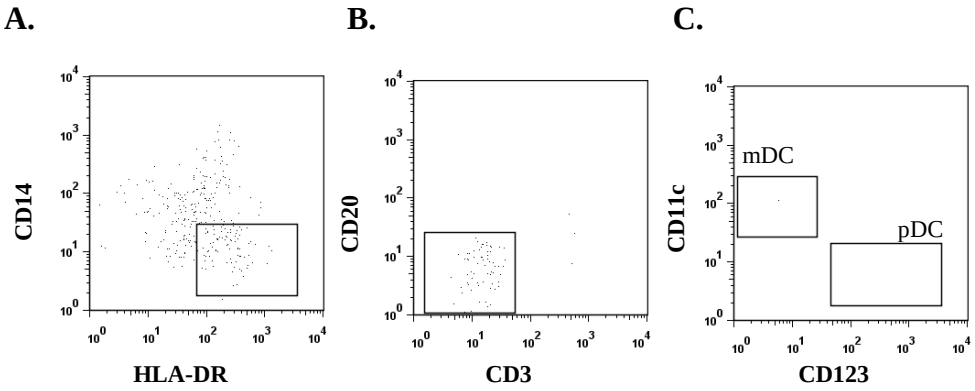

Figure 6.5. Identification of dendritic cells
Phenotypic determination of dendritic (DC) cells. **A.** The parent gate identified HLA-DR^{Bright}CD14- cells by HLA-DR versus CD14 plot from the monocyte grandparent gates. **B.** HLA-DR^{Bright}CD14-CD3- CD20- cells were identified from the parent gate. **C.** HLA-DR^{Bright}CD14-CD3-CD20- CD123-CD11c+ myeloid dendritic cells (mDC) and HLA-DR^{Bright}CD14-CD3-CD20- CD123+CD11c- plasmacytoid dendritic cells (pDC) by CD123 versus CD11c plot.

Plasma Viral Load

Plasma viral loads and definitions are described in Appendix IV.

Statistical Analysis

For data evaluation, controls were non-SIV infected macaques and SIV infected subjects were grouped into periods defined as early and chronic (Appendix II). Macaques developing AIDS were fast and slow progressors.

Marrow and blood T lymphocyte, B lymphocyte, plasma cell, immature B cell, NK cell, and dendritic cells gating strategies were compared between FSC vs. SSC and CD45 vs. SSC plots. Percentages of immunophenotypic populations for control and SIV infected macaques were compared using the Mann Whitney non-parametric unpaired t test, and correlations were determined using non-parametric Spearman correlation coefficients (GraphPad Software; San Diego, CA).

Graphs represent the means and SEM. Significant differences were defined as $p \leq 0.05$.

RESULTS

Percentages of CD3+ T Lymphocytes During SIV Infection

T lymphocytes were defined as CD3+ cells. T lymphocytes were maintained in BM during SIV but steadily lost in blood over time (Figure 6.6). BM CD3+ T lymphocytes were highly represented in the $CD45^{Bright}$ gate (R11) but only represented a minor population in the marrow lymphocyte gate for control macaques, thus the gating strategies did not correlate (Table 6.6). In BM, $\geq$70% of CD3+ T lymphocytes were $CD45^{Bright}$ with the remainder of CD3+ T lymphocytes detected in $CD45^{DimToNegative}$ and low SSC gate (R10). Circulating lymphocytes were predominantly CD3+ T lymphocytes in control macaques by both gating strategies confirmed by moderate correlation for comparison of gates (Table 6.3). In WB, $\geq$97% of CD3+ T lymphocytes were $CD45^{Bright}$.

CD7, a marker of CD3+ T lymphocytes, is expressed early during maturation in pre-thymic lymphocytes and maintained on the cell (Bodey 1994). CD2 is another early maturation marker expressed in post-thymic lymphocytes also maintained on the cell (Bodey 1994). BM of controls contained mostly CD3+CD2-CD7- T lymphocytes by FSC vs. SSC plot but CD3+CD2+CD7+ T lymphocytes by CD45 vs. SSC plot (Figure 6.7). CD3+CD2-CD7+ T lymphocytes were decreased in BM post-infection. CD3+CD2+CD7+ and CD3+CD2-CD7- T lymphocytes were minimally decreased early in SIV disease then in the chronic phase approached control levels. Early in infection CD2+CD7- lymphocytes were increased then returned to control levels. Most circulating CD3+ T cells co-expressed CD2 and CD7~60% with fewer cells that expressed only CD2 (15%) in control macaques (Figure 6.8). CD3+CD2-CD7+ lymphocytes were maintained in WB while CD2+CD7+ lymphocytes were lost and early in infection CD2+CD7- lymphocytes were increased then returned to control macaque levels. CD3+CD2-CD7- T lymphocytes increased post-infection.

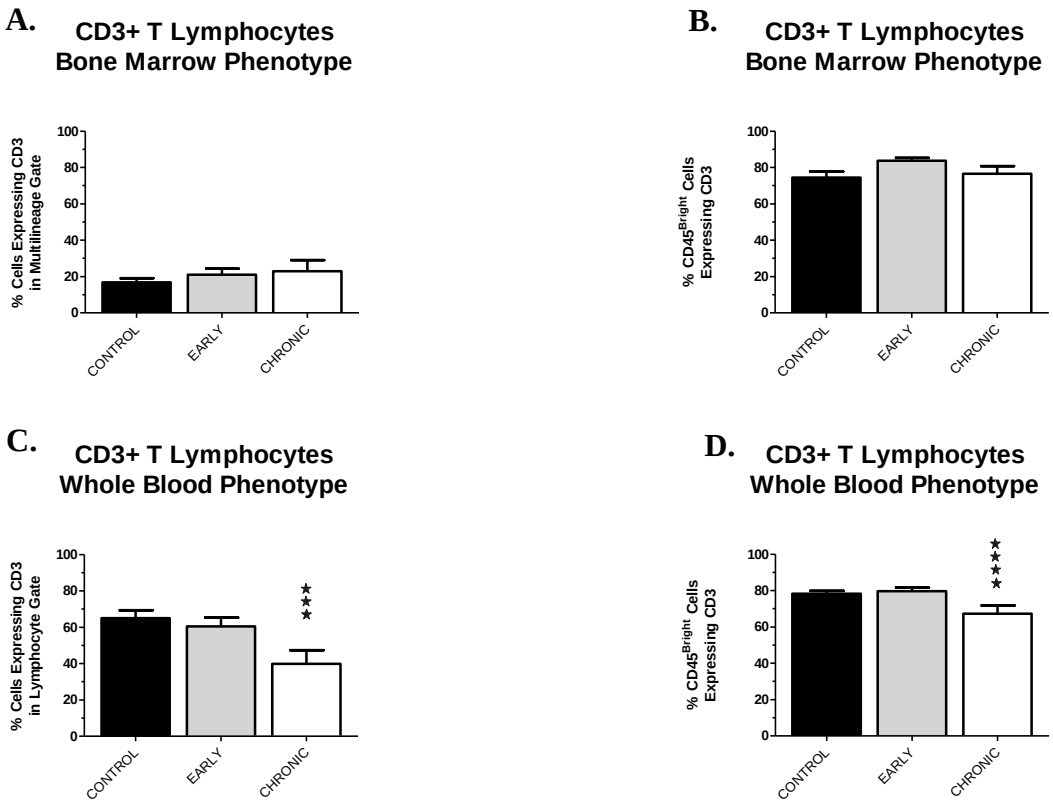

Figure 6.6. Bone marrow and whole blood percentages of T lymphocytes during SIV infection

Percentages of cells expressing CD3 in bone marrow (BM) and whole blood (WB) populations by T lymphocyte gating strategy as described in text for **A-B.** bone marrow and **C-D.** whole blood. Comparison of control cohort to early and chronic periods during SIV infection by Mann Whitney t tests (***$p \leq 0.01$ and ****$p \leq 0.05$). Percentages are shown as mean $\pm$ SEM.

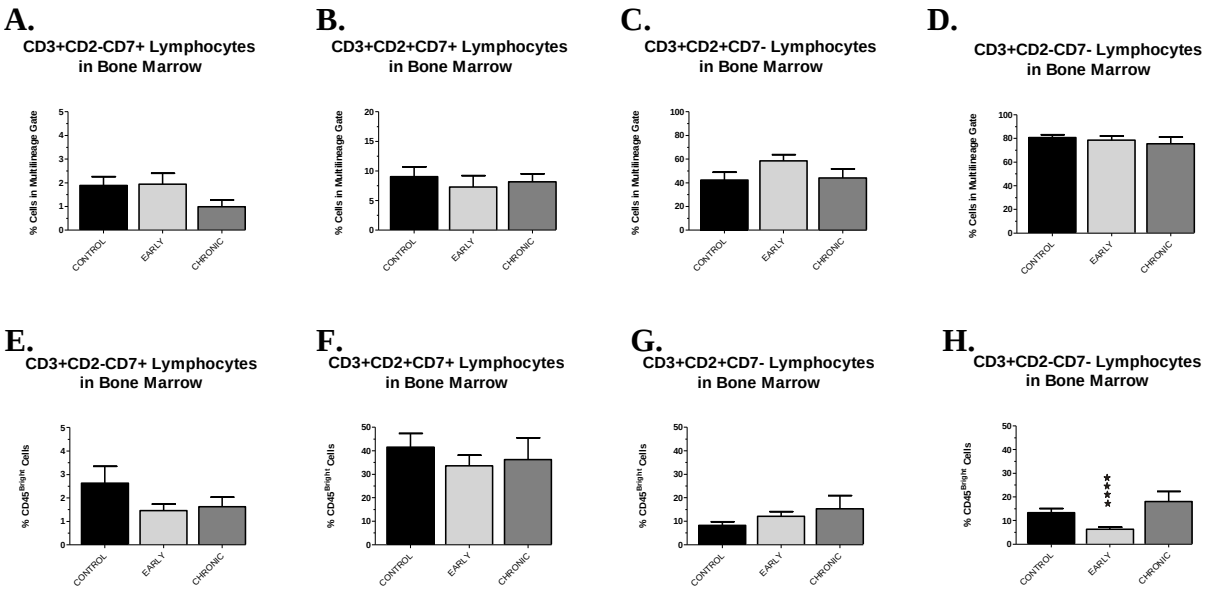

Figure 6.7. Expression of early markers on T lymphocytes in bone marrow during SIV infection

Percentages of CD2 and CD7 on CD3+ T lymphocytes by early T lymphocyte gating strategy as described in text. Lymphocytes in the **A-D** multilineage gate in FSC versus SSC plot and **E-F** marrow lymphocyte gate in CD45 versus SSC plot. Comparison of control cohort to early and chronic periods during SIV infection by Mann Whitney t tests (****$p \leq 0.05$). Percentages are shown as mean $\pm$ SEM.

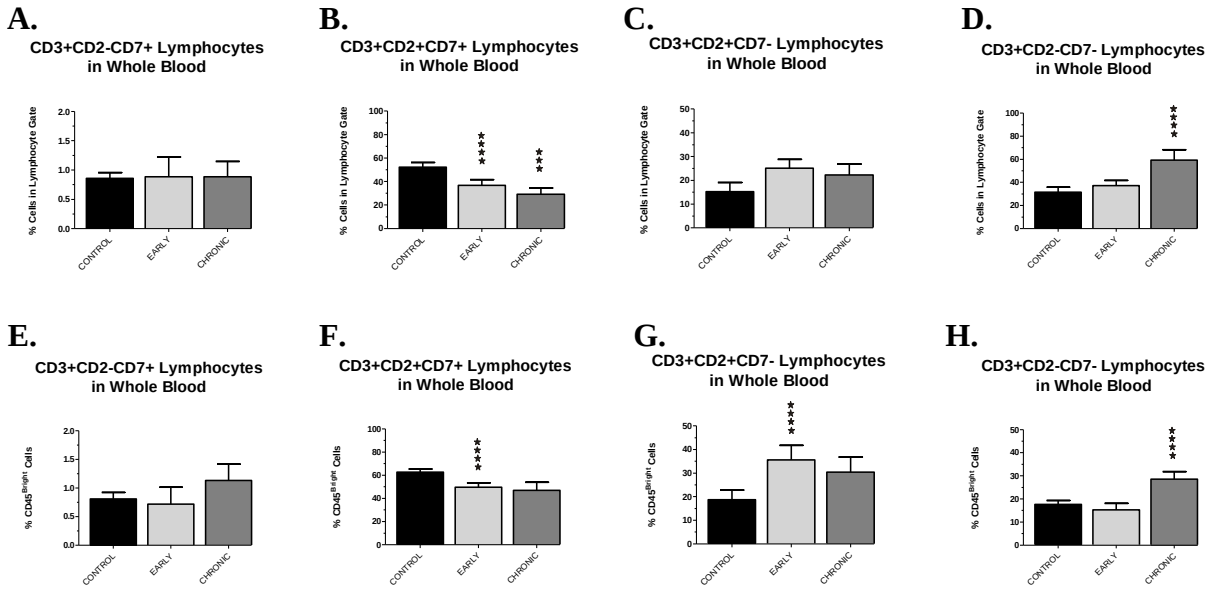

Figure 6.8. Expression of early markers on T lymphocytes in whole blood during SIV infection

Percentages of expression of CD2 and CD7 on CD3+ T lymphocytes by early T lymphocyte gating strategy as described in text. Lymphocytes in the **A-D** lymphocyte gate in FSC versus SSC plot and **E-F** CD45 lymphocyte gate in CD45 versus SSC plot. Comparison of control cohort to early and chronic periods during SIV infection by Mann Whitney t tests (***$p \leq 0.01$ and ****$p \leq 0.05$). Percentages are shown as mean $\pm$ SEM.

Viral loads positively correlated with BM and WB CD3+ T lymphocytes gated by CD45 (Spearman r =0.5294, p=0.0350) and (Spearman r =0.6122, p=0.0117) respectively. Moreover, viral loads negatively correlated with BM CD3+CD2-CD7- T lymphocytes (Spearman r = -0.5559, p=0.0254). BM CD3+CD2+7+ T lymphocytes and CD3+CD2+CD7- comparisons between FSC vs. SSC and CD45 vs. SSC gating strategies positively correlated (Table 6.2) while all WB phenotypes positively correlated (Table 6.3).

Table 6.2. Correlation of CD3+ T Lymphocyte Gated Populations Comparison Between FSC versus SSC Plot (R2 gate) and CD45 versus SSC Plot (R11 gate) for Bone Marrow

Bone Marrow Phenotype	Spearman r Coefficient	p value
CD3+ T Lymphocyte	0.1643	NS
CD3+CD2-CD7+ T Lymphocyte	0.3000	NS
CD3+CD2+CD7+ T Lymphocyte	0.6478	0.0006
CD3+CD2+CD7- T Lymphocyte	0.7139	<0.0001
CD3+CD2-CD7- T Lymphocyte	-0.0761	NS

NS = no significance

Table 6.3. Correlation of CD3+ T Lymphocyte Gated Populations Comparison Between FSC versus SSC Plot (R6 gate) and CD45 versus SSC Plot (R18 gate) for Whole Blood

Whole Blood Phenotype	Spearman r Coefficient	p value
CD3+ T Lymphocyte	0.5788	0.0038
CD3+CD2-CD7+ T Lymphocyte	0.7369	0.0002
CD3+CD2+CD7+ T Lymphocyte	0.6207	0.0021
CD3+CD2+CD7- T Lymphocyte	0.7967	<0.0001
CD3+CD2-CD7- T Lymphocyte	0.5426	0.0091

NS = no significance

Percentages of CD20+ B Lymphocytes During SIV Infection

B lymphocytes were defined as CD20+ cells. BM CD20+ B lymphocytes represented higher percentages of lymphocytes in bone marrow (~30%) than WB (~20%). Further, 50% of BM CD20+ B cells co-expressed CD38, 20% co-expressed IgM, and less than 10% co-expressed

IgG in control macaques (Figure 6.9, Figure 6.10, and Figure 6.11). Expression of CD45 intensity on CD20+ B lymphocytes was 33% $CD45^{Dim}$, 33% $CD45^{Moderate}$, and 33% $CD45^{Bright}$ in BM while $\geq$97% of circulating cells were $CD45^{Bright}$. B lymphocytes in BM were depressed post infection with apparently equal losses for total B cells as well as CD38+, IgM+ and IgG+ expressing B cells and in the chronic phase for IgG+ B cells. WB B lymphocytes early in infecttion approached the control level (increased) mainly due to a rise in IgM+ B cells in the chronic phase. IgG+ B cells were consistently depleted post-infection in blood. Correlations with viral load were not observed for B lymphocytes. Gating of B lymphocytes by the FSC vs. SSC or CD45 vs. SSC lymphocyte populations were moderately to highly correlated for all populations (Table 6.4 and Table 6.5).

Percentages of Plasma Cells and Immature B Lymphocytes During SIV Infection

Plasma cells were defined as CD3-CD20-CD38+CD138+ cells and immature B cells were defined as CD3-CD20-CD38+CD138- cells. Plasma cells and immature B lymphocytes were less than 1% of the lymphocyte population at 10 fold higher in WB than BM with predominance in the $CD45^{DimToNegative}$ gate for control macaques R17 and R10 respectively (Figure 6.12 and Figure 6.13). Immature B cells were present only in BM of the $CD45^{Bright}$ gate (R11) and barely detectable in the WB gate (R18). Plasma cells decreased post-infection in WB and BM with greatest depression in the chronic phase. A rise of $CD45^{Bright}$ plasma cells was noted in the early phase in BM. Immature B cells increased post-infection with apex in the early phase. Plasma cells and immature B cells were not correlated to viral loads. Bone marrow was highly correlated while whole blood gating was moderately correlated for gating strategies between FSC vs. SSC and the sum of both CD45 vs. SSC populations (Table 6.6 and Tabel 6.7).

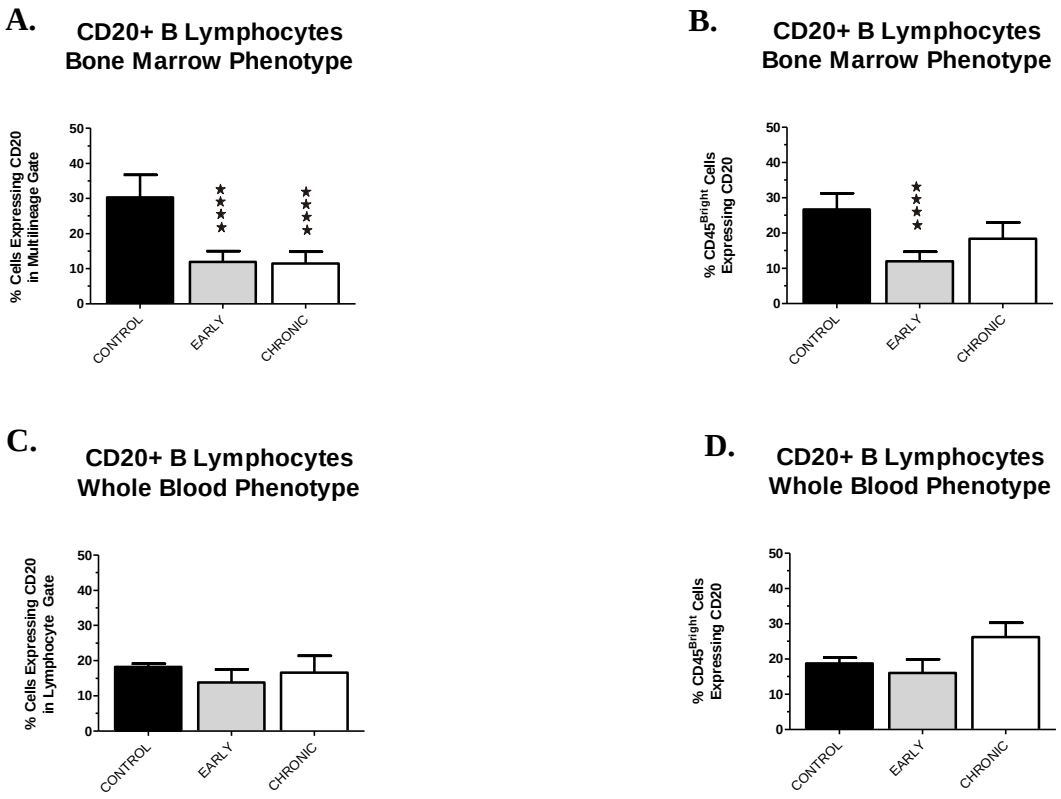

Figure 6.9. Bone marrow and whole blood percentages of B lymphocytes during SIV infection

Percentages of cells expressing CD20 in bone marrow (BM) and whole blood (WB) populations by B lymphocyte gating strategy as described in text for **A-B.** bone marrow and **C-D.** whole blood. Comparison of control cohort to early and chronic periods during SIV infection by Mann Whitney t tests (****$p \leq 0.05$). Percentages are shown as mean $\pm$ SEM.

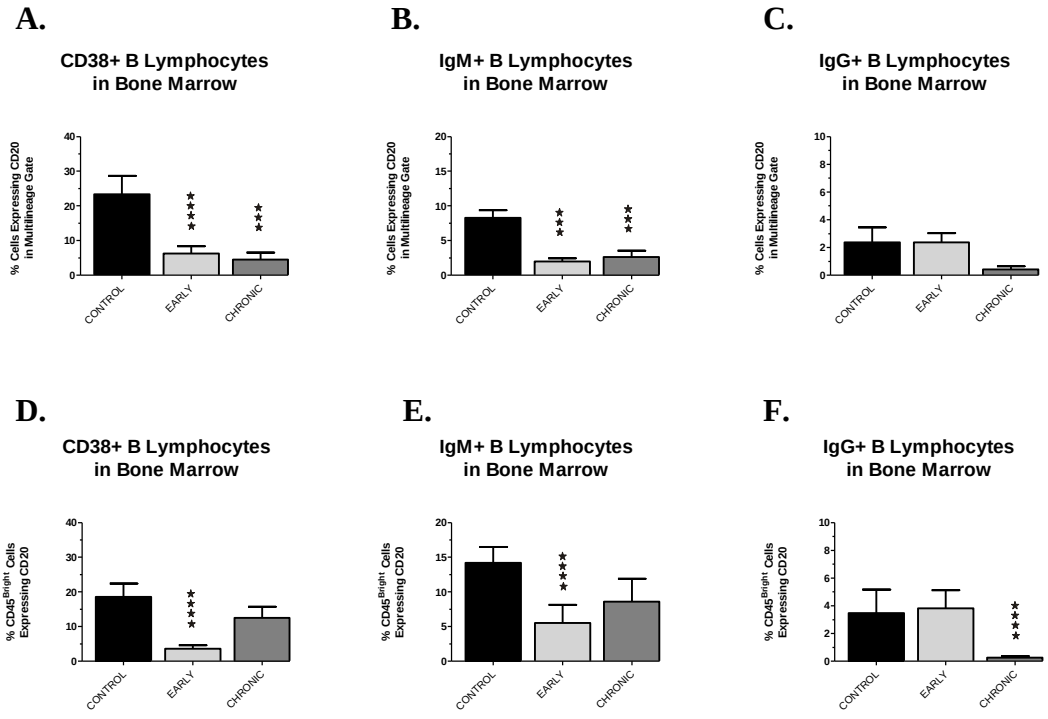

Figure 6.10. Expression of CD38 and antibody markers on B lymphocytes in bone marrow during SIV infection

Percentages of CD38 and antibody markers by CD20+ B lymphocytes by B lymphocyte gating strategy as described in text. Lymphocytes in the **A-D** multilineage gate in FSC versus SSC plot and **E-F** marrow lymphocyte gate in CD45 versus SSC plot. **A.** CD20+CD38+ lymphocytes. **B.** CD20+IgM+ lymphocytes. **C.** CD20+IgG+ lymphocytes. **D.** $CD45^{Bright}$CD20+CD38+ lymphocytes. **E.** $CD45^{Bright}$ CD20+IgM+ lymphocytes. **F.** $CD45^{Bright}$ CD20+IgG+ lymphocytes. Comparison of control cohort to early and chronic periods during SIV infection by Mann Whitney t tests (***$p \leq 0.01$ and ****$p \leq 0.05$). Percentages are shown as mean $\pm$ SEM.

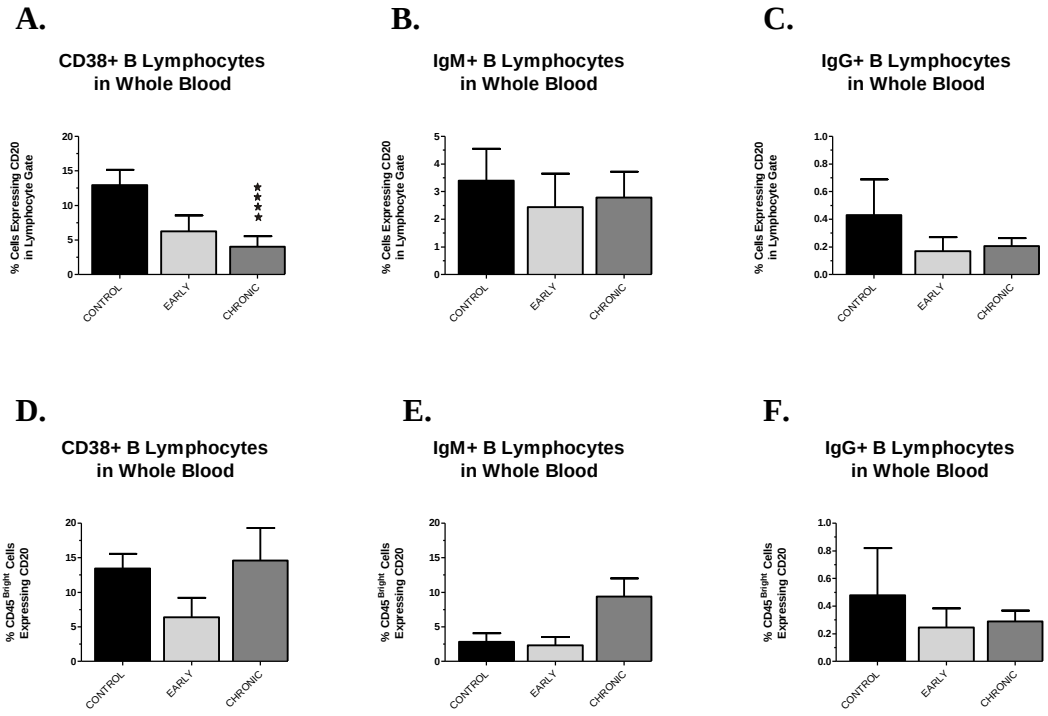

Figure 6.11. Expression of CD38 and antibody markers on B lymphocytes in whole blood during SIV infection

Percentages of expression of CD38 and antibody markers on CD20+ B lymphocytes by B lymphocyte gating strategy as described in text. Lymphocytes in the **A-C** lymphocyte gate in FSC versus SSC plot and **E-F** CD45 lymphocyte gate in CD45 versus SSC plot. Comparison of control cohort to early and chronic periods during SIV infection by Mann Whitney t tests (****$p \leq 0.05$). Percentages are shown as mean $\pm$ SEM.

Table 6.4.Correlation of CD20+ B Lymphocyte Gated Populations Comparison Between FSC versus SSC Plot (R2 gate) and CD45 versus SSC Plot (R11 gate) for Bone Marrow

Bone Marrow Phenotype	Spearman r Coefficient	p value
CD20+ B Lymphocyte	0.7549	0.0001
CD20+CD38+ B Lymphocyte	0.6541	0.0018
CD20+IgM+ B Lymphocyte	0.7865	<0.0001
CD20+IgG- B Lymphocyte	0.9402	<0.0001

Table 6.5. Correlation of CD20+ B Lymphocyte Gated Populations Comparison Between FSC versus SSC Plot (R6 gate) and CD45 versus SSC Plot (R18 gate) for Whole Blood

Whole Blood Phenotype	Spearman r Coefficient	p value
CD20+ B Lymphocyte	0.6586	0.0016
CD20+CD38+ B Lymphocyte	0.6586	0.0016
CD20+IgM+ B Lymphocyte	0.6213	0.0035
CD20+IgG- B Lymphocyte	0.832	<0.0001

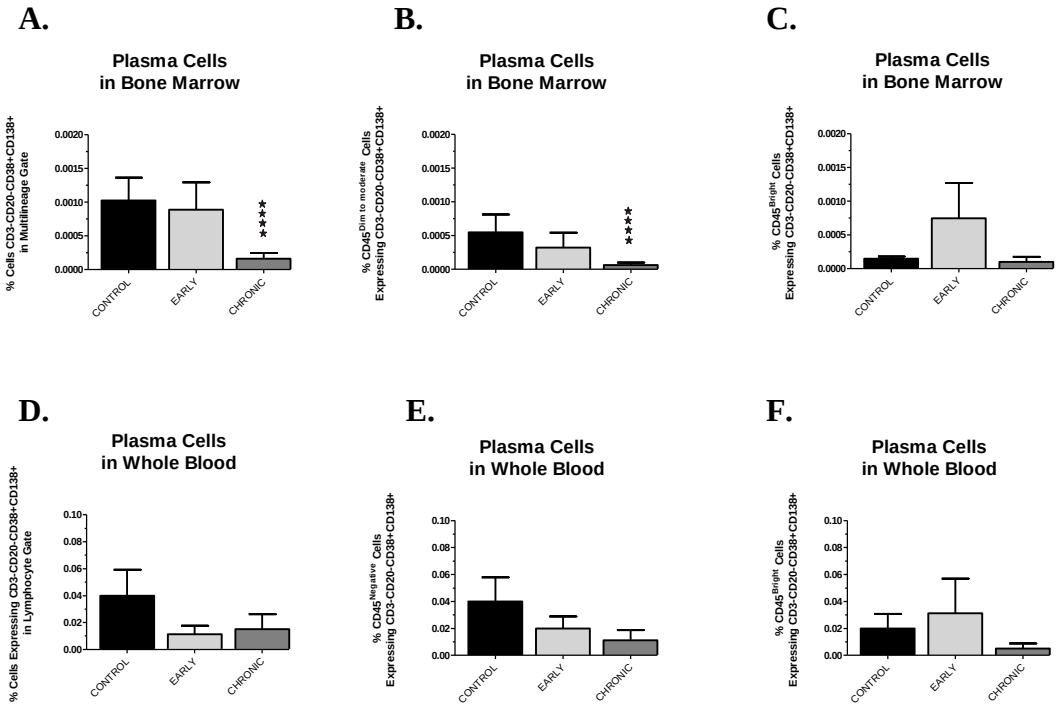

Figure 6.12. Bone marrow and whole blood percentages of plasma cells during SIV infection

Percentages of CD3-CD20- cells expressing CD38 and CD138 in **A-C** bone marrow (BM) and **D-F** whole blood (WB) populations by plasma cell gating strategy as described in text. Comparison of control cohort to early and chronic periods during SIV infection by Mann Whitney t tests (****$p \leq 0.05$). Percentages are shown as mean $\pm$ SEM.

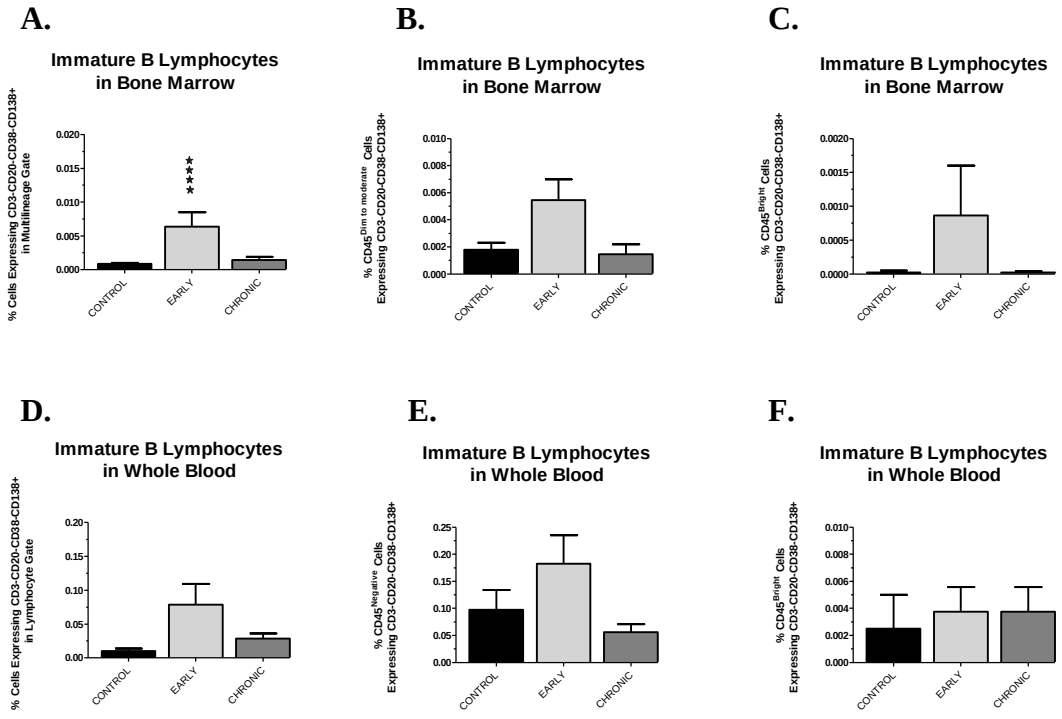

Figure 6.13. Bone marrow and whole blood percentages of immature B lymphocytes during SIV infection

Percentages of CD3-CD20- cells expressing CD38 and CD138 in **A-C** bone marrow (BM) and **D-F** whole blood (WB) populations by immature B lymphocyte gating strategy as described in text. Comparison of control cohort to early and chronic periods during SIV infection by Mann Whitney t tests (****$p \leq 0.05$). Percentages are shown as mean $\pm$ SEM.

Table 6.6.Correlation of Plasma Cell and Immature B Lymphocyte Gated Populations Comparison Between FSC versus SSC Plot (R2 gate) and CD45 versus SSC Plots (R10 + R11 gates) for Bone Marrow

Bone Marrow Phenotype	Spearman r Coefficient	p value
CD3-CD20-CD38+CD138+ Plasma Cell	0.8700	<0.0001
CD3-CD20-CD38-CD138+ Immature B Lymphocyte	0.7957	<0.0001

Table 6.7. Correlation of Plasma Cell and Immature B Lymphocyte Gated Populations Comparison Between FSC versus SSC Plot (R6 gate) and CD45 versus SSC Plots (R17 + R18 gates) for Whole Blood

Whole Blood Phenotype	Spearman r Coefficient	p value
CD3-CD20-CD38+CD138+ Plasma Cell	0.5789	0.0075
CD3-CD20-CD38-CD138+ Immature B Lymphocyte	0.5285	0.0166

Percentages of Natural Killer Cells During SIV Infection

NK cells were defined as CD3-CD20-CD8+CD335+ cells. Natural killer cells were less than 6% of the lymphocyte population for BM and WB with BM populations 2X higher than WB in controls (Figure 6.14). Higher percentages of NK cells were $CD45^{Bright}$. NK cells were decreased post-infection in BM. WB NK cells varied by gating strategy but overall were spared. NK cells did not correlate with plasma viral loads. Nk gating strategies did not correlate between gating strategies for BM or WB (Table 6.8 and Table 6.9).

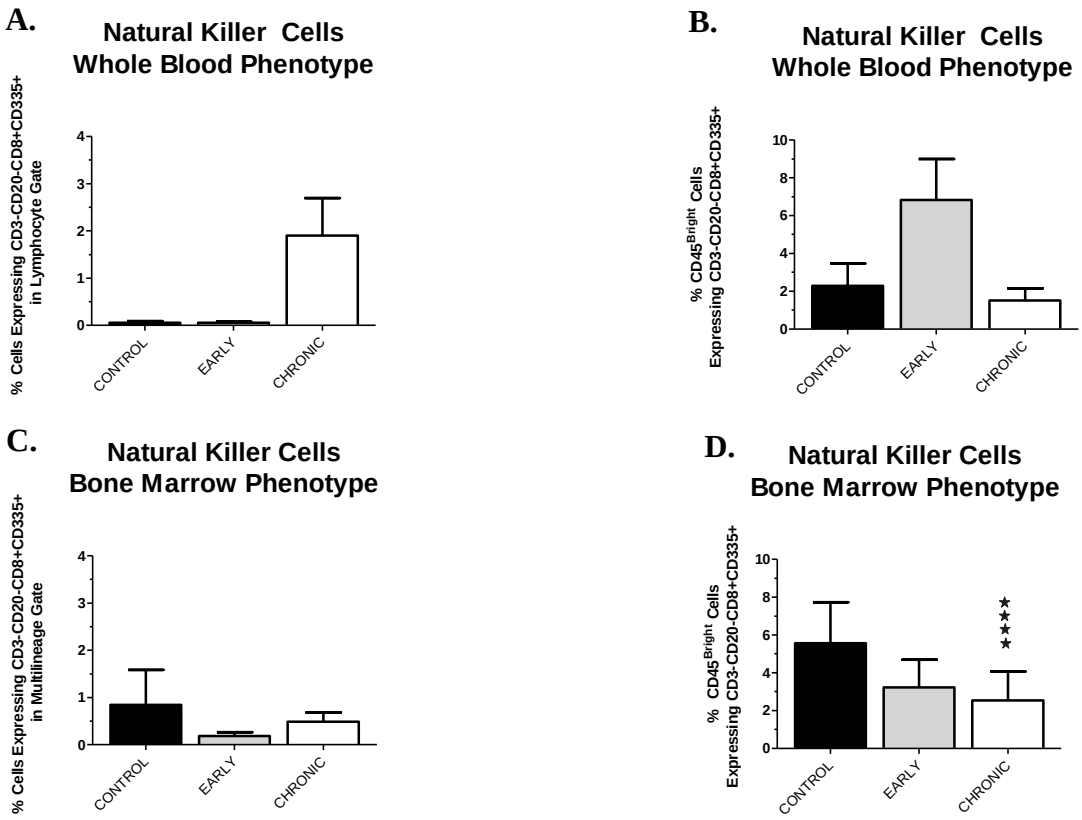

Figure 6.14. Bone marrow and whole blood percentages of natural killer cells during SIV infection
Percentages of CD3-CD20-CD8+ cells expressing CD335 in **A-B** bone marrow (BM) and **C-D** whole blood (WB) populations by natural killer gating strategy as described in text. Comparison of control cohort to early and chronic periods during SIV infection by Mann Whitney t tests (****$p \leq 0.05$). Percentages are shown as mean $\pm$ SEM.

Table 6.8. Correlation of Natural Killer Cell Gated Populations Comparison Between FSC versus SSC Plot (R2 gate) and CD45 versus SSC Plot (R11 gate) for Bone Marrow

Bone Marrow Phenotype	Spearman r Coefficient	p value
CD3-CD20-CD8+CD335+ Natural Killer Cell	0.4341	NS

NS = not significant

Table 6.9. Correlation of Natural Killer Cell Gated Populations Comparison Between FSC versus SSC Plot (R6 gate) and CD45 versus SSC Plots (R18 gate) for Whole Blood

Whole Blood Phenotype	Spearman r Coefficient	p value
CD3-CD20-CD38+CD335+ Natural Killer Cell	-0.1001	NS

NS = not significant

Percentages of Dendritic Cells During SIV Infection

Dendritic cells were defined as HLA-DR^{Bright}CD14-CD3-CD20- and additionally for mDC CD11cCD123 or pDC CD11cCD123. Dendritic cells were minor populations within blood and marrow monocyte populations that consisted of predominantly mDC and fewer pDC in control macaques (Figure 6.10). For infected RM, mDC were below the control population level for BM and WB. Depletion of pDC in chronic infection by CD45 gating was detected but increased by FSC gating, however both gating strategies showed a rise in the early phase in BM and WB. Correlations for gating of dendritic cells were present for BM and WB comparing FSC vs. SSC lymphoid and lymphocyte gating to CD45 vs. SSC R12 and R19 gating respectively (Table 6.10 and Table 6.11). Viral loads did not correlate with dendritic cells.

DISCUSSION

Phenotypic analyses of lymphocyte and dendritic cell subsets were analyzed during SIV infection. Immunophenotyping in the previous chapter (Chapter 5) and findings within the current chapter established percentages of BM lymphocytes. In control macaques, the BM FSC lymphoid gate was defined by CD45 and CD14 plots as ~20% CD3+ T lymphocytes, ~20% CD20+ B lymphocytes, ~20% erythroid lineage including lineage negative immature

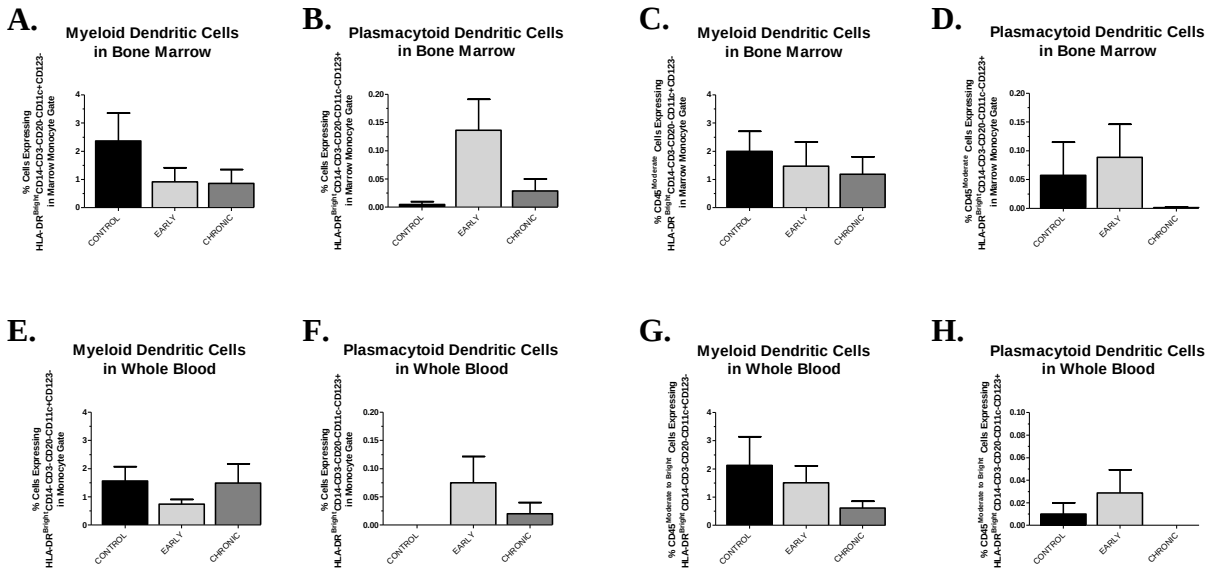

Figure 6.15. Bone marrow and whole blood percentages of dendritic cells during SIV infection

Percentages of HLA-DR^{Bright}CD14-CD3-CD20- cells expressing CD11c and CD123 in bone marrow (BM) and whole blood (WB) populations by dendritic cell gating strategy as described in text. **A-B** Dendritic cells in marrow monocyte gate. **C-D** CD45^{Moderate} dendritic cells in marrow. **E-F** Dendritic cells in blood monocyte gate. **G-H** CD45$^{Moderate\ to\ bright}$ dendritic cells in blood. Comparison of control cohort to early and chronic periods during SIV infection by Mann Whitney t tests (no difference). Percentages are shown as mean $\pm$ SEM.

Table 6.10. Correlation of Dendritic Cell Gated Populations Comparison Between FSC versus SSC Plot (R3 gate) and CD45 versus SSC Plot (R12 gate) for Bone Marrow

Bone Marrow Phenotype	Spearman r Coefficient	p value
HLA-DR^{Bright}CD14-CD3-CD20-CD11c+CD123- Myeloid Dendritic Cell	0.8923	<0.0001
HLA-DR^{Bright}CD14-CD3-CD20-CD11c-CD123+ Plasmacytoid Dendritic Cell	0.8724	<0.0001

Table 6.11. Correlation of Dendritic Cell Gated Populations Comparison Between FSC versus SSC Plot (R7 gate) and CD45 versus SSC Plot (R19 gate) for Whole Blood

Whole Blood Phenotype	Spearman r Coefficient	p value
HLA-DR^{Bright}CD14-CD3-CD20-CD11c+CD123- Myeloid Dendritic Cell	0.6269	0.0031
HLA-DR^{Bright}CD14-CD3-CD20-CD11c-CD123+ Plasmacytoid Dendritic Cell	0.4676	0.0376

hematopoietic cells, ~5% immature hematopoietic cells, ~2 % NK cells, ~2% immature myeloid cells, and <1% plasma cells and immature B cells. $CD45^{Bright}$ BM mature lymphocytes were ~6% of nucleated cells composed of ~70% CD3+ T lymphocytes, ~30% CD20+ B lymphocytes, <2% NK cells, and <1% plasma cells and immature B cells.

Good correlations for gating by FSC vs. SSC compared to CD45 vs. SSC were found for monocytes and lymphocytes, similar to findings in Chapter 5. CD3+ T cells represented about 1/5 of cells in the multilineage population of controls with moderate to bright expression of CD45. In blood, lymphocytes were predominantly CD3+ and $CD45^{Bright}$ in controls similar to BM findings in the $CD45^{Bright}$ gate. However, careful attention must be paid to gating schemes for identification of BM T cells as CD3+ T have variable staining intensity for CD45. Circulating cells can be gated through CD45 or FSC gates. WB T cells and WB B cells were >95% CD45Bright with high correlations present between gating strategies indicating CD45 is not necessary to identify circulating T and B lymphocytes.

Multilineage gating of BM revealed CD3+ cells were predominantly CD2-CD7, a highly unexpected finding. However, this in not completely unanticipated because CD2 and CD7 are maturation markers we hypothesized would discriminate immature CD3+ T cells or precursors. In blood or scondary lymphoid tissues, CD3+ cells would be expected to express both CD7 and CD2 as the T cell receptor is rearranged and surface expression of CD3 manifests during thymic development after expression of CD7 and before expression of CD2. Findings of decreased expression of early maturation markers were poorly described in the literature especially for bone marrow. Possible explanations would be down-regulation in the BM compartment, binding of CD2 and CD7 by antibodies or other ligands, *de novo* lymphocyte production in bone marrow, or undefined recirculation patterns.

Control macaques had similar percentages in BM and WB respectively by different gating strategies, with good correlations for total B cells and subsets. IgM B cells were found in higher percentages in BM while IgG B cells were found in higher percentages in circulation for control macaques. Plasma cells and immature B cells were found in higher percentages in the $CD45^{DimToModerate}$ gate versus the $CD45^{Bright}$ gate for BM and WB in control macaques. For control macaques, most NK cells were $CD45^{Bright}$.

In Chapter 5 we showed that during SIV infection, BM monocytes were maintained yet there was a loss of BM granulocytes and early loss of BM lymphocytes while circulating lymphocytes declined. This study showed CD3+ T cells were maintained in BM during SIV infection and circulating T cells were lost in the chronic phase. Loss of circulating T cells or lymphopenia has been a defining feature of HIV, AIDS, and SIV (C.D.C. 1982; Henrickson 1983; Veazey 1998). BM $CD45^{Bright}$ gating of T cells revealed mature lymphocytes were CD2+CD7+ similar to circulating T cells.

In WB the percentage of CD3+CD2+CD7+ cells represented the major circulating population but these varied for BM by gating strategy in control macaques. CD3+CD2-CD7- T lymphocytes increased by percentage in circulation post-infection while maintained in BM. CD3+CD2+CD7+ T cells were maintained in BM by percentage but $CD45^{Bright}$CD3+CD2+CD7+ mature T cells decreased post-infection in BM and WB. BM and WB CD3+CD2+CD7- immature T cell percentages peaked early in SIV infection then fell in chronic infection. BM and WB CD3+CD2-CD7- T cells increased early in infection but later decreased in BM.

B lymphocytes decreased post-infection in BM and WB including CD38+ activated B cells. IgM secreting mature B cells were maintained in WB but declined in BM by percentage post-infection. IgG secreting mature B cells were low in BM and WB with depletion of IgG B

cells in the chronic phase of BM. Early in SIV infection RM revealed loss of circulating B cells including loss of IgG and IgM secreting cells with decreased function (Kuhrt 2010; Peruchon 2009). Replenishment of circulating B cells has been reported to be slower for IgM than IgG B cells without return to pre-infection levels (Kuhrt 2010). One theory for B cell loss is depletion or re-distribution into other lymphoid compartments (Kuhrt 2010). Our study observed loss of B cells in BM, ruling out sequestration or increased production in this lymphoid compartment.

Post-infection plasma cells were depressed in BM and WB; however $CD45^{Bright}$ gating revealed an increase in the early phase. Immature B lymphocytes in BM and WB increased during the early phase then dropped to near control macaque levels in the chronic phase. In HIV patients, plasma cells were decreased early and late during infection without restoration post-ART therapy (Bussmann 2010).

NK cells in BM and WB were low in the early phase then depressed in the chronic phase. $CD45^{Bright}$ NK cells were increased in the early phase. Early in SIV infection circulating NK cells were decreased in the RM and in chronic infection (Pereira 2008; Peruchon 2009). Possible theories for loss of NK cells include overstimulation, necrosis, increased apoptosis or switching of NK cell receptors (Pereira 2008).

Circulating mDC were low post-infection in BM and WB. pDC were increased post-infection in blood but this was only noted in the early phase of infection in BM. HIV-1 acute and chronic infected patients showed losses of pDC and mDC (Brown K. N. 2007; McKenna 2005). Losses of DC in HIV patients was reported from blood and lymph nodes suggesting a loss and not a redistribution during infection (Brown K. N. 2007). HIV infected DC have been reported to ineffectively work as APCs because they cannot appropriately stimulate T cells (McKenna 2005).

Although the lymphocytes in SIV infection were maintained by both phenotypic and morphologic analyses, only the T cells were maintained while B cells, plasma cells, and NK cells declined for bone marrow and whole blood. Monocytes were also maintained during SIV infection though we found losses of mDC without losses of pDC in bone marrow and whole blood. Our study found lower numbers of DC in bone marrow and whole blood with maintenance of T cells in bone marrow but loss in whole blood. Transfection of HIV by 'escort' cells was recently shown by *in vitro* culture experiments using a CXCR4/CCR5 HIV-1 virus with 'host' human cells that monocyte-derived dendritic cells and not peripheral blood mononuclear cells enhanced virus infection (Sealy 2009). Maintenance of T cells in bone marrow with loss of DC suggests DC may be more likely to be infected in bone marrow compared to circulating cells.

SUMMARY

During SIV infection, BM percentages of CD3+ T cells were maintained as CD3+CD2+CD7+ T cells, B cells, plasma cells, NK cells, monocytoid dendritic cells and plasmacytoid dendritic cells, only in the early phase, declined. Concurrently during SIV infection, circulating percentages of T cells, CD3+CD2+CD7+ T cells, B cells, plasma cells, NK cells, and monocytoid dendritic cells declined while plasmacytoid dendritic cells increased. Findings were representative of reports in HIV and SIV. Antigen presenting cells and lymphocytes showed corollary declines during infection in whole blood while bone marrow lymphocytes were maintained. Findings suggest infected cells of bone marrow may be mononuclear DC cells and less likely CD3+ T cells which will be examined in the following chapter. Finally, immunophenotyping revealed T cells, NK cells, plasma cells, and immature B cells were variable for CD45 staining in bone marrow indicating gating schemes should be clearly identified for reporting of these populations during SIV infection.

REFERENCES

Andersen, H., Rossio, J.L., Coalter, V., Poore, B., Martin, M.P., Carrington, M., and Lifson, J.D. (2004). Characterization of rhesus macaque natural killer activity against a rhesus-derived target cell line at the single-cell level. Cellular immunology *231*, 85-95.

Baumgarth, N. (2004). B-cell immunophenotyping. Methods in cell biology *75*, 643-662.

Blom, B., and Spits, H. (2006). Development of human lymphoid cells. Annu Rev Immunol *24*, 287-320.

Bodey, B. (1994). Development of lymphopoiesis as a function of the thymic microenvironment. Use of CD8+ cytotoxic T lymphocytes for cellular immunotherapy of human cancer. In Vivo *8*, 915-943.

Brown, K.N., Trichel, A., and Barratt-Boyes, S.M. (2007). Parallel loss of myeloid and plasmacytoid dendritic cells from blood and lymphoid tissue in simian AIDS. J Immunol *178*, 6958-6967.

Bussmann, B.M., Reiche, S., Bieniek, B., Krznaric, I., Ackermann, F., and Jassoy, C. (2010). Loss of HIV-specific memory B-cells as a potential mechanism for the dysfunction of the humoral immune response against HIV. Virology *397*, 7-13.

C.D.C. (1982). Opportunistic Infections and Kaposi's Sarcoma among Haitians in the United States Morbidity and Mortality Weekly Report *31*, 353-354,360-361.

Coates, P.T., Barratt-Boyes, S.M., Zhang, L., Donnenberg, V.S., O'Connell, P.J., Logar, A.J., Duncan, F.J., Murphey-Corb, M., Donnenberg, A.D., Morelli, A.E., *et al.* (2003). Dendritic cell subsets in blood and lymphoid tissue of rhesus monkeys and their mobilization with Flt3 ligand. Blood *102*, 2513-2521.

Della Bella, S., Giannelli, S., Taddeo, A., Presicce, P., and Villa, M.L. (2008). Application of six-color flow cytometry for the assessment of dendritic cell responses in whole blood assays. Journal of immunological methods *339*, 153-164.

Henrickson, R.V., Maul, D.H., Osborn, K.G., Sever, J.L., Madden, D.L., Ellingsworth, L.R., Anderson, J.H., Lowenstine, L.J., and Gardner, M.B. (1983). Epidemic of acquired immunodeficiency in rhesus monkeys. Lancet *1*, 388-390.

Kuhrt, D., Faith, S.A., Leone, A., Rohankedkar, M., Sodora, D.L., Picker, L.J., and Cole, K.S. (2010). Evidence of early B-cell dysregulation in simian immunodeficiency virus infection: rapid depletion of naive and memory B-cell subsets with delayed reconstitution of the naive B-cell population. J Virol *84*, 2466-2476.

Loken, M.R., Shah, V.O., Dattilio, K.L., and Civin, C.I. (1987). Flow cytometric analysis of human bone marrow. II. Normal B lymphocyte development. Blood *70*, 1316-1324.

Martin-Martin, L., Almeida, J., Hernandez-Campo, P.M., Sanchez, M.L., Lecrevisse, Q., and Orfao, A. (2009). Immunophenotypical, morphologic, and functional characterization of maturation-associated plasmacytoid dendritic cell subsets in normal adult human bone marrow. Transfusion *49*, 1692-1708.

McKenna, K., Beignon, A.S., and Bhardwaj, N. (2005). Plasmacytoid dendritic cells: linking innate and adaptive immunity. J Virol *79*, 17-27.

Medina, F., Segundo, C., Campos-Caro, A., Salcedo, I., Garcia-Poley, A., and Brieva, J.A. (2003). Isolation, maturational level, and functional capacity of human colon lamina propria plasma cells. Gut *52*, 383-389.

Morice, W.G., Hanson, C.A., Kumar, S., Frederick, L.A., Lesnick, C.E., and Greipp, P.R. (2007). Novel multi-parameter flow cytometry sensitively detects phenotypically distinct plasma cell subsets in plasma cell proliferative disorders. Leukemia *21*, 2043-2046.

Noessner, E., and Schleypen, J.S. (2007). The Complexity of Natural Killer Cells, pp. 1621.

Nowakowski, G.S., Witzig, T.E., Dingli, D., Tracz, M.J., Gertz, M.A., Lacy, M.Q., Lust, J.A., Dispenzieri, A., Greipp, P.R., Kyle, R.A., *et al.* (2005). Circulating plasma cells detected by flow cytometry as a predictor of survival in 302 patients with newly diagnosed multiple myeloma. Blood *106*, 2276-2279.

Pereira, L.E., Johnson, R.P., and Ansari, A.A. (2008). Sooty mangabeys and rhesus macaques exhibit significant divergent natural killer cell responses during both acute and chronic phases of SIV infection. Cellular immunology *254*, 10-19.

Peruchon, S., Chaoul, N., Burelout, C., Delache, B., Brochard, P., Laurent, P., Cognasse, F., Prevot, S., Garraud, O., Le Grand, R., *et al.* (2009). Tissue-specific B-cell dysfunction and generalized memory B-cell loss during acute SIV infection. PLoS One *4*, e5966.

Rawstron, A.C., Davies, F.E., DasGupta, R., Ashcroft, A.J., Patmore, R., Drayson, M.T., Owen, R.G., Jack, A.S., Child, J.A., and Morgan, G.J. (2002). Flow cytometric disease monitoring in multiple myeloma: the relationship between normal and neoplastic plasma cells predicts outcome after transplantation. Blood *100*, 3095-3100.

Sealy, R., Jones, B.G., Surman, S.L., and Hurwitz, J.L. (2009). Short communication: The dead cell: a potent escort for HIV type 1 transinfection. AIDS research and human retroviruses *25*, 1123-1128.

Shah, V.O., Civin, C.I., and Loken, M.R. (1988). Flow cytometric analysis of human bone marrow. IV. Differential quantitative expression of T-200 common leukocyte antigen during normal hemopoiesis. J Immunol *140*, 1861-1867.

Sims, G.P., Ettinger, R., Shirota, Y., Yarboro, C.H., Illei, G.G., and Lipsky, P.E. (2005). Identification and characterization of circulating human transitional B cells. Blood *105*, 4390-4398.

Smock, K.J., Perkins, S.L., and Bahler, D.W. (2007). Quantitation of plasma cells in bone marrow aspirates by flow cytometric analysis compared with morphologic assessment. Archives of pathology & laboratory medicine *131*, 951-955.

Spits, H. (2002). Development of alphabeta T cells in the human thymus. Nature reviews *2*, 760-772.

Szabolcs, P., Park, K.D., Reese, M., Marti, L., Broadwater, G., and Kurtzberg, J. (2003). Absolute values of dendritic cell subsets in bone marrow, cord blood, and peripheral blood enumerated by a novel method. Stem cells (Dayton, Ohio) *21*, 296-303.

Szczepanski, T., van der Velden, V.H., and van Dongen, J.J. (2006). Flow-cytometric immunophenotyping of normal and malignant lymphocytes. Clin Chem Lab Med *44*, 775-796.

Upham, J.W., Lundahl, J., Liang, H., Denburg, J.A., O'Byrne, P.M., and Snider, D.P. (2000). Simplified quantitation of myeloid dendritic cells in peripheral blood using flow cytometry. Cytometry *40*, 50-59.

Veazey, R.S., DeMaria, M., Chalifoux, L.V., Shvetz, D.E., Pauley, D.R., Knight, H.L., Rosenzweig, M., Johnson, R.P., Desrosiers, R.C., and Lackner, A.A. (1998). Gastrointestinal tract as a major site of CD4+ T cell depletion and viral replication in SIV infection. Science *280*, 427-431.

Warren, H.S. (2005). The Eighth Human Leucocyte Differentiation Antigen (HLDA8) Workshop: natural killer cell section report. Cellular immunology *236*, 17-20.

Wei, S., Kryczek, I., and Zou, W. (2006). Regulatory T cell compartmentalization and trafficking. Blood.

CHAPTER 7: VIRAL COPIES OF SIV ARE READILY PRESENT IN BONE MARROW YET FEW MONONUCLEAR HEMATOPOIEITIC BONE MARROW CELLS ARE OBSERVED TO BE INFECTED IN THE COURSE OF SIV DISEASE

INTRODUCTION

As early as 3 days post-infection, bone marrow hyperplasia, consisting of myeloid hyperplasia with a left shift that increases the myeloid: erythroid ratio and megakaryocyte hyperplasia are evident (Mandell 1993). RM studies of bone marrow hematopoietic cells have found virus in bone marrow as early as 2 weeks post SIV infection by *in vivo* and *in vitro* techniques (Watanabe 1990). These early bone marrow changes may be the result of direct viral infection of T cells and macrophages (Mandell 1993). Mononuclear cells have been identified as reservoir for HIV in BM (Louache 1992; Neal 1995). Hematopoietic cells and stromal cells can be infected during HIV infection; however, dysfunction of the stromal support system has been proposed to cause bone marrow changes in hematopoiesis (Douek 2003). Our prior studies have found hematologic abnormalities and bone marrow changed affecting circulating cells (Chapter 3- 6).

The objective of this study was to determine numbers and phenotype of SIV infected cells in bone marrow during progressive SIV disease. We hypothesized mononuclear cells would be infected in bone marrow in very low proportions compared to total nucleated cells. We performed semi-quantitative and quantitative analyses of bone marrow to detect SIV RNA and DNA.

MATERIAL AND METHODS

Experimental Database II-IV

Experimental database and definitions are described in Appendix II. .

Hematologic Data and Definitions

Hematologic data and definitions are described in Appendix I.

Whole Blood Absolute CD4+ Lymphocyte Count

Flow cytometry analysis and whole blood absolute CD4+ lymphocyte count are described in Appendix III.

Plasma Viral Load

Plasma viral loads and definitions are described in Appendix IV.

SIV *In situ* Hybridization

SIV RNA and DNA non-radioactive *in situ* hybridization (ISH) was performed on bone marrow sections as previously described including appropriate positive and negative controls (Borda 2004; Kitagawa 1991; Veazey 1998; Wang 2007). RNA ISH was performed for all infected subjects in ED IV listed in Table II.5 (Appendix II) and DNA ISH was performed on randomly selected SIV infected macaques listed in Table 7.2. Formalin fixed paraffin-embedded bone marrow tissue sections and controls were deparaffinated in xylene followed by hydration in serial alcohol rinses ending in a final distilled diethylpyrocarbonate (DEPC) water rinse. On day 1, tissues were incubated in 0.2M HCl followed by a 1X sodium citrate (SSC) wash and antigen retrieval was performed by steam in 0.01M citrate buffer at pH 6.0 with a conventional microwave. A 60 minute pre-hybridization incubation was performed followed by overnight incubation at 45°C in hybridization buffer with either SIV RNA digoxigenin labeled probe (Lofstrand Labs Limited; Gaithersburg, MD) or SIV DNA digoxigenin labeled probe (TNPRC Molecular Core, gifted from Terri Rasmussen) for detection of SIV RNA and SIV DNA ISH respectively. Short washes in successive 1X SSC dilutions were conducted on day 2 and excess 1X SSC was removed and tissues incubated in protein block (Serum Free Protein Blocker,

DAKO; Carpenteria, CA). Appropriately diluted sheep Fab fragments of anti-digoxigenin antibody (Roche Diagnostics; Indianapolis, IN) were applied and sections were incubated overnight in dark humidified chambers at 4°C. Two post-hybridization buffers were applied to wash tissues on day 3 and sections were developed with the chromogen nitro blue tetrazolium chloride/5-Bromo-4-chloro-3-indolyl phosphate (NBT-BCIP) (Roche). SIV infected cells were distinguished by brown intranuclear staining. For RNA ISH, 3 hour NBT-BCIP incubation was performed. Twenty-seven hour incubation with NBT-BCIP was performed for DNA ISH. A blinded evaluation of non-overlapping fields covering the entire section was performed by one microscopist using a Zeiss Axiostar Plus microscope (Zeiss; Thornwood, NY) was performed. Photographs were taken of representative sections using a 40X objective on a Leica DMLb microscope (Leica; Bannockburn, IL) using Spot Insight color camera and Spot Imaging Software (Diagnostic Instruments; Sterling Heights, MI).

SIV RNA Fluorescent *In situ* Hybridization and Combined Fluorescent Immunohistochemistry detection by Confocal Microscopy

Fluorescent in situ hybridization (FISH) and fluorescent immunohistochemistry (FIHC) were performed on selected infected macaques in Table 7.2 and appropriate controls as previously described (Borda 2004; Wang 2008b; Wang 2007). Bone marrow and mesenteric lymph node tissue were evaluated from eight infected RM from ED II and eight infected RM from ED III by FISH. Tissues from subjects from ED II were triple labeled for detection of SIV by FISH and by HAM56 and infected lymphocytes by CD3 by FIHC.

Briefly, ISH was completed and sections were incubated overnight in 1X tris buffered saline (TBS). A fluorescent antibody was applied in lieu of a chromogen on day 3. After overnight incubation, three serial 1X SSC washes were performed then tissues were incubated in 1X diluted protein block (5X In Situ Hybridization Blocking Solution, Vector Laboratories;

Burlingame, CA) for 30 minutes. Appropriately diluted sheep Fab fragments of anti-digoxigenin antibody (Roche Diagnostics; Indianapolis, IN) were applied and sections were incubated for 60 minutes in dark humidified chambers. Three serial 1X TBS washes were performed followed by incubation with Permanent Red for 20 minutes. SIV RNA was detected by permanent fast red which fluoresces at 568 nm. FIHC was performed afterward, for a select group of ED II macaques, following incubation in 1X TBS overnight. On day 4, tissues were incubated for 60 minutes with 10% normal goat serum (NGS) (Gibco; Carlsbad, CA) followed by incubation with the primary antibody (macrophage) HAM56 diluted in NGS and incubated for another 60 minutes (Table 7.1). Three serial washes in PBS-fish skin gelatin (FSG)-Tx100 then PBS-FSG were followed by incubation with the secondary antibody appropriately diluted in NGS for another 60 minutes (Table 7.1). Three serial washes in PBS-FSG-TX100 and PBS-FSG were performed. Tissues were incubated overnight in PBS-FSG then the FIHC protocol was repeated on day 5 using CD3 as the primary antibody with an appropriate secondary antibody (Table 7.1).

Sections were examined by confocal microscopy at the TNPRC Confocal Microscopy Core. A Leica TCS SP2 confocal microscope with three lasers was utilized (Leica Microsystems; Exton, PA) to image serial optical slices of 750 um^2 with a 20x objective.

Table 7.1. Primary and Secondary Antibody Staining for Fluorescent Immunohistochemistry of Experimental Database II

	Macrophage Staining	**Lymphocyte Staining**
Primary Antibody Reagent, dilution Clone Resource	 HAM56, 1:20 Mouse anti-human macrophage DAKO; Carpenteria, CA	 CD3 1:1000 Rabbit anti-human, Clone DAKO; Carpenteria, CA
Secondary Antibody Reagent, dilution Fluorochrome Resource	 Goat anti-mouse IgM, 1:500 FITC Alexa 488 Invitrogen; Carlsbad, CA	 Goat anti-rabbit IgG1 1:1000 Far-red Alexa 633 Invitrogen; Carlsbad, CA

Grading of SIV Infected Tissues

Subjective grading of bone marrow and lymph node tissue by ISH and FISH was performed as previously described (Borda 2004). A blinded evaluation by one microscopist of all fields per bone marrow tissue and 5 fields of lymph node tissue was performed by light microscopy using a Zeiss Axiostar Plus microscope with a 20X objective (Zeiss; Thornwood, NY). Grading was 0 if no infected cells were detected (-); 1 to 10 infective cells detected in all microscopic fields (+); and greater than 10 infective cells detected in all microscopic fields (++).

Quantifying SIV Infected Cells in Tissues

FISH staining of bone marrow and lymph node of select SIV infected subjects were quantitatively evaluated for numbers of SIV infected cells/mm^2 as previously described (Wang 2007). A blinded evaluation by one microscopist of random, non-touching fields per tissue was performed by confocal microscopy. Five microscopic fields were evaluated and SIV positive staining cells were manually counted and means calculated and reported as SIV infected cells/mm^2 per tissue.

DNA Polymerase Chain Reaction Analysis

DNA polymerase chain reaction (PCR) was performed with appropriate controls as previously described (Poonia 2006; Vajdy 2001). Bone marrow collected from select ED III subjects (Table 7.3) at necropsy was snap frozen in Tissue-Tek O.C.T. Compound (Sakura Finetek; Torrance, CA) then in dry-ice cooled isopentylbutane and maintained at -80°C. Six frozen sections at 10µm each were prepared for DNA extraction and SIV DNA PCR analysis. DNA extraction was performed as per manufacturer directions for tissue (DNeasy Blood and Tissue Kit, Qiagen; Valencia, CA). Tissue was washed in phosphate buffered saline (PBS) and digested/lysed with Proteinase K. Binding of DNA was performed then washed with a final

elution step. Spectrophotometric analysis of nucleic acid material was performed and all levels were >10µg/mL. DNA primers were SIV specific (Integrated DNA Technologies; San Diego, CA). DNA PCR analysis was performed using a Robocycler Gradient 40 analyzer (Stratagene; La Jolla, CA). A minimum of 35 rounds of amplification were performed to detect viral fragments.

Real Time Polymerase Chain Reaction Analysis

Quantitative real time PCR (qRT-PCR) analysis was performed as previously described (Mohan 2008). Bone marrow tissue was collected from eight ED III subjects at necropsy in RNA later (Ambion; Austin, TX) then frozen and maintained at -80°C. Bone marrow tissue was then defrosted and approximately a 1/2 cm^2 specimen was prepared for RNA extraction and SIV qRT-PCR. RNA extraction was performed as per manufacturer directions (Rneasy Mini Kit, Qiagen; Valencia, CA) with DNase digestion (RNase-free DNase Kit, Qiagen; Valencia, CA). Tissue was washed in PBS and disrupted/homogenized. DNase digestion was performed. Then, binding of RNA was performed followed by washes with a final elution step. Spectrophotometric analysis of nucleic acid material was performed and each sample was standardized to 50µg/mL. RNA primers were SIV specific (TNPRC Molecular Core, gifted from Terri Rasmussen). qRT-PCR was performed using the RT PCR 7500 Fast Real Time PCR System (Applied Biosystems, Inc.; Foster City, CA).

Statistical Analysis

For data evaluation, controls were non-SIV infected macaques and SIV infected subjects were grouped into periods defined as early and chronic based on disease progression as chronic asymptomatic SIV disease (ASY), chronic advanced SIV disease (ASD), and AIDS (Appendix II). Macaques developing AIDS were fast and slow progressors at $\geq$260 DPI.

Statistical difference, $p \leq 0.05$, for periods of SIV infection in SIV infected macaques was determined using the Mann Whitney non-parametric unpaired t test and correlations were determined using non-parametric Spearman correlation coefficients GraphPad Prism with Significance was considered as (GraphPad Software; La Jolla, CA). Spearman correlation and p values for correlations of gating strategies were defined in tables. Data are shown as means $\pm$ SEM. Ss

Percentages of immunophenotypic populations for control and SIV infected macaques were compared using the Mann Whitney non-parametric unpaired t test, and correlations were determined using non-parametric Spearman correlation coefficients GraphPad Prism with significance was considered as (GraphPad Software; San Diego, CA).

Graphs represent the means and SEM. Significant differences were defined as $p \leq 0.05$.

RESULTS

Plasma Viral Load and Whole Blood Absolute CD4+ Lymphocyte Counts During SIV Infection

Viral load (Table IV.1 and Table IV.2 in Appendix IV) and CD4+ lymphocyte counts (Table III.1 and Table III.2 in Appendix III) were determined for all SIV infected RM (ED IV) from blood obtained on the day of necropsy. A trend of increased viral load and decreased CD4 counts was noted though the ASD period had the highest viral load and AIDS had the lowest CD4 counts but correlations were not identified (Figure 7.1). CD4+ lymphocyte counts were significantly different from early through AIDS period ($p \leq 0.0001$), ASY to AIDS period ($p=0.0016$), and ASD to AIDS period ($p=0.0042$). Viral load was significantly different for early to ASY period ($p=0.0004$), early to AIDS period ($p=0.0110$), and ASY to ASD periode ($p=0.0281$).

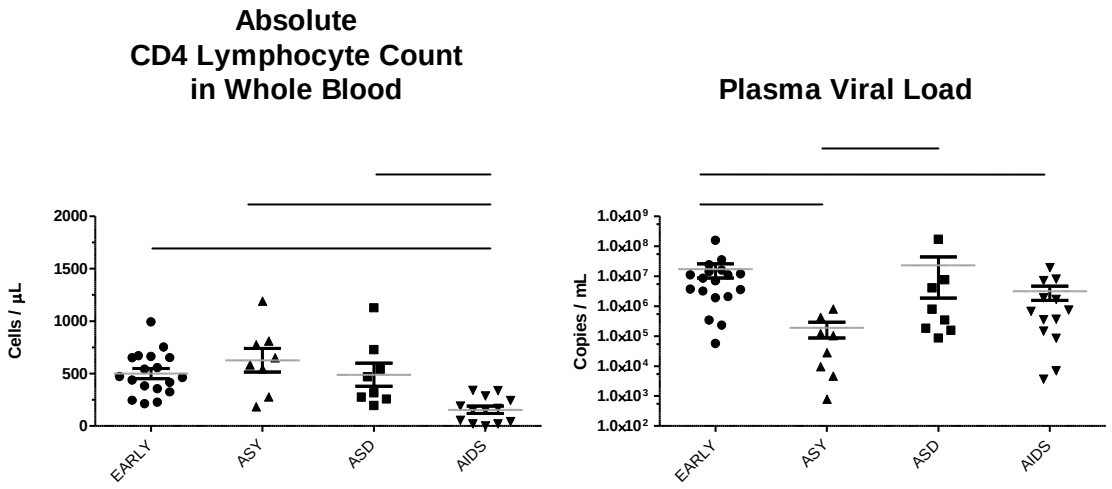

Figure 7.1. CD4 lymphocyte count and plasma viral load for SIV infected macaques
SIV viral load copies during various phases of SIV disease. Phases of SIV infection were early, chronic asymptomatic SIV disease (ASY), chronic advanced SIV disease (ASD), and AIDS. Comparison of various phases of SIV infection by Mann Whitney t tests (**p≤0.001, ***p≤0.01, and ****p≤0.05). Values are shown as mean ± SEM.

Detection of Cellular Viral RNA and DNA in Bone Marrow During SIV Infection

ISH was performed on bone marrow of SIV infected macaques with few positive results. For RNA detection, SIV infected cells were observed in bone marrow tissue from 2 of 47 macaques (HG49 and FT46) (Figure 7.2 and Table 7.2). For DNA detection, bone marrow from 2 of 6 macaques (AL07 and HG56) identified virus (Figure 7.3 and Table 7.2 and Table 7.3).

FISH with FIHC was performed on BM and mesenteric lymph node tissue for 8 infected macaques and FISH only was performed on BM and mesenteric lymph node tissue for 8 other infected macaques (Table 7.2). SIV infected cells were detected for 3/16 infected subjects (BV13, FT46 and HG49). Phenotype of infected cells revealed HAM56+ macrophages, CD3+ T cells, double and single positive cells, and HAM56-CD3- cells (Figure 7.4). Rare giant multi-nucleated cells were SIV positive in lymphoid tissue but HAM56-CD3-.

Table 7.2. SIV Detection in Bone Marrow and Lymph Node Tissue

Subject ID[a]	DPI[b]	RNA ISH BM[c]	DNA ISH BM[d]	RNA FISH BM[e]	RNA FISH LN[f]
BA57	8	-	NP[g]	-	++
BV13	8	-	NP	+	++
AV91	10	-	NP	-	++
HI63	13	-	NP	-	++
M992	13	-	NP	-	++
BI58	22	-	NP	-	++
FT46	71	+	-	+	++
DI28	80	-	NP	-	++
FE53	140	-	-	+	++
HG49	145	+	-	-	++
HI68	155	-	-	NP	NP
HG56	156	-	+	-	++
N998	180	-	NP	-	++
AL07	195	-	+	NP	NP
L164	195	-	NP	-	++
HG58	283	-	-	NP	NP
R544	414	-	NP	-	++
BE64	742	-	NP	-	++
P045	809	-	NP	-	++

ID = identification; b) DPI = days post-inoculation; c) RNA ISH BM = RNA *in situ* hybridization of bone marrow tissue; d) DNA ISH BM = RNA *in situ* hybridization of bone marrow tissue; e) RNA FISH BM = RNA fluorescent *in situ* hybridization of bone marrow tissue; f) RNA FISH BM = RNA fluorescent *in situ* hybridization of lymph node tissue; g) NP = not performed; Subjective grading scale as defined in text

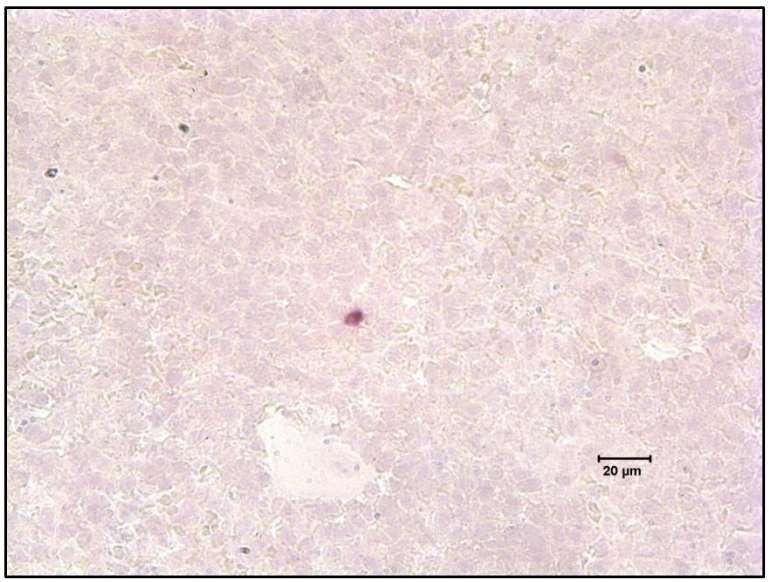

Figure 7.2. SIV viral RNA in bone marrow
Photomicrograph of RNA SIV *in situ* hybridization staining in bone marrow for macaque FT46 that identified an infected cell (brown color). Field represents a 40X objective image (400X) on a Leica DMLb microscope (Leica; Bannockburn, IL) using Spot Insight color camera and Spot Imaging Software (Diagnostic Instruments; Sterling Heights, MI).

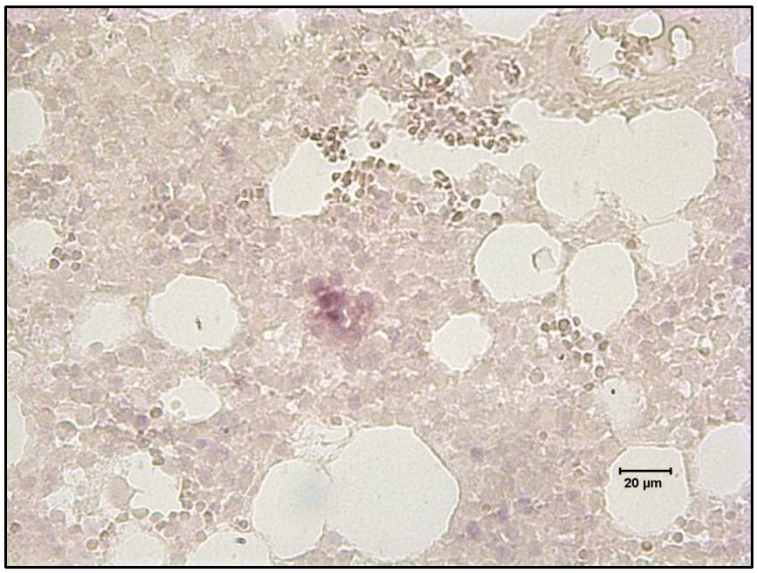

Figure 7.3. SIV viral DNA in bone marrow
Photomicrographs of DNA SIV *in situ* hybridization staining in bone marrow for macaque AL07 that identified viral DNA in a few cells (brown color). Field represents a 40X objective image (400X) on a Leica DMLb microscope (Leica; Bannockburn, IL) using Spot Insight color camera and Spot Imaging Software (Diagnostic Instruments; Sterling Heights, MI).

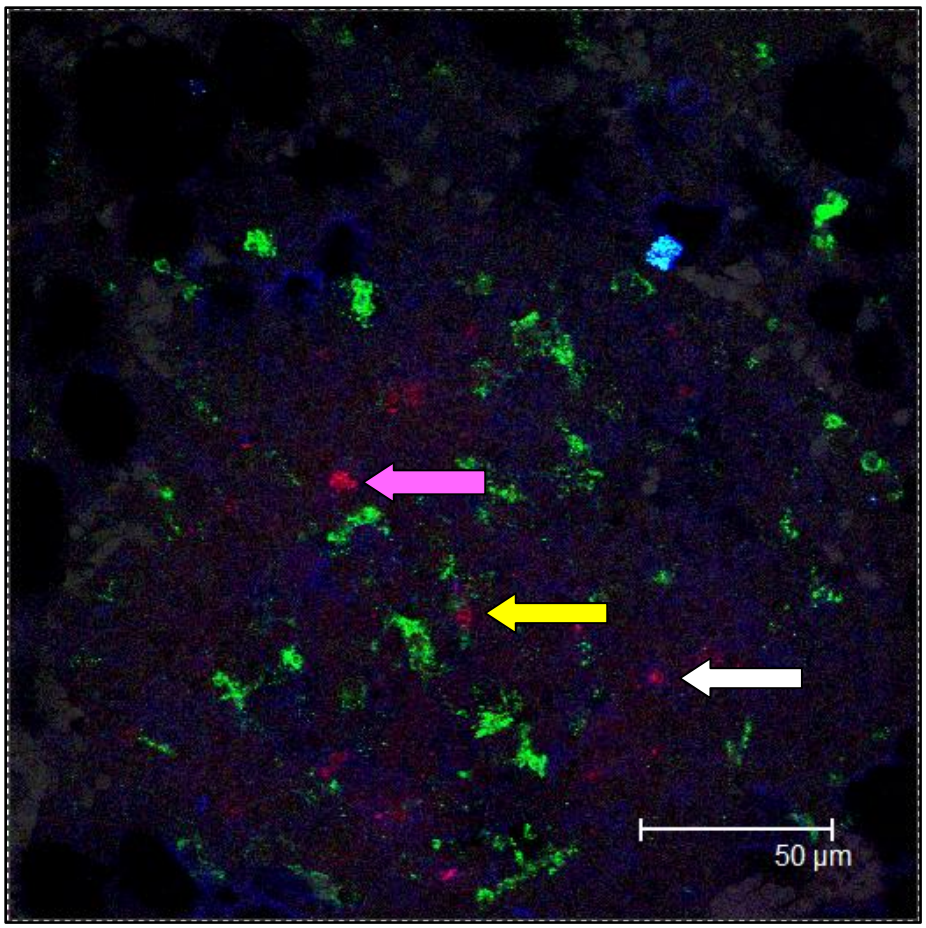

Figure 7.4. Immunophenotypic SIV detection in bone marrow
Photomicrograph of Rhesus macaque BV13 fluorescent *in situ* hybridization and immunohistochemical staining of bone marrow tissue. SIV *in situ* hybridization represented in red, HAM56 macrophages represented in green, CD3 lymphocytes represented in blue. Infected cells are identified as SIV+HAM56-CD3+ (white arrow), SIV+HAM56+CD3- (yellow arrow) and SIV+HAM56-CD3- (pink arrow). Field represents a 100X objective image using a Leica TCS SP2 confocal microscope (Leica Microsystems; Exton, PA).

Viral DNA Was Detected in Bone Marrow Tissue During SIV Infection

Ultrasensitive PCR for detection of SIV DNA in bone marrow tissue revealed positive results (Table 7.3). The first PCR analysis revealed positive results for HG49, FE53, HG56, and HI68 found in the first panel in Figure 7.5. Increased cycles of analysis revealed positive results for AV91, HI63, BA57, and M992 depicted in the second panel in Figure 7.5. Finally >39 cycles revealed positive results for AL07 and FA14 depicted in the third panel in Figure 7.5.

Table 7.3. Polymerase Chain Reaction (PCR) Detection of Viral DNA in Bone Marrow

Subject Identification	DNA PCR
Acute	
AV91	+
BA57	+
HI63	+
M992	+
Chronic	
AL07	+
FA14	+
FE53	+
HG49	+
HG56	+
HG58	+
HI68	+

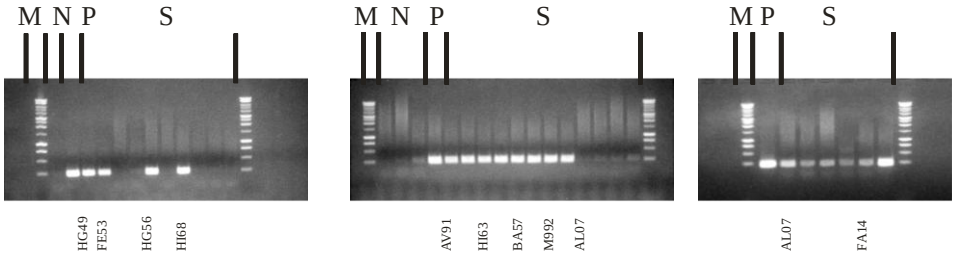

Figure 7.5. SIV viral DNA in bone marrow tissue
Polymerase chain reaction (PCR) for viral DNA SIV in bone marrow tissue in three panels. N is the negative macaque control. P is the positive macaque control. S is bone marrow tissue from the SIV infected Rhesus macaque subjects. PCR as defined in text.

SIV Virus was Quantifiable During SIV Infection

qRT-PCR was performed on bone marrow from four early infected RM AV91, BA57, HI63 and M992 and four chronically infected RM FE53 (symptomatic), FT46 (symptomatic), HG49 and (asymptomatic), HG56 (AIDS) (Table 7.4). RNA was detectable by PCR for all SIV infected animals without correlation to ISH or FISH detection. Viral load was correlated to numbers of SIV infected cells in lymph node (Spearman r=0.7381, p value=0.0458). qRT-PCR bone marrow analysis was negatively correlated to numbers of SIV infected cells in bone marrow (Spearman r= -0.7326, p value=0.0458).

DISCUSSION

Our findings of few infected cells in bone marrow during all periods of SIV infection is supported by findings of others (Doweiko 1993; Harbol 1994). We identified only 4% of RM with infected BM cells by SIV RNA ISH which is lower than reported by Kitagawa et al. at 65% (15/23) subjects (Kitagawa 1991). HIV was detected by RNA ISH in marrow of 16% (6/37) of HIV infected people including those with AIDS (Weiser 1996). By DNA ISH analysis of marrow, we detected 28% infection (2/7). RNA ISH findings were not consistent. Only 1 macaque was detected with infected bone marrow cells by both *in situ* techniques (FT46), but mesenteric lymph node tissue from all SIV infected subjects was positive at all post-inoculation stages of SIV.

Morphologic examination of ISH and FISH SIV tissues revealed SIV infected T lymphocytes, macrophages, and unclassified CD3-HAM56- cells. However, the number of infected cells was too low in marrow to determine the predominant infected cell type. The unclassified CD3-HAM56- cells were mononuclear cells and not multi-nucleated cells such as osteoclasts or megakaryocytes. Interestingly, prior reports of SIV infected marrow cells are

Table 7.4. Detection of SIV

Subject ID[a]	DPI[b]	Plasma Viral Load x 10^4 copies/mL	qRT-PCR[c] copies/mL	RNA ISH M[d]	RNA FISH BM[e] cells/mm^2	SIV RNA FISH LN[f] cells/mm^2	DNA ISH BM[g]	DNA PCR[h]
BA57	8	1428	508	-	0	11.36	NP	+
AV91	10	15719	1904	-	0	26.83	NP[e]	+
HI63	13	2431	1032	NP	0	4.16	NP	+
M992	13	3494	3424	-	0	4.61	NP	+
FT46	71	17079	96	+	0.68	13.73	-	NP
FE53	140	34	21	-	0.23	2.03	-	+
HG49	145	10	122	+	0	2.93	-	NP
HG56	152	1952	1660	-	0	6.75	+	+

ID = identification; b) DPI = days post-inoculation; c) qRT-PCR = quantitative real time polymerase chain reaction; d) RNA ISH BM = RNA *in situ* hybridization of bone marrow tissue; e) RNA FISH BM = RNA fluorescent *in situ* hybridization of bone marrow tissue; f) RNA FISH BM = RNA fluorescent *in situ* hybridization of lymph node tissue; g) DNA ISH BM = RNA *in situ* hybridization of bone marrow tissue; h) DNA PCR = DNA polymerase chain reaction

predominantly macrophage or monocyte lineage cells rather than lymphoid cells especially early in infection (Kitagawa 1991; Mandell 1995). BM macrophages or monocytes were observed to be infected at 1-2 copies per 100 cells in HIV patients by Davis et al. (Davis 1991).

Macrophages were found to be HIV positive from HIV infected cultures of BM from healthy human donors (Canque 1995). Both pDCs and mDCs can be infected with HIV-1 (McKenna 2005). HIV-infected BM mononuclear cells, predominantly CD3+ lymphocytes at a rate of 10-200 HIV copies per 1000 CD3+ T lymphocytes, were detected in symptomatic HIV patients without evidence of infection within CD34+ cells, CFU-GM colonies, or macrophage progenitors (Davis 1991).

Studies have produced conflicting information regarding HIV and its ability to infect CD34+ hematopoietic stem cells. *In vitro* studies demonstrated HIV to infect marrow stem cells and thus produce fewer colony forming units in culture (Harbol 1994). CD34+ bone marrow mononuclear were infected *in vitro* were with HIV89.6 (Carter 2010) and HIV-1 (Folks 1988). Other studies have documented few HIV patients with HIV-1 DNA in CD34+ hematopoietic stem cells (Harbol 1994). CD34+ from BM of asymptomatic HIV infected patients was not positive for HIV RNA (Neal 1995). In patients with high viral loads, CD34+ cells isolated from bone marrow mononuclear cells obtained by BM aspirate were found to express the HIV89.6 clone Gag protein (Carter 2010). Also in HIV human patients on HAART therapy with undetectable viral loads, CD34+ cells isolated from bone marrow mononuclear cell fractions, obtained by BM aspirates, had quantifiable HIV DNA viral genomes (Carter 2010).

HIV has been detected in megakaryocytes of 10/10 AIDS patients with TCP by *in situ* hybridization for RNA based on morphologic appearance (Zucker-Franklin 1989a). One SIV infected RM was reported with infected megakaryocytes by *in situ* hybridization identification

which displayed severe lymphoid depletion and was co-infected with type D retrovirus serotype-1 (Kitagawa 1991). HIV was reported to infect megakaryocytes by CXCR4 co-receptor and monocytic cells by CCR5 co-receptor in BM despite both co-receptors being expressed on both cell types (Lee B. 1999).

Viral DNA was detected in BM in 2 macaques by ISH and in 11/11 (100%) macaques by PCR. Only 5/11 macaques had both ISH and PCR performed and one macaque, HG56, was positive by both techniques. BM aspirate from advanced HIV disease and AIDS patients were detected with proviral DNA in 1-10% of CD4+ T lymphocytes and low numbers of CD14+ monocyte/macrophages and rarely in CD34+ cells and absent in macrophage progenitors (Davis 1991). Viral HIV DNA was found in plasmacytoid and monocytoid dendritic cells isolated from HIV patients (Donaghy 2003). Proviral DNA was not detected from CFU-GM progenitor cells derived *in vitro* from CD34+ cells isolated from bone marrow aspirates of HIV infected patients (Davis 1991). HIV viral DNA could not be detected in sorted BM CD34+ hematopoietic stem cells from HIV patients (Marandin 1996) (De Luca 1993) though Re et al. identified viral DNA copies in CD34+BM cells from 1/11 HIV patients (Re 1993). Viral DNA was not detected from CD34+ BM cells in SHIV infected cynomolgus macaques (Thiebot 2001).

Davis et al estimated fewer than 1 per 200 CFU-GM cells in BM may be infected with HIV viral DNA (Davis 1991). Viral DNA was not detected by PCR in CD34+ sorted bone marrow cells from RM infected with different strains of SIV (van Wely 1993). One week post-HIV infection of *in vitro* CD34+ BM cells with a negative Gag expression followed by addition of GM-CSF and TNF-α allowed detection of Gag expression (Carter 2010). Hillyer et al. identified a weak signal for SIVsmm9 virus by PCR in CFU-GM progenitor cells derived from infected RM (Hillyer 1993b). Culture of BM cells from HIV infected patients did not reveal

detection of RNA or proviral detection in CFU-E, BFU-E, CFU-GM, or CFU-MK (Louache 1992). Davis et al. proposed transmission of virus from progenitor to differentiated cells is highly unlikely (Davis 1991).

We quantified SIV RNA from 8/8 subjects including 1/8 identified by both ISH and FISH, 1/8 identified by ISH, and 1/8 identified by FISH. Even though did not observed infected cells in all macaques, DNA or RNA was present in most. Positive identification of virus is limited by ability of the test to detect a minimum number of viral copies.

We identified only chronically infected macaques with quantifiable SIV and observed positive cells in BM despite quantifiable SIV in early macaques also. Weiser et al further concluded HIV active replication of bone marrow did not occur in all stages of infection as in other lymphoid organs (Weiser 1996). We conclude active infection and viral DNA are present in BM, notably in the chronic periods during progressive SIV infection and recommend multiple techniques be used for detection of SIV in bone marrow. Testing to determine integration of viral DNA is also recommended.

SUMMARY

SIV was detected in bone marrow by multiple techniques. RNA copies of SIV could be quantitated at all phases of infection while microscopic observation could only be detected in the chronic phases. Copies of RNA present in BM were negatively correlated to numbers of SIV infected cells in marrow. DNA copies of SIV were also detected at all phases of infection by polymerase chain reaction while microscopic observation could only be detected in the chronic phases. Low numbers of bone marrow cells were infected with SIV including macrophages, CD3+ T lymphocytes, and unclassified mononuclear cells. Evaluation of subsets of T cells in the following chapter will elucidate shifts during chronic infection.

REFERENCES

Borda, J.T., Alvarez, X., Kondova, I., Aye, P., Simon, M.A., Desrosiers, R.C., and Lackner, A.A. (2004). Cell tropism of simian immunodeficiency virus in culture is not predictive of in vivo tropism or pathogenesis. The American journal of pathology *165*, 2111-2122.

Canque, B., Marandin, A., Rosenzwajg, M., Louache, F., Vainchenker, W., and Gluckman, J.C. (1995). Susceptibility of human bone marrow stromal cells to human immunodeficiency virus (HIV). Virology *208*, 779-783.

Carter, C.C., Onafuwa-Nuga, A., McNamara, L.A., Riddell, J.t., Bixby, D., Savona, M.R., and Collins, K.L. HIV-1 infects multipotent progenitor cells causing cell death and establishing latent cellular reservoirs. Nat Med.

Davis, B.R., Schwartz, D.H., Marx, J.C., Johnson, C.E., Berry, J.M., Lyding, J., Merigan, T.C., and Zander, A. (1991). Absent or rare human immunodeficiency virus infection of bone marrow stem/progenitor cells in vivo. Journal of virology *65*, 1985-1990.

De Luca, A., Teofili, L., Antinori, A., Iovino, M.S., Mencarini, P., Visconti, E., Tamburrini, E., Leone, G., and Ortona, L. (1993). Haemopoietic CD34+ progenitor cells are not infected by HIV-1 in vivo but show impaired clonogenesis. British journal of haematology *85*, 20-24.

Donaghy, H., Gazzard, B., Gotch, F., and Patterson, S. (2003). Dysfunction and infection of freshly isolated blood myeloid and plasmacytoid dendritic cells in patients infected with HIV-1. Blood *101*, 4505-4511.

Douek, D.C., Picker, L.J., and Koup, R.A. (2003). T cell dynamics in HIV-1 infection. Annu Rev Immunol *21*, 265-304.

Doweiko, J.P. (1993). Hematologic aspects of HIV infection. AIDS (London, England) *7*, 753-757.

Folks, T.M., Kessler, S.W., Orenstein, J.M., Justement, J.S., Jaffe, E.S., and Fauci, A.S. (1988). Infection and replication of HIV-1 in purified progenitor cells of normal human bone marrow. Science *242*, 919-922.

Harbol, A.W., Liesveld, J.L., Simpson-Haidaris, P.J., and Abboud, C.N. (1994). Mechanisms of cytopenia in human immunodeficiency virus infection. Blood reviews *8*, 241-251.

Hillyer, C.D., Lackey, D.A., 3rd, Villinger, F., Winton, E.F., McClure, H.M., and Ansari, A.A. (1993). CD34+ and CFU-GM progenitors are significantly decreased in SIVsmm9 infected rhesus macaques with minimal evidence of direct viral infection by polymerase chain reaction. Am J Hematol *43*, 274-278.

Kitagawa, M., Lackner, A.A., Martfeld, D.J., Gardner, M.B., and Dandekar, S. (1991). Simian immunodeficiency virus infection of macaque bone marrow macrophages correlates with disease progression in vivo. The American journal of pathology *138*, 921-930.

Lee, B., Ratajczak, J., Doms, R.W., Gewirtz, A.M., and Ratajczak, M.Z. (1999). Coreceptor/chemokine receptor expression on human hematopoietic cells: biological implications for human immunodeficiency virus-type 1 infection. Blood *93*, 1145-1156.

Louache, F., Henri, A., Bettaieb, A., Oksenhendler, E., Raguin, G., Tulliez, M., and Vainchenker, W. (1992). Role of human immunodeficiency virus replication in defective in vitro growth of hematopoietic progenitors. Blood *80*, 2991-2999.

Mandell, C.P., Jain, N.C., Miller, C.J., and Dandekar, S. (1995). Bone marrow monocyte/macrophages are an early cellular target of pathogenic and nonpathogenic isolates of simian immunodeficiency virus (SIVmac) in rhesus macaques. Laboratory investigation; a journal of technical methods and pathology *72*, 323-333.

Mandell, C.P., Jain, N.C., Miller, C.J., Marthas, M., and Dandekar, S. (1993). Early hematologic changes in rhesus macaques (Macaca mulatta) infected with pathogenic and nonpathogenic isolates of SIVmac. J Med Primatol *22*, 177-186.

Marandin, A., Katz, A., Oksenhendler, E., Tulliez, M., Picard, F., Vainchenker, W., and Louache, F. (1996). Loss of primitive hematopoietic progenitors in patients with human immunodeficiency virus infection. Blood *88*, 4568-4578.

McKenna, K., Beignon, A.S., and Bhardwaj, N. (2005). Plasmacytoid dendritic cells: linking innate and adaptive immunity. J Virol *79*, 17-27.

Mohan, M., Aye, P.P., Borda, J.T., Alvarez, X., and Lackner, A.A. (2008). CCAAT/enhancer binding protein beta is a major mediator of inflammation and viral replication in the gastrointestinal tract of simian immunodeficiency virus-infected rhesus macaques. The American journal of pathology *173*, 106-118.

Neal, T.F., Holland, H.K., Baum, C.M., Villinger, F., Ansari, A.A., Saral, R., Wingard, J.R., and Fleming, W.H. (1995). CD34+ progenitor cells from asymptomatic patients are not a major reservoir for human immunodeficiency virus-1. Blood *86*, 1749-1756.

Poonia, B., Nelson, S., Bagby, G.J., and Veazey, R.S. (2006). Intestinal lymphocyte subsets and turnover are affected by chronic alcohol consumption: implications for SIV/HIV infection. Journal of acquired immune deficiency syndromes (1999) *41*, 537-547.

Re, M.C., Zauli, G., Gibellini, D., Furlini, G., Ramazzotti, E., Monari, P., Ranieri, S., Capitani, S., and La Placa, M. (1993). Uninfected haematopoietic progenitor (CD34+) cells purified from the bone marrow of AIDS patients are committed to apoptotic cell death in culture. AIDS (London, England) *7*, 1049-1055.

Thiebot, H., Louache, F., Vaslin, B., de Revel, T., Neildez, O., Larghero, J., Vainchenker, W., Dormont, D., and Le Grand, R. (2001). Early and persistent bone marrow hematopoiesis defect in simian/human immunodeficiency virus-infected macaques despite efficient reduction of viremia by highly active antiretroviral therapy during primary infection. Journal of virology *75*, 11594-11602.

Vajdy, M., Veazey, R., Tham, I., deBakker, C., Westmoreland, S., Neutra, M., and Lackner, A. (2001). Early immunologic events in mucosal and systemic lymphoid tissues after intrarectal inoculation with simian immunodeficiency virus. J Infect Dis *184*, 1007-1014.

van Wely, M., Slachmuylders, J.F., Visser, T.P., Dubbes, R.H., Niphuis, H., Heeney, J.L., and Wagemaker, G. (1993). Isolation of uninfected immature hematopoietic cells from bone marrow of simian immunodeficiency virus infected rhesus monkeys. Transplant Proc *25*, 1279-1280.

Veazey, R.S., DeMaria, M., Chalifoux, L.V., Shvetz, D.E., Pauley, D.R., Knight, H.L., Rosenzweig, M., Johnson, R.P., Desrosiers, R.C., and Lackner, A.A. (1998). Gastrointestinal tract as a major site of CD4+ T cell depletion and viral replication in SIV infection. Science *280*, 427-431.

Wang, X., Pahar, B., Rasmussen, T., Alvarez, X., Dufour, J., Rasmussen, K., Lackner, A.A., and Veazey, R.S. (2008). Differential cross-reactivity of monoclonal antibody OPD4 (anti-CD45RO) in macaques. Dev Comp Immunol *32*, 859-868.

Wang, X., Rasmussen, T., Pahar, B., Poonia, B., Alvarez, X., Lackner, A.A., and Veazey, R.S. (2007). Massive infection and loss of CD4+ T cells occurs in the intestinal tract of neonatal rhesus macaques in acute SIV infection. Blood *109*, 1174-1181.

Watanabe, M., Ringler, D.J., Nakamura, M., DeLong, P.A., and Letvin, N.L. (1990). Simian immunodeficiency virus inhibits bone marrow hematopoietic progenitor cell growth. J Virol *64*, 656-663.

Weiser, B., Burger, H., Campbell, P., Donelan, S., and Mladenovic, J. (1996). HIV type 1 RNA expression in bone marrows of patients with a spectrum of disease. AIDS research and human retroviruses *12*, 1551-1558.

Zucker-Franklin, D., and Cao, Y.Z. (1989). Megakaryocytes of human immunodeficiency virus-infected individuals express viral RNA. Proceedings of the National Academy of Sciences of the United States of America *86*, 5595-5599.

CHAPTER 8: CD4 T CELLS ARE MAINTAINED AND CD8 T CELLS ARE INCREASED IN BONE MARROW DURING SIV INFECTION

INTRODUCTION

Loss of circulating CD4+ T cells is a hallmark of SIV and HIV disease (Veazey 1998). Activated, memory CD4+ T cells co-expressing CCR5 expression are depleted during SIV infection in secondary and tertiary lymphoid tissues (Veazey 1998; Veazey 2000a). Recently, $\beta7^{High}$CD4+ circulating T cells have been observed to decrease parallel with CD4+CCR5+ T cell loss within the gastrointestinal tract even as circulating CD4+CCR5+ T cells approach pre- SIV infection levels (Wang 2009). Until recently, BM CD4+ lymphocytes during SIV infection were poorly characterized. Paiardini et al. reported during SIV infection, BM CD4+ lymphocytes proliferate at lower levels compared to non-SIV infected RM indicating loss of homeostatic mechanisms (Paiardini 2009).

The objective of this study was to determine absolute changes in lymphocytes population in WB and BM tissue. Our prior studies evaluated percentages of lymphocytes in whole blood (Chapter 3) and bone marrow (Chapter 4-6) during early and chronic stages of SIV. In whole blood we defined increased percentages but steadily declining absolute numbers during SIV disease. Prior studies have reported T cells migrate through blood within the body including bone marrow (Di Rosa 2005; Palendira 2008). Sopper et al. determined the lymphoid organ with highest numbers of lymphocytes was the thymus, followed by the spleen, lymph node, bone marrow, spleen, blood and lung in the RM (Sopper 2003). Moreover, we defined increased BM cellularity during chronic SIV infection (Chapter 4) and increased percentages of BM lymphocytes during chronic infection (Chapter 5 and Chapter 6). Further, we described maintenance of lymphocytes in BM as APCs declined during SIV disease (Chapter 6). Finally,

we established viral RNA and DNA were easily detected in BM during SIV infection, yet productively infected mononuclear cells were rare (Chapter 7).

We hypothesized absolute numbers of T lymphocytes would decrease in the bone marrow compartment for CD4+ and CD8+ lymphocytes including naïve, memory, and activated subsets during progressive SIV infection and independent of the whole blood compartment lymphocyte. We additionally hypothesized the dual loss of lymphocytes in WB and BM would trigger compsensatory changes in lymphocyte homeostasis and regulation between the compartments. Bone marrow was analyzed by immunohistochemistry, flow cytometry, and absolute counts for comparison with blood to determine both percent and absolute values for select lymphocyte subsets.

MATERIAL AND METHODS

Experimental Database II

Experimental database and definitions are described in Appendix II.

Hematologic Data and Definitions

Hematologic data and definitions are described in Appendix I.

Flow Cytometry Analysis

Whole blood and BM tissue collection, flow cytometry preparation, flow cytometry acquisition, flow cytometry analysis, and definitions are described in Appendix III. Immunophenotype of hematopoietic cells was performed for select populations (Table 8.1) based on multiple gating strategies in a particular order relating to grandparent, parent, sibling, and terminal populations. All antibodies were from BD Biosciences (San Jose, CA).

Table 8.1. Lymphocyte Phenotypic Panels for Four Color Flow Cytometry by Antibody and Clone

Flow Cytometry Panel	FITC	PE	PerCP	APC
Lymphocyte Panel I	CD3 Clone SP34-2	CD8 Clone SK1	CD20 Clone L27	CD4 Clone L200
Lymphocyte Panel II	CD20 Clone L27	CD3 Clone SP34-2	CD8 Clone SK1	CD4 Clone L200
Lymphocyte Panel III	CD3 Clone SP34-2	CD20 Clone L27	CD8 Clone SK1	CD4 Clone L200
Early Lymphocyte Panel	CD7 Clone M-T701	CD137 Clone 4B4-1	CD8 Clone SK1	CD4 Clone L200
Proliferation Lymphocyte Panel I	BrdU Clone 3D4	CD3 Clone SP34-2	CD8 Clone SK1	CD4 Clone L200
Proliferation Lymphocyte Panel II	BrdU Clone 3D4	CD195 Clone 3A9	CD8 Clone SK1	CD4 Clone L200
Proliferation Lymphocyte Panel III	Ki67 Clone B56	β7 Clone FIB504	CD8 Clone SK1	CD4 Clone L200
Proliferation Lymphocyte Panel IV	Ki67 Clone B56	CD195 Clone 3A9	CD8 Clone SK1	CD4 Clone L200
Naïve and Memory Lymphocyte Panel	CD95 Clone DX2	CD28 Clone CD28.2	CD8 Clone SK1	CD4 Clone L200
Naïve and Memory and Lymph Node Tissue Homing Molecule Lymphocyte Panel	CD45RA Clone 5H9	CD62L Clone SK11	CD8 Clone SK1	CD4 Clone L200
Early Activation Lymphocyte Panel	CD25 Clone M-A251	CD69 Clone L78	CD8 Clone SK1	CD4 Clone L200
Late Activation Lymphocyte Panel	CD45RA Clone 5H9	HLA-DR Clone L243	CD8 Clone SK1	CD4 Clone L200
Integrin Gut Associated Lymphoid Tissue Homing Molecule Lymphocyte Panel	CD45RA Clone 5H9	βeta7 (β7) Clone FIB504	CD8 Clone SK1	CD4 Clone L200
CCR5 Chemokine Receptor (CD195) Lymphocyte Panel	CD45RA Clone 5H9	CD195 Clone 3A9	CD8 Clone SK1	CD4 Clone L200
CXCR4 Chemokine Receptor (CD184) Lymphocyte Panel	CD45RA Clone 5H9	CD184 Clone 12G5	CD8 Clone SK1	CD4 Clone L200
CXCR3 Chemokine Receptor (CD183) Lymphocyte Panel	CD45RA Clone 5H9	CD183 Clone	CD8 Clone SK1	CD4 Clone L200

Identification of Lymphocytes

Lymphocyte phenotype panels in Table 8.1 were utilized to define populations using Boolean gating schemes as previously described (Veazey 2000b). Lymphocytes were identified in bone marrow and whole blood by first gating through lymphocytes (Figure 8.1). Lymphocyte subsets were then identified as CD4+ or CD8+ or CD7+ (early maturation marker) cells as shown in Figure 8.2B and 8.2C and 8.2D respectively. CD4+ and CD8+ subsets were identified in four quadrant gating as single, double positive, or negative populations in Figure 8.2F. For

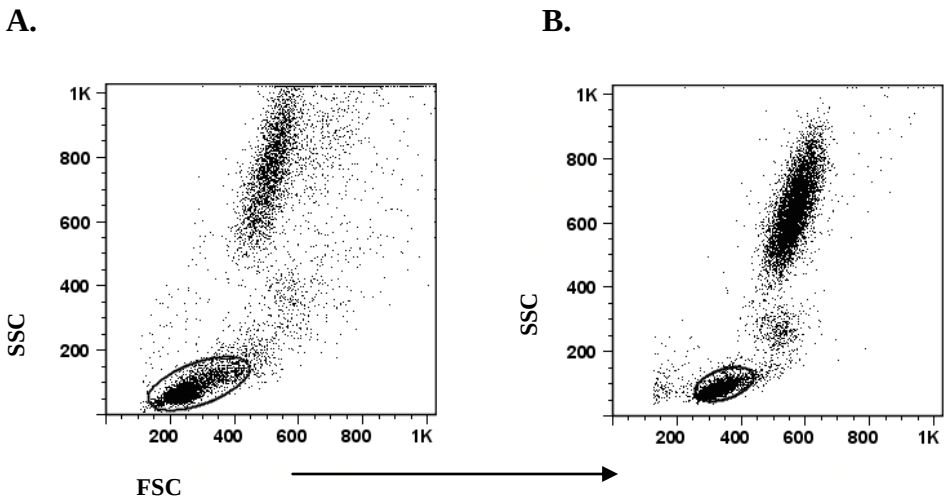

Figure 8.1. Lymphocyte populations in bone marrow and whole blood
Phenotypic gating of lymphocyte populations by FSC versus SSC gating dot plots by multilineage gate of bone marrow (**A.**) and lymphocyte gate of whole blood (**B.**). Lymphocytes are delineated by the oval gates.

identification of T lymphocytes, the CD3+ population was identified (Figure 8.2A) first then subsequent gates were applied (Figure 8.2B-E). Lymphocyte populations were detected using the lymphocyte panel and early lymphocyte panel defined in Table 8.1.

Proliferation Lymphocyte Phenotypic Panel

Proliferating lymphocytes were identified by bromodeoxyuridine (BrdU) while lymphocytes active in the cell cycle were identified by Ki67 in bone marrow and whole blood (Table 8.1). Lymphocytes were identified in bone marrow and whole blood as shown in Figure 8.1 and Figure 8.2. Four terminal phenotypes or gates were identified within the parent gate. The terminal gate was identified by the proliferation marker, either BrdU or Ki67, vs. lymphocyte marker, either CD4 or CD8, plot for determination of double positive cells (Figure 8.3).

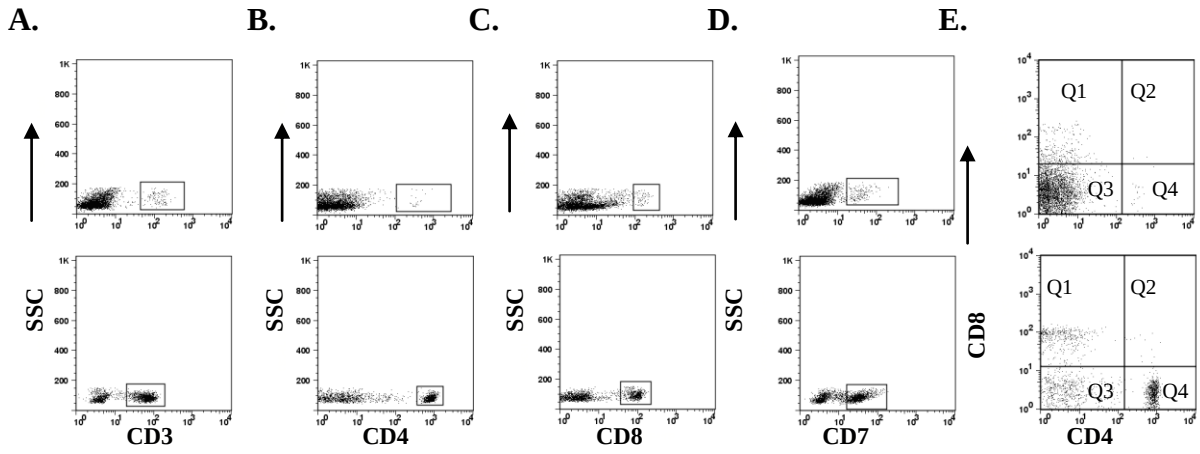

Figure 8.2. Phenotypic identification of lymphocyte subsets
Phenotypic identification of lymphocytes in bone marrow (upper panels) and whole blood (lower panel) by gating from the parent lymphoid or lymphocyte gate by FSC versus SSC plot respectively. **A.** CD3+ lymphocytes by CD3 versus SSC plot. B. CD4+ lymphocytes by CD4 versus SSC plot. **C.** CD8+ lymphocytes by CD8 versus SSC plot. **D.** CD7+ early lymphocytes by CD7 versus SSC plot. E. Four quadrant gating CD4 versus CD8 identified quadrants (Q) as Q1 or CD4-CD8+; Q2 or CD4+CD8+; Q3 or CD4-CD8-; and Q4 or CD4+CD8- lymphocytes. Cells were identified as described in text.

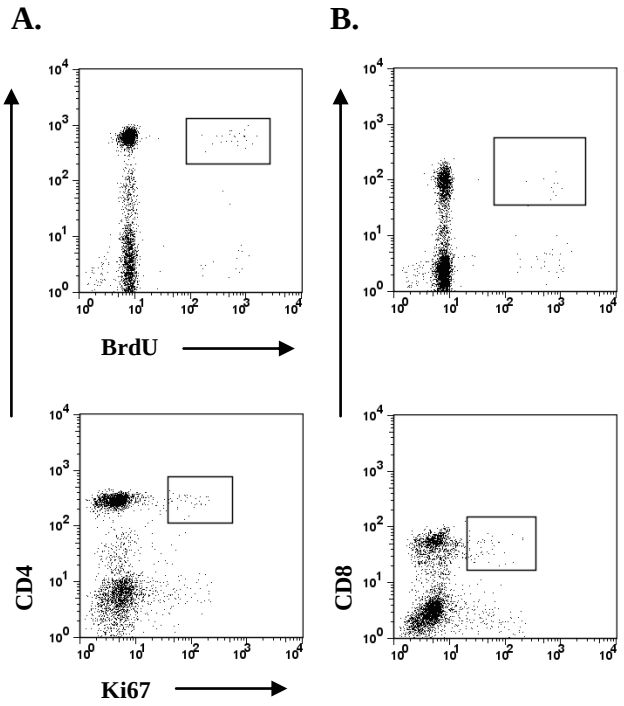

Figure 8.3. Phenotypic identification of proliferating CD4 and CD8 lymphocytes
Phenotypic identification of proliferating lymphocytes in bone marrow and whole blood by gating from the parent lymphoid or lymphocyte gate by FSC versus SSC plot respectively. **A.** BrdU+CD4+ lymphocytes by BrdU versus CD4 plot (upper panel) and Ki67+CD4+ lymphocytes by Ki67 versus CD4 plot (lower panel). **B.** BrdU+CD8+ lymphocytes by BrdU versus CD8 plot (upper panel) and Ki67+CD8+ by Ki67 versus CD8 plot (lower panel). Cells were identified as described in text.

Naïve and Memory, Tissue Homing, Activation, and Chemokine Receptor Lymphocyte Phenotypic Panels

Lymphocytes were identified in bone marrow and whole blood as shown in Figure 8.1 and Figure 8.2. The terminal phenotype was from the parent gates as a four quadrant gate of the FITC antibody vs. the PE antibody for each panel as defined in Table 8.1. Four quadrant gating single positive, double positive, and negative populations (Figure 8.4). FL1 included CD95, CD25, and CD45RA as defined in Table 8.1. FL2 included CD28, CD69, CD62L, HLA-DR, β7, CD195, CD184, and CD183 as defined in Table 8.1. Total cells were the sum of all positive populations.

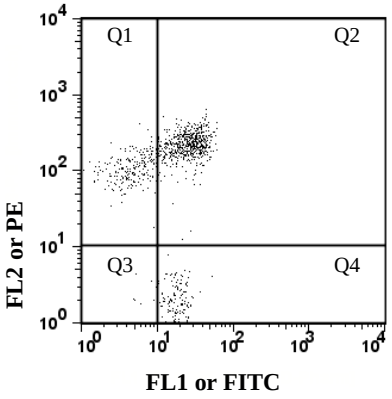

Figure 8.4. Phenotypic identification of lymphocytes by four quadrant gating
Phenotypic identification of naïve, memory, homing, and activated lymphocytes also chemokine receptors on lymphocytes in bone marrow and whole blood by gating described in Table 8.1. The terminal gates of interest were determined by four quadrant gating of FL1 or FITC versus FL2 or PE dot: FL1 or FITC vs. FL2 or PE defined quadrants as Q1 or FL1-FL2+ or single positive FL2, Q2 or FL1+FL2+ or double positive, Q3 or FL1-FL2- or double negative, and Q4 or FL1+FL2- or single positive FL1 lymphocytes.

Plasma Viral Load

Plasma viral loads and definitions are described in Appendix IV.

Quantitation of Macrophages and Lymphocytes in Bone Marrow Tissue

Five μm sections of formalin fixed paraffin-embedded bone marrow tissue were processed for macrophage and CD3 T lymphocyte IHC staining. IHC was performed as previously described (Borda 2004; Wang 2008b). Briefly, tissue sections were fixed in xylene then rehydrated in alcohol gradients and finally distilled water. Antigen retrieval was achieved by steam in 1X citrate buffer pH 6.0 for 20 minutes and then cooled slides were washed in TBS solution. A tissue protein block with DAKO Protein Blocker, Serum Free (Carpenteria, CA) was performed followed with a tissue peroxidase block using DAKO Peroxidase Blocking Reagent (DAKO). After a TBS wash, tissue was incubated with mouse anti-human HAM56 macrophage antibody (DAKO) for 60 minutes. Slides were washed again in TBS and peroxidase amplification was implemented with VectaStain Elite Peroxidase ABC Kit (Vector Laboratories;

Burlingame, CA) per manufacturer direction followed by another TBS wash. Macrophages were detected by DAB chromogen (DAKO) developed for 4 minutes. Following an overnight TBS incubation and wash, the tissue was treated as before by protein block, TBS wash, peroxidase block, and TBS wash. Rabbit anti-human CD3 antibody (DAKO) was applied for 60 minutes. A TBS wash and amplification was performed with a biotin free alkaline phosphatase system by Biocare Medical Mach3 Probe and Polymer system (Biocare; Concord, CA) per manufacturer directions. CD3+ T lymphocytes were detected by Ferangi blue (Biocare) chromogen after 5 minutes development. Tissues were incubated overnight in TBS then air dried and cover slipped. Tissues were imaged using a 20X objective on a Leica DMLb microscope (Leica; Bannockburn, IL) with Spot Insight color camera and Spot Imaging Software (Diagnostic Instruments; Sterling Heights, MI). Each tissue section was examined and 5 random non-touching fields were collected. Image-Pro Plus 4.0 (Media Cybernetics; Silver Springs, MD) software allowed the images to be manually blindly counted for Ham56+ brown cells and CD3+ blue cells within a standard area reported as mean cells/mm^2 from an area of 2800 mm^2 per image (Figure 8.5).

Quantitation of Lymphocyte Subsets in Bone Marrow and Whole Blood

BM absolute numbers were determined. Percentages of CD3+CD4+ and CD3+CD8+ lymphocytes within BM determined by flow cytometry were multiplied by the mean CD3 absolute lymphocyte count from the IHC analysis of bone marrow tissue for each subject to obtain absolute numbers of CD3+CD4+ and CD3+CD8+ lymphocytes respectively. Next, T lymphocyte numbers in marrow were multiplied by the lymphocyte percentage of CD4+ or CD8+ subsets. The resultant new product was the absolute bone marrow immunophenotype lymphocyte count (ILC) defined as lymphocytes/mm^2 for each subset.

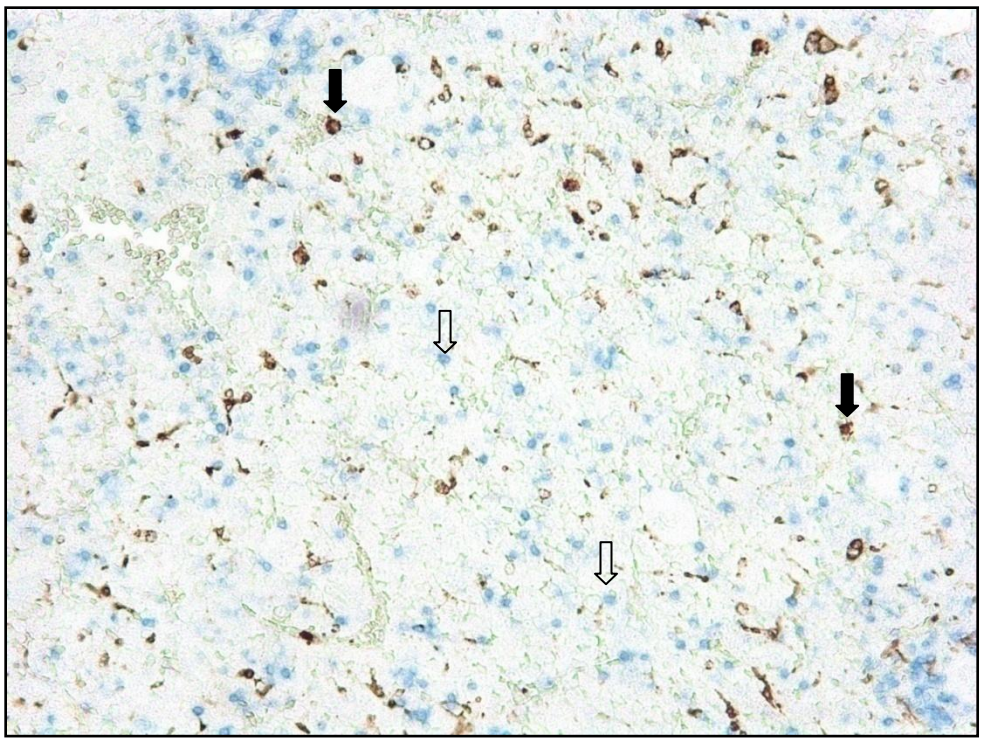

Figure 8.5. Identification of lymphocytes and macrophages in bone marrow tissue
Image representative of immunohistochemical staining for CD3+ lymphocytes (blue cells, open arrow) and macrophages (brown cells, closed arrow) in a paraffin embedded bone marrow tissue section. Field represents a 20X objective image (200X) on a Leica DMLb microscope (Leica; Bannockburn, IL) using Spot Insight color camera and Spot Imaging Software (Diagnostic Instruments; Sterling Heights, MI).

WB absolute numbers were determined suing CBC data. Percentages of CD4+ and CD8+ lymphocytes within the flow cytometry WB lymphocyte gate were multiplied by the absolute lymphocyte count from the CBC analysis for each individual subject to obtain absolute numbers of CD4+ and CD8+ lymphocytes respectively. Next, T lymphocyte numbers in marrow were multiplied by the lymphocyte percentage of CD4+ or CD8+ subsets. The resultant new product was the absolute bone marrow defined as 10^3 lymphocytes/µL.

Statistical Analysis

For data evaluation, controls were non-SIV infected macaques and SIV infected subjects were grouped into periods defined as early and chronic based on disease progression as chronic

asymptomatic SIV disease (ASY), chronic advanced SIV disease (ASD), and AIDS (Appendix II). Macaques developing AIDS were slow progressors at ≥260 DPI.

Percentages and absolute numbers of immunophenotypic populations for control and SIV infected macaques were compared for differences using the Mann Whitney non-parametric unpaired t test and correlations were determined using non-parametric Spearman r correlation coefficients in GraphPad Prism with significance considered as $p \leq 0.05$ (GraphPad Software; La Jolla, CA). Means of data are represented by graphs where error bars represent the SEM.

Percentages and absolute numbers of immunophenotypic populations for control and SIV infected macaques were compared using the Mann Whitney non-parametric unpaired t test, and correlations were determined using non-parametric Spearman correlation coefficients (GraphPad Software; San Diego, CA).

Graphs represent the means and SEM. Significant differences were defined as $p \leq 0.05$.

RESULTS

Phenotyping Lymphocyte Populations During SIV Infection

Lymphocyte populations were compared during progressive SIV infection in the marrow and blood compartment by FSC vs. SSC plot (Figure 8.6). The BM phenotypic lymphocyte gate demonstrated a decline in the early phase and stabilization in the chronic phase, though stages by clinical disease varied which was supported by our prior study (Chapter 5 and Chapter 6). Early in infection, BM showed a decrease while WB maintained percentages, however both compartments peaked in the ASY period followed by drop in the ASD and AIDS periods in SIV. Of note, the BM multilineage gate represented immature hematopoietic cells and the erythroid lineage cells, so further determination of lymphocytes and subsets was needed to ascertain changes in SIV infection .

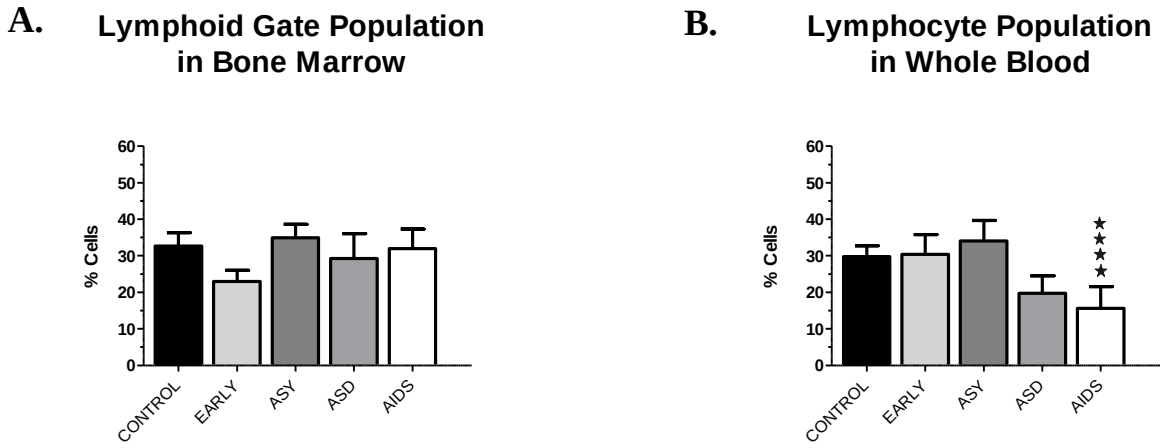

Figure 8.6. Percentages of total cells in phenotypic lymphocyte gates of bone marrow and whole blood during SIV

Mean lymphocyte populations by FSC versus SSC plots during SIV infection. **A.** Percentage of cells in lymphoid gate of bone marrow. **B.** Percentage of cells in lymphocyte gate of whole blood. Mann Whitney t tests compared populations between control cohort and each infected time period of SIV (****$p \leq 0.05$). Infected time periods were early, ASY was chronic asymptomatic group, ASD was advanced SIV disease or chronic symptomatic group, and AIDS displayed as mean values $\pm$ SEM.

Percentages of Lymphocytes that Expressed the Early CD7+ Lymphocyte Phenotype During SIV Infection

CD7 is expressed on T lymphocytes starting early in the maturation process. Percentages of lymphocytes from control RM that expressed the early maturation T lymphocyte phenotype were ~ 10X higher in WB than BM (Figure 8.7). CD7 expression on CD8+ lymphocytes in BM (>60%) but CD4+ in WB (>60%) for control macaques (Figure 8.8). Overall, percentages of CD7+ lymphocytes decreased post-infection in both BM and WB compartments expressed as a steady decline for WB (Figure 8.7) which mimicked the lymphocyte gated populations. Peak populations for CD8+ lymphocytes in both compartments occurred during AIDS while in the same phase CD4+ lymphocytes were the most depressed. BM CD7+CD4+ and CD7+CD8+ cells negatively correlated (Spearman coefficient = -0.3748, p = 0.0265). WB CD7+CD4+ lymphocytes declined post-infection while in the same periods CD7+CD8+ lymphocytes

increased. Phenotypic evaluation of specific lymphocyte populations was performed to examine if loss in early lymphocytes of both compartments translated to loss of mature lymphocytes.

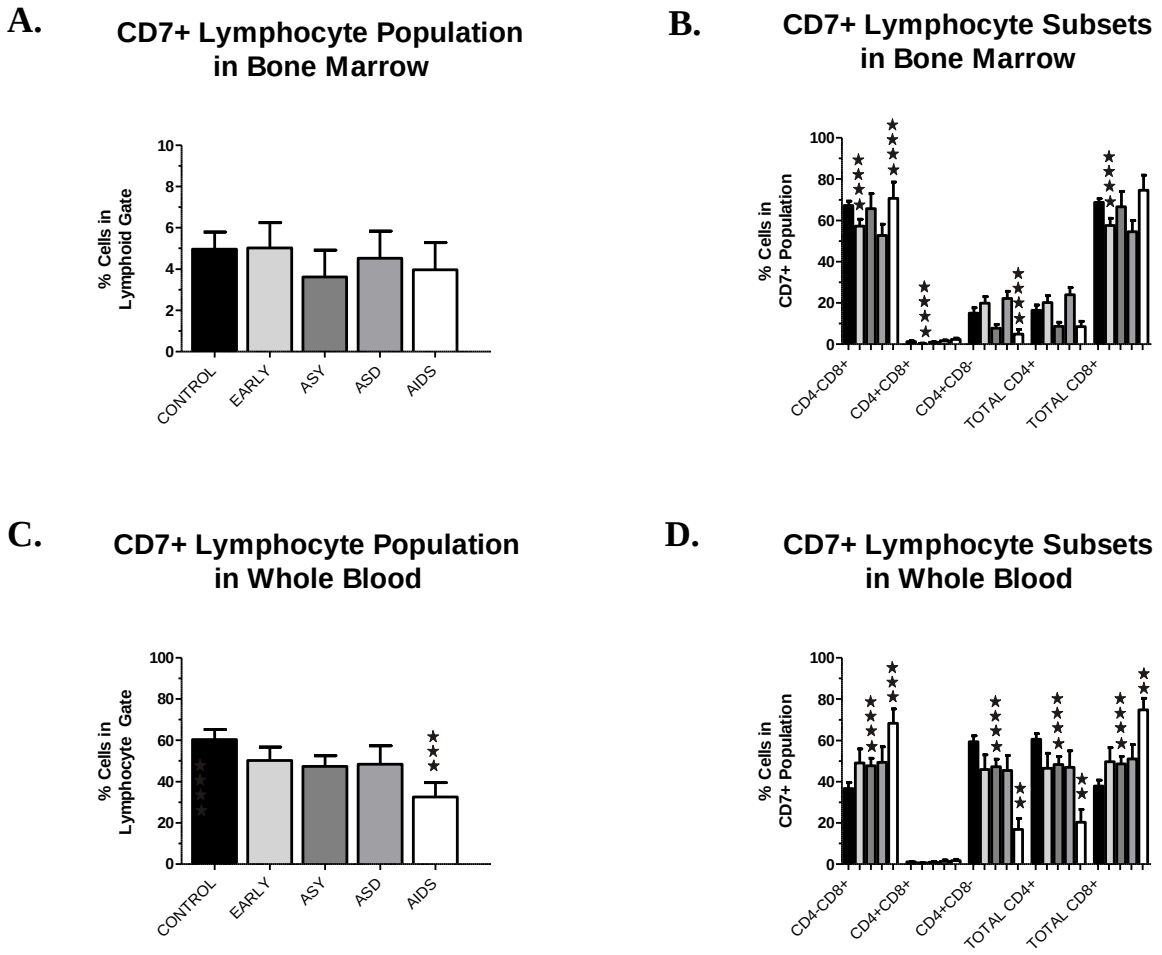

Figure 8.7. Percentages of early maturation markers expressed on lymphocytes in bone marrow and whole blood during SIV

Expression of CD7, an early maturation marker, on lymphocyte subsets during SIV infection. **A.** Percentages of CD7+ lymphocytes in bone marrow. **B.** Percentages of CD7+ lymphocytes in whole blood. **C.** CD4 versus CD8 expression on CD7 lymphocytes in bone marrow by percentage. **D.** CD4 versus CD8 expression on CD7 lymphocytes in whole blood by percentage. Mann Whitney t tests compared populations between control cohort and each infected time period of SIV (**$p \leq 0.001$, ***$p \leq 0.01$, and ****$p \leq 0.05$). Infected time periods were early, ASY was chronic asymptomatic group, ASD was advanced SIV disease or chronic symptomatic group, and AIDS displayed as mean values $\pm$ SEM.

Percentages of T Lymphocytes During SIV Infection

Percentages of T lymphocytes were ~ 7X higher in WB than BM for control macaques (Figure 8.8). Based on CD3+ phenotype, nearly 50% of BM T cells and nearly 80% of WB T cells expressed CD7 in control macaques. Mature BM T lymphocyte populations remained fairly stable during progressive SIV infection compared to loss in circulation by phenotypic analysis. In the ASY phase, BM CD3+ cells were depressed but rebounded in later phases. However, depression of WB CD3+ cells was noted early in infection with failed attempts to rebound as disease progressed to AIDS. Absolute numbers of lymphocytes were determined to verify BM lymphocytes were maintained during SIV disease.

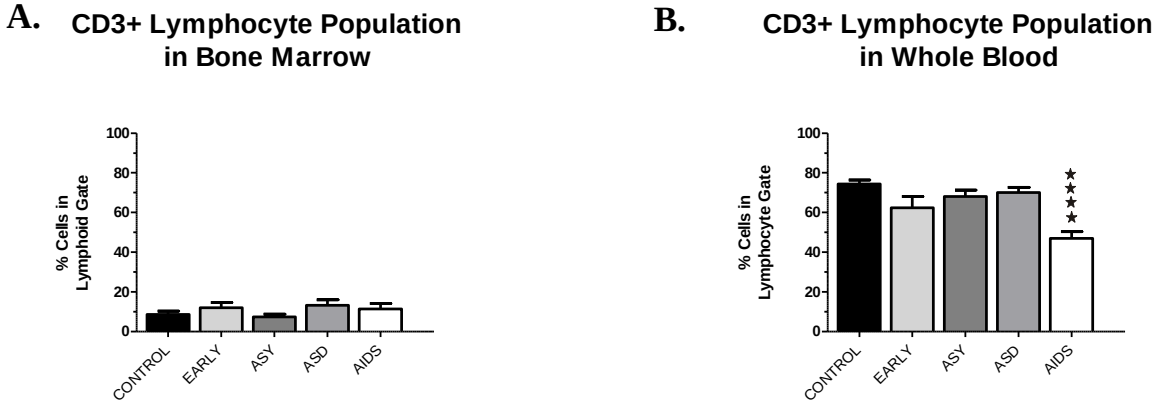

Figure 8.8. Percentages of CD3+ lymphocytes in bone marrow and whole blood during SIV Percentage of CD3+ T lymphocytes during SIV infection in **A.** bone marrow and **B.** whole blood by percentage. Mann Whitney t tests compared populations between control cohort and each infected time period of SIV (****$p \leq 0.05$). Infected time periods were early, ASY was chronic asymptomatic group, ASD was advanced SIV disease or chronic symptomatic group, and AIDS displayed as mean values $\pm$ SEM.

Absolute Numbers of T Lymphocytes During SIV Infection

Post-infection, absolute numbers of T lymphocytes and macrophages in BM determined by IHC analysis increased compared to control macaques, with the smallest increase in the ASY period and highest in the ASD period (Figure 8.9). The ratio of CD3+ lymphocytes to HAM56+

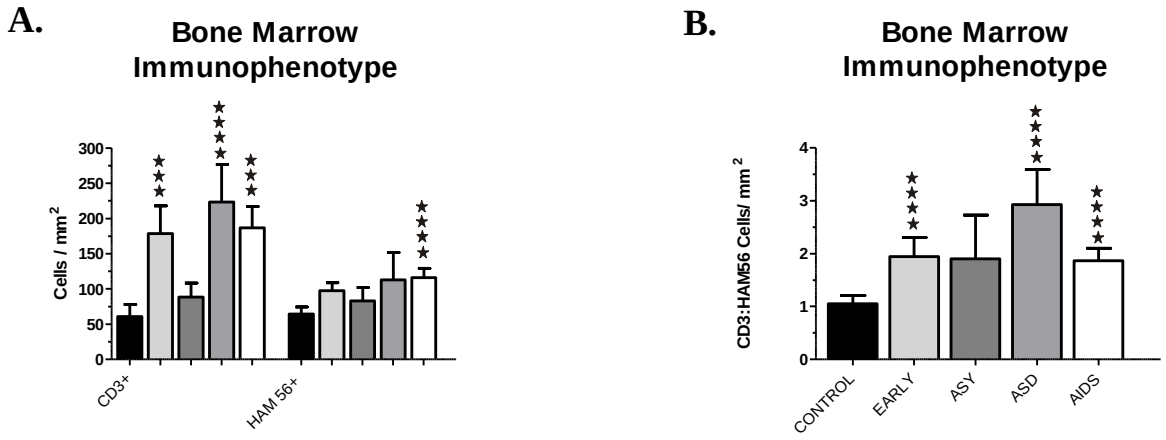

Figure 8.9. Absolute numbers of CD3 lymphocytes and macrophages in bone marrow during SIV

Immunohistochemical evaluation of bone marrow tissue for CD3 T lymphocytes and HAM56 (macrophages) in SIV. **A.** Absolute numbers of CD3+ T lymphocytes and macrophages. **B.** The ratio of CD3+ T lymphocytes to HAM56 macrophages in bone marrow. Mann Whitney t tests compared populations between control cohort and each infected time period of SIV (***$p \leq 0.01$, and ****$p \leq 0.05$). Infected time periods were early, ASY was chronic asymptomatic group, ASD was advanced SIV disease or chronic symptomatic group, and AIDS displayed as mean values $\pm$ SEM.

macrophages was 1 for control macaques while infected macaque ratios were 1.5-2X higher than controls. Meanwhile, absolute numbers of total lymphocytes dropped during the same SIV phases (Figure 8.10). Absolute numbers of several lymphocyte subsets were calculated to characterize the increase in the BM compartment in relation to the loss of the WB compartment.

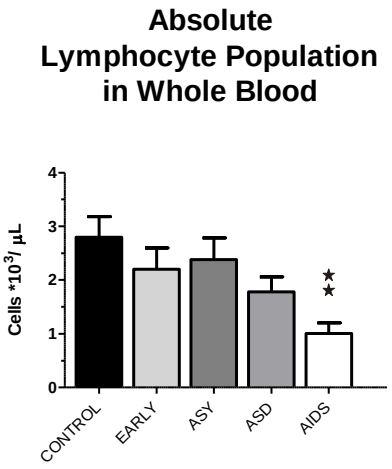

Figure 8.10. Absolute numbers of lymphocytes in whole blood during SIV
Absolute numbers of whole blood lymphocytes by CBC analysis during SIV infection. Mann Whitney t tests compared populations between control cohort and each infected time period of SIV (**$p \leq 0.001$). Infected time periods were early, ASY was chronic asymptomatic group, ASD was advanced SIV disease or chronic symptomatic group, and AIDS displayed as mean values $\pm$ SEM.

Absolute Numbers of Lymphocytes During SIV Infection

CD3+ T lymphocytes in bone marrow of control RM were predominantly composed of CD8+ cells (~75%) and fewer CD4+ cells (~25%) by percentage and absolute numbers with a CD4:CD8 ratio less than 1, the opposite of WB for naïve RM (Figure 8.11). Whole blood had higher percentages of CD4+ lymphocytes ~50% of the lymphocyte population compared to CD8+ lymphocytes at <30% of lymphocytes in controls for a CD4:CD8 percent ratio greater than 1. For control macaques, the WB CD4:CD8 ratio was about 2X higher than the BM CD4:CD8 ratio.

Figure 8.11. Percentages and absolute numbers of CD3, CD4, and CD8 lymphocytes in bone marrow and whole blood during SIV

Expression of CD3, CD4, and CD8 on lymphocytes during SIV infection by percent and absolute numbers in bone marrow and whole blood. **A**. Percent lymphocytes in bone marrow. **B**. Absolute lymphocyte numbers in bone marrow. **C**. CD3+CD4+ to CD3+CD8+ ratio of bone marrow percent lymphocytes. **D**. CD3+CD4+ to CD3+CD8+ ratio of bone marrow absolute lymphocytes. **E**. Percent lymphocytes in whole blood. **F**. Absolute lymphocyte numbers in whole blood. **G**. CD4+ to CD8+ ratio of whole blood percent lymphocytes. **H**. CD4+ to CD8+ ratio of whole blood absolute lymphocytes. Mann Whitney t tests compared populations between control cohort and each infected time period of SIV (**$p \leq 0.001$, ***$p \leq 0.01$, and ****$p \leq 0.05$). Infected time periods were early, ASY was chronic asymptomatic group, ASD was advanced SIV disease or chronic symptomatic group, and AIDS displayed as mean values $\pm$ SEM.

Figure on next page.

A.

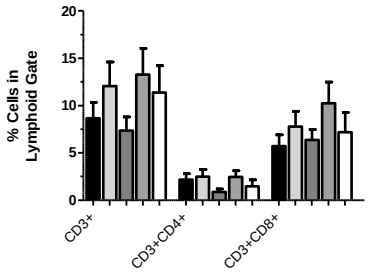
Lymphocyte Population
by Percentage
in Bone Marrow
% Cells in
Lymphoid Gate
20
15
10
5
0
CD3+
CD3+CD4+
CD3+CD8+

B.

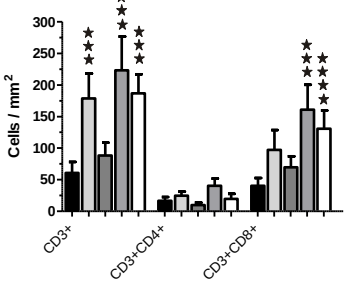
Lymphocyte Population
by Absolute Numbers
in Bone Marrow
Cells / mm2
300
250
200
150
100
50
0
CD3+
CD3+CD4+
CD3+CD8+

C.

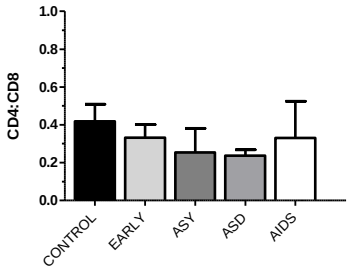
Lymphocyte Percentage Cell
Ratio in Bone Marrow
CD4:CD8
1.0
0.8
0.6
0.4
0.2
0.0
CONTROL
EARLY
ASY
ASD
AIDS

D.

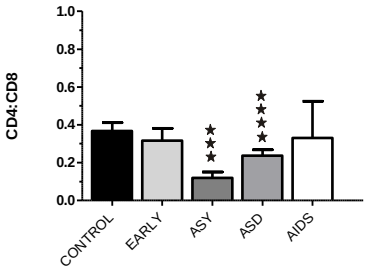
Lymphocyte Absolute Cell
Ratio in Bone Marrow
CD4:CD8
1.0
0.8
0.6
0.4
0.2
0.0
CONTROL
EARLY
ASY
ASD
AIDS

E.

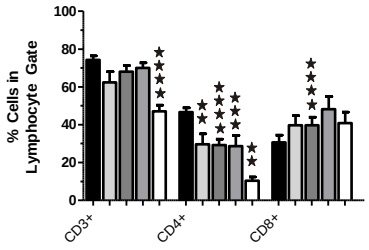
Lymphocyte Population
by Percentage
in Whole Blood
% Cells in
Lymphocyte Gate
100
80
60
40
20
0
CD3+
CD4+
CD8+

F.

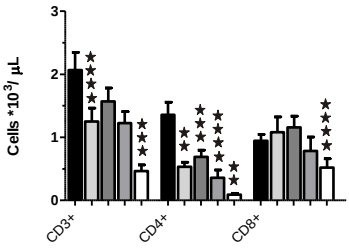
Lymphocyte Population
by Absolute Numbers
in Whole Blood
Cells *10-3/ µL
3
2
1
0
CD3+
CD4+
CD8+

G.

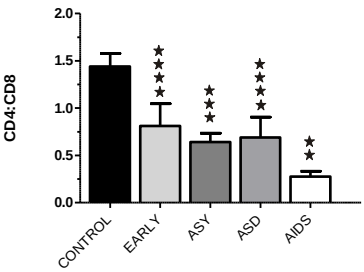
Lymphocyte Percentage Cell
Ratio in Whole Blood
CD4:CD8
2.0
1.5
1.0
0.5
0.0
CONTROL
EARLY
ASY
ASD
AIDS

H.

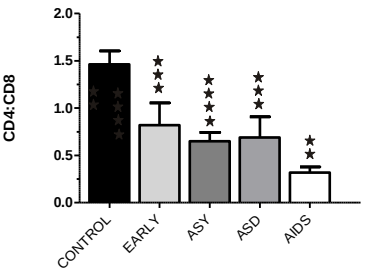
Lymphocyte Absolute Cell
Ratio in Whole Blood
CD4:CD8
2.0
1.5
1.0
0.5
0.0
CONTROL
EARLY
ASY
ASD
AIDS

BM lymphocytes by percent and absolute numbers revealed increases in lymphocytes during SIV infection which were mostly attributed to increased CD3+CD8+ lymphocytes and to a lesser extent CD3+CD4+ lymphocytes. Absolute numbers of CD4+ BM lymphocytes were maintained near control levels but depressed in the ASY and AIDS period. Absolute numbers of CD8+ BM lymphocytes in progressive infection were about 2-3X higher than in controls with peak in later periods ($p \leq 0.05$). Post-infection, BM CD3+, CD3+CD4+, and CD3+CD8+ lymphocytes were highest in the ASD period and lowest in the ASY period.
Infected macaques had low levels of circulating lymphocytes in later phases, especially the AIDS phase, for CD3+, CD4+, and CD8+ lymphocytes. CD8+ lymphocytes were elevated initially during SIV infection but dropped in absolute numbers in advanced stages while CD3+ and CD4+ lymphocytes remained depressed. Post-infection, WB CD3+, CD4+, and CD8+ lymphocytes were highest in the ASY phase and lowest in the AIDS phase.

For both compartments, the CD4:CD8 ratio was never restored to control levels in infected macaques. CD4:CD8 ratios were decreased post-infection with depression in the ASY phase for BM ($p<0.05$) and in AIDS for WB ($p<0.05$).

Similar patterns of total CD8+ and CD4+ lymphocytes were observed for both compartments (Figure 8.12). In both compartments, double positive (CD4+CD8+) lymphocytes were minimally changed by percentage or absolute number during SIV disease. Interestingly, BM CD3+ double negative (CD4-CD8-) lymphocytes were increased during infection ($p<0.05$) similar to BM CD3+CD4+ lymphocytes. In fact, BM CD3+CD4-CD8- lymphocytes were found in greater numbers than CD3+CD4+CD8- for the early and AIDS stages of SIV disease. A moderate negative correlation was observed between CD3+ lymphocyte WB and BM absolute

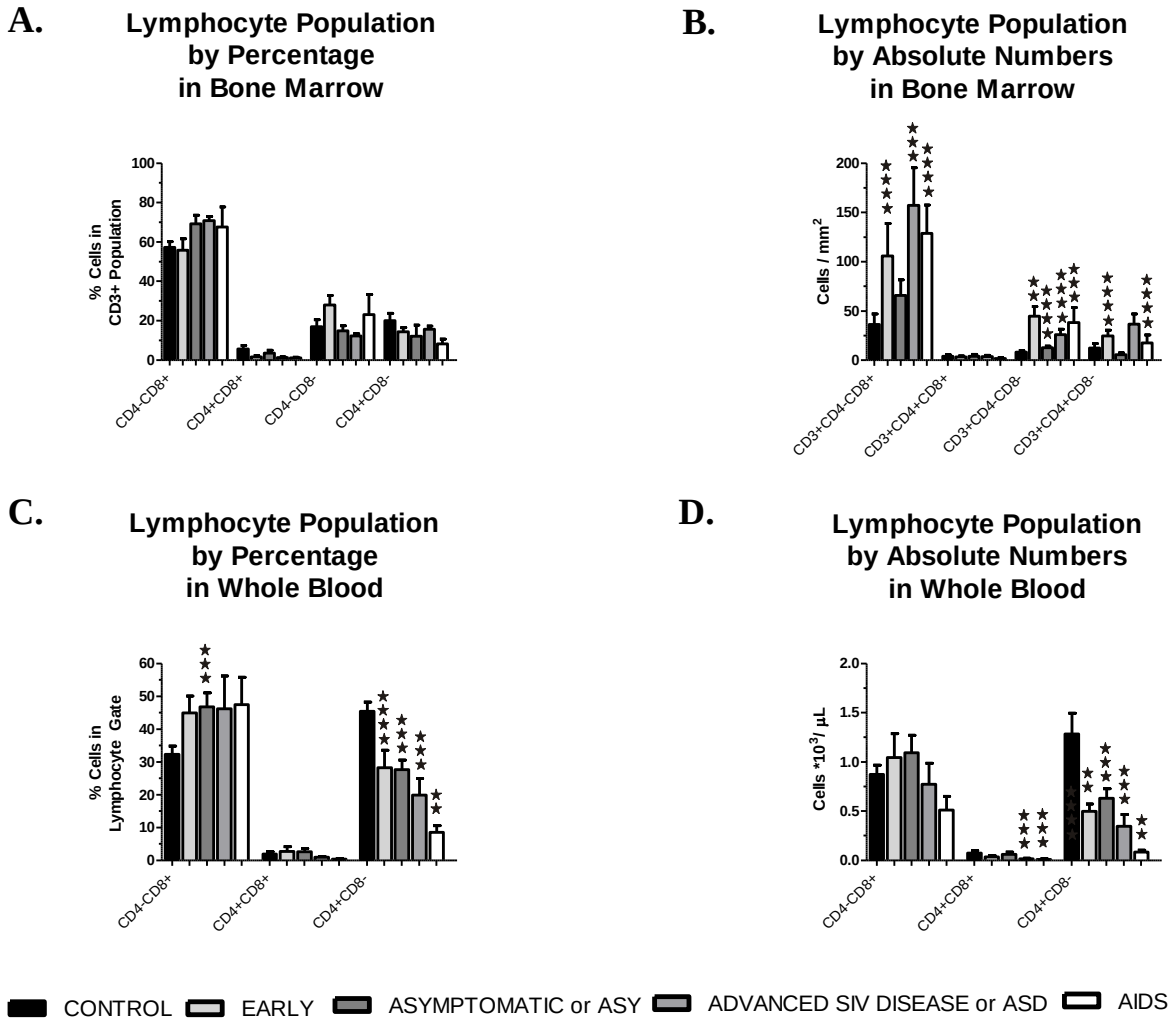

Figure 8.12. Percentages and absolute numbers of CD4/CD8 lymphocytes in bone marrow and whole blood during SIV

Expression of CD4 and CD8 on lymphocytes during SIV infection by percent and absolute numbers in bone marrow and whole blood. **A**. Percent T lymphocytes in bone marrow. **B**. Absolute T lymphocyte numbers in bone marrow. **C**. Percent lymphocytes in whole blood. **D**. Absolute lymphocyte numbers in whole blood. Mann Whitney t tests compared populations between control cohort and each infected time period of SIV (**$p \leq 0.001$, ***$p \leq 0.01$, and ****$p \leq 0.05$). Infected time periods were early, ASY was chronic asymptomatic group, ASD was advanced SIV disease or chronic symptomatic group, and AIDS displayed as mean values $\pm$ SEM.

numbers (Spearman coefficient = -0.4960, p = 0.0033). Correlations were not observed between WB and BM absolute CD4+ lymphocytes or WB and BM absolute CD8+ lymphocytes.

Lymphocyte Subset Proliferation During SIV Infection

BrdU is incorporated into lymphocytes during the S phase (synthesis) during cell replication while Ki67 staining identified lymphocytes within all active stages of cell cycle replication excluding G_0 or resting cells (Figure 8.13 and Figure 8.14 respectively). Controls revealed most BM CD3+CD4+ lymphocytes in the active phases of the cell cycle were replicating confirmed by both percent and absolute number. Absolute numbers of BM CD3+CD8+ lymphocytes revealed $1/10^{th}$ were actively replicating in controls. Control macaques expressed nearly equal numbers of proliferating CD3+CD4+ and CD3+CD8+ lymphocytes in BM though more CD3+CD8+ cells were in the active cell cycle. Proliferating lymphocytes of controls were similar between percent and absolute number in blood with 20% CD4+ lymphocytes and 30% CD8+ lymphocytes replicating. The ratio of S phase by BrdU staining to all active cell cycle stages by Ki67 staining or proliferation ratio was higher for the BM CD3+CD4+ lymphocyte compartment compared to the WB compartment but lower for BM CD3+CD8+ lymphocytes than WB in control subjects (Table 8.2).

Active cell cycle (Ki67) and proliferating (BrdU) CD3+CD4+ BM lymphocytes were similar in patterns with declines in the early and AIDS periods of SIV. CD3+CD8+ BM lymphocytes were increased both by BrdU and Ki67 expression post-infection. Significant differences in the chronic period for CD4+ BM lymphocytes were noted consistent with cell cycle dysregulation also in the early and AIDS periods for CD8+ BM lymphocytes. The CD4:CD8 BM ratios were variable due to differences in absolute numbers during the stages of SIV (Table 8.3).

Figure 8.13. Percentages and absolute numbers of CD4 and CD8 proliferating lymphocytes (BrdU+) in bone marrow and whole blood during SIV

Expression of BrdU on lymphocytes during SIV infection by percent and absolute numbers in bone marrow and whole blood to detect S phase of the cell cycle or replication as described in text. **A**. Percent CD4+ BrdU+ lymphocytes in bone marrow. **B**. Absolute CD3+CD4+ BrdU+ lymphocyte numbers in bone marrow. **C**. Percent CD4+ BrdU+ lymphocytes in whole blood. **D**. Absolute CD4+ BrdU+ lymphocyte numbers in whole blood. **E**. Percent CD8+ BrdU+ lymphocytes in bone marrow. **F**. Absolute CD3+CD8 BrdU+ lymphocyte numbers in bone marrow. **G**. Percent CD8+ BrdU+ lymphocytes in whole blood. **H**. Absolute CD8+ BrdU+ numbers in whole blood. Mann Whitney t tests were performed between control cohort and each infected time period of SIV (****$p \leq 0.05$). Infected time periods were early, ASY was chronic asymptomatic group, ASD was advanced SIV disease or chronic symptomatic group, and AIDS displayed as mean values $\pm$ SEM.

Figure on next page.

A.

BrdU+ Lymphocyte Population in Bone Marrow

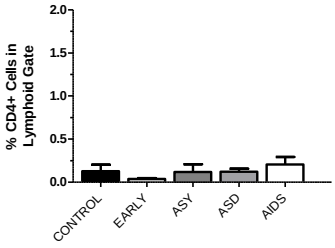

B.

CD3+BrdU+CD4+ Lymphocyte Population in Bone Marrow

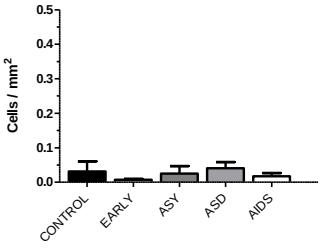

C.

BrdU+ Lymphocyte Population in Whole Blood

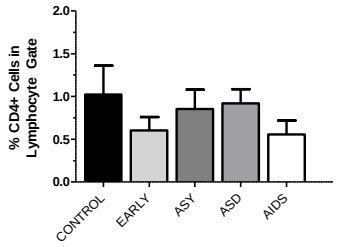

D.

BrdU+CD4+ Lymphocyte Population in Whole Blood

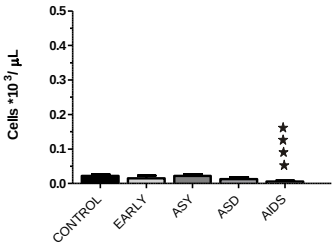

E.

BrdU+ Lymphocyte Population in Bone Marrow

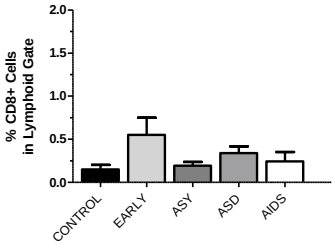

F.

CD3+BrdU+CD8+ Lymphocyte Population in Bone Marrow

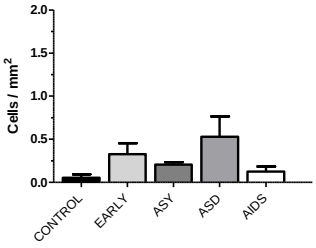

G.

BrdU+ Lymphocyte Population in Whole Blood

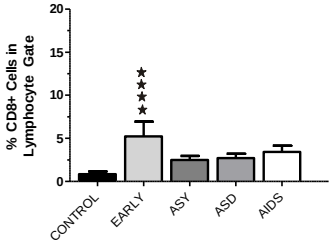

H.

BrdU+CD8+ Lymphocyte Population in Whole Blood

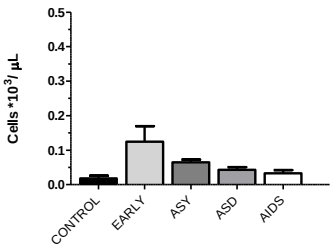

Figure 8.14. Percentages and absolute numbers of CD4 and CD8 lymphocytes within the active cell cycle (Ki67+) in bone marrow and whole blood during SIV
Expression of Ki67 on lymphocytes during SIV infection by percent and absolute numbers in bone marrow and whole blood to detect cells active in the cell cycle or non-resting cells as described in text. **A**. Percent CD4+ Ki67+ lymphocytes in bone marrow. **B**. Absolute CD3+CD4+ Ki67+ lymphocyte numbers in bone marrow. **C**. Percent CD4+ Ki67+ lymphocytes in whole blood. **D**. Absolute CD4+ Ki67+ lymphocyte numbers in whole blood. **E**. Percent CD8+ Ki6+ lymphocytes in bone marrow. **F**. Absolute CD3+CD8 Ki67+ lymphocyte numbers in bone marrow. **G**. Percent CD8+ Ki67+ lymphocytes in whole blood. **H**. Absolute CD8+ Ki6+ lymphocyte numbers in whole blood. Mann Whitney t tests were performed between control cohort and each infected time period of SIV (***$p \leq 0.01$, and ****$p \leq 0.05$). Infected time periods were early, ASY was chronic asymptomatic group, ASD was advanced SIV disease or chronic symptomatic group, and AIDS displayed as mean values $\pm$ SEM.

Figure on next page.

A.

Ki67+ Lymphocyte Population in Bone Marrow

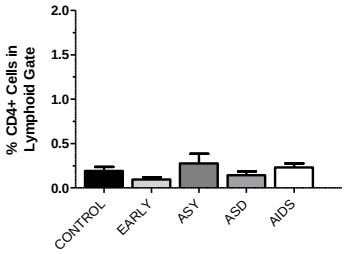

B.

CD3+Ki67+CD4+ Lymphocyte Population in Bone Marrow

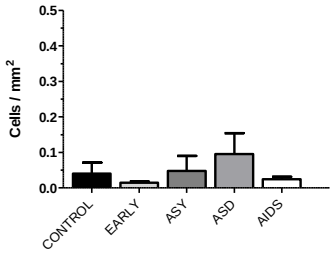

C.

Ki67+ Lymphocyte Population in Whole Blood

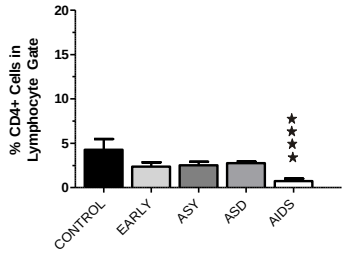

D.

Ki67+CD4+ Lymphocyte Population in Whole Blood

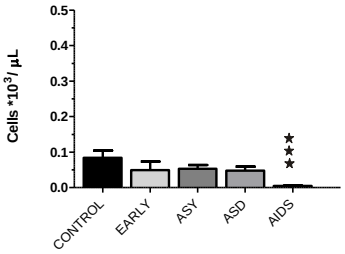

E.

Ki67+ Lymphocyte Population in Bone Marrow

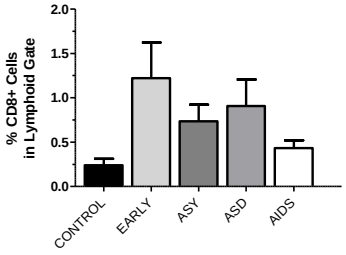

F.

CD3+Ki67+CD8+ Lymphocyte Population in Bone Marrow

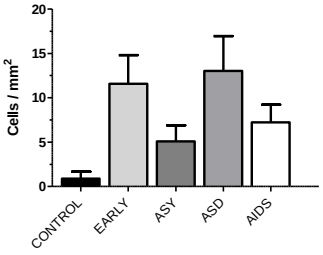

G.

Ki67+ Lymphocyte Population in Whole Blood

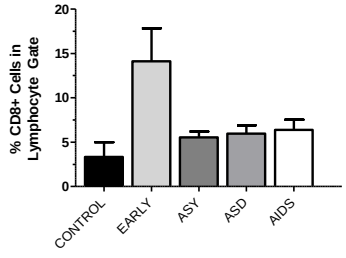

H.

Ki67+CD8+ Lymphocyte Population in Whole Blood

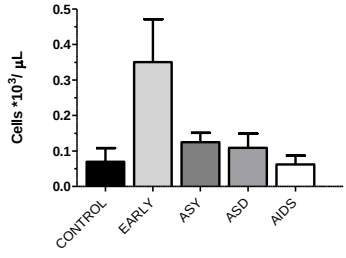

CD4+ lymphocytes expressing Ki67 decreased post-infection in blood but proliferation was low only in the ASY period. Similar patterns of BrdU+ expression CD8+ WB lymphocytes. The ratio of BrdU to Ki67 of circulating lymphocytes increased in CD4+ cells suggesting cell cycle regulation was disturbed (Table 8.2). Nonetheless, absolute numbers varied for WB CD4+ and CD8+ lymphocytes characterized by significantly decreased ratios of CD4 to CD8 ratios with variations of up to 80% lower than control macaques post-infection (Table 8.3).

Table 8.2. Mean BrdU to Ki67 Ratio of Absolute Numbers of Lymphocytes During Progressive SIV Infection

BrdU:Ki67 Lymphocyte Ratio	Control	Early	Asymptomatic	Symptomatic	AIDS
CD3+CD4+ Bone Marrow	0.656	0.641	0.3655****	0.403****	0.831
CD3+CD8+ Bone Marrow	0.073	0.032	0.031	0.061	0.044
CD4+ Whole Blood	0.277	0.316	0.420	0.446	1.092
CD8+ Whole Blood	0.380	0.347	0.392	0.586	0.506

Comparison of control cohort to various phases of SIV infection by Mann Whitney t tests (****p<0.05)

Table 8.3. Mean CD4:CD8 Ratio of Absolute Numbers of Lymphocytes During Progressive SIV Infection

CD4:CD8 Lymphocyte Ratio	Control	Early	Asymptomatic	Symptomatic	AIDS
BrdU Bone Marrow	0.313	0.062	0.111	0.078	2.384
Ki67 Bone Marrow	0.069	0.002	0.008	0.005	0.052
BrdU Whole Blood	1.489	0.243***	0.338	0.289****	0.404
Ki67 Whole Blood	1.928	0.358***	0.477****	0.388	0.168****

Comparison of control cohort to various phases of SIV infection by Mann Whitney t tests (**p<0.001, ***p<0.01, and ****p<0.05)

Memory Lymphocytes During SIV Infection

Naïve and memory lymphocytes were evaluated for changes during SIV disease by CD95 versus CD28 staining as three subsets: naïve lymphocytes CD95-CD28+; central memory (CM) lymphocytes CD95+CD28+; and effector memory (EM) lymphocytes, CD95+CD28- (Pitcher 2002) (Figure 8.15). Another classification of naïve and memory lymphocytes by CD45RA

versus CD62L staining was used to identify four subsets: CD45RA+CD62L+ naïve cells; CD45RA-CD62L+ central memory cells; CD45RA-CD62L- effector memory cells; and CD45RA+CD62L- cells represent terminally differentiated effector memory (TDEM) lymphocytes and recently activated naïve lymphocytes (Kaur 1998; Koopman 2004; Ostrowski 1999) (Figure 8.16).

In controls, BM CD4+ naïve and CM lymphocytes were about equal in numbers by different gating, but EM and TDEM were present by CD45RA strategy and minimal by CD95/28 strategies. WB CD4+ naïve and EM lymphocytes were about equal in numbers by different gating yet only CM cells were detected by CD95/28 gating and only TDEM cells by CD62L gating. BM CD8+ naïve and memory cells were equal in numbers for CD95/CD28 strategies but EM > TDEM > naïve > CM for CD45RA gating. For CD8+ WB lymphocytes, naïve cells > TDEM > EM > CM for CD45RA gating but naïve and memory populations were equal in number by CD95/CD28 strategies. BM CD8+ naïve and memory cells were about double BM CD4+ numbers in control macaques. Naïve CD4+ and CD8+ lymphocytes were equally represented in circulation for control macaques while CD4+ WB memory cells were about double CD8+ WB memory cells.

Naïve BM CD4+ and CD8+ lymphocytes increased in the early and ASD phases and were maintained at near control levels in the ASY and AIDS periods. Naïve circulating CD4+ and CD8+ lymphocytes were low post-infection with near depletion in AIDS.

CM CD8+ lymphocytes were increased post-infection which was also noted for CD4+ CM lymphocytes except in the ASY period. CM BM cells were minimally detected by CD45RA gating. WB CM lymphocytes were low post-infection for CD4+ and maintained for CD8+ cells until AIDS when all were nearly eliminated.

Figure 8.15. Percentages and absolute numbers of CD4 and CD8 CD95/CD28 naïve and memory lymphocytes in bone marrow and whole blood during SIV
Expression of CD95 and CD28 on lymphocytes during SIV infection by percent and absolute numbers in bone marrow and whole blood to detect naïve and memory lymphocytes as described in text. **A**. Percent CD4+ lymphocytes in bone marrow. **B**. Absolute CD3+CD4+ lymphocyte numbers in bone marrow. **C**. Percent CD4+ lymphocytes in whole blood. **D**. Absolute CD4+ lymphocyte numbers in whole blood. **E**. Percent CD8+ lymphocytes in bone marrow. **F**. Absolute CD3+CD8+ lymphocyte numbers in bone marrow. **G**. Percent CD8+ lymphocytes in whole blood. **H**. Absolute CD8+ lymphocyte numbers in whole blood. Mann Whitney t tests compared populations between control cohort and each infected time period of SIV (**$p \leq 0.001$, ***$p \leq 0.01$, and ****$p \leq 0.05$). Infected time periods were early, ASY was chronic asymptomatic group, ASD was advanced SIV disease or chronic symptomatic group, and AIDS displayed as mean values $\pm$ SEM.

Figure on next page.

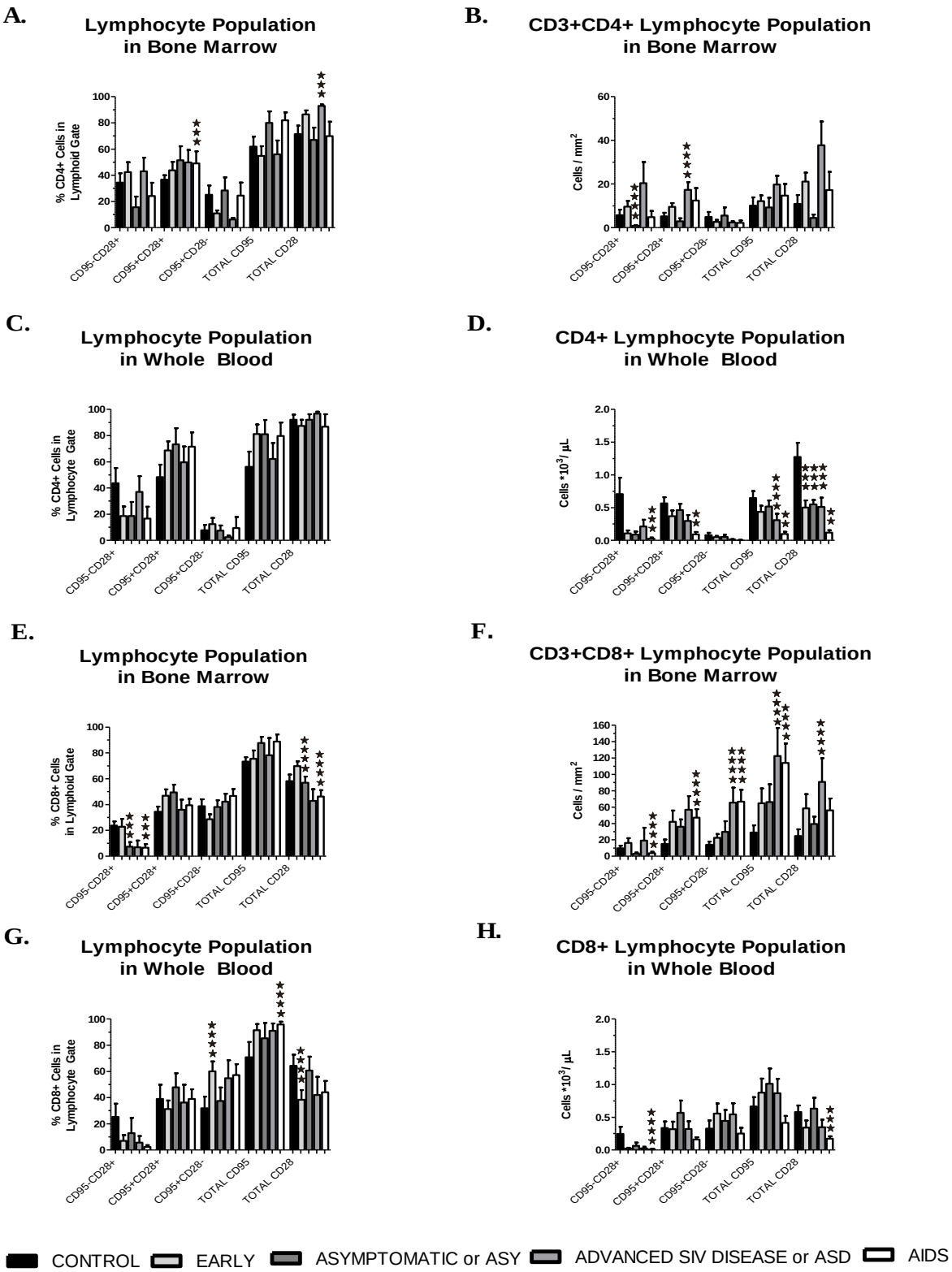
A.
Lymphocyte Population in Bone Marrow
% CD4+ Cells in Lymphoid Gate
B.
CD3+CD4+ Lymphocyte Population in Bone Marrow
Cells / mm2
C.
Lymphocyte Population in Whole Blood
% CD4+ Cells in Lymphocyte Gate
D.
CD4+ Lymphocyte Population in Whole Blood
Cells *10³/ µL
E.
Lymphocyte Population in Bone Marrow
% CD8+ Cells in Lymphoid Gate
F.
CD3+CD8+ Lymphocyte Population in Bone Marrow
Cells / mm2
G.
Lymphocyte Population in Whole Blood
% CD8+ Cells in Lymphocyte Gate
H.
CD8+ Lymphocyte Population in Whole Blood
Cells *10³/ µL
CD95-CD28+
CD95+CD28+
CD95+CD28-
TOTAL CD95
TOTAL CD28
CONTROL
EARLY
ASYMPTOMATIC or ASY
ADVANCED SIV DISEASE or ASD
AIDS

Figure 8.16. Percentages and absolute numbers of CD4 and CD8 CD45RA/CD62L naïve and memory lymphocytes in bone marrow and whole blood during SIV
Expression of CD45RA and CD62L on lymphocytes during SIV infection by percent and absolute numbers in bone marrow and whole blood to detect naïve and memory lymphocytes as described in text. **A**. Percent CD4+ lymphocytes in bone marrow. **B**. Absolute CD3+CD4+ lymphocyte numbers in bone marrow. **C**. Percent CD4+ lymphocytes in whole blood. **D**. Absolute CD4+ lymphocyte numbers in whole blood. **E**. Percent CD8+ lymphocytes in bone marrow. **F**. Absolute CD3+CD8+ lymphocyte numbers in bone marrow. **G**. Percent CD8+ lymphocytes in whole blood. **H**. Absolute CD8+ lymphocyte numbers in whole blood. Mann Whitney t tests compared populations between control cohort and each infected time period of SIV (***$p \leq 0.01$, and ****$p \leq 0.05$). Infected time periods were early, ASY was chronic asymptomatic group, ASD was advanced SIV disease or chronic symptomatic group, and AIDS displayed as mean values $\pm$ SEM.

Figure on next page.

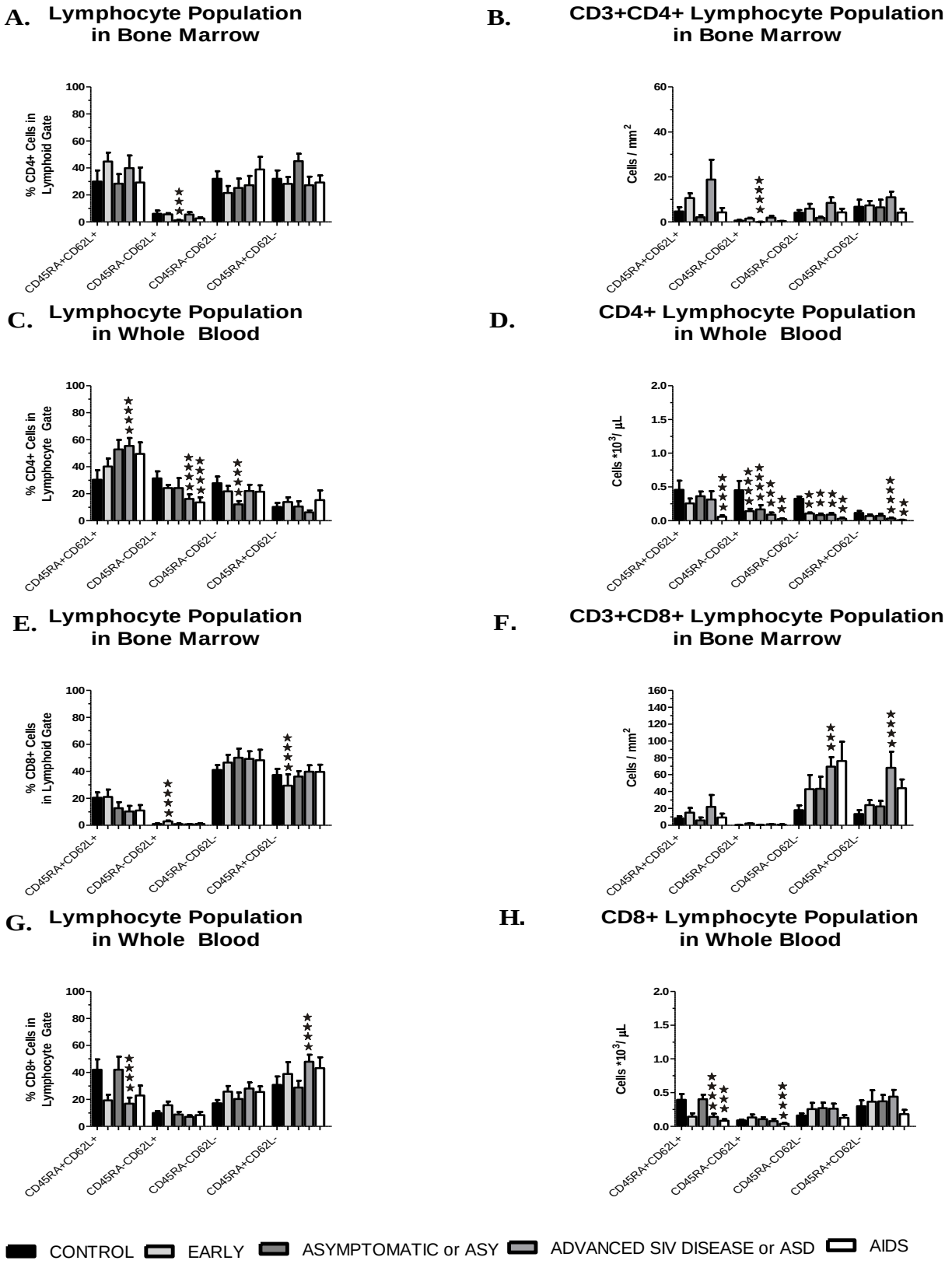
A.
Lymphocyte Population in Bone Marrow
% CD4+ Cells in Lymphoid Gate
B.
CD3+CD4+ Lymphocyte Population in Bone Marrow
Cells / mm2
C.
Lymphocyte Population in Whole Blood
% CD4+ Cells in Lymphocyte Gate
D.
CD4+ Lymphocyte Population in Whole Blood
Cells *10^3/ µL
E.
Lymphocyte Population in Bone Marrow
% CD8+ Cells in Lymphoid Gate
F.
CD3+CD8+ Lymphocyte Population in Bone Marrow
Cells / mm2
G.
Lymphocyte Population in Whole Blood
% CD8+ Cells in Lymphocyte Gate
H.
CD8+ Lymphocyte Population in Whole Blood
Cells *10^3/ µL
CD45RA+CD62L+
CD45RA-CD62L+
CD45RA-CD62L-
CD45RA+CD62L-
CONTROL
EARLY
ASYMPTOMATIC or ASY
ADVANCED SIV DISEASE or ASD
AIDS

BM EM CD4+ lymphocytes by CD45RA gating followed the naïve BM CD4+ memory pattern. However, CM CD4+ BM lymphocytes by CD95/CD28 gating were decreased post-infection. BM EM CD8+ BM lymphocytes were increased post-infection especially in later periods. WB EM CD4+ lymphocyte declined over time post-infection with greatest loss in AIDS while CD8+ lymphocytes were increased until finally depleted in AIDS. The same pattern of EM was observed for TDEM in blood.

Early and Late Activation of Lymphocytes During SIV Infection

Lymphocyte subsets were classified using both early (CD69) and late (CD25, HLA-DR) markers of immune activation. CD25-CD69+ cells were considered very early activated, CD25+CD69- was considered a mid-stage marker, CD25+CD69+ was an early to middle stage marker, and HLA-DR+ was a late marker for lymphocyte activation. Incongruity was observed between the percentage and absolute phenotype for circulating CD4+ lymphocytes while other subsets were congruent.

Early to middle stage activated cells (Figure 8.17) and late stage activated cells (Figure 8.18) were examined in bone marrow and whole blood. In control macaques, activated CD4+ BM lymphocytes were represented by late > early > middle > early to middle stages. For CD4+ WB lymphocytes in circulation, numbers of activated cells were late > middle > early > early to middle stages. CD4+ lymphocytes were found in all stages of activation while CD8+ lymphocytes expressed early stages > later stages in BM and WB but middle and middle to late stages were not observed.

BM CD4+ lymphocytes displayed increased numbers of early and middle stage activated cells early during infection that waned in AIDS, while late and early-to-middle stage activated cells slowly increased over time. Circulating CD4+ lymphocytes showed decreased activation

Figure 8.17. Percentages and absolute numbers of CD4 and CD8 CD25/CD69 activated lymphocytes in bone marrow and whole blood during SIV

Expression of CD25 and CD69 on lymphocytes during SIV infection by percent and absolute numbers in bone marrow and whole blood to detect activated lymphocytes as described in text. **A**. Percent CD4+ lymphocytes in bone marrow. **B**. Absolute CD3+CD4+ lymphocyte numbers in bone marrow. **C**. Percent CD4+ lymphocytes in whole blood. **D**. Absolute CD4+ lymphocyte numbers in whole blood. **E**. Percent CD8+ lymphocytes in bone marrow. **F**. Absolute CD3+CD8+ lymphocyte numbers in bone marrow. **G**. Percent CD8+ lymphocytes in whole blood. **H**. Absolute CD8+ lymphocyte numbers in whole blood. Mann Whitney t tests compared populations between control cohort and each infected time period of SIV (**$p \leq 0.001$, ***$p \leq 0.01$, and ****$p \leq 0.05$). Infected time periods were early, ASY was chronic asymptomatic group, ASD was advanced SIV disease or chronic symptomatic group, and AIDS displayed as mean values $\pm$ SEM.

Figure on next page.

A.

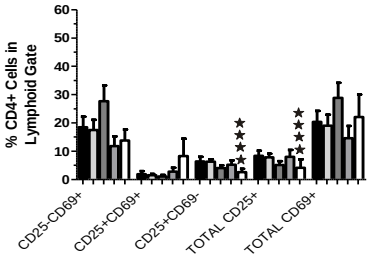

B.

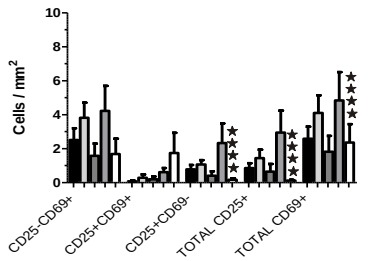

C.

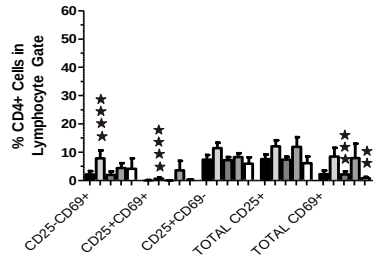

D.

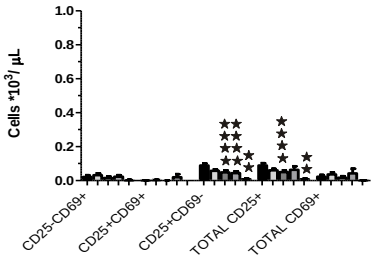

E.

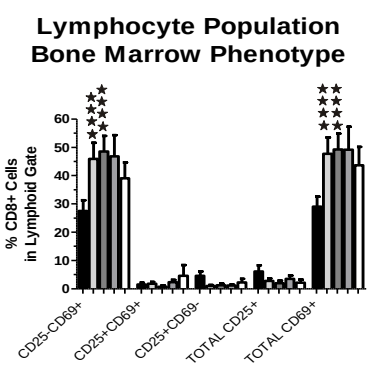

F.

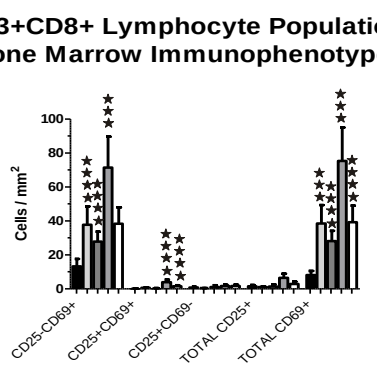

G.

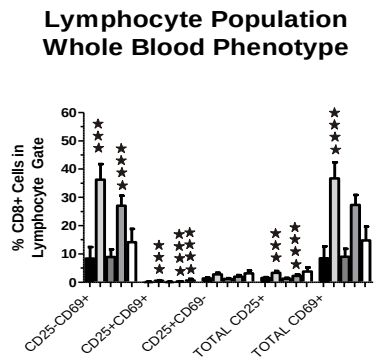

H.

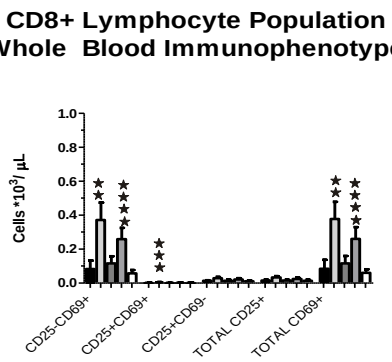

CONTROL EARLY ASYMPTOMATIC or ASY ADVANCED SIV DISEASE or ASD AIDS

Figure 8.18. Percentages and absolute numbers of CD4 and CD8 CD45RA/HLA-DR activated lymphocytes in bone marrow and whole blood during SIV
Expression of CD45RA and HLA-DR on lymphocytes during SIV infection by percent and absolute numbers in bone marrow and whole blood to detect activated lymphocytes. **A**. Percent CD4+ lymphocytes in bone marrow. **B**. Absolute CD3+CD4+ lymphocyte numbers in bone marrow. **C**. Percent CD4+ lymphocytes in whole blood. **D**. Absolute CD4+ lymphocyte numbers in whole blood. **E**. Percent CD8+ lymphocytes in bone marrow. **F**. Absolute CD3+CD8+ lymphocyte numbers in bone marrow. **G**. Percent CD8+ lymphocytes in whole blood. **H**. Absolute CD8+ lymphocyte numbers in whole blood. Mann Whitney t tests compared populations between control cohort and each infected time period of SIV (***$p \leq 0.01$, and ****$p \leq 0.05$). Infected time periods were early, ASY was chronic asymptomatic group, ASD was advanced SIV disease or chronic symptomatic group, and AIDS displayed as mean values $\pm$ SEM.

Figure on next page.

A. **Lymphocyte Population in Bone Marrow**

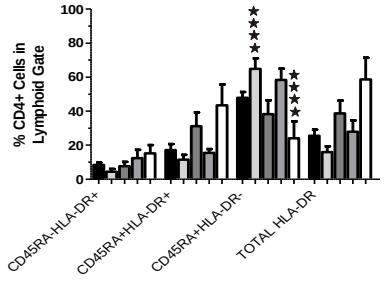

B. **CD3+CD4+ Lymphocyte Population in Bone Marrow**

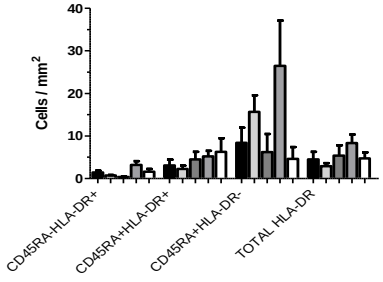

C. **Lymphocyte Population in Whole Blood**

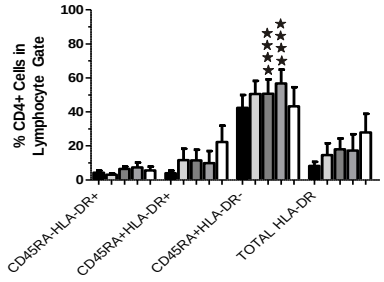

D. **CD4+ Lymphocyte Population in Whole Blood**

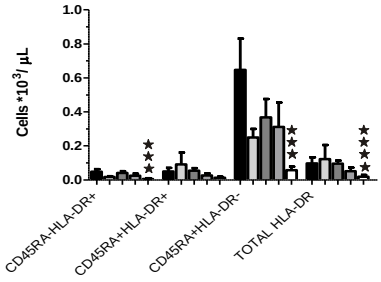

E. **Lymphocyte Population in Bone Marrow**

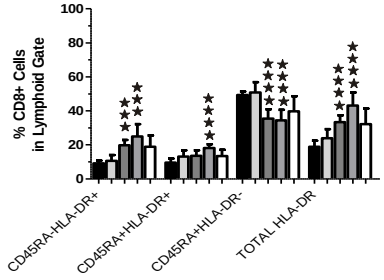

F. **CD3+CD8+ Lymphocyte Population in Bone Marrow**

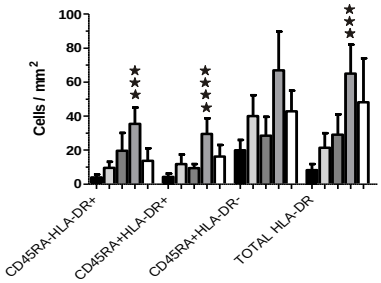

G. **Lymphocyte Population in Whole Blood**

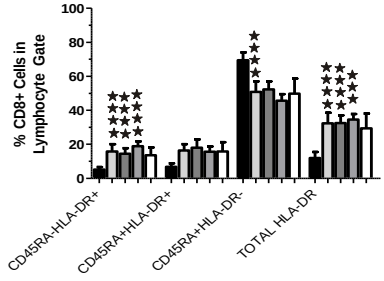

H. **CD8+ Lymphocyte Population in Whole Blood**

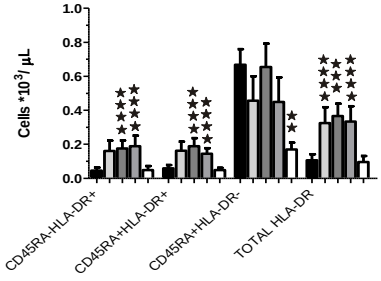

CONTROL EARLY ASYMPTOMATIC or ASY ADVANCED SIV DISEASE or ASD AIDS

post-infection with significant loss in AIDS. Increases in early and late activation CD8+ lymphocytes were noted during progressive infection that were maintained in BM, but declined in blood in AIDS.

Homing Molecule Expression on Lymphocytes During SIV Infection

Molecules on lymphocytes important for homing to secondary or tertiary lymphoid tissues were evaluated during SIV infection. Subjects were not available in the early phase for evaluation of the intestinal homing molecule β7.

BM lymphocytes expressing β7 were observed in marrow and blood (Figure 8.19). For control macaques, BM CD8+ lymphocytes expressed β7 ~2X greater than CD4+ BM lymphocytes which was also observed for WB CD8+CD45RA- β7 cells compared to WB CD4+CD45RA- β7 cells. In BM, CD8+ lymphocytes post-infection were increased compared to the controls while CD4+ lymphocytes were decreased compared to the control group. Whole blood CD4+ cells displayed decreased numbers of intestinal homing lymphocytes with near depletion in AIDS compared to controls while CD8+ cells were similar in number except in the ASY period.

CD62L (L selectin receptor) is considered important for homing to peripheral lymphoid tissue (PeLT) (Figure 8.20) (Sallusto 1999). Higher numbers of CD4+ BM, CD4+ WB, and CD8+ BM lymphocytes expressed CD62L than β7 for controls. CD8+ lymphocytes in blood of control RM were about equal in numbers for expression of both homing markers. BM lymphocytes were more variable in patterns during SIV disease with peak in the ASD period and depression in the ASY and AIDS periods. Circulating lymphocytes had decreased expression of CD62L as disease progressed with depletion in AIDS.

Figure 8.19. Percentages and absolute numbers of CD4 and CD8 expressing mucosal homing molecule marker β7 in bone marrow and whole blood during SIV
Co-expression of CD45RA and β7 on lymphocytes during SIV infection by percent and absolute numbers in bone marrow and whole blood to detect intestinal homing lymphocytes as described in text. **A**. Percent CD4+ lymphocytes in bone marrow. **B**. Absolute CD3+CD4+ lymphocyte numbers in bone marrow. **C**. Percent CD4+ lymphocytes in whole blood. **D**. Absolute CD4+ lymphocyte numbers in whole blood. **E**. Percent CD8+ lymphocytes in bone marrow. **F**. Absolute CD3+CD8+ lymphocyte numbers in bone marrow. **G**. Percent CD8+ lymphocytes in whole blood. **H**. Absolute CD8+ lymphocyte numbers in whole blood. Mann Whitney t tests compared populations between control cohort and each infected time period of SIV (***$p \leq 0.01$, and ****$p \leq 0.05$). Infected time periods were early, ASY was chronic asymptomatic group, ASD was advanced SIV disease or chronic symptomatic group, and AIDS displayed as mean values $\pm$ SEM.

Figure on next page.

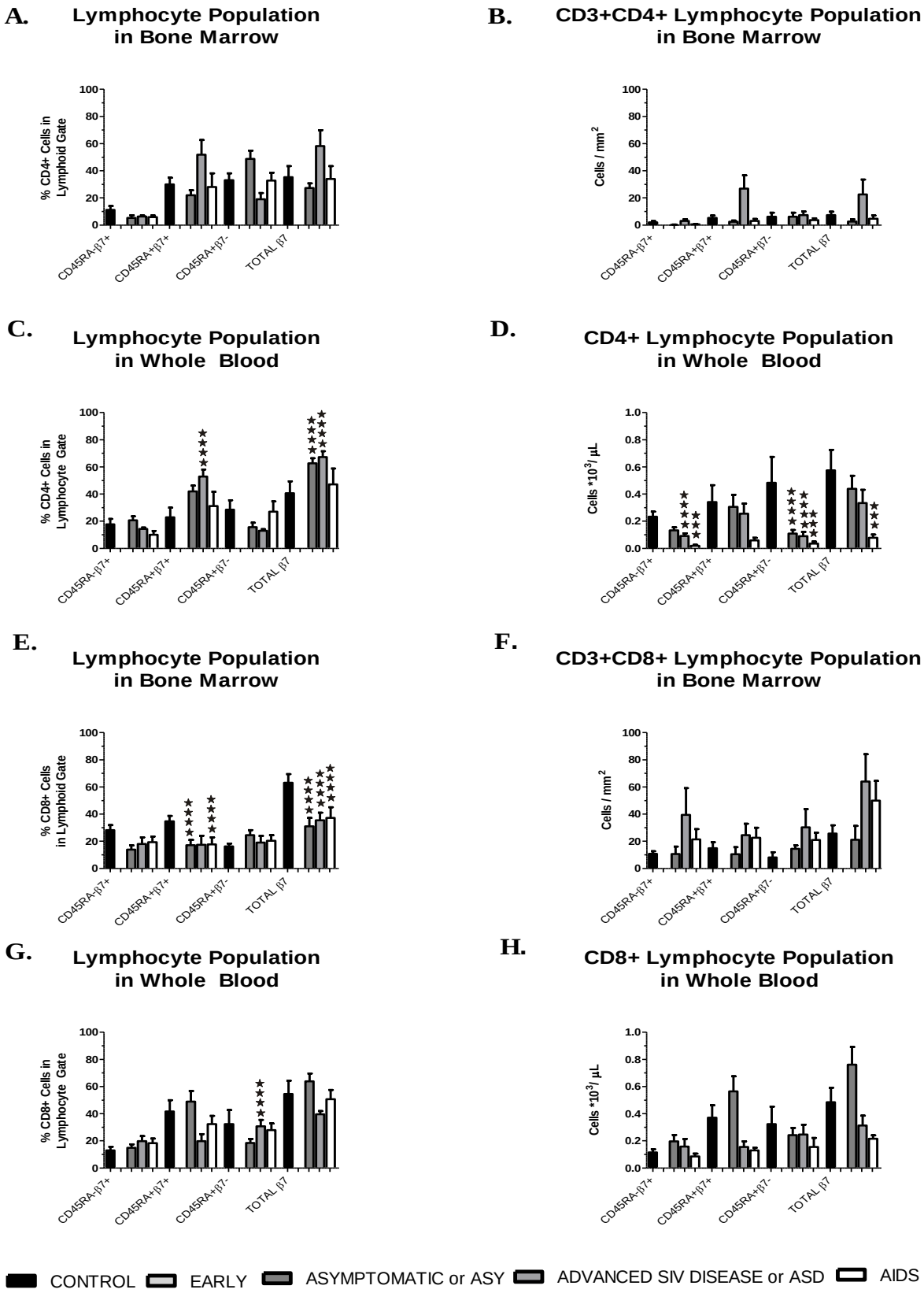
A.
Lymphocyte Population in Bone Marrow
% CD4+ Cells in Lymphoid Gate
B.
CD3+CD4+ Lymphocyte Population in Bone Marrow
Cells / mm2
C.
Lymphocyte Population in Whole Blood
% CD4+ Cells in Lymphocyte Gate
D.
CD4+ Lymphocyte Population in Whole Blood
Cells *10^3/ µL
E.
Lymphocyte Population in Bone Marrow
% CD8+ Cells in Lymphoid Gate
F.
CD3+CD8+ Lymphocyte Population in Bone Marrow
Cells / mm2
G.
Lymphocyte Population in Whole Blood
% CD8+ Cells in Lymphocyte Gate
H.
CD8+ Lymphocyte Population in Whole Blood
Cells *10^3/ µL
CD45RA-β7+
CD45RA+β7+
CD45RA+β7-
TOTAL β7
CONTROL
EARLY
ASYMPTOMATIC or ASY
ADVANCED SIV DISEASE or ASD
AIDS

Figure 8.20. Percentages and absolute numbers CD62L+ CD4 and CD8 lymphocytes in bone marrow and whole blood during SIV

Expression of CD45RA and CD62L on lymphocytes during SIV infection by percent and absolute numbers in bone marrow and whole blood to detect homing lymphocytes as described in text. **A**. Percent CD4+ lymphocytes in bone marrow. **B**. Absolute CD3+CD4+ lymphocyte numbers in bone marrow. **C**. Percent CD4+ lymphocytes in whole blood. **D**. Absolute CD4+ lymphocyte numbers in whole blood. **E**. Percent CD8+ lymphocytes in bone marrow. **F**. Absolute CD3+CD8+ lymphocyte numbers in bone marrow. **G**. Percent CD8+ lymphocytes in whole blood. **H**. Absolute CD8+ lymphocyte numbers in whole blood. Mann Whitney t tests compared populations between control cohort and each infected time period of SIV (**$p \leq 0.001$, ***$p \leq 0.01$, and ****$p \leq 0.05$). Infected time periods were early, ASY was chronic asymptomatic group, ASD was advanced SIV disease or chronic symptomatic group, and AIDS displayed as mean values $\pm$ SEM.

Figure on next page.

A. **Lymphocyte Population in Bone Marrow**

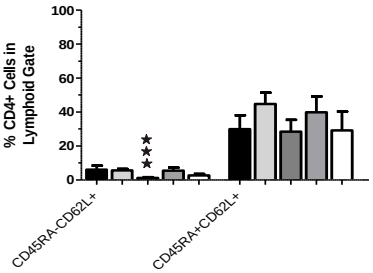

B. **CD3+CD4+ Lymphocyte Population in Bone Marrow**

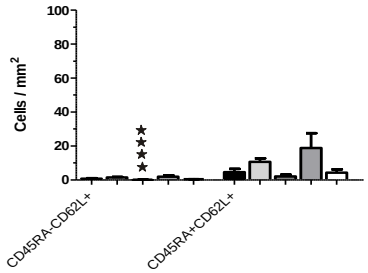

C. **Lymphocyte Population in Whole Blood**

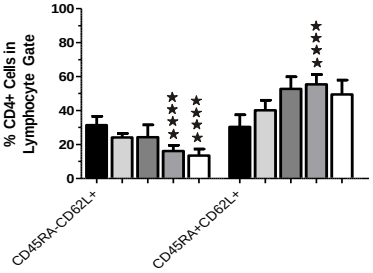

D. **CD4+ Lymphocyte Population in Whole Blood**

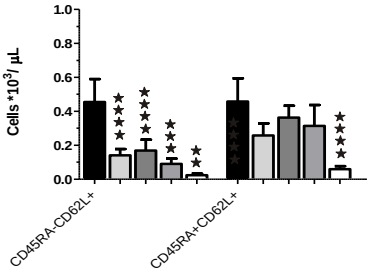

E. **Lymphocyte Population in Bone Marrow**

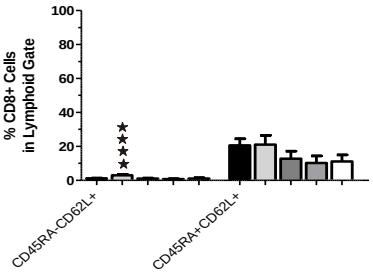

F. **CD3+CD8+ Lymphocyte Population in Bone Marrow**

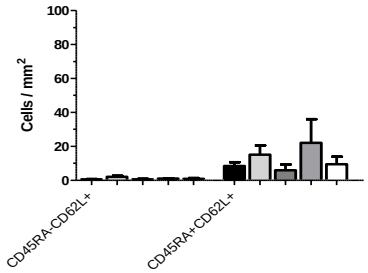

G. **Lymphocyte Population in Whole Blood**

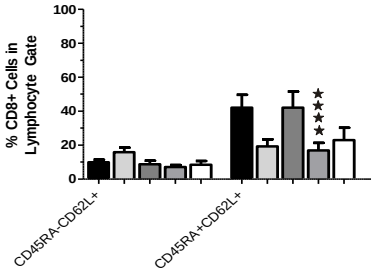

H. **CD8+ Lymphocyte Population in Whole Blood**

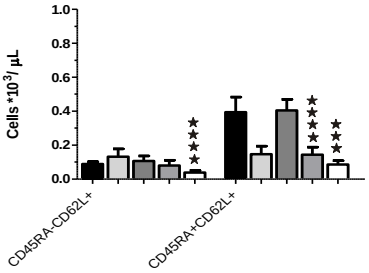

CONTROL EARLY ASYMPTOMATIC or ASY ADVANCED SIV DISEASE or ASD AIDS

Expression of Chemokine Receptors on Lymphocytes During SIV Infection

Chemokine receptors were evaluated during progressive SIV disease including CCR5 (CD195) (Figure 8.21), CXCR4 (CD184) (Figure 8.22), and CXCR3 (CD183) (Figure 8.23). Differences for CD4+ WB lymphocytes between percent and absolute numbers were detected. Control macaques expressed higher levels of CXCR3 than CCR5 or CXCR4 on BM CD8+ T cells while CD4+ T cell expression of CXCR4 was higher than CCR5 or CXCR3. Compared to WB, BM CD8+ T cells had higher CXCR3 (1.6X) and CCR5 (2X) expression, though not equal in proportion, and lower (1.5X) CXCR4 expression in controls. BM CD4+ T cells were equal to WB for CXCR3 expression, 1.5X lower compared to WB for CXCR4 expression and nearly 4X higher than WB CCR5 expression.

In control macaques, BM CD4+CD45RA+ lymphocytes, BM CD8+CD45RA+ lymphocytes, blood CD4+CD45RA-, and blood CD8+ CD45RA+ T lymphocytes had CXCR4 > CXCR3 > CCR5 expression. In control macaques, BM T cells CD8+CD45RA- lymphocytes had CXCR3 > CCR5 > CXCR4 expression. BM T cells CD4+CD45RA- T lymphocytes and circulating CD8+CD45RA- T lymphocytes in control macaques had CCR5 > CXCR3 > CXCR4 expression. Circulating T cells CD4+CD45RA+ lymphocytes in control macaques had CXCR4 > CCR5 > CXCR3 expression.

Bone marrow CD4+ lymphocytes showed minimal changes with respect to CCR5 expression during SIV infection while circulating CD4+ lymphocytes displayed significant loss of CCR5. CD8+ lymphocytes showed increased expression of CCR5 during SIV infection in BM and WB often with significant differences ($p \leq 0.05$). Total CCR5 expression on lymphocytes was nearly depleted in AIDS except for CD8+ circulating lymphocytes. Early during SIV infection and again in the ASD period, CXCR4 expression rose on CD4+ and CD8+

Figure 8.21. Percentages and absolute numbers of CD4 and CD8 lymphocytes expressing CCR5 in bone marrow and whole blood during SIV

Expression of CD45RA and CD195 (CCR5) on lymphocytes during SIV infection by percent and absolute numbers in bone marrow and whole blood to detect chemokine receptor CCR5 on lymphocytes. **A**. Percent CD4+ lymphocytes in bone marrow. **B**. Absolute CD3+CD4+ lymphocyte numbers in bone marrow. **C**. Percent CD4+ lymphocytes in whole blood. **D**. Absolute CD4+ lymphocyte numbers in whole blood. **E**. Percent CD8+ lymphocytes in bone marrow. **F**. Absolute CD3+CD8+ lymphocyte numbers in bone marrow. **G**. Percent CD8+ lymphocytes in whole blood. **H**. Absolute CD8+ lymphocyte numbers in whole blood. Mann Whitney t tests compared populations between control cohort and each infected time period of SIV (**$p \leq 0.001$, ***$p \leq 0.01$, and ****$p \leq 0.05$). Infected time periods were early, ASY was chronic asymptomatic group, ASD was advanced SIV disease or chronic symptomatic group, and AIDS displayed as mean values $\pm$ SEM.

Figure on next page.

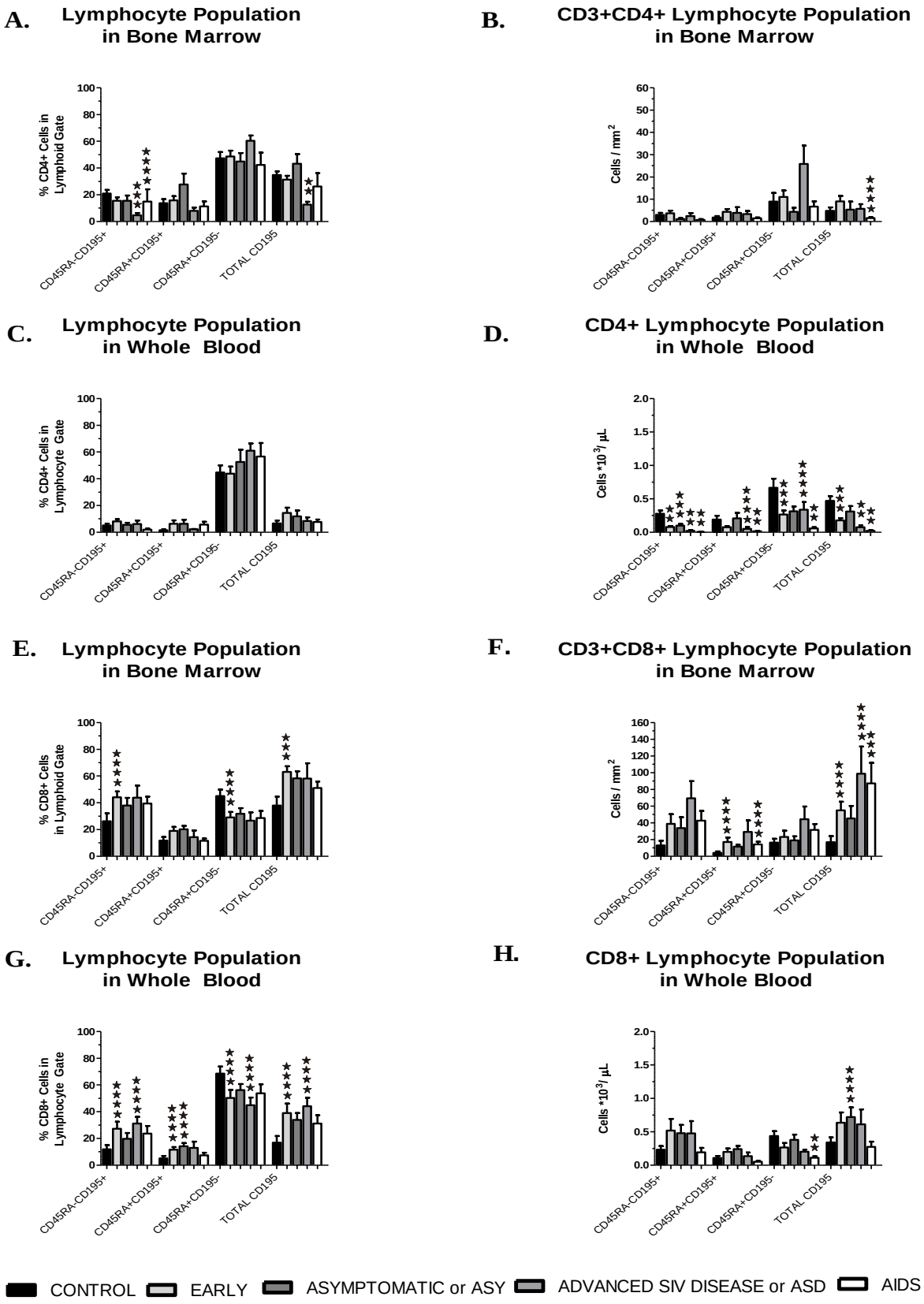
A.
Lymphocyte Population in Bone Marrow
% CD4+ Cells in Lymphoid Gate
B.
CD3+CD4+ Lymphocyte Population in Bone Marrow
Cells / mm2
C.
Lymphocyte Population in Whole Blood
% CD4+ Cells in Lymphocyte Gate
D.
CD4+ Lymphocyte Population in Whole Blood
Cells *10-3/ µL
E.
Lymphocyte Population in Bone Marrow
% CD8+ Cells in Lymphoid Gate
F.
CD3+CD8+ Lymphocyte Population in Bone Marrow
Cells / mm2
G.
Lymphocyte Population in Whole Blood
% CD8+ Cells in Lymphocyte Gate
H.
CD8+ Lymphocyte Population in Whole Blood
Cells *10-3/ µL
CD45RA-CD195+
CD45RA+CD195+
CD45RA+CD195-
TOTAL CD195
CONTROL
EARLY
ASYMPTOMATIC or ASY
ADVANCED SIV DISEASE or ASD
AIDS

Figure 8.22. Percentages and absolute numbers of CD4 and CD8 lymphocytes expressing CXCR4 in bone marrow and whole blood during SIV

Expression of CD45RA and CD184 (CXCR4) on lymphocytes during SIV infection by percent and absolute numbers in bone marrow and whole blood to detect chemokine receptor CXCR4 on lymphocytes. **A**. Percent CD4+ lymphocytes in bone marrow. **B**. Absolute CD3+CD4+ lymphocyte numbers in bone marrow. **C**. Percent CD4+ lymphocytes in whole blood. **D**. Absolute CD4+ lymphocyte numbers in whole blood. **E**. Percent CD8+ lymphocytes in bone marrow. **F**. Absolute CD3+CD8+ lymphocyte numbers in bone marrow. **G**. Percent CD8+ lymphocytes in whole blood. **H**. Absolute CD8+ lymphocyte numbers in whole blood. Mann Whitney t tests compared populations between control cohort and each infected time period of SIV (**$p \leq 0.001$, ***$p \leq 0.01$, and ****$p \leq 0.05$). Infected time periods were early, ASY was chronic asymptomatic group, ASD was advanced SIV disease or chronic symptomatic group, and AIDS displayed as mean values $\pm$ SEM.

Figure on next page.

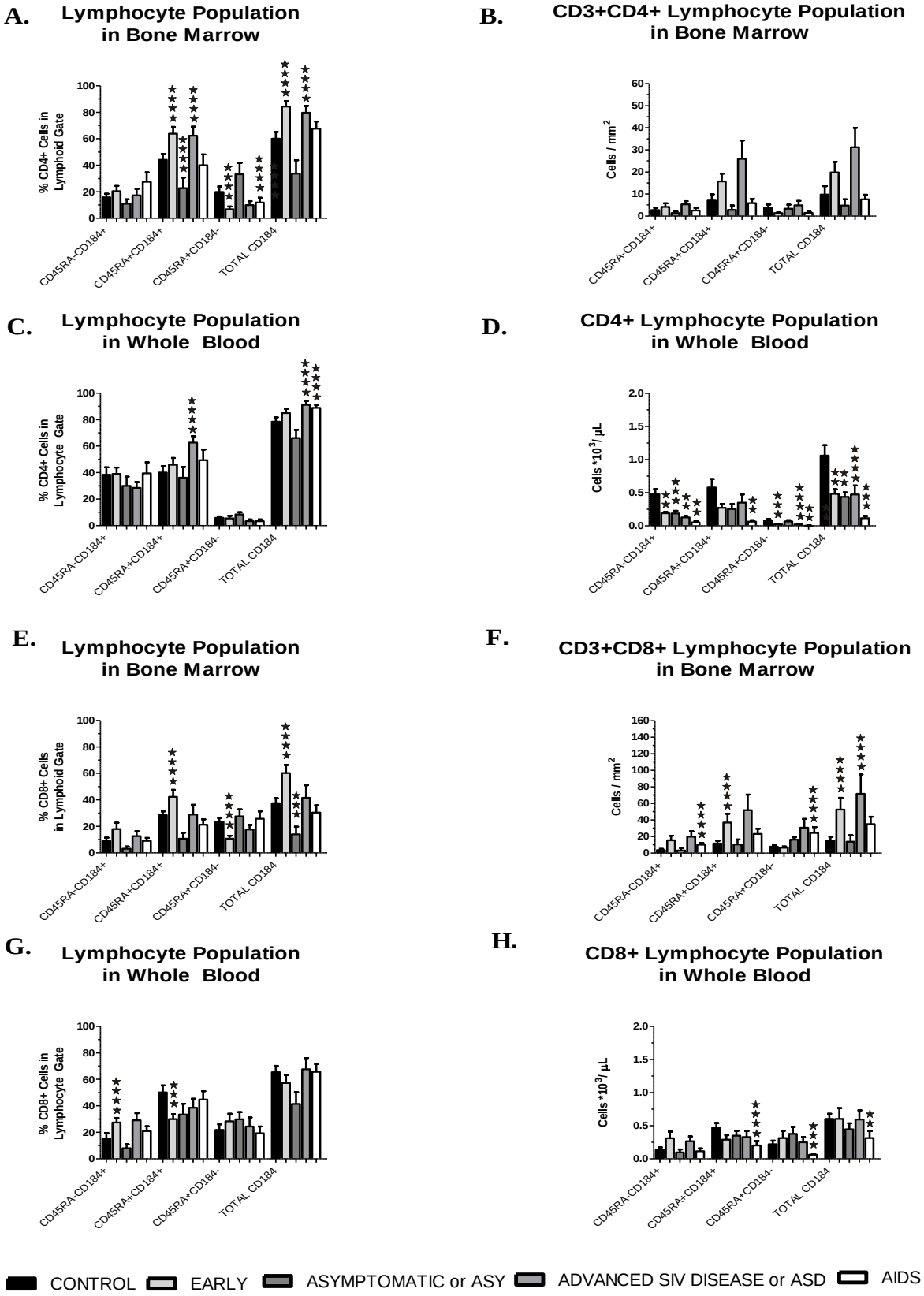
A.
Lymphocyte Population in Bone Marrow
% CD4+ Cells in Lymphoid Gate
B.
CD3+CD4+ Lymphocyte Population in Bone Marrow
Cells / mm2
C.
Lymphocyte Population in Whole Blood
% CD4+ Cells in Lymphocyte Gate
D.
CD4+ Lymphocyte Population in Whole Blood
Cells *10-3/ µL
E.
Lymphocyte Population in Bone Marrow
% CD8+ Cells in Lymphoid Gate
F.
CD3+CD8+ Lymphocyte Population in Bone Marrow
Cells / mm2
G.
Lymphocyte Population in Whole Blood
% CD8+ Cells in Lymphocyte Gate
H.
CD8+ Lymphocyte Population in Whole Blood
Cells *10-3/ µL
CD45RA-CD184+
CD45RA+CD184+
CD45RA+CD184-
TOTAL CD184
CONTROL
EARLY
ASYMPTOMATIC or ASY
ADVANCED SIV DISEASE or ASD
AIDS

Figure 8.23. Percentages and absolute numbers of CD4 and CD8 lymphocytes expressing CXCR3 in bone marrow and whole blood during SIV

Expression of CD45RA and CD183 (CXCR3) on lymphocytes during SIV infection by percent and absolute numbers in bone marrow and whole blood to detect chemokine receptor CXCR3 on lymphocytes. **A**. Percent CD4+ lymphocytes in bone marrow. **B**. Absolute CD3+CD4+ lymphocyte numbers in bone marrow. **C**. Percent CD4+ lymphocytes in whole blood. **D**. Absolute CD4+ lymphocyte numbers in whole blood. **E**. Percent CD8+ lymphocytes in bone marrow. **F**. Absolute CD3+CD8+ lymphocyte numbers in bone marrow. **G**. Percent CD8+ lymphocytes in whole blood. **H**. Absolute CD8+ lymphocyte numbers in whole blood. Mann Whitney t tests compared populations between control cohort and each infected time period of SIV (***$p \leq 0.01$, and ****$p \leq 0.05$). Infected time periods were early, ASY was chronic asymptomatic group, ASD was advanced SIV disease or chronic symptomatic group, and AIDS displayed as mean values $\pm$ SEM.

Figure on next page.

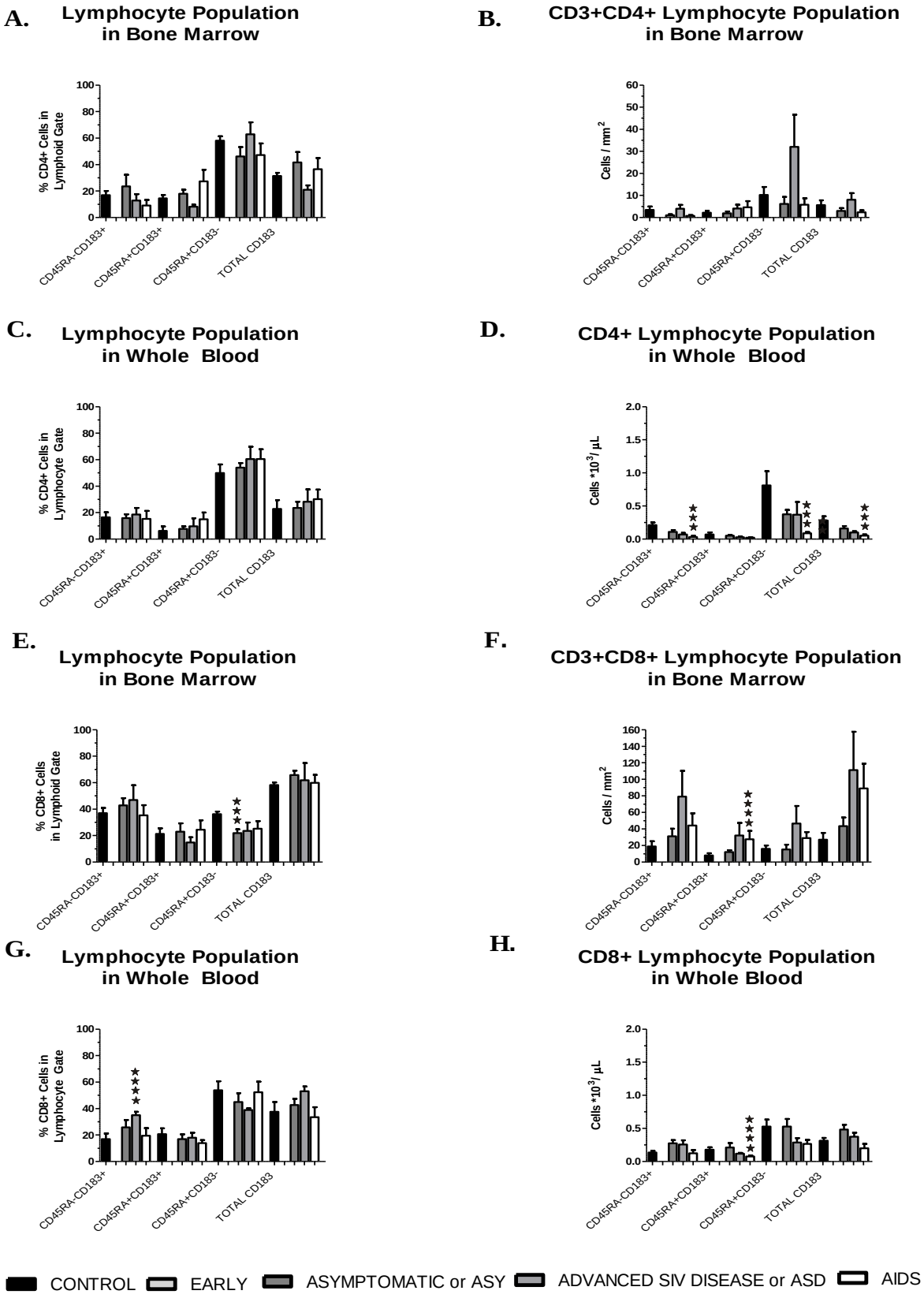
A.
Lymphocyte Population in Bone Marrow
% CD4+ Cells in Lymphoid Gate
B.
CD3+CD4+ Lymphocyte Population in Bone Marrow
Cells / mm2
C.
Lymphocyte Population in Whole Blood
% CD4+ Cells in Lymphocyte Gate
D.
CD4+ Lymphocyte Population in Whole Blood
Cells *10^3/ µL
E.
Lymphocyte Population in Bone Marrow
% CD8+ Cells in Lymphoid Gate
F.
CD3+CD8+ Lymphocyte Population in Bone Marrow
Cells / mm2
G.
Lymphocyte Population in Whole Blood
% CD8+ Cells in Lymphocyte Gate
H.
CD8+ Lymphocyte Population in Whole Blood
Cells *10^3/ µL
CD45RA-CD183+
CD45RA+CD183+
CD45RA+CD183-
TOTAL CD183
CONTROL
EARLY
ASYMPTOMATIC or ASY
ADVANCED SIV DISEASE or ASD
AIDS

lymphocytes in BM and WB mostly noted on CD45RA+CD184+ lymphocytes. However, CD8+ circulating lymphocytes showed higher expression on CD45RA-CD184+ memory lymphocytes. Additionally CXCR4 total expression was lowest in AIDS except for CD8+ WB cells. For CXCR3 lymphocyte expression, decreases were observed post-infection with depression in AIDS except for CD8+ BM cells.

Plasma Viral Load and the Bone Marrow Lymphocyte Phenotype

Plasma viral load was high during progressive SIV infection (Figure 8.24). Significant differences were observed between the early and ASY period (p=0.0029) also the early and AIDS period (p= 0.0367). The pattern of changes in viral load during progressive infection was similar to the BM compartment changes in patterns of lymphocytes for the following: BM CD4:CD8 lymphocyte ratio, CD3+CD8+ BM lymphocytes, BrdU+CD3+CD8+ BM lymphocytes, Ki67+CD3+CD8+ BM lymphocytes, central memory CD3+CD8+CD95+CD28+ BM lymphocytes, naïve CD3+CD8+CD45RA+HLA-DR- BM lymphocytes, late activation CD3+CD8+CD25-CD69+ BM lymphocytes, and CD3+CD8+ BM lymphocytes expressing the CXCR4 and CCR5 chemokine receptors. A correlation was noted between the mean BM lymphocyte population and to viral load for only total CXCR4 on CD3+CD8+ BM lymphocytes as a moderate negative correlation (Spearman r= -0.5852, p value=0.0021).

DISCUSSION

Our prior analysis of BM revealed the lymphoid gate by FSC vs. SSC plot encompassed lymphocytes of varying CD45 intensity or higher percentages when strictly using the $CD45^{Bright}$ gate of mature lymphocytes from CD45 vs. SSC plots (Chapter 5 and Chapter 6). Therefore we chose to utilize the multilineage gate for determination of BM lymphocytes. Our prior phenotypic study 40% lymphocytes consisting of 20% T cells and 20% B cells, 2 % NK cells,

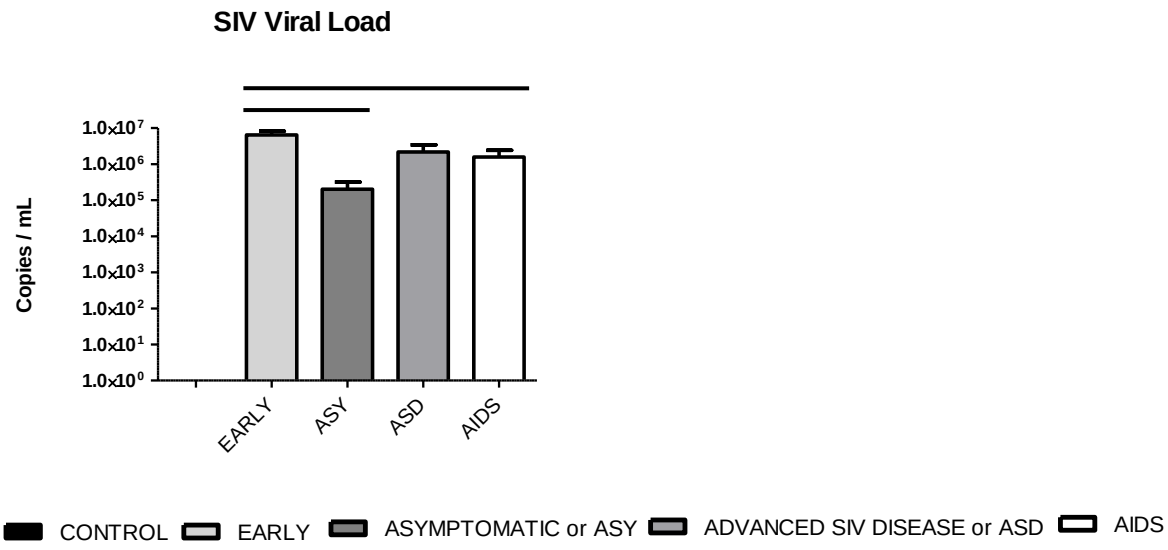

Figure 8.24. Plasma viral load during SIV
SIV plasma viral RNA copies during various phases of SIV disease. Mann Whitney t tests compared populations between control cohort and each infected time period of SIV (***$p \leq 0.01$, and ****$p \leq 0.05$). Infected time periods were early, ASY was chronic asymptomatic group, ASD was advanced SIV disease or chronic symptomatic group, and AIDS displayed as mean values $\pm$ SEM.

<1% plasma cells and immature B cells as well as 20% erythroid lineage including lineage negative immature hematopoietic cells and 5% immature hematopoietic cells (Chapter 5 and Chapter 6). In our earlier WB study, we found the lymphocyte gate of FSC vs. SSC was equally representative of $CD45^{Bright}$ circulating lymphocyte population and that the blood lymphocyte gate consist of (>90%) with few immature hematopoietic cells and metarubricytes (when present) (Chapter 5 and Chapter 6).

Important differences were detected between marrow and blood in control macaques. CD4:CD8 ratios greater than 1 for WB and less than 1 for BM were detected in the control group. Further, the BM T lymphocytes comprised nearly 3X higher CD8+ lymphocytes than CD4+ lymphocytes whereas WB lymphocytes were conversely represented higher CD4+ lymphocytes ~1.5X higher than CD8+ lymphocytes in control macaques as previously reported

(Mattapallil 2004; Paiardini 2009; Veazey 2000a). Our finding of increased BM CD8+ T cells compared to CD4+ T cells with a lower BM T cell CD4:CD8 ratio compared to peripheral blood was supported by similar findings in humans (Palendira 2008) and RM (Paiardini 2009; Sopper 2003).

Studies in mice, macaques, and humans revealed CD8+ memory T cells in BM were represented in higher percentages than naïve phenotype (Mazo 2005; Paiardini 2009; Palendira 2008). Further, Paiardini et al. observed the proliferation in BM of T cells resulted in a larger pool of memory lymphocytes in non-SIV infected RM which supports our data (Paiardini 2009). Studies of mice revealed post-immunization CD4+ and CD8+ T cells increased in BM (Di Rosa 2003). Human studies of BM CD8+ T cell responsiveness to viruses revealed Epstein Barr virus (EBV)-specific cells were found in higher levels than cytomegalovirus (CMV)-specific cells (Palendira 2008). Also, studies in mice have revealed adoptive transfer of memory phenotype T results in higher seeding of BM compared to lymph node (Di Rosa 2003). Prior mouse and human studies suggest BM is important for trafficking of memory cells suggesting T cell recruitment to BM may be involved in the host response to certain viruses (Di Rosa 2003; Palendira 2008). Selective depletion of either CD4+ or CD8+ T cells in BM of non-SIV infected RM resulted in rapid proliferation of the lost lymphocytes and return to pre-depletion levels respectively indicating BM is involved in T cell homeostasis (Paiardini 2009). Paiardini et al. referred to BM as the 'preferred site for proliferation of T cells in NHP' (Paiardini 2009). Murine studies have identified memory CD4+ T cells home to bone marrow within 3-8 weeks post-inoculation with LPS (Tokoyoda 2009).

Our study found high CCR5 expression on BM CD8+ T cells, of control macaques, at about twice levels in blood supported by human findings (Palendira 2008). However, CXCR3

expression of control macaque CD8+ T cells was disparate compared to humans, with control macaques having higher expression on BM compared to higher expression on blood CD8+ lymphocytes in humans (Palendira 2008).

We hypothesized absolute numbers of T lymphocytes in BM would decrease during SIV infection and our study revealed CD3+BM lymphocytes were increased at all stages during SIV infection similar to our prior findings of increased percentage (Chapter 4-6) and reported by Sopper et al. (Sopper 2003). In fact, macrophages were also increased at all stages of SIV infection as opposed to minimal increases of monocyte lineage cells observed in our earlier studies (Chapter 4-6). Circulating CD3+ T cells were decreased during SIV infection as previously reported (Sopper 2003). Absolute CD3 lymphocytes negatively correlated between the WB and BM compartments as circulating lymphocytes were decreased and BM lymphocytes were increased during progressive SIV disease. Absolute numbers of circulating lymphocytes declined in WB during SIV which was also detected in our earlier studies (Chapter 3-4) and opposite from BM lymphocyte observations (Chapter 5-6). Of note, WB percentage loss in this study was observed for the later stages of SIV. In spite of CD3 correlation, total CD4 and CD8 lymphocytes in whole blood and bone marrow compartments were rarely correlated during SIV disease.

We hypothesized decreases during all phases of infection for BM CD3+CD8+ lymphocytes and CD3+CD4+ lymphocytes, yet this was demonstrated only for the ASD and AIDS periods for CD4+ T cells. Post-infection, total BM T cells were increased, mainly attributed to increases in CD8+ cells and maintenance or minimal increases in CD4+ cells. Post-infection within BM, proliferation of CD8+ T cells increased as proliferation of CD4+ T cells decreased by BrdU, but both subsets shwoed increases by Ki67 staining. Our findings for

BM CD4+ cell Ki67 proliferation was supported by Ki67 staining by Sopper et al. as increased for the asymptomatic phase and decline in the AIDS phase toward non-SIV infected rates (Sopper 2003). We observed decreased BM CD4+ T cells in the asymptomatic phase but Sopper et al. observed increases during the same phase (Sopper 2003). We observed minimal loss of BM CD4+ T cells in the AIDS phase compared to minimal increases observed by Sopper et al. for the AIDS phase (Sopper 2003). For CD8+ our findings of BM proliferation were in agreement with Sopper et al. for BM. Chronic immune stimulation in the presence of active viral replication is one theory for maintenance/proliferation of CD4 lymphocytes during progressive SIV infection (Sopper 2003). Sopper et al. further thought increased proliferation of CD4 lymphocytes leads to increased destruction of CD4 lymphocytes during SIV infection (Sopper 2003). Conversely, increased proliferation of CD8 lymphocytes leads to increased numbers as CD8 lymphocytes are spared during SIV infection (Sopper 2003). Our demonstration of maintenance of BM CD4+ lymphocytes during SIV infection by percent and absolute numbers rejected our original hypothesis and suggested the WB and BM lymphoid compartments were under different homeostatic mechanisms.

Absolute numbers of CD8+ BM lymphocytes were increased all SIV phases characterized by increased proliferation, CM cells, EM cells, TDEM cells, early stage activation cells, and chemokine receptor expression. Further, CD8+ naïve and PLT homing BM lymphocytes were increased in early and ASD periods and CD8+ BM ASD and AIDS phases increased for GALT homing and chemokine expression. Absolute numbers of CD8+ circulating lymphocytes were increased in early and ASY periods for proliferation, active cell cycle, EM, TDEM, and early activation. Decreases in absolute circulating CD8+ lymphocytes in the ASD phase were noted but most examined subsets were increased. Decreases in absolute numbers of

circulating CD8+ lymphocytes in AIDS were observed for proliferation, memory, activation, and β7 expression.

BM CD4+ absolute numbers of naïve cells, EM cells, early activation cells, PeLT homing cells, and CXCR4 expressing T lymphocytes were increased in early and ASD periods while decreased ASY and AIDS periods. Absolute CD4+ BM lymphocytes were increased in the early phase for CM cells, early to middle stage activation cells, and for CCR5 chemokine expression. Decreased absolute numbers of CD4+ BM lymphocytes were in the ASY phase for CM cells, middle stage activation cells, GALT homing cells, and CXCR3 chemokine expression. CD4+ BM lymphocytes were increased in the ASD phase for proliferation, cell cycle, CM cells, TDEM cells, activation all stages, β7 expression, and CXCR3 chemokine expression. Finally, CD4+ BM lymphocytes were decreased in AIDS for proliferation, cell cycle, TDEM cells, GALT homing cells, CXCR3 and CCR5 expression. Chemokine receptor expression was maintained on CD4+ BM T cells. WB CD4+ lymphocytes were decreased post-infection with few exceptions.

We examined several subsets of lymphocytes in bone marrow and whole blood. CD3+ circulating lymphocytes declined post-infection as previously reported in RM (Mattapallil 2004). SIV infection demonstrated loss of CD4+ circulating cells in all phases but increases in CD8+ lymphocytes in the early and ASY periods or asymptomatic groups then dropped in the ASD and AIDS periodss or symptomatic groups as supported by Sopper et al. (Sopper 2003). Loss of CD4+ WB lymphocytes has been previously reported in SIV (Mattapallil 2004; Nishimura 2007; Sopper 2003; Veazey 2000a) as early as 3 DPI and peak at 10-14 DPI (Mattapallil 2005). WB CD8+ lymphocytes were maintained during SIV infection until later in infection (Mattapallil

2004). Absolute numbers of CD4+ circulating lymphocytes were decreased during SIV infection for all examined subsets.

Proliferation of lymphocyte subsets was evaluated. In our study, lymphocytes were mostly in a resting state of the cell cycle in WB and BM control macaques and SIV infected macaques supported by findings in peripheral blood lymphocytes of HIV patients (Cannavo 2001). In our study, overall percentages of proliferating T cells in control macaques in BM was nearly 1/10 less of WB levels. Proliferating T cells in circulation were predominantly CD8+ cells, but proliferating CD4+ cells were noted in low numbers as also previously reported (Kaur 2000; Sopper 2003).

We found increased cell cycle activity and proliferation during SIV in CD8+ cells of BM and WB as previously reproted (Paiardini 2009; Sopper 2003). However, we observed decreased cell activity and proliferation in CD4+ cells in WB, and depletion in AIDS. In BM we also found depletion in AIDS as reported by by Paiardini et al (Paiardini 2009). We detected increases in WB until AIDS and post-infection in BM as reported by Sopper et al. (Sopper 2003). SIVmac251 inoculated RM were reported with proliferating WB CD8+ T cells at 11 DPI and CD4+ T cells at 16 DPI (Benlhassan-Chahour 2003).

Circulating CD4+ and BM CD3+CD4+ lymphocytes showed cell cycle alterations in chronic infection notably in AIDS phases, particularly with reference to BrdU:Ki67 and CD4:CD8 proliferation ratios. Chaves and Kallas reported HIV patients, without ART, showed similar findings including increased CD4+ peripheral blood mononuclear cells (PBMC) in the S phase without the ability to proceed normally into G_2 and mitosis, or an acquired arrest as compared to healthy subjects (Chaves 2004). Proliferating lymphocytes from SIV infected macaques in blood displayed lower absolute numbers of BrdU+CD8+ (S phase) in the early and

ASY periods. Monceaux et al. reported increased proliferation of circulating CD8+ lymphocytes post-infection (Monceaux 2005). Our results showed similar cell cycle changes in CD4+ lymphocytes between the two compartments during chronic infection, suggesting multiple lymphoid sites were equally affected, while CD8+ cell cycle function was apparently preserved in WB. Also, dysregulation of the cell cycle was observed for BM CD8+ lymphocytes in the early and AIDS phases.

Cell cycle perturbations or cell cycle dysfunction were noted as increased cyclin B1 levels on peripheral blood lymphocytes of non-ART HIV patients which corrected with ART therapy (Cannavo 2001). However, dysregulation was interrupted based on the the finding of G_1/S levels of cyclin B and AGNORs in a resting G_0 lymphocyte not committed to entering the cell cycle (Cannavo 2001). *In vitro* studies have shown lack of degradation is the cause of Cyclin B overexpression in lymphocytes of HIV patients and not necessarily reflection of an increased production (Cannavo 2001). Thus, dampering of degradation may be due to a defect in protein degradation involving the ubiquitin-proteasome pathway (Cannavo 2001). In HIV-infected patients, dysregulated lymphocytes appear to be more susceptible to "cell cycle-related" apoptosis versus control lymphocytes in *in vitro* studies (Cannavo 2001). HIV-infected patients undergoing treatment that reduces viral load and overall immune activation have decreased lymphocyte cell turnover and decreased lymphocyte proliferation (Cannavo 2001). The lower proliferation rates allow lymphocytes to regain function of defective protein degradation and thus have appropriate levels of cyclin B and AGNORs (Cannavo 2001). Increased cyclin B1 levels from peripheral blood lymphocytes *in vitro* was also reported in chronically infected SIV RM (Paiardini 2006).

Naïve and memory lymphocytes were evaluated by different panels. CD4+ T cells usually follow a linear progression from naïve cell to effector memory cell to central memory cells, but central memory cells may also be generated from earlier activated T cells (Obhrai 2006; Sallusto 2004). Homeostatic or "self-renewal" proliferation of memory cells occurs but is mechanistically different from antigenic "pluripotent" memory proliferation (Kaech 2002). BM T cells in control RM were found to be equally represented in naïve and memory populations in our study by percentage and absolute number for CD4+ cells but absolute number only for CD8+ cells in CD95 versus CD28 strategies. BM CD3+CD4+ and CD3+CD8+ naïve and CM lymphocytes were increased in the early and ASD phase as circulating CD4+ and CD8+ subsets were low post-infection at the same period. CD4+ naïve and memory cells in both lymphoid compartments were decreased in the ASY period. Effector memory and TDEM CD8+ lymphocytes were increased in BM and circulation, except in AIDS, during progressive SIV disease as CD4+ BM cells were maintained and CD4+ circulating lymphocytes were steadily depleted. In AIDS, all subsets were depleted except CD8+ BM memory cells. CD45RA vs. CD62L plots defined CM bone marrow lymphocytes in lower numbers than represented by CD95 vs. CD28 plots but patterns were similar. Koopman et al. discovered circulating CD4+CD45RA+CD62L+ naïve cells increased as CD4+CD45RA+CD62L- memory or recently activate naïve cells decreased which was supported by our findings in percentages, but all were decreased by absolute numbers (Koopman 2001). We observed low numbers of BM CD4+ central memory CD45RA-CD62L+ in control macaques as reported in mice as an absence of CD4+CD62L+ CM BM cells (Tokoyoda 2009).

In the early and ASD phases, BM CD8+, WB CD8+ and BM CD4+ lymphocytes shared increased early and late stage activation markers. In ASY period of infection, CD8+ early and

late stage activated lymphocytes were increased in both compartments. In AIDS, activated CD8+ BM cells increased and WB decreased. BM CD3+CD4+ lymphocytes displayed increased activation in AIDS for early to middle, and late stage activation markers. Decreased CD4+ early and early to middle stage activated cells were noted for both lymphocyte compartments. Activation markers were rarely detected on circulating CD4+ lymphocytes consistent with findings of low absolute numbers of CD4+ lymphocytes.

We observed lymphocytes homing to secondary and tertiary lymphoid tissues in BM. Expression of CD4+β7+ circulating lymphocytes decreased post-infection as previously reported (Mattapallil 2004; Wang 2009). In fact, BM CD4+β7+ lymphocytes were decreased post-infection in parallel to circulating cells. BM T lymphocytes were increased in the early period for CD62L expression while a decline was noted for WB lymphocytes. BM CD4+ and CD8+ homing lymphocytes were decreased in the ASY and increased in the ASD phase. WB CD4+ and CD8+ homing lymphocytes were decreased in the early, ASY and AIDS phases. BM CD4+ homing cells were decreased in the AIDS phases as BM CD8+ lymphocytes were increased in AIDS.

Our study revealed most circulating CD8+ and CD4+ lymphocytes of control macaques co-expressed CXCR4 in higher numbers than CCR5, as supported by findings of others (Monceaux 2005; Veazey 2000a). We also noted BM T cells had higher expression of CXCR4 on cells. Further we demonstrated CD8+ lymphocytes with CCR5 expression were spared post-infection including CD45RA+/- phenotype which was supported by findings of others (Monceaux 2005; Veazey 2000a). Numbers of CD4+ circulating lymphocytes with CXCR4 and CCR5 expression declined post-infection however, Veazey et al. noted selective decline in

CD4+CCR5+ memory populations versus the CXCR4 expressing cells especially early in infection (Veazey 2000a).

We hypothesized the lymphocyte compartments would be differ between BM and WB. Divergences between the lymphocyte compartments were observed as were similar patterns in infection. Percentages of BM CD7+ lymphocytes were opposite between CD4+ and CD8+ lymphocytes for each phase of SIV infection. Percentages of CD7+ lymphocytes were decreased for circulating CD4+ cells and increased for circulating CD8+ cells post-infection. Our findings suggest regulation was preserved during progressive infection for BM CD3+CD8+ lymphocytes which responded with increases in total numbers of several subsets post-infection. Drop in BM cells during the ASY and AIDS phases corresponds to loss for CD3+CD4+ lymphocytes but decline in CD3+CD8+ from the prior phase. BM CD3+CD4+ lymphocytes were maintained in early and ASD phases indicating regulation was not lost but may have been blunted compared to the BM CD3+CD8+ responses. Circulating CD8+ lymphocytes were increased post-infection signifying regulation was also maintained till loss of cells in AIDS but interestingly, cells expressing PeLT homing signals were lost during all phases of infection. As reported consistently in SIV, homeostasis was lost for circulating CD4+ lymphocytes in essentially all subsets examined.

The difference between the compartments was more defined for CD4 lymphocytes in all periods and in AIDS for CD8+ lymphocytes. In BM, early and ASD periods had increased subsets of lymphocytes the ASY period had decreased subsets of lymphocytes which was similar to the trend post-infection for marrow cellularity and M:E ratio. Several theories for these changes exists including increased virus in BM, increased CD3+ apoptosis, or loss of cytokine regulation. AIDS phase showed fairly consistent lower numbers of CD4+ and CD8+

circulating cells as well as CD3+CD4+ BM lymphocytes, but increased CD3+CD8+ BM lymphocytes. Viral load was not correlated to BM changes during progressive SIV infection. Absolute numbers of CD4+ BM T cells were maintained in BM but lost in WB post-infection while CD8+ BM T cells were increased in parallel with WB until AIDS which is supported by findings of Sopper et al. (Sopper 2003).

SUMMARY

Progressive SIV infection in Rhesus macaques was studied in both bone marrow and whole blood by percent and absolute numbers for several lymphocyte subsets during early and chronic phases of SIV infection categorized by day post-inoculation and observance of clinical signs and AIDS. The objective of this study was to evaluate differences in subsets to determine if regulation of lymphocytes was disrupted by subset or by lymphocyte compartment, in either BM or WB, during SIV infection. Absolute CD3+ T lymphocytes increased in BM during infection characterized by increased CD3+CD8+ lymphocytes, the predominant phenotype in control macaques, and maintenance of CD3+CD4+ in early but not late infection. BM did not show loss of lymphocyte regulation, however, the CD3+CD4+ proliferative response was blunted compared to the observed increase in cellularity for CD3+CD8+ during all phases of SIV. Overall, BM CD3+CD4+, WB CD4+, and WB CD8+ lymphocytes were decreased in AIDS while BM CD3+CD8+ lymphocytes were increased.

Our study was supported by earlier findings in BM. BM T lymphocytes are predominantly CD8 in control macaques compared to CD4 dominance in WB. Bone marrow T lymphocytes are maintained during SIV infection characterized by increases in CD8+ phenotype and preservation of CD4+ phenotypes except in chronic asymptomatic and AIDS phases. Blunted response of BM CD3+CD4+ lymphocytes may be due to increased virus in BM,

increased apoptosis, or loss of cytokine regulation. Further studies in BM will aid in defining the cause for minimal BM T lymphocyte response of CD4+ T cells and subsets.

REFERENCES

Benlhassan-Chahour, K., Penit, C., Dioszeghy, V., Vasseur, F., Janvier, G., Riviere, Y., Dereuddre-Bosquet, N., Dormont, D., Le Grand, R., and Vaslin, B. (2003). Kinetics of lymphocyte proliferation during primary immune response in macaques infected with pathogenic simian immunodeficiency virus SIVmac251: preliminary report of the effect of early antiviral therapy. Journal of virology *77*, 12479-12493.

Borda, J.T., Alvarez, X., Kondova, I., Aye, P., Simon, M.A., Desrosiers, R.C., and Lackner, A.A. (2004). Cell tropism of simian immunodeficiency virus in culture is not predictive of in vivo tropism or pathogenesis. The American journal of pathology *165*, 2111-2122.

Cannavo, G., Paiardini, M., Galati, D., Cervasi, B., Montroni, M., De Vico, G., Guetard, D., Bocchino, M.L., Picerno, I., Magnani, M., *et al.* (2001). Abnormal intracellular kinetics of cell-cycle-dependent proteins in lymphocytes from patients infected with human immunodeficiency virus: a novel biologic link between immune activation, accelerated T-cell turnover, and high levels of apoptosis. Blood *97*, 1756-1764.

Chaves, M.M., and Kallas, E.G. (2004). Cell cycle distribution of CD4+ lymphocytes in HIV-1-infected subjects. Cytometry B Clin Cytom *62*, 46-51.

Di Rosa, F., and Pabst, R. (2005). The bone marrow: a nest for migratory memory T cells. Trends in immunology *26*, 360-366.

Di Rosa, F., and Santoni, A. (2003). Memory T-cell competition for bone marrow seeding. Immunology *108*, 296-304.

Kaech, S.M., Wherry, E.J., and Ahmed, R. (2002). Effector and memory T-cell differentiation: implications for vaccine development. Nat Rev Immunol *2*, 251-262.

Kaur, A., Grant, R.M., Means, R.E., McClure, H., Feinberg, M., and Johnson, R.P. (1998). Diverse host responses and outcomes following simian immunodeficiency virus SIVmac239 infection in sooty mangabeys and rhesus macaques. Journal of virology *72*, 9597-9611.

Kaur, A., Hale, C.L., Ramanujan, S., Jain, R.K., and Johnson, R.P. (2000). Differential dynamics of CD4(+) and CD8(+) T-lymphocyte proliferation and activation in acute simian immunodeficiency virus infection. Journal of virology *74*, 8413-8424.

Koopman, G., Niphuis, H., Haaksma, A.G., Farese, A.M., Casey, D.B., Kahn, L.E., Mann, D., MacVittie, T.J., Woulfe, S.L., and Heeney, J.L. (2004). Increase in plasmacytoid and myeloid dendritic cells by progenipoietin-1, a chimeric Flt-3 and G-CSF receptor agonist, in SIV-Infected rhesus macaques. Hum Immunol *65*, 303-316.

Koopman, G., Niphuis, H., Newman, W., Kishimoto, T.K., Maino, V.C., and Heeney, J.L. (2001). Decreased expression of IL-2 in central and effector CD4 memory cells during progression to AIDS in rhesus macaques. AIDS (London, England) *15*, 2359-2369.

Mattapallil, J.J., Douek, D.C., Hill, B., Nishimura, Y., Martin, M., and Roederer, M. (2005). Massive infection and loss of memory CD4+ T cells in multiple tissues during acute SIV infection. Nature *434*, 1093-1097.

Mattapallil, J.J., Letvin, N.L., and Roederer, M. (2004). T-cell dynamics during acute SIV infection. AIDS (London, England) *18*, 13-23.

Mazo, I.B., Honczarenko, M., Leung, H., Cavanagh, L.L., Bonasio, R., Weninger, W., Engelke, K., Xia, L., McEver, R.P., Koni, P.A., *et al.* (2005). Bone marrow is a major reservoir and site of recruitment for central memory CD8+ T cells. Immunity *22*, 259-270.

Monceaux, V., Viollet, L., Petit, F., Ho Tsong Fang, R., Cumont, M.C., Zaunders, J., Hurtrel, B., and Estaquier, J. (2005). CD8+ T cell dynamics during primary simian immunodeficiency virus infection in macaques: relationship of effector cell differentiation with the extent of viral replication. J Immunol *174*, 6898-6908.

Nishimura, Y., Igarashi, T., Buckler-White, A., Buckler, C., Imamichi, H., Goeken, R.M., Lee, W.R., Lafont, B.A., Byrum, R., Lane, H.C., *et al.* (2007). Loss of naive cells accompanies memory CD4+ T-cell depletion during long-term progression to AIDS in Simian immunodeficiency virus-infected macaques. Journal of virology *81*, 893-902.

Obhrai, J.S., Oberbarnscheidt, M.H., Hand, T.W., Diggs, L., Chalasani, G., and Lakkis, F.G. (2006). Effector T cell differentiation and memory T cell maintenance outside secondary lymphoid organs. J Immunol *176*, 4051-4058.

Ostrowski, M.A., Chun, T.W., Justement, S.J., Motola, I., Spinelli, M.A., Adelsberger, J., Ehler, L.A., Mizell, S.B., Hallahan, C.W., and Fauci, A.S. (1999). Both memory and CD45RA+/CD62L+ naive CD4(+) T cells are infected in human immunodeficiency virus type 1-infected individuals. Journal of virology *73*, 6430-6435.

Paiardini, M., Cervasi, B., Engram, J.C., Gordon, S.N., Klatt, N.R., Muthukumar, A., Else, J., Mittler, R.S., Staprans, S.I., Sodora, D.L., *et al.* (2009). Bone marrow-based homeostatic proliferation of mature T cells in nonhuman primates: implications for AIDS pathogenesis. Blood *113*, 612-621.

Paiardini, M., Cervasi, B., Sumpter, B., McClure, H.M., Sodora, D.L., Magnani, M., Staprans, S.I., Piedimonte, G., and Silvestri, G. (2006). Perturbations of cell cycle control in T cells contribute to the different outcomes of simian immunodeficiency virus infection in rhesus macaques and sooty mangabeys. Journal of virology *80*, 634-642.

Palendira, U., Chinn, R., Raza, W., Piper, K., Pratt, G., Machado, L., Bell, A., Khan, N., Hislop, A.D., Steyn, R., *et al.* (2008). Selective accumulation of virus-specific CD8+ T cells with unique homing phenotype within the human bone marrow. Blood *112*, 3293-3302.

Pitcher, C.J., Hagen, S.I., Walker, J.M., Lum, R., Mitchell, B.L., Maino, V.C., Axthelm, M.K., and Picker, L.J. (2002). Development and homeostasis of T cell memory in rhesus macaque. J Immunol *168*, 29-43.

Sallusto, F., Geginat, J., and Lanzavecchia, A. (2004). Central memory and effector memory T cell subsets: function, generation, and maintenance. Annu Rev Immunol *22*, 745-763.

Sallusto, F., Lenig, D., Forster, R., Lipp, M., and Lanzavecchia, A. (1999). Two subsets of memory T lymphocytes with distinct homing potentials and effector functions. Nature *401*, 708-712.

Sopper, S., Nierwetberg, D., Halbach, A., Sauer, U., Scheller, C., Stahl-Hennig, C., Matz-Rensing, K., Schafer, F., Schneider, T., ter Meulen, V., *et al.* (2003). Impact of simian immunodeficiency virus (SIV) infection on lymphocyte numbers and T-cell turnover in different organs of rhesus monkeys. Blood *101*, 1213-1219.

Tokoyoda, K., Zehentmeier, S., Hegazy, A.N., Albrecht, I., Grun, J.R., Lohning, M., and Radbruch, A. (2009). Professional memory CD4+ T lymphocytes preferentially reside and rest in the bone marrow. Immunity *30*, 721-730.

Veazey, R.S., DeMaria, M., Chalifoux, L.V., Shvetz, D.E., Pauley, D.R., Knight, H.L., Rosenzweig, M., Johnson, R.P., Desrosiers, R.C., and Lackner, A.A. (1998). Gastrointestinal tract as a major site of CD4+ T cell depletion and viral replication in SIV infection. Science *280*, 427-431.

Veazey, R.S., Mansfield, K.G., Tham, I.C., Carville, A.C., Shvetz, D.E., Forand, A.E., and Lackner, A.A. (2000a). Dynamics of CCR5 expression by CD4(+) T cells in lymphoid tissues during simian immunodeficiency virus infection. Journal of virology *74*, 11001-11007.

Veazey, R.S., Tham, I.C., Mansfield, K.G., DeMaria, M., Forand, A.E., Shvetz, D.E., Chalifoux, L.V., Sehgal, P.K., and Lackner, A.A. (2000b). Identifying the target cell in primary simian immunodeficiency virus (SIV) infection: highly activated memory CD4(+) T cells are rapidly eliminated in early SIV infection in vivo. Journal of virology *74*, 57-64.

Wang, X., Pahar, B., Rasmussen, T., Alvarez, X., Dufour, J., Rasmussen, K., Lackner, A.A., and Veazey, R.S. (2008). Differential cross-reactivity of monoclonal antibody OPD4 (anti-CD45RO) in macaques. Dev Comp Immunol *32*, 859-868.

Wang, X., Xu, H., Gill, A.F., Pahar, B., Kempf, D., Rasmussen, T., Lackner, A.A., and Veazey, R.S. (2009). Monitoring alpha4beta7 integrin expression on circulating CD4+ T cells as a surrogate marker for tracking intestinal CD4+ T-cell loss in SIV infection. Mucosal Immunol *2*, 518-526.

CHAPTER 9: APOPTOSIS OF T LYMPHOCYTES IN BONE MARROW DURING SIV INFECTION IS MINIMAL

INTRODUCTION

Theories of bone marrow hematopoiesis dysfunction include the following: infectious disease, anti-microbial therapy, cytokine or chemokine regulated suppression, ART therapy, HIV infection of hematopoietic stem cells, HIV protein derived suppression, HIV infection of mesenchymal or mononuclear cells involved in hematopoiesis, apoptosis, BM stromal changes, and cytokine soluble factors that suppress hematopoiesis (Marandin 1996; Isgro 2005). SIV infection in BM was shown to occur in T cells and macrophages (Chapter 7) and reported to occur in dendritic cells (Donaghy 2003). Bystander apoptosis or direct viral killing of cells through apoptosis may occur during SIV and HIV infection (Isgro 2005).

One theory for increased BM apoptosis may be cell-to-cell interaction in BM between SIV infected T cells, macrophages, and dendritic cells may disrupt cytokine production and lead to increased apoptosis of BM cells (Bucur 2000). Our earlier findings revealed increased T cells, macrophages, and plasmacytoid DC but decreased monocytoid dendritic cells during SIV infection (Chapter 5, Chapter 6, and Chapter 8). *In vitro* evaluation of T cell apoptosis from SIV infected macaques has been reportedly due to FAS/CD95 pathway or spontaneous apoptosis (Arnoult 2003). Prior HIV studies reported increased apoptosis of T cells after *in vitro* incubation (Gougeon 1996).

The objective of this study was to define apoptosis of BM CD4+ T cells in the Rhesus macaque and confirm loss during progressive SIV infection. We hypothesized increased BM T cell apoptosis would mirror whole blood during SIV. Additionally, we hypothesized apoptosis would be fueled by increased pro-apoptotic cytokines in bone marrow tissue. Whole blood was analyzed to detect parallel changes in the bone marrow. Flow cytometry was utilized to

determine apoptosis by the activated caspase 3 (AC3) in BM and WB. Tissue detection of apoptosis by AC3 and terminal deoxynucleotidyl transferase (Tdt) deoxyuridine-triphosphatase (dUTP) nick end labeling (TUNEL) was performed to visualize bone marrow apoptotic cells. Cytokine analysis was performed on plasma and supernatant from stimulated bone marrow mononuclear cells.

MATERIAL AND METHODS

Experimental Database III

Experimental database and definitions are described in Appendix II.

Hematologic Data and Definitions

Hematologic data and definitions are described in Appendix I.

Flow Cytometry Analysis

Whole blood and BM tissue collection, flow cytometry preparation, flow cytometry acquisition, flow cytometry analysis, and definitions are described in Appendix III.

Activated Caspase 3

AC3 (PE, clone C92-605) and CD3 (PB, clone SP34-2) antibodies were from BD Biosciences (San Jose, CA) and utilized to detect apoptotic T lymphocytes using flow cytometry. T lymphocytes were determined by gates in bone marrow (multilineage gate) and whole blood (lymphocyte gate) as earlier described (Chapter 5-6). The gate of interest was defined as CD3+AC3+ using the CD3 vs. AC3 plot (Figure 9.1).

Plasma Viral Load

Plasma viral loads and definitions are described in Appendix IV.

Apoptosis Detection in Bone Marrow Tissue Sections

BM tissue and appropriate control tissues were analyzed for apoptosis by double labeling fluorescent *in situ* and fluourescent immunohistochemistry. Tissues were prepared through

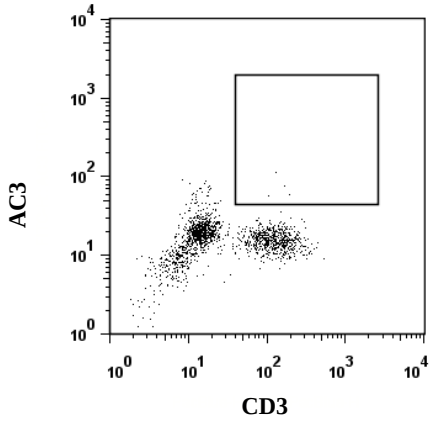

Figure 9.1. Identification of apoptotic T lymphocytes
Phenotypic determination of apoptotic T lymphocytes. CD3+AC3+ T lymphocytes by CD3 versus AC3 plot. Cells were identified as described in text.

antigen retrieval for FISH as described in Chapter 7 and FICH was performed as described in Chapter 8 using previously described methods (Borda 2004; Kitagawa 1991; Veazey 1998; Wang 2008b; Wang 2007). I*n situ* TUNEL was performed on BM sections per manufacturer directions (ApopTag Fluorescein In Situ Apoptosis Detection Kit, Chemicon International; Temicula, CA). Briefly, slides were incubated with equilibration buffer was for 60 minutes at room temperature in dark humidified chambers and then incubated with Tdt for 90 minutes in dark humidified chambers at 37°C. The reaction was stopped with stop/wash buffer followed by four serial TBS washes. TUNEL reaction was detected by tissue incubation with anti-digoxigenin FITC labeled conjugate for 30 minutes at room temperature in a dark humidified chamber.

FIHC was performed after serial TBS washes. Tissue was incubated in protein block (Serum Free Protein Blocker, DAKO; Carpenteria, CA) for 30 minutes at room temperature in dark humidified chambers. First, primary antibody rabbit anti-human polyclonal activated caspase 3 (AC3) (Abcam; Cambridge, MA) was incubated for 60 minutes at room temperature

on tissues followed by PBS-FSG washes. A secondary antibody, goat anti-rabbit conjugated to fast red Alexa 568 (Invitrogen; Carlsbad, CA) was incubated on tissues for 30 minutes at room temperature for detection of AC3. Finally, after PBS washes the slides were coverslipped with aqueous anti-quenching medium.

Slides were imaged for fluorescence with flourescent microscopy at the TNPRC Confocal Core Microscopy Center. A Leica DMR microscope was utilized (Leica Microsystems; Exton, PA) to view five serial non-touching fields under the 100x objective. The mean number of cells detected for single labeling of TUNEL or AC3 and double labeling with TUNEL and AC3 fluorescence was calculated in each of five high power fields (hpf).

Cytokine Analysis of Plasma and Whole Blood

Plasma for cytokine analysis was separated from heparinized whole blood by centrifugation and frozen at -80°C. Ficoll preparation was used to isolate the mononuclear fraction of marrow cells collected during necropsy. The bone marrow mononuclear cells (BMMC) were diluted in enriched RPMI media for a final dilution of $1x10^5$/mL. Then, 100µL of BMMC from each subject was plated in triplicate into 96 well plates. Stimulation media was prepared from sterile RPMI media with phytohemagluttinin (PHA) (Gibco, Invitrogen; Carlsbad, CA) for a desired final concentration of 50ng/mL, phorbol 12-myristate 13-acetate (PMA) (Sigma-Aldrich; St. Louis, MO) for a desired final concentration of 100ng/mL, and calcium ionophore (Sigma-Aldrich; St. Louis, MO) for a desired final concentration of 250ng/uL then frozen in aliquots. Stimulation media defrosted to room temperature was added at 1:2 ratio per well and cells were stimulated for 18 hours in a 37°C incubator with 5% CO_2. Post-incubation, plates were centrifuged at 200 x g for 5 minutes and 100 µL of supernatant was retrieved from each well and frozen at -80°C. Supernatants from stimulated cells were utilized for cytokine

analysis. Before and after stimulation of BMMC, monolayer of cells were observed by an inverted microscope and nucleated cells were present.

A magnetic bead array analysis was performed to detect cytokine concentrations as previously described (Giavedoni 2005; Ramesh 2009). Batch analysis of plasma and stimulated BMMC supernatant was performed in duplicate. Cytokines consisted of pre-mixed anti-cytokine labelled beads designed to detect 27 cytokines (Table 9.1) (Bio-Plex Human Cytokine 27-Plex Panel Group I, Bio-Rad). Controls for the analysis were RPMI media used as a blank and the manufacturer provided low and high standard controls for each cytokine per manufacturer instructions (Bio-Plex Cytokine Assay, Bio-Rad Laboratories; Hercules, CA). BMMC supernatants were diluted 1:100 prior to analysis per manufacturer directions (Bio-Plex Cytokine Assay). The multiplex assay plate was prepared per manufacturer directions (Bio-Plex Cytokine Assay). Detection of cytokines by was performed on the multiplex assay plate analyzer using the Bio-Plex 200 Suspension Array Luminex System and Bio-Plex Manager Software (Bio-Rad). The low standard was utilized for lower and upper limit detection of cytokines as pg/mL. Indeterminate cytokine values were defined as results below the lower limit of the low standard for each cytokine.

Statistical Analysis

For data evaluation, controls were non-SIV infected macaques and SIV infected subjects were grouped into periods defined as early and chronic (Appendix II). Macaques developing AIDS were fast and slow progressors.

Apoptosis and cytokine concentrations for control and SIV infected macaques were compared for differences using the Mann Whitney non-parametric unpaired t test and correlations were determined using non-parametric Spearman r correlation coefficients in

Table 9.1. Cytokine Profile

Cytokine	Cytokine Name	Possible Source for Production of Cytokine by these cells:
IL-1β	Interleukin 1β	Macrophages, monocytes, dendritic cells
IL-1ra	Interleukin 1ra	Macrophages, monocytes, dendritic cells
IL-2	Interleukin 2	T lymphocytes
IL-4	Interleukin 4	Basophils
IL-5	Interleukin 5	T lymphocytes, mast cells, eosinophils
IL-6	Interleukin 6	T lymphocytes, macrophages, osteoblasts, smooth muscle cells in blood vessels
IL-7	Interleukin 7	Stromal cells of bone marrow and thymus
IL-8	Interleukin 8	Macrophages, endothelial cells
IL-9	Interleukin 9	T lymphocytes
IL-10	Interleukin 10	Monocytes, T lymphocytes
IL-12 (p70)	Interleukin 12	Dendritic cells, macrophages
IL-13	Interleukin 13	T lymphocytes
IL-15	Interleukin 15	Macrophages
IL-17	Interleukin 17	T lymphocytes
Eotaxin	Eotaxin	Macrophages
FGF basic	Basic Fibroblast Growth Factor	
CSF-G	Granulocyte Colony Stimulating Factor	Macrophages, T lymphocytes, mast cells, endothelial cells, fibroblasts
CSF-GM	Granulocyte-Macrophage Colony Stimulating Factor	Macrophages, T lymphocytes, mast cells, endothelial cells, fibroblasts
IFN-γ	Interferon gamma	Natural killer cells, lymphocytes, cytotoxic lymphocytes
IP-10	Interferon Inducible Protein 10	Monocytes, endothelial cells, keratinocytes
MCP-1 (MCAF)	Monocyte Chemotactic Protein 1 or CCL2 or Monocyte Chemotactic and Activating Factor	Monocytes, vascular endothelial cells, osteoblasts, smooth muscle cells
MIP-1α	Macrophage Inflammatory Protein 1 alpha or CCL3	Macrophages
MIP-1β	Macrophage Inflammatory Protein 1 beta or CCL4	Macrophages, T cells, B cells
PDGF	Platelet Derived Growth Factor dimer BB	Megakaryocytes, stored in platelets
RANTES	Regulated upon Activation, normal T cell Expressed and Secreted or CCL5	T lymphocytes
TNF-α	Tumor Necrosis Factor alpha	Macrophages, monocytes, neutrophils, T lymphocytes, NK cells
VEGF	Vascular Endothelial Growth Factor	Macrophages

GraphPad Prism with significance considered as $p \leq 0.05$ (GraphPad Software; La Jolla, CA). Means of data are represented by graphs where error bars represent the SEM.

Percentages of immunophenotypic populations for control and SIV infected macaques were compared using the Mann Whitney non-parametric unpaired t test, and correlations were determined using non-parametric Spearman correlation coefficients GraphPad Prism with significance was considered as (GraphPad Software; San Diego, CA).

Graphs represent the means and SEM. Significant differences were defined as $p \leq 0.05$.

RESULTS

Apoptosis in Bone Marrow Tissue Sections During SIV Infection

Very low numbers of marrow cells were noted to undergo apoptosis in bone marrow tissue by evaluation of AC3 and TUNEL staining of BM tissue sections. Cells were considered apoptotic if staining for AC3 and TUNEL was intranuclear, however low numbers of cells stained for AC3 within the cytoplasm of infected and non-infected macaques. This intracytoplasmic staining for AC3 was often considered phagocytic debris from cells undergoing apoptosis.

Detection of apoptosis by AC3 revealed higher numbers of BM apoptotic cells compared to TUNEL or double labeling (Figure 9.2). In non-infected macaques, the mean of less than 1 cell per hpf was observed as apoptotic. During early SIV infection, apoptotic cells were significantly decreased in number, but increased during the chronic period. By double labeling for AC3 and TUNEL in BM tissue in the chronic period, less than 1 cell/hpf was apoptotic by TUNEL compared to >1 cell/hpf for apoptosis by AC3.

Apoptosis of T Lymphocytes During SIV Infection

Percentages of CD3+ T lymphocytes undergoing apoptosis were identified by AC3 staining using flow cytometry. Few marrow and blood CD3+ T lymphocytes were detected as apoptotic (<0.02%) and percentages remained stable during SIV infection for bone marrow and whole blood with minimal decrease in the chronic phase (Figure 9.3). Due to low detection of apoptotic T cells, further phenotyping of apoptotic cells was not performed.

Plasma Cytokines During SIV Infection

Early during SIV infection, rises were detected for the following: IL-1ra (p=0.0035), IL-2 (p=0.047), IL-4 (p=0.047), IL-15 (0.0239), eotaxin (p=0.0312), MCP-1 (p=0.0078), TNF-α

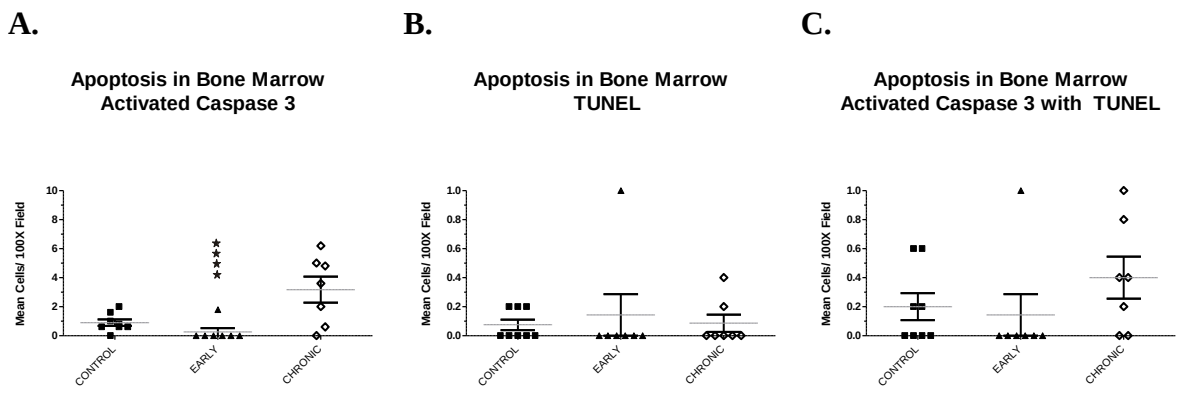

Figure 9.2. Detection of apoptosis in bone marrow tissue
Fluorescent immunohistochemistry staining for activated caspase 3 (AC3) and fluorescent *in situ* terminal deoxynucleotidyl transferase (Tdt) deoxyuridine-triphosphatase (dUTP) nick end labeling (TUNEL) analysis for apoptosis was performed. Difference between control cohort to early and chronic periods of SIV infection were compared by Mann Whitney t tests (****$p \leq 0.05$). Representation of mean values (grey line) $\pm$ SEM.

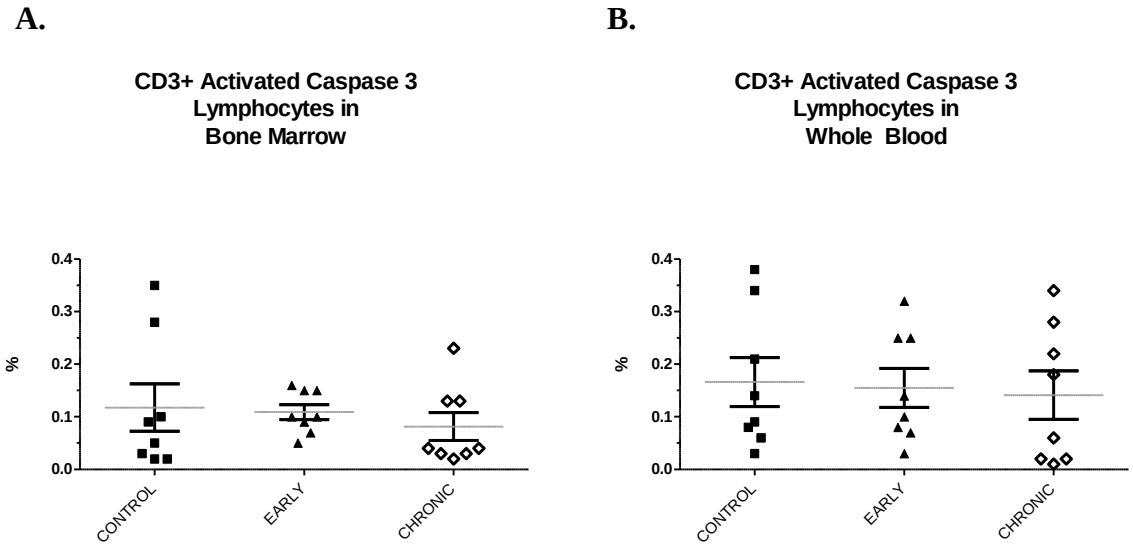

Figure 9.3. Apoptosis of T lymphocytes in bone marrow and whole blood
Percentages of T lymphocytes detected by activated caspase 3 for apoptosis in **A.** bone marrow and **B.** whole blood. Difference between control cohort to early and chronic periods of SIV infection were compared by Mann Whitney t tests (****$p \leq 0.05$). Representation of mean values (grey line) $\pm$ SEM.

(p=0.0307), IL-5, Il-7, CSF-G, CSF-GM, INF-γ, IP-10, and RANTES. During the chronic period, increases continued for IL-1ra (p=0.0035), IL-15, MCP-1 (p=0.0099), and TNF-α (Figure 9.4). The other cytokines that increased during the early phase were decreased or unchanged

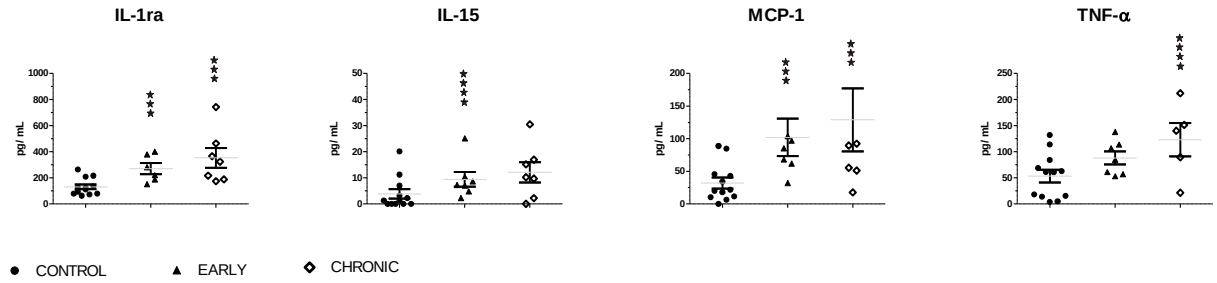

Figure 9.4. Plasma cytokine concentrations increased during SIV
Difference between control cohort to early and chronic periods of SIV infection were compared by Mann Whitney t tests (****$p \leq 0.05$). Representation of mean values (grey line) $\pm$ SEM.

during the chronic perod (Figure 9.5). RANTES was increased in the early period, then decreased in the chronic phase of SIV infection (Figure 9.6). PDGF was decreased during the early period, and then increased later during infection (Figure 9.6). IL-6, IL-8, and IL-17 were decreased in the chronic period, without any change during early SIV infection (Figure 9.7).

Bone Marrow Supernatant Cytokine Concentration During SIV Infection

Cytokine concentrations from the supernatant of stimulated bone marrow mononuclear cells were detected only for IL-8, and MIP-1β, cytokines secreted by macrophages. Comparison of cytokine concentrations between controls and infected RM did not reveal significance, however MIP-1β showed an upward trend post-infection but IL-8 remained unchanged (Figure 9.8). BMMC supernatant analysis was indeterminate for IL-1ra, IL-2, IL-4, IL-5, IL-6, IL-7, IL-9, IL-10, IL-12 (p70), IL-13, IL-15, IL-17, Eotaxin, FGF basic, G-CSF, GM-CSF, IFN-γ, IP-10, MCP-1 (MCAF), MIP-1α, PDGF bb, RANTES, TNF-α, and VEGF.

DISCUSSION

Apoptosis of marrow cells by AC3 was observed to significantly decrease early during SIV infection and then increase later during infection within bone marrow. Even though changes in apoptosis were noted in marrow, few cells were detected to be undergoing apoptosis.

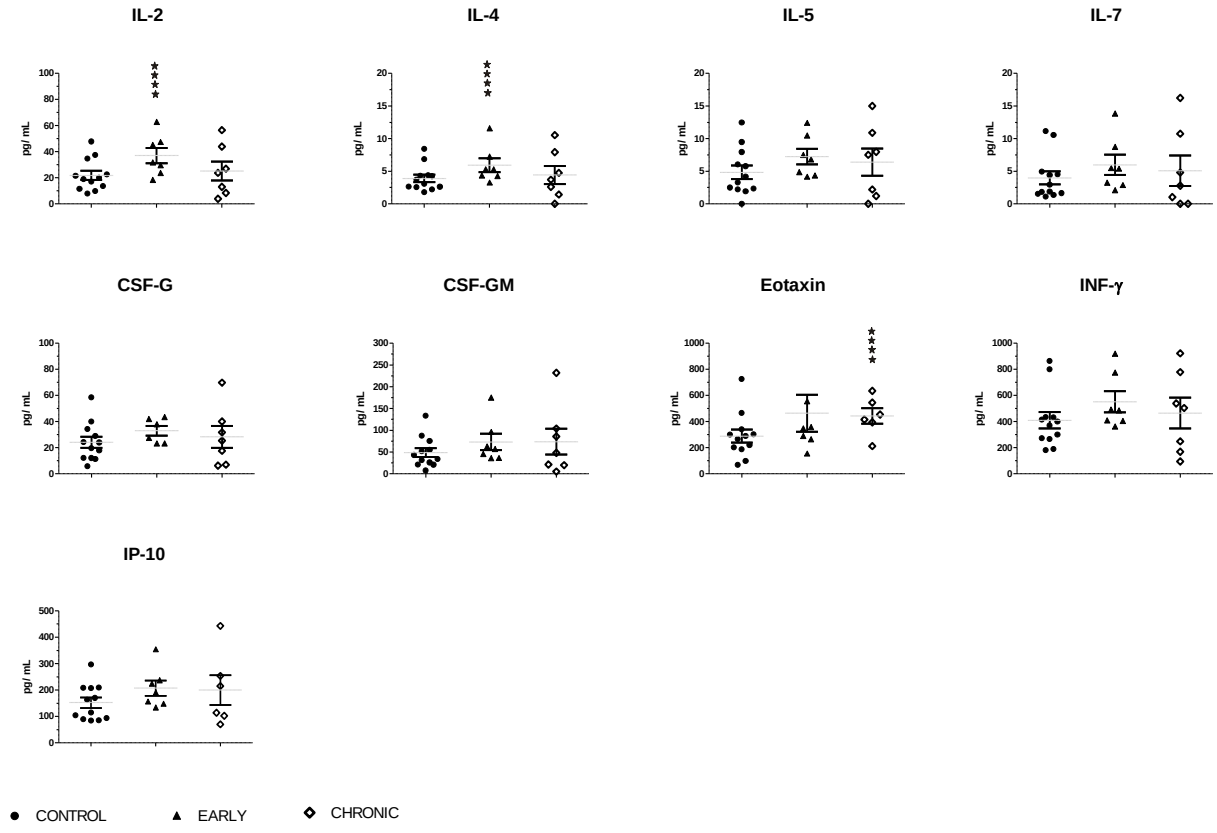

Figure 9.5. Plasma cytokine concentrations increased early during SIV infection
Difference between control cohort to early and chronic periods of SIV infection were compared by Mann Whitney t tests (****$p \leq 0.05$). Representation of mean values (grey line) $\pm$ SEM.

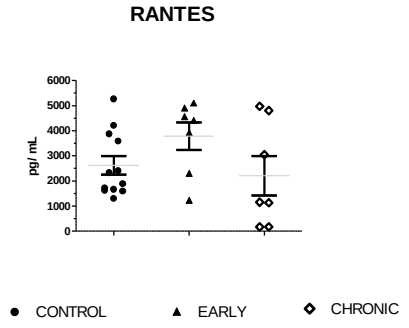

Figure 9.6. Plasma cytokine concentrations were variable during SIV infection
Difference between control cohort to early and chronic periods of SIV infection were compared by Mann Whitney t tests (****$p \leq 0.05$). Representation of mean values (grey line) $\pm$ SEM.

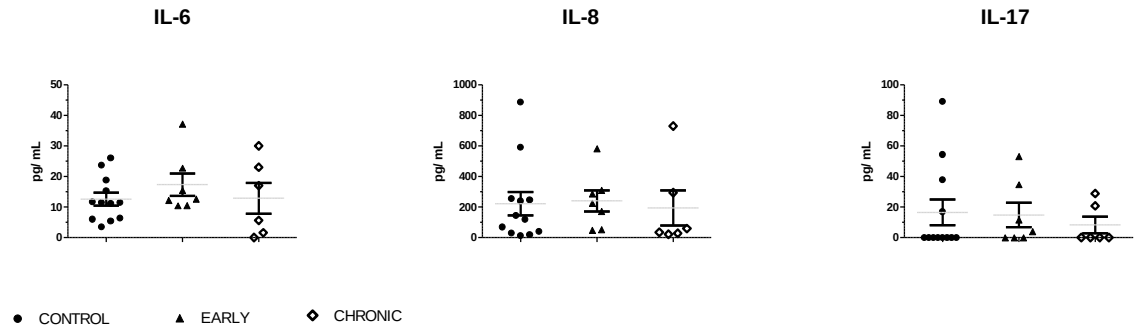

Figure 9.7. Plasma cytokine concentrations decreased during SIV infection
Difference between control cohort to early and chronic periods of SIV infection were compared by Mann Whitney t tests (****$p \leq 0.05$). Representation of mean values (grey line) $\pm$ SEM.

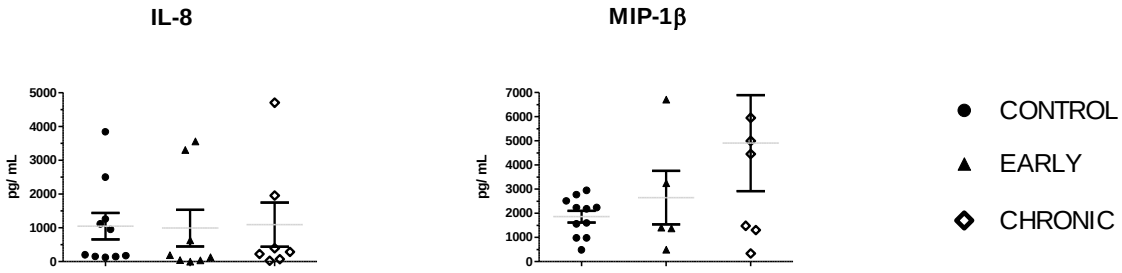

Figure 9.8. Cytokine concentrations in supernatant from stimulated bone marrow cells during SIV infection
Difference between control cohort to early and chronic periods of SIV infection were compared by Mann Whitney t tests (no differences). Representation of mean values (grey line) $\pm$ SEM.

By flow analysis of apoptosis in marrow and blood, the percentages indicated apoptosis of CD3+ T lymphocytes to be a rare event that was unchanged during SIV infection. Our finding was consistent with blood lymphocytes from chronically SIV infected RM that had similar levels of apoptosis to non-SIV infected RM detected by AC3 (Paiardini 2006). Paiardini et al. detected higher levels of activated caspase 8 (AC8) in SIV infected RM compared to non-infected macaques (Paiardini 2006). AC8 is an initiator caspase upstream from AC3 in the FAS mediated apoptosis pathway (Elmore 2007). Within lamina propria of SIV infected RM, increased apoptosis of CD4+ and not CD8+ T cells was identified by TUNEL and AC3 (Li 2005)

Theile et al. reported AIDS patients were observed with increased apoptosis in BM identified by TUNEL compared to non-HIV infected people (Thiele 1997). In addition Theile et al. indetified similar bone marrow changes for non-AIDS patients with myelitis and myelodysplasia suggestive of premature cell death or ineffective hematopoiesis (Thiele 1997). Theile et al. proposed that detection of apoptosis may be impeded by efficient removal of apoptotic cells by tissue macrphages (Thiele 1997). Further Theile et al. suggested apoptosis may result in recruitment of macrophages which in turn could secrete cytokines to enhance apoptosis (Thiele 1997). We observed by apoptosis staining in BM tissue the presence of intracytoplasmic fluorescence for AC3 suggestive of phagocytosed debris from apoptotic cells, however this was noted in control and infected macaques. We also found several cytokines increase post-infection in BMMC, a fraction of which likely contained macrophages. However, MIP-1β (a chemoattractant for granulocytes) was only increased in early and later periods. Moreover, TNF-α in plasma was continually elevated post-infection which can induce apoptosis (Thiele 1997).

Our finding of increased MIP-1β in marrow supernatant was supported by similar findings in BMMC from HIV patients receiving ART (Dallalio 1999). In additon, TNF and

RANTES were also found to elevated by Dallalio et al. in HIV patients (Dallalio 1999). We detected increases in plasma TNF early and late during SIV infection but only during the early phase for RANTES. Our study demonstrated BMMC supernatant levels of MIP-1β was higher post-infection compared to control macaques supported by reports of significantly higher concentrations by ELISA in supernatant from BM aspirates of HIV infected patients than non-infected (Dallalio 1999). IL-1β and IFN-γ were not detectable in bone marrow supported by minimal detection by ELISA from BM aspirates of HIV patients (Dallalio 1999). BM aspirate supernatant from HIV patients revealed significant increases in TNF-α and MIP-1α from non-HIV infected patients and minimal changes in RANTES by ELISA determination (Dallalio 1999).

Cytokine analysis of supernatant from long term bone marrow culture cells (LTBMC) infected with HIV did not reveal differences compared to control cultures for IL-1α, IL-3, IL-6, MIP-1α, TGF-β, and TNF-α (Marandin 1995). In our study, IL-1α, MIP-1α, and TGF-β were not detectable in supernatant. In our study IL-6, MIP-1α, and TNF-α were low in accordance with HIV studies (Marandin 1995) but IL-6 was high in HIV studies (Marandin 1995). Also stromal cells in LTBMC from HIV infected cultures were able to support hematopoiesis compared to non-infected LTBMC cultures (Marandin 1995).

IL-7 supports survival of CD8+ naïve cells while IL-7 and IL-15 support expansion of memory cells (Koopman 2001). IL-2 and IL-4 can support proliferation of CD8+ memory cells (Koopman 2001). IL-7 supports survival of CD4+ naïve, memory, and effector cells (Koopman 2001). IL-2 inhibits effector cells during priming but prevents apoptosis during the contraction phase for CD4+ lymphocytes (Koopman 2001).

Limitation of this study was BMMC supernatant stimulation performed to determine cytokine levels during SIV infection. Cellular composition of the BMMC may not have

supported detection of cytokines. Monocytes, macrophages, and lymphocytes secrete several of the cytokines analyzed and should have been represented in the mononuclear ficoll preparation but flow analysis was not performed to confirm the phenotype of BMMC before or after stimulation. It is unknown what concentration or ratio of cells is needed in bone marrow to detect cytokine levels, though previous studies have detected concentrations of cytokines in marrow supernatant. The dilution factor may have been a hindrance to detection. The dilution factor for supernatant was chosen at 1:100 per manufacturer recommendations, but several cytokines were not recorded because the level of detection was below the lower limit of the standard. Cytokine concentrations in supernatant may be undetectable, even without dilution, but optimal for cell-to-cell interface within bone marrow tissue. Microarray analysis to detect upregulation of genes that target cytokine production found with BMMC fractions may reveal changes during SIV infection.

SUMMARY

In vivo apoptosis of T cells is minimally changed during SIV infection in bone marrow and whole blood. Cytokine analysis of supernatant from bone marrow mononuclear cells of infected macaques did not reveal increases in pro-apoptotic cytokines. Plasma cytokine levels from the same macaques revealed pro-inflammatory cytokines. Our hypothesis was rejected for increased apoptosis in bone marrow of T cells.

REFERENCES

Arnoult, D., Petit, F., Lelievre, J.D., Lecossier, D., Hance, A., Monceaux, V., Hurtrel, B., Ho Tsong Fang, R., Ameisen, J.C., and Estaquier, J. (2003). Caspase-dependent and -independent T-cell death pathways in pathogenic simian immunodeficiency virus infection: relationship to disease progression. Cell death and differentiation *10*, 1240-1252.

Borda, J.T., Alvarez, X., Kondova, I., Aye, P., Simon, M.A., Desrosiers, R.C., and Lackner, A.A. (2004). Cell tropism of simian immunodeficiency virus in culture is not predictive of in vivo tropism or pathogenesis. The American journal of pathology *165*, 2111-2122.

Bucur, S.Z., Gillespie, T.W., Lee, M.E., Adams, J.W., Bray, R.A., Villinger, F., Ansari, A.A., and Hillyer, C.D. (2000). Hematopoietic response to lineage-non-specific (rrIL-3) and lineage-specific (rhG-CSF, rhEpo, rhTpo) cytokine administration in SIV-infected rhesus macaques is related to stage of infection. Journal of medical primatology *29*, 47-56.

Dallalio, G., North, M., McKenzie, S.W., and Means, R.T., Jr. (1999). Cytokine and cytokine receptor concentrations in bone marrow supernatant from patients with HIV: correlation with hematologic parameters. J Investig Med *47*, 477-483.

Donaghy, H., Gazzard, B., Gotch, F., and Patterson, S. (2003). Dysfunction and infection of freshly isolated blood myeloid and plasmacytoid dendritic cells in patients infected with HIV-1. Blood *101*, 4505-4511.

Elmore, S. (2007). Apoptosis: a review of programmed cell death. Toxicol Pathol *35*, 495-516.

Giavedoni, L.D. (2005). Simultaneous detection of multiple cytokines and chemokines from nonhuman primates using luminex technology. Journal of immunological methods *301*, 89-101.

Gougeon, M.L., Lecoeur, H., Dulioust, A., Enouf, M.G., Crouvoiser, M., Goujard, C., Debord, T., and Montagnier, L. (1996). Programmed cell death in peripheral lymphocytes from HIV-infected persons: increased susceptibility to apoptosis of CD4 and CD8 T cells correlates with lymphocyte activation and with disease progression. J Immunol *156*, 3509-3520.

Kitagawa, M., Lackner, A.A., Martfeld, D.J., Gardner, M.B., and Dandekar, S. (1991). Simian immunodeficiency virus infection of macaque bone marrow macrophages correlates with disease progression in vivo. The American journal of pathology *138*, 921-930.

Koopman, G., Niphuis, H., Newman, W., Kishimoto, T.K., Maino, V.C., and Heeney, J.L. (2001). Decreased expression of IL-2 in central and effector CD4 memory cells during progression to AIDS in rhesus macaques. AIDS (London, England) *15*, 2359-2369.

Li, Q., Duan, L., Estes, J.D., Ma, Z.M., Rourke, T., Wang, Y., Reilly, C., Carlis, J., Miller, C.J., and Haase, A.T. (2005). Peak SIV replication in resting memory CD4+ T cells depletes gut lamina propria CD4+ T cells. Nature *434*, 1148-1152.

Marandin, A., Canque, B., Coulombel, L., Gluckman, J.C., Vainchenker, W., and Louache, F. (1995). In vitro infection of bone marrow-adherent cells by human immunodeficiency virus type 1 (HIV-1) does not alter their ability to support hematopoiesis. Virology *213*, 245-248.

Marandin, A., Katz, A., Oksenhendler, E., Tulliez, M., Picard, F., Vainchenker, W., and Louache, F. (1996). Loss of primitive hematopoietic progenitors in patients with human immunodeficiency virus infection. Blood *88*, 4568-4578.

Paiardini, M., Cervasi, B., Sumpter, B., McClure, H.M., Sodora, D.L., Magnani, M., Staprans, S.I., Piedimonte, G., and Silvestri, G. (2006). Perturbations of cell cycle control in T cells contribute to the different outcomes of simian immunodeficiency virus infection in rhesus macaques and sooty mangabeys. Journal of virology *80*, 634-642.

Ramesh, G., Borda, J.T., Gill, A., Ribka, E.P., Morici, L.A., Mottram, P., Martin, D.S., Jacobs, M.B., Didier, P.J., and Philipp, M.T. (2009). Possible role of glial cells in the onset and progression of Lyme neuroborreliosis. J Neuroinflammation *6*, 23.

Thiele, J., Zirbes, T.K., Wiemers, P., Lorenzen, J., Kvasnicka, H.M., and Fischer, R. (1997). Incidence of apoptosis in HIV-myelopathy, myelodysplastic syndromes and non-specific inflammatory lesions of the bone marrow. Histopathology *30*, 307-311.

Veazey, R.S., DeMaria, M., Chalifoux, L.V., Shvetz, D.E., Pauley, D.R., Knight, H.L., Rosenzweig, M., Johnson, R.P., Desrosiers, R.C., and Lackner, A.A. (1998). Gastrointestinal tract as a major site of CD4+ T cell depletion and viral replication in SIV infection. Science *280*, 427-431.

Wang, X., Pahar, B., Rasmussen, T., Alvarez, X., Dufour, J., Rasmussen, K., Lackner, A.A., and Veazey, R.S. (2008). Differential cross-reactivity of monoclonal antibody OPD4 (anti-CD45RO) in macaques. Dev Comp Immunol *32*, 859-868.

Wang, X., Rasmussen, T., Pahar, B., Poonia, B., Alvarez, X., Lackner, A.A., and Veazey, R.S. (2007). Massive infection and loss of CD4+ T cells occurs in the intestinal tract of neonatal rhesus macaques in acute SIV infection. Blood *109*, 1174-1181.

CHAPTER 10: CONCLUSION

We hypothesized bone marrow is a site of increased apoptosis for CD4+ T lymphocytes during SIV/HIV infection causing depletion of this subset in the marrow. Potential mechanisms of CD4+ T lymphocyte loss in the bone marrow include the following: (1) direct viral infection of CD4+ T cells and destruction (Harbol 1994; Paiardini 2009); (2) "bystander apoptosis" of CD4+ T cells as an effect from nearby virally infected bone marrow cells (Chen 2002; Li 2005; Paiardini 2009); or (3) apoptosis and/or defective lymphopoiesis leading to lack of reconstitution secondary to chronic immune stimulation during SIV/HIV infection (Harbol 1994; Paiardini 2009). The accelerated apoptosis may be from direct cell infection and loss or the result of "bystander apoptosis" from nearby infected cells or viral proteins. For true bystander apoptosis to be a mechanism of destruction, any CD4+ T lymphocytes could potentially undergo programmed cell death regardless of chemokine receptor expression, but this could also be dependent on cell activation.

First, we demonstrated the Rhesus macaque model for progressive SIV disease parallels HIV disease of humans with regard to hematologic abnormalities detected on a complete blood count. Lymphopenia, neutropenia, anemia, thrombocytopenia, and eosinophilia are common in prevalence and distrubtion during progressive SIV disease. The SIV model of RM was validated for study of hematologic abnormalities in HIV disease.

We then confirmed the Rhesus macaque model for SIV disease mimics HIV disease of humans with regard to observable bone marrow changes by an objective detailed morphologic assessment. We documented marrow panhypercellularity (especially in the AIDS phase), BM fibrosis, BM lymphoid aggregations, BM iron depletion, and increased BM CD34+ hematopoietic stem cells during progressive SIV disease that was similar to findings during HIV disease. The BM myeloid to erythroid ratio is mostly maintained with minimal loss of myeloid

lineage cells and increase of erythroid lineage cells post-infection. Despite observed changes in BM, during progressive infection the marrow was able to respond appropriately to peripheral needs by increase production of hematopoietic cells especially noted in AIDS. The SIV model of RM was validated for study of bone marrow changes in HIV disease.

We established a percent increase in the erythroid and lymphoid lineages, maintenance of the monocytic lineage, and drop in the granulocytic lineage during progressive SIV disease in macaques by phenotypic analysis of marrow hematopoeitic cell lineages by flow cytometry. Our phenotypic analysis of BM was similar to our morphologic analysis of BM during SIV with respect to increased T lymphocytes and erythroid cells, lack of change in monocytes, and loss of granulocytes. Further, we determined the increase in marrow lymphocytes was due to CD3+ T lymphocytes while B lymphocytes, plasma cells, NK cells, and DC cells decreased in the marrow during progressive SIV disease. As T lymphocytes increased in BM, antigen presenting dendritic cells in BM and WB decreased suggestive of a loss and not redistribution of cells.

We quantified viral copies of RNA in BM during progressive SIV infection in macaques with minimal observable detection of infective cells except in chronic phases. Viral DNA wasdetected by polymerase chain reaction during progressive SIV infection also with rare observable productively infected cells in BM. Hematopoietic cells infected with SIV were macrophages, CD3+ T lymphocytes, and other mononuclear cells in BM.

We demonstrated the percentage increase in BM T cells post-SIV infection in macaques translated to increased absolute numbers of CD3+ T lymphocytes during SIV infection predominantly by CD8+ T cells. Suprisingly, unlike WB, BM CD4+ T lymphocytes were maintained during progressive SIV infection with evidence of proliferation. Our hypothesis of loss of CD4+ T lymphocytes during progressive SIV infection was rejected based on this unexpected finding.

We observed few apoptotic cells were present in bone marrow for control and SIV infected RM. Flow cytometry analysis of apoptosis of CD3+ cells revealed low percentages of cells were undergoing apoptosis as determined by detection of activated caspase 3 expression during SIV. Bone marrow cytokine concentrations from supernatant of stimulated marrow mononuclear cells detected rare cytokines while plasma detected pro-inflammatory cytokines during progressive SIV infection.

Theories for loss of CD4+ T lymphocytes in marrow were rejected in this study due to lack of loss of these cells in bone marrow during various periods of SIV infection in the RM. Few productively SIV infected cells were detected in marrow though RNA and DNA viral copies were detected by PCR so direct viral destruction or bystander apoptosis of CD4+ T lymphocytes is unlikely. Low numbers of marrow cells were undergoing apoptosis so virally induced apoptosis of CD4+ T lymphocytes is unlikely. Cytokine expression was minimally detected in stimulated BM mononuclear cells so chronic immune stimulation affecting marrow cytokine production was not detected to halt or prevent lymphopoiesis of T lymphocytes.

Neutropenia was a consistent finding in SIV infected RM especially in progressive disease. Myeloid loss of granulocytic cells and not monocytic cells was noted in the BM during SIV infection though the BM cellularity increased. Maintenance of CD4+ T lymphocytes in BM was detected during progressive SIV infection. Future studies are needed to determine relevance of these factors during SIV and HIV.

Our findings suggest bone marrow and whole blood are under different homeostatic mechanisms. CD8+ T lymphocytes were able to respond during progressive SIV infection though CD4+ T lymphocytes were maintained but did not increase. Proliferation in BM of CD4+ and CD8+ T lymphocytes indicates bone marrow tissue can support lymphopoiesis during SIV infection but cell cycle dysfunction was evident for CD4 cells.

Our study of marrow raises the question that bone marrow may be a *de novo* site of CD4+ T lymphocyte production and provide CD4+ T lymphocytes to enter circulation and may be the "tap" in the purported "tap and drain" mechanism of CD4+ T lymphocyte loss and turnover (Chen 2002). Lymphocyte numbers may be increased in bone marrow following infection because of redistribution or increased migration from or decreased emigration to peripheral blood and lymphoid tissues. HIV infected patients demonstrated significant increases of CD4+ T lymphocytes migrating from peripheral blood to bone marrow compared to uninfected people by *in vivo* CD4 lymphocyte autologous nuclear labeling studies (Chen 2002).

Future studies in bone marrow lymphocyte homeostasis may provide clues to changes identified during SIV and HIV infection.

REFERENCES

Chen, J.J., Huang, J.C., Shirtliff, M., Briscoe, E., Ali, S., Cesani, F., Paar, D., and Cloyd, M.W. (2002). CD4 lymphocytes in the blood of HIV(+) individuals migrate rapidly to lymph nodes and bone marrow: support for homing theory of CD4 cell depletion. Journal of leukocyte biology *72*, 271-278.

Harbol, A.W., Liesveld, J.L., Simpson-Haidaris, P.J., and Abboud, C.N. (1994). Mechanisms of cytopenia in human immunodeficiency virus infection. Blood reviews *8*, 241-251.

Li, Q., Duan, L., Estes, J.D., Ma, Z.M., Rourke, T., Wang, Y., Reilly, C., Carlis, J., Miller, C.J., and Haase, A.T. (2005). Peak SIV replication in resting memory CD4+ T cells depletes gut lamina propria CD4+ T cells. Nature *434*, 1148-1152.

Paiardini, M., Cervasi, B., Engram, J.C., Gordon, S.N., Klatt, N.R., Muthukumar, A., Else, J., Mittler, R.S., Staprans, S.I., Sodora, D.L., *et al.* (2009). Bone marrow-based homeostatic proliferation of mature T cells in nonhuman primates: implications for AIDS pathogenesis. Blood *113*, 612-621.

APPENDIX I: HEMATOLOGIC DATA AND DEFINITIONS

All hematologic values were generated from a single ethylenediaminetetraacetic acid (EDTA) anti-coagulated sample of whole blood processed the same day and analyzed on a hematology analyzer at the TNPRC Clinical Pathology Core Laboratory. EDTA blood for CBCs collected on day of sacrifice was obtained immediately prior to humane euthanasia. EDTA blood was maintained at room temperature on a rocker until CBC analysis was performed. CBC data with values outside of the reference ranges/intervals or those flagged for any reason were always evaluated microscopically by review of a modified Wright stained blood smear.

CBCs were evaluated from day 0 of SIV inoculation serially over time till day of sacrifice for SIV infected subjects in ED I (Appendix II). Control subjects in ED I had one CBC evaluated. Subjects in ED II, ED III, and ED IV (Appendix II) had one CBC evaluated on the day of sacrifice.

Samples collected prior to Sept 1, 2001 were analyzed using a Coulter T540 hematology analyzer (Beckman Coulter; Fullerton, CA) and samples collected after 2001 were generated using an ADVIA 120 hematology analyzer (Bayer; Tarrytown, NY). However, prior to this transition, extensive quality control testing was performed to ensure consistency of data collection and analysis between the two instruments (data not shown). Subjects included in ED I utilized both hematologic analyzers. Subjects included in ED II -IV utilized only the ADVIA 120 hematologic analyzer.

Hematologic conditions were interpreted by observed laboratory parameters. Abnormalities were defined based upon CBC reference intervals for the Rhesus macaque. Cytopenia or decreased values were defined as the following: leukopenia (white blood cell (WBC) count <6,600 cells/µL); lymphopenia (absolute lymphocyte count <2,600 cells/µL); monocytopenia (absolute monocyte count <100 cells/µL); neutropenia (absolute neutrophil count

<2,200 cells/µL); and TCP without gross or microscopic evidence of platelet clumping (platelet count < 193,000 cells/µL). Cytosis or cytophilia were defined as the following: leukocytosis (total WBC count >15,500 cells/µL); basophilia (absolute basophil count >100 cells/µL); eosinophilia (absolute eosinophil count >400cells/µL); lymphocytosis (absolute lymphocyte count >8,600 cells/µL); monocytosis (absolute monocyte count >600 cells/µL); and neutrophilia (absolute neutrophil count >5,600 cells/µL; and reticulocytosis (reticulocyte count >212x10^9 cells/µL).

Anemia was defined as a low hematocrit value (hematocrit <34.8%). Anemia was further characterized by MCV and MCHC values. Microcytosis was defined as a decreased MCV value (<63.7 fL), normocytosis was defined as a MCV value within the reference interval (63.7-86.9 fL) and macrocytosis was defined as an increased MCV value (>86.9 fL). Anemia was also classified as hypochromic or normochromic by the MCHC value. Hypochromia was defined as a decreased MCHC value (<28.9 g/dL) and normochromia was defined as a MCHC value within the reference interval (28.9-35.4 g/dL). Reticulocytosis was defined as regenerative during an anemic condition. Reticulocyte count was performed for ED II and III.

Mean platelet volume (reference interval 7.0-12.0 fL) was evaluated for ED II and III.

APPENDIX II: EXPERIMENTAL DATABASE

RESEARCH SUBJECTS

Four experimental databases were utilized that consisted of different control and SIV infected RM and different designations of stages during SIV infection defined as periods. ED I was utilized in Chapter 3. ED II was utilized in Chapter 4, Chapter 7, and Chapter 8. ED III was utilized in Chapter 5, Chapter 6, Chapter 7, and Chapter 9. ED IV was utilized in Chapter 7.

Controls were uninfected or non-inoculated for SIV and changed for each ED. Asian RM were chosed for the SIV animal model of HIV disease at the TNRPC. Rhesus macaques were inoculated by once by either intravenous (IV), intra-vaginal (INVG), or intra-rectal (IR) route with either of SIVmac239, SIVmac251, or SIVB670.

IV administration was performed according to TNPRC SOP 3.18.2 Intraveous Inoculation of Nonhuman Primates. INVG administration was performed according to TNPRC SOP 3.19.2 Intravaginal Inoculation of Nonhuman Primates. IR administration was performed according to TNPRC SOP 3.49.2 Intra-rectal inoculation of Nonhuman Primates. Subjects were at least 1.75 years of age at time of inoculation. Control subjects were naïve for SIV inoculation and age-matched. Further, all animals were devoid of SIV-related experimental treatment, therapy, or vaccination throughout the study.

All RM subjects were sedated for examinations, procedures, and/or transport to the necropsy suite per TNPRC SOP 3.1.2 Chemical Restraint of Nonhuman Primates for Examination and Minor Procedures by TNPRC veterinarians. Venipuncture was performed according to TNPRC SOP 3.10.3 Blood Collection by Venipuncture in Nonhuman Primates. Select RM were intra-peritoneally injected with bromodeoxyuridine (BrdU) 24 hours prior to humane sacrifice.

Control macaques in ED I were not sacrificed after sample collection. Control macaques in ED II-III were humanely euthanized at the termination of their study protocol as were SIV infected macaques. Additionally, SIV infected RM were humanely euthanized for intractable illness prior to termination of their study protocol. Throughout the study, clinical signs were monitored and recorded by TNPRC veterinarians. Euthanasia was performed according to TNPRC SOP 3.23.2 Euthanasia Procedures in Nonhuman Primates. Necropsy included gross evaluation of multiple organs and tissues for each subject along with sample collection obtained by a necropsy prosector and/or veterinary pathologist. Multiple samples from organs/tissues were taken from each subject for histopathologic review by a TNPRC veterinary pathologist. Either absence of significant lesions, no significant lesions found (NSF), or presence of disease processes were confirmed by histopathological examination of multiple organs/tissues obtained from necropsy. Samples were obtained at necropsy and disease was confirmed by gross and histopathological examination of multiple organs/tissues.

DEFINITIONS OF PERIODS DURING SIV INFECTION

For data evaluation, inoculated subjects were grouped based on progression of infection as control, early, and chronic periods of SIV infection. Early, chronic, and AIDS periods consisted of SIV inoculated macaques. Early subjects were 1-42 days post-inoculation (DPI) at humane sacrifice. The chronic subjects were >42 DPI. AIDS subjects were chronically infected with clinical signs and disease consistent with AIDS criteria.

The chronic time period was subdivided for ED II and ED IV by clinical signs and disease process, based on the 2008 World Health Organization (WHO) and CDC classification for HIV. The chronic group was subdivided into 3 phases based on clinical signs ascertained by TNPRC laboratory animal veterinarians and necropsy diagnosis of disease as asymptomatic SIV disease (ASY), advanced SIV disease (ASD), and acquired immune deficiency syndrome

(AIDS). ASY subjects were without clinical signs of disease at humane sacrifice and without necropsy diagnosis of disease. ASD subjects or "sick" macaques displayed clinical signs of disease with confirmed necropsy diagnosis of disease but lacking AIDS defined diseases at humane sacrifice. AIDS was defined based on the 1993 Centers for Disease Control (CDC) guidelines of encephalitis, lymphoid tumors, or opportunistic infections (OI). AIDS subjects had classic clinical signs and disease consistent with AIDS criteria. The progression to AIDS was defined as fast or slow progressors.

EXPERIMENTAL DATABASE I-IV

Experimental Database I

The 21 infected subjects ranged in age from 1.77-12.2 years of age at inoculation (mean 4.98 years) as defined in Table II.1. Three male and two female RM were examined in the SIVmac239 group with an average of 691 DPI (range 359-1113 DPI), six males were examined in the SIVmac251 group with an average of 814 DPI (range 536-1071 DPI), and five male and five females were examined in the SIVB670 group with an average of 454 DPI (range 278-776 DPI). Criteria for diagnosis of AIDS remained fairly consistent between groups except for animal BE53, inoculated with SIVmac251, diagnosed with multi-organ lymphoma. Each infected RM had at least one CBC drawn during each successive stage of infection. Thirty-one control RM consisted of twenty-two male and nine female macaques whose ages ranged from 2.24 to 9.72 years (mean of 5.10 years). Controls are defined in Table II.2.

Experimental Database II

Thirty-nine Indian RM were included in this study (Table II.1). Control subjects consisted of eight RM, 3 male and 5 female with an average age of 7.6 years at sacrifice (range 3-10 years). Ten early subjects, within 8-22 DPI, were all inoculated IV with SIVmac251, 8 male and 2 female with an average of 7.2 years at sacrifice (range 3-20 years). At 63-181 DPI

Table II.1. SIV Inoculated Rhesus Macaque Experimental Database I

Subject ID[a]	Sex	Age at Inoculation, Years	SIV Inoculum	Days Post-Inoculation at Sacrifice	AIDS Diagnosis
BR20	M[b]	6.35	mac239	389	Pneumocystis pneumonia
EE54	F[c]	2.75	mac239	359	Pneumocystis pneumonia
I553	F	12.20	mac239	646	Pneumocystis pneumonia
P045	M	8.46	mac239	1113	Pneumocystis pneumonia
T798	M	6.22	mac239	949	Intestinal mycobacteriosis
AE55	M	5.10	mac251	658	Pneumocystis pneumonia
BE53	M	3.33	mac251	536	Lymphoma, multi-organ
BE65	M	3.33	mac251	1071	Intestinal mycobacteriosis
BI33	M	5.17	mac251	899	Pneumocystis pneumonia
BT51	M	4.03	mac251	990	Intestinal mycobacteriosis
P503	M	10.31	mac251	730	Pneumocystis pneumonia
G010	F	1.95	B670	390	Meningoencephalitis
G055	F	2.31	B670	343	Meningoencephalitis
G143	M	1.93	B670	445	Cryptospordiosis
G164	M	1.87	B670	776	Meningoencephalitis
J714	M	2.02	B670	317	Pneumocystis pneumonia
N073	M	3.88	B670	510	Intestinal mycobacteriosis
N217	F	9.91	B670	546	Intestinal mycobacteriosis
P337	M	2.04	B670	517	Intestinal mycobacteriosis
R544	F	7.87	B670	414	Meningoencephalitis
T270	F	1.77	B670	278	Cryptospordiosis

a) ID= identification; b) M = male; c) F = female

Table II.2. Controls in Experimental Database I

Subject ID[a]	Sex	Age, Years
CE04	F[b]	9.72
CF18	F	8.55
CT13	M[c]	6.47
DF51	M	6.41
DF99	M	6.38
DJ11	M	6.16
DN57	M	5.46
DR15	F	5.91
DR48	F	5.89
DV24	F	5.84
DV66	M	5.38
EA27	M	5.90
EB45	M	5.31
EB50	M	5.28
EF56	F	5.87
EL18	M	4.92
EL50	M	4.36
EL52	F	4.81
EM96	F	4.76
EP43	M	4.29
ER34	F	4.48
FG52	M	3.35
FH22	M	3.33
FH43	M	3.33
FH71	M	3.31
FJ20	M	3.14
FJ65	M	3.14
FJ68	M	3.13
FP79	M	2.28
FT10	M	2.24
FT46	M	2.23

a) ID= identification; b) F = female; c) M = male

were seven ASY subjects inoculated with SIVmac251, 5 male by IR route and 2 female by INVG route with an average age of 5.8 years at sacrifice (range 4-10 years). The ASD subjects were two male and three female subjects inoculated IV with SIVmac251 and one female was inoculated INVG with SIVB670 that ranged 63-959 DPI with an average age of 7.4 years at sacrifice (range 4-13). Finally, AIDS subjects were 414-1071 DPI and consisted of three male and one female subject inoculated IV with SIVmac251, three males inoculated with SIVmac239, and one female inoculated INVG with SIVB670 with an average of 9.4 years at sacrifice (range 6-14). AIDS subjects were slow progressors or $\geq$260 DPI at humane sacrifice.

Experimental Database III

Twenty-four Asian RM were included in this study (Table II.2). Control subjects consisted of twelve female Indian RM with an average age of 9.9 years at sacrifice (4-16 years). All experimental subjects were infected with SIVmac251. Eight early subjects, within 8-13 DPI, were all inoculated IV with SIVmac251, 1 male and 7 females with an average age of 10.3 years at sacrifice (range 5-14 years). Eight chronic subjects, within 71-1068 DPI, were all inoculated with SIVmac251, 5 females by INVG route, 2 females by IV route, and 1 male by IR route with an average of 8.7 years at sacrifice (range 3-11). Chronic RM included 1 asymptomatic, 2 symptomatic, and 5 AIDS subjects. AIDS subjects were fast progressors with clinical signs and disease consistent with AIDS criteria for ED II. AIDS diagnoses were all different including OIs, lymphoma, and encephalitis. All RM were of Indian origin except 1 female in AIDS.

Experimental Database IV

Experimental database II and III were combined to form a single cohort of only SIV infected macaques divided into early (18 RM), ASY (8 RM), ASD (8 RM), and AIDS (13 RM) periods based on definitions for ED II including forty-seven subjects. The AIDS group included fast and slow progressors.

Table II.3. Experimental Database II

Subject ID[a]	Sex	Age at Sacrifice, years	DPI[b] at Sacrifice	SIV Inoculum, Route	Period of Infection, Necropsy Diagnosis	BrdU[c] Administration
CONTROL						
AJ79	F[d]	7.19			Control, NSF[e]	+[f]
BB05	M[g]	6.91			Control, NSF	-[h]
EH70	F	3.01			Control, NSF	+
EH80	F	3.01			Control, NSF	+
EH95	F	3.00			Control, NSF	+
H741	M	15.73			Control, NSF	+
L750	M	12.12			Control, NSF	+
R534	F	10.21			Control, NSF	+
EARLY						
AV63	F	4.37		mac251, IV[i]	Early, NSF	+
AV85	F	8.16	21	mac251, IV	Early, LH[j]	+
BA17	M	8.28	12	mac251, IV	Early, LH	+
BI58	M	3.19	22	mac251, IV	Early, LH	-
BN37	M	2.53	21	mac251, IV	Early, LH	-
BV13	M	3.33	8	mac251, IV	Early, LH	+
C419	M	20.27	9	mac251, IV	Early, NSF	+
CB74	M	3.25	21	mac251, IV	Early, LH	+
L880	M	11.33	10	mac251, IV	Early, LH	+
T139	M	7.26	13	mac251, IV	Early, LH	+
CHRONIC						
BV74	M	4.73	63	mac251, IR[k]	ASY[l], LH	+
CF35	M	4.51	91	mac251, IR	ASY, LH	+
DB53	M	5.12	77	mac251, IR	ASY, LH	-
DE09	M	3.59	76	mac251, IR	ASY, LH	-
DI28	M	3.53	80	mac251, IR	ASY, LH	-
N998	F	10.13	180	mac251, INVG[m]	ASY, LH	+
R908	F	8.91	181	mac251, INVG	ASY, LH	-
AP53	F	6.44	63	mac251, IV	ASD[n], Septicemia, Bacterial pneumonia	-
BD78	M	3.93	205	mac251, IV	ASD, Pulmonary infarct, Thrombosis	+
BE64	F	5.30	742	mac251, IV	ASD, Right heart failure	+
CD95	F	7.73	924	mac251, IV	ASD, Advanced colitis	+
L164	F	12.93	195	B670, INVG	ASD Pericardial and abdominal effusion	+
V205	M	8.11	959	mac251, IV	ASD, Intestinal amyloidosis	+
AE55	M	6.93	658	mac251, IV	AIDS[o], Pneumocystosis and Cryptosporidiosis	+
BA25	M	10.71	544	mac239, IV	AIDS, Pneumocystosis	-
BE65	M	6.31	1071	mac251, IV	AIDS, *Mycobacterium avium* pneumonia	+
BI33	M	7.67	899	mac251, IV	AIDS, Pneumocystosis	-
I553	F	14.00	646	mac251, IV	AIDS, Pneumocystosis	-
P045	M	11.56	809	mac239, IV	AIDS, Pneumocystosis	+
R544	F	9.03	414	B670, INVG	AIDS, Meningoencephalitis	+
T798	M	8.86	949	mac239, IV	AIDS, *Mycobacterium avium* pneumonia	+

a) ID = identification; b) DPI = days post-inoculation; c) BrdU = bromodeoxyuridine; d) F = female; e) NSF = no significant lesions found; f) + = positive for BrdU administration; g) M = male; h) - = negative for BrdU administration; i) IV = intravenous; j) LH = Lymphoid hyperplasia; k) IR = intra-rectal; l) ASY = asymptomatic disease; m) INVG = intra-vaginal; n) ASD = advanced SIV disease; o) AIDS = acquired immune deficiency syndrome

Table II.4. Experimental Database III

Subject ID[a]	Sex	Age at Sacrifice, years	DPI[b] at Sacrifice	SIV Inoculum, Route	Period of Infection, Necropsy Diagnosis	BrdU[c] Administration
CONTROL						
AG71	F[d]	11.07			Control, NSF[e]	+[f]
BB01	F	13.03			Control, NSF	+
CC10	F	8.93			Control, NSF	+
GN70	F	10.11			Control, NSF	+
HI54	F	5.39			Control, NSF	+
HI55	F	4.44			Control, NSF	+
HI56	F	4.43			Control, NSF	+
HI57	F	4.59			Control, NSF	+
EARLY						+
AV91	M[g]	14.08	10	mac251, IV[h]	Early, LH[i]	+
BA57	F	14.01	8	mac251, IV	Early, LH	+
HI52	F	5.43	7	mac251, IV	Early, LH	+
HI53	F	6.60	8	mac251, IV	Early, LH	+
HI58	F	6.64	12	mac251, IV	Early, LH	+
HI63	F	6.54	12	mac251, IV	Early, LH	+
M992	F	16.06	13	mac251, IV	Early, LH	+
T108	F	13.12	8	mac251, IV	Early, LH	+
CHRONIC						+
HG49	F	11.25	145	mac251, INVG[j]	ASY[k], Lymphoid hyperplasia	+
FE53	M	4.11	140	mac251, IR[l]	ASD[m], Pulmonary infarct, Vasculopathy	+
FT46	M	3.04	71	mac251, IR	ASD, Severe gastroenteritis	+
AL07	F	11.43	195	mac251, INVG	AIDS[n], *Mycobacterium avium*	+
FA14	F	9.50	1068	mac251, IV	AIDS, Pneumocystosis pneumonia	+
HG56	F	10.67	152	mac251, INVG	AIDS, Gastric lymphoma	+
HG58	F	9.97	283	mac251, INVG	AIDS, Encephalitis	+
HI68	F	9.83	155	mac251, INVG	AIDS, Cytomegalovirus, Vasculitis	+

a) ID = identification; b) DPI = days post-inoculation; c) BrdU = bromodeoxyuridine; d) F = female; e) NSF = no significant lesions found; f) + = positive for BrdU administration; g) M = male; h) IV = intravenous; i) LH = Lymphoid hyperplasia; j) INVG = intra-vaginal; k) ASY = asymptomatic disease; l) ; IR = intra-rectal; m) ASD = advanced SIV disease; n) AIDS = acquired immune deficiency syndrome

Table II.5. Experimental Database IV

Subject ID[a]	Sex	Age at Sacrifice, years	DPI[b] at Sacrifice	SIV Inoculum, Route	Period of Infection, Necropsy Diagnosis
Early					
AV63	F[c]	4.37		mac251, IV[d]	Early, NSF[e]
AV85	F	8.16	21	mac251, IV	Early, LH[f]
AV91	M[g]	14.08	10	mac251, IV	Early, LH
BA17	M	8.28	12	mac251, IV	Early, LH
BA57	F	14.01	8	mac251, IV	Early, LH
BI58	M	3.19	22	mac251, IV	Early, LH
BN37	M	2.53	21	mac251, IV	Early, LH
BV13	M	3.33	8	mac251, IV	Early, LH
C419	M	20.27	9	mac251, IV	Early, NSF
CB74	M	3.25	21	mac251, IV	Early, LH
HI52	F	5.43	7	mac251, IV	Early, LH
HI53	F	6.6	8	mac251, IV	Early, LH
HI58	F	6.64	12	mac251, IV	Early, LH
HI63	F	6.54	12	mac251, IV	Early, LH
L880	M	11.33	10	mac251, IV	Early, LH
M992	F	16.06	13	mac251, IV	Early, LH
T108	F	13.12	8	mac251, IV	Early, LH
T139	M	7.26	13	mac251, IV	Early, LH
ASY[h]					
BV74	M	4.73	63	mac251, IR[i]	ASY, LH
CF35	M	4.51	91	mac251, IR	ASY, LH
DB53	M	5.12	77	mac251, IR	ASY, LH
DE09	M	3.59	76	mac251, IR	ASY, LH
DI28	M	3.53	80	mac251, IR	ASY, LH
HG49	F	11.25	145	mac251, INVG[j]	ASY, Lymphoid hyperplasia
N998	F	10.13	180	mac251, INVG	ASY, LH
R908	F	8.91	181	mac251, INVG	ASY, LH
ASD[k]					
AP53	F	6.44	63	mac251, IV	ASD, Septicemia, Bacterial pneumonia
BD78	M	3.93	205	mac251, IV	ASD, Pulmonary infarct, Thrombosis
BE64	F	5.3	742	mac251, IV	ASD, Right heart failure
CD95	F	7.73	924	mac251, IV	ASD, Advanced colitis
FE53	M	4.11	140	mac251, IRl	ASD, Pulmonary infarct, Vasculopathy
FT46	M	3.04	71	mac251, IR	ASD, Severe gastroenteritis
L164	F	12.93	195	B670, INVG	ASD Pericardial and abdominal effusion
V205	M	8.11	959	mac251, IV	ASD, Intestinal amyloidosis

Table II.5 continued on next page

AIDS[l]					
AE55	M	6.93	658	mac251, IV	AIDS, Pneumocystosis and Cryptosporidiosis
AL07	F	11.43	195	mac251, INVG	AIDS, *Mycobacterium avium*
BA25	M	10.71	544	mac239, IV	AIDS, Pneumocystosis
BE65	M	6.31	1071	mac251, IV	AIDS, *Mycobacterium avium* pneumonia
BI33	M	7.67	899	mac251, IV	AIDS, Pneumocystosis
FA14	F	9.5	1068	mac251, IV	AIDS, Pneumocystosis pneumonia
HG56	F	10.67	152	mac251, INVG	AIDS, Gastric lymphoma
HG58	F	9.97	283	mac251, INVG	AIDS, Encephalitis
HI68	F	9.83	155	mac251, INVG	AIDS, Cytomegalovirus, Vasculitis
I553	F	14	646	mac251, IV	AIDS, Pneumocystosis
P045	M	11.56	809	mac239, IV	AIDS, Pneumocystosis
R544	F	9.03	414	B670, INVG	AIDS, Meningoencephalitis
T798	M	8.86	949	mac239, IV	AIDS, *Mycobacterium avium* pneumonia

a) ID = identification; b) DPI = days post-inoculation; c) F = female; d) IV = intravenous; e) NSF = no significant lesions found; f) LH = Lymphoid hyperplasia; g) M = male; h) ASY = asymptomatic; i) IR = intra-rectal; j) INVG = intra-vaginal; k) ASD = advanced SIV disease; l) AIDS = acquired immune deficiency syndrome

APPENDIX III: FLOW CYTOMETRY ANALYSIS

WHOLE BLOOD COLLECTION

Whole blood was obtained immediately prior to euthanasia into EDTA tubes. All WB samples were maintained at room temperature on a blood rocker till processed.

BONE MARROW TISSUE COLLECTION

Bone marrow necropsy collection from the femur was obtained within 30 minutes post-sacrifice. Bone marrow examination by ante-mortem and post-mortem has been reported to be comparable (Switzer 1967). Marrow tissue was harvested for formalin fixation and fresh tissue was suspended in 10mL of an enriched RPMI media solution. The enriched media solution consisted of 500mL RPMI 1640 IX without glutamine (Mediatech; Herndon, VA); 25mL Standard Fetal Bovine Serum (HyClone; Logan, UT); 5mL BioWhittaker™ Penicillin Streptomycin with 10,000 U Pen/mL and 10,000 µg Strep/mL (Cambrex; Walkersville, MD); 5mL BioWhittaker™ L-glutamine 200mM solution is 0.85% NaCl solution (Cambrex; Walkersville, MD); and 5mL HyQ® Hepes 1M solution (HyClone; Logan, UT).

The BM sample in media was thoroughly mixed by vortex then centrifuged at 400 x g for 7 minutes (Beckman Coulter Allegra™ 6R Centrifuge; Beckman Coulter, Inc.; Fullerton, CA). The supernatant and fat was discarded. The bone marrow cell pellet was resuspended in 2 mL of the enriched media and thoroughly vortexed. Resuspended bone marrow was filtered through nylon mesh and placed into a clean tube. Prior to flow cytometry staining, 20µL of processed bone marrow sample and 180µL of trypan blue were mixed and live cells counted using a hemocytometer. Final dilution of $1x10^7$/mL live cells was performed with the enriched RPMI media solution. Processed bone marrow tissue was maintained on ice until flow cytometry staining.

FLOW CYTOMETRY STAINING OF WHOLE BLOOD AND BONE MARROW TISSUE

Human or non-human primate antibodies from commercial distributors or NIH were optimized for flow cytometric analysis in the Rhesus macaque for whole blood and bone marrow tissue. Antibody panels were prepared for detection of specific cell populations as detailed in each chapter. Single antibodies or an antibody cocktail composed of multiple single fluorochrome antibodies were applied to each tube based upon the pre-determined panel. Appropriate volume and dilution of antibodies were added for each tube. Each subject had multiple tubes included in a batch to determine phenotypic characteristics of specific cell populations. Appropriate compensation tubes were included within each batch of subject samples. Surface staining was performed for each sample. Intracellular staining for detection of proliferation and apoptosis was performed after surface staining.

Antibodies were directly conjugated to the following fluorochromes: Allophycocyanin (APC), Allophycocyanin Cyanine 7 (APC-Cy7), *Anemonia mojona* Cyanine (AmCyan), Fluorescein isothiocyanate (FITC), Pacific Blue (PacBlue or PacBl), Peridinin Chlorophyll Protein (PerCP), Peridinin Chlorophyll Protein Cyanine 5.5 (PerCP-Cy5.5), Phycoerythrin (PE), Phycoerythrin Texas Red (PE-Tx RED or PE-TxR), Phycoerythrin Cyanine 5 (PE-Cy5), Phycoerythrin Cyanine 7 (PE-Cy7), and Quantom dots 655 (QDOT 655).

Flow Cytometry Compensation Tubes

Compensation sample tubes utilized whole blood samples from a RM subject. One compensation tube was unstained blood cells. Other compensation tubes comprised an individual antibody for each fluorochrome used in the pre-determined panels. Each fluorochrome was represented in the compensation panel. Compensation antibody tubes were dictated by the fluorochromes analyzed and defined lymphocyte populations.

Flow Cytometry Surface Staining

Surface staining was performed with appropriately diluted antibodies and compensation tubes as previously described (Veazey 2000b). Briefly, monoclonal antibody for surface staining was incubated with 10^6 cells of WB or BM samples in100µL aliquots for 30 minutes in the dark at 4°C. Red blood cell lysis was performed with a 1X BD FACS Lysing Solution 1X as directed by the manufacturer and incubated for 10 minutes at room temperature in the dark (BD Biosciences; San Jose, CA). A short wash in 3mL of phosphate buffered saline (PBS) at 400 x g for 7 minutes followed. The supernatant was discarded leaving a cell pellet. Samples to be analyzed for surface staining only were fixed as detailed below. Samples to be analyzed for intracellular markers were fixed and processed as described later.

The cell pellet was fixed. For four color flow cytometry, fixation was in 300 µL per sample of 2% paraformaldehyde. For multi-color flow cytometry, fixation was in 300 µL per sample of BD Stabilizing Fixative as directed by the manufacturer (BD Biosciences). All fixed samples were maintained at 4°C until analysis.

Flow Cytometry Intracellular Staining

After surface staining, flow cytometry samples processed for intracellular staining to detect proliferation by Ki67 and bromodeoxyuridine (BrdU) or apoptosis by activated caspase 3 (AC3). Samples were maintained at 4°C in the dark after intracellular staining till analysis.

Intracellular staining for detection of proliferation during G_1, S, G_2 and mitosis phases of the cell cycle by Ki67 was performed after surface staining as previously described (Kaur 2000). Cells were fixed with 600µL of 4% paraformaldehyde for 30 minutes in the dark at room temperature. Cells were permeabilized by a wash in 2mL of a 0.1% saponin-PBS solution. The sample was decanted and the pellet was incubated with 20µL of Ki67 antibody for 30 minutes at room temperature in the dark. A final wash in 0.1% saponin-PBS solution with supernatant

discard was performed and cells were fixed with 300µL of 2% paraformaldehyde and stored overnight.

Intracellular staining for detection of proliferation during the S phase or DNA synthesis of the cell cycle by BrdU staining was performed as previously described (Wang 2008a). RM had been inoculated intra-peritoneal with BrdU 24 hours prior to sacrifice. BrdU was administered at 60mg/kg of body weight diluted in sterile PBS to a final dilution of 20mg BrdU/mL of PBS. After surface staining, cells in the sample were fixed and permeabilized with 100µL of BD Cytofix/Cytoperm Fixation and Permeabilization buffer (BD Biosciences) for 15 minutes on ice in the dark. A wash with 3mL of 1X BD Perm Wash buffer (BD Biosciences), at 400 x g for 7 minutes followed by discard of the supernatant formed a cell pellet. The pellet was incubated with 100µL of deoxyribonuclease (DNAse) (Sigma-Aldrich; St. Louis, MO) for 60 minutes at 37°C in a humidified incubator with 5% CO_2. Another wash followed by incubation with 20µL of anti-BrdU antibody for 30 minutes at room temperature in the dark. A final wash with supernatant discard was performed and cells were fixed with 300µL of 2% paraformaldehyde and ready for analysis.

Intracellular staining for detection of apoptosis by activated caspase 3 was performed after surface staining. Cells in the sample were permeabilized with 250µL of BD Cytofix/Cytoperm (BD Biosciences) fixation and permeabilization buffer for 20 minutes at 4°C in the dark. A wash with 1X BD Perm Wash buffer (BD Biosciences), diluted per manufacturer instructions from 10X, at 400 x g for 7 minutes followed by discard of the supernatant. The pellet was incubated with 15µL of activated caspase 3 antibody and 50µL of 1X BD Perm Wash buffer (BD Biosciences), per tube, for 60 minutes at room temperature in the dark. A final wash with supernatant discard was performed and cells were fixed with 300µL of 1% paraformaldehyde.

FLOW CYTOMETRY ACQUISTION

Flow cytometry evaluation of samples, surface and intracellular staining, was performed within 24 hours of cell preparation as a batch including compensation tubes. Flow cytometry analysis by a flow cytometer was performed in the TNPRC Flow Cytometry Core Laboratory.

Four color flow cytometry analysis was performed on the BD FACSCalibur Flow Cytometer (BD Biosciences) with Macintosh Operating System 10.4.1 (Apple Software; Cupertino, CA). Data acquisition was obtained by Cell Quest Pro 5.2.1 (BD Biosciences). A minimum of 20,000 events was recorded for each sample.

Multi-color flow cytometry analysis was performed when samples contained five or more fluorochromes. Multi-color flow cytometry analysis was performed on the BD LSRII (BD Biosciences) with BD FACSDiva operating system and acquisition software (BD Biosciences). A minimum of 10,000 events was recorded for each sample.

FLOW CYTOMETRY DATA ANALYSIS

Flow cytometry data acquired from the TNPRC flow cytometry core laboratory was analyzed by using FlowJo for Windows (Tree Star, Inc.; Ashland, OR). Basic gating is depicted in Figure III.1. Gating strategies to identify specific populations of interest are defined by chapter. Immunophenotype of cells was reported in percentages.

Flow Cytometry Compensation Tubes

Fluorescence identified as negative or positive signal for each fluorochrome served as controls for gating of panels in a compensation tube panel as described by Walker et al (Walker 2004b). Selection for absence or presence of fluoruescence for a selected fluorochrome tagged to a single specific antibody established negative and positive signals respectively (Figure 2.1). Compensation tubes allowed setting of flow cytometry analyzers to properly detect antibodies within ranges of fluorescence and minimized spectral overlap.

WHOLE BLOOD ABSOLUTE CD4+ LYMPHOCYTE COUNT

The whole blood absolute CD4+ lymphocyte count for each Rhesus macaques infected with SIV was determined for experimental database II (Table III.1) and experimental database III (Table III.1). The whole blood lymphocyte phenotypic population was identified by the parent gate of forward scatter versus side scatter plot (Figure III.1). The gate of interest was identified from the parent gate as CD4 versus side scatter plot to reveal CD4+ lymphocytes as percentages of total lymphocytes. The immunophenotype percentage of CD4+ lymphocytes was multiplied by the absolute lymphocyte and the final number was the whole blood absolute CD4+ lymphocyte count of cells/μL.

Table III.1. Whole Blood Absolute CD4 Lymphocyte Count for Experimental Database II

ED II[a] Subject ID[b]	Absolute CD4 Lymphocyte Count cells/μL
AV63	463
AV85	670
BA17	416
BI58	558
BN37	542
BV13	752
C419	383
CB74	992
L880	212
T139	355
BV74	775
CF35	546
DB53	277
DE09	1192
DI28	810
N998	584
R908	653
AP53	1127
BD78	729
BE64	258
CD95	543
L164	317
V205	195
AE55	150
BA25	169
BE65	288
BI33	150
I553	21
P045	2
R544	190
T798	43

a) ED II = experimental database II
b) ID = identification

ED III[a] Subject ID[b]	Absolute CD4 Lymphocyte Count cells/μL
AV91	472
BA57	246
HI52	664
HI53	325
HI58	651
HI63	438
M992	227
T108	653
AL07	56
FA14	244
FE53	469
FT46	279
HG49	184
HG56	339
HG58	341
HI68	22

a) ED III = experimental database III
b) ID = identification

REFERENCES

Kaur, A., Hale, C.L., Ramanujan, S., Jain, R.K., and Johnson, R.P. (2000). Differential dynamics of CD4(+) and CD8(+) T-lymphocyte proliferation and activation in acute simian immunodeficiency virus infection. Journal of virology *74*, 8413-8424.

Switzer, J.W. (1967). Bone marrow composition in the adult rhesus monkey (Macaca mulatta). J Am Vet Med Assoc *151*, 823-829.

Veazey, R.S., Tham, I.C., Mansfield, K.G., DeMaria, M., Forand, A.E., Shvetz, D.E., Chalifoux, L.V., Sehgal, P.K., and Lackner, A.A. (2000). Identifying the target cell in primary simian immunodeficiency virus (SIV) infection: highly activated memory CD4(+) T cells are rapidly eliminated in early SIV infection in vivo. Journal of virology *74*, 57-64.

Walker, J.M., Maecker, H.T., Maino, V.C., and Picker, L.J. (2004). Multicolor flow cytometric analysis in SIV-infected rhesus macaque. In Methods in cell biology, Z. Darzynkiewicz, M. Roederer, and H.J. Tanke, eds. (Elsevier), pp. 535-557.

Wang, X., Das, A., Lackner, A.A., Veazey, R.S., and Pahar, B. (2008). Intestinal double-positive CD4+CD8+ T cells of neonatal rhesus macaques are proliferating, activated memory cells and primary targets for SIVMAC251 infection. Blood *112*, 4981-4990.

APPENDIX IV: PLASMA VIRAL LOAD

VIRAL LOAD

Plasma samples were processed from EDTA whole blood collected at necropsy and frozen at -80°C. Thawed plasma samples were analyzed for quantitative analysis of SIV. Plasma viral load was determined by bDNA assay (Siemens Clinical Laboratory; Berkeley, CA) as previously described (Smith S. M. 1999) from frozen plasma samples. Nucleic acid hybridization technique for the quantitation of SIVmac or SIVsm in RM plasma by detection of genomic RNA SIV was performed. The hybridization probe detects the *pol* gene in an SIV RNA 4.0 branched DNA (bDNA) assay. Viral load was reported as RNA copies/mL of plasma.

Experimental Database Plasma Viral Load

For ED II, thirty-nine Indian RM were included in this study but only Rhesus macaques inoculated with SIV had viral loads determined (Table IV.1).

For ED III, twenty-four Asian RM were included in this study but only Rhesus macaques inoculated with SIV had viral loads determined (Table IV.1).

Table IV.1. Experimental Database Plasma Viral Load

ED II[a] Subject ID[b]	Plasma Viral Load x 10^4 copies/mL
AJ79	
BB05	
EH70	
EH80	
EH95	
H741	
L750	
R534	
AV63	190.00
AV85	23.00
BA17	1100.00
BI58	1200.00
BN37	34.00
BV13	1600.00
C419	1100.00
CB74	210.00
L880	700.00
T139	320.00
BV74	0.08
CF35	12.17
DB53	2.86
DE09	0.97
DI28	82.02
N998	42.76
R908	0.47
AP53	410.00
BD78	8.60
BE64	79.00
CD95	15.65
L164	770.00
V205	18.24
AE55	75.00
BA25	67.26
BE65	8.55
BI33	36.13
I553	189.54
P045	714.89
R544	170.00
T798	0.37

b) a) ED II = experimental database II
c) b) ID = identification
d)
e)

ED III[a] Subject ID[b]	Plasma Viral Load x 10^4 copies/mL
AG71	
BB01	
CC10	
GN70	
HI54	
HI55	
HI56	
HI57	
AV91	15719.00
BA57	1428.82
HI52	370.06
HI53	355.57
HI58	849.60
HI63	2431.09
M992	3494.98
T108	5.73
AL07	37.46
FA14	14.90
FE53	34.35
FT46	17079.80
HG49	10.49
HG56	1952.27
HG58	0.71
HI68	807.62

ED III = experimental database III
ID = identification

REFERENCES

Smith, S.M., Holland, B., Russo, C., Dailey, P.J., Marx, P.A., and Connor, R.I. (1999). Retrospective analysis of viral load and SIV antibody responses in rhesus macaques infected with pathogenic SIV: predictive value for disease progression. AIDS research and human retroviruses *15*, 1691-1701.

APPENDIX V: COPYRIGHT PERMISSION

Permission was granted from the publisher (Figure V.1) and author (Figure V.2) to use the schematic found in Chapter 2 (Gupta 2007).

ELSEVIER LICENSE
TERMS AND CONDITIONS

Mar 26, 2010

This is a License Agreement between Amy F Gill ("You") and Elsevier ("Elsevier") provided by Copyright Clearance Center ("CCC"). The license consists of your order details, the terms and conditions provided by Elsevier, and the payment terms and conditions.

All payments must be made in full to CCC. For payment instructions, please see information listed at the bottom of this form.

Supplier	Elsevier Limited The Boulevard,Langford Lane Kidlington,Oxford,OX5 1GB,UK
Registered Company Number	1982084
Customer name	Amy F Gill
Customer address	P.O. Box 14763 Baton Rouge, LA 70898
License Number	2396651047336
License date	Mar 26, 2010
Licensed content publisher	Elsevier
Licensed content publication	Autoimmunity Reviews
Licensed content title	Susceptibility of naïve and subsets of memory T cells to apoptosis *via* multiple signaling pathways
Licensed content author	Sudhir Gupta, Sastry Gollapudi
Licensed content date	August 2007
Volume number	6
Issue number	7
Pages	6
Type of Use	Thesis / Dissertation
Portion	Figures/tables/illustrations
Number of Figures/tables/illustrations	1
Format	Both print and electronic
You are an author of the Elsevier article	No
Are you translating?	No
Order Reference Number	
Expected publication date	May 2010

Figure V.1. Copyright permission from publisher

Original Message-----
From: Gupta, Sudhir [mailto:sgupta@uci.edu]
Sent: Fri 3/26/2010 11:03 AM
To: Gill, Amy
Subject: RE: T cell apoptosis article 2007
Yes, You may use the figure from my article.

Sudhir Gupta, MD, Ph.D., MACP
Editor-in-Chief, Journal of Clinical Immunology
Professor of Medicine, Pathology & Laboratory Medicine, and Microbiology & Molecular Genetics
Chief, Basic and Clinical Immunology
Director, Jeffery Modell Diagnostic Center for Primary Immunodeficiencies
University of California
Irvine, CA 92697
Phone: (949) 824-5818
Fax: (949) 824-4362
e-mail: sgupta@uci.edu
Director of Scientific Development
The Sass Foundation for Medical Research, Inc.
New York
President and Director
Foundation for Primary Immunodeficiency Diseases (FPID)
California

_____
From: Gill, Amy [afgill@tulane.edu]
Sent: Friday, March 26, 2010 8:53 AM
To: Gupta, Sudhir
Subject: T cell apoptosis article 2007

Dear Dr. Gupta,

I am writing my dissertation on research in SIV infection of rhesus macaques evaluating bone marrow effects. My reserach is based upon the theory apoptosis of bone marrow cells increases during infection. I have referenced your article Autoimmunity Reviews 6 (2007) 476-481 and would like to include Figure 1 in my dissertation. May I have permission from you and contacts for the journal to secure copyright permission? I appreciate your attention to this matter and thank you for your help.

Respectfully,
Amy Gill

Amy F. Gill, D.V.M.
T32 Postdoctorate Trainee
Tulane National Primate Research Center
Division of Comparative Pathology
18703 Three Rivers Road
Covington, LA 70433
Office 985-871-6508
Fax 985-871-6591
Email afgill@tulane.edu

Figure V.2. Copyright permission from author

REFERENCES

Gupta, S., and Gollapudi, S. (2007). Susceptibility of naive and subsets of memory T cells to apoptosis via multiple signaling pathways. Autoimmun Rev *6*, 476-481.

VITA

Amy F.Gill was born in Baton Rouge, Louisiana, where she graduated from Saint Joseph's Academy in May 1987. She attended undergraduate school in the College of Basic Sciences at Louisiana State University in Baton Rouge, Louisiana. After successful admittance to the Louisiana State University School of Veterinary Medicine in Baton Rouge, Louisiana, with only three years of undergraduate work, she earned her Doctorate of Veterinary Medicine in May 1994. She practiced small animal veterinary medicine in East Baton Rouge Parish, St. Tammany Parish, Tangipahoa Parish and Washington Parish until return to academia in 2003. She entered a combined residency and graduate program in the Department of Pathobiological Sciences at the Louisiana State University School of Veterinary Medicine in Baton Rouge, Louisiana, in May 2003. She completed a three year residency in veterinary clinical pathology under Professor Stephen Gaunt. Pursuant to finishing her residency program she was accepted into a T32 Postdoctoral Fellowship for her doctoral research completed at the Tulane National Primate Research Center under Professor Ronald S. Veazey. She is a candidate for the degree of Doctor of Philosophy.